REFERENCE

ProQuest LLC.
789 East Eisenhower Parkway
P.O. Box 1346
Ann Arbor, MI 48106 – 1346

LONG TERM PERFORMANCE OF CONCRETE REPAIR IN HIGHWAY STRUCTURES

Finbarr J. O'Flaherty

A thesis submitted in partial fulfilment of the requirements of
Sheffield Hallam University
for the degree of Doctor of Philosophy

March 1998

Collaborating Organisations
Department of Transport
V.A. Crookes (Contracts) Ltd.
Flexcrete Ltd.
M.J. Gleeson (Group) PLC

ABSTRACT

In recent years, the number of reinforced concrete structures requiring repair and rehabilitation has increased considerably. This is due mainly to the corrosion of the reinforcing steel within the concrete which has become contaminated with a highly corrosive environment containing chlorides and carbon dioxide. Specification of repair materials at present, in accordance with BD 27/86 [1], is based on an inadequate understanding of the interaction between the substrate concrete and repair material. Cracking may occur in the early ages after application of the repair material due to the restraint to shrinkage provided by the substrate concrete and steel reinforcement. This would have serious durability consequences which would aid the onset of further corrosion. Furthermore, it is not clear at present if an efficient composite interaction is developed between the repair patch and substrate concrete in the long term to enable the repair patch to carry external load, or if the repair patch just acts as a barrier to protect the steel reinforcement from further corrosion.

This research relates the basic properties of repair materials (elastic modulus, shrinkage and creep) to the long term performance of repair materials applied to actual concrete highway structures and simulated laboratory repairs. The research forms part of a LINK project sponsored by three companies and the Department of Transport. Three deteriorating highway structures were selected for concrete repairs. The repairs were monitored over the long term to gain an understanding of the interaction between the repair material, substrate concrete and steel reinforcement. These were Gunthorpe Bridge, a three span reinforced concrete arch bridge, crossing the River Trent to the east of Nottingham, Lawns Lane Bridge, carrying part of the M1 near Wakefield in West Yorkshire, and finally, Sutherland Street Bridge, carrying the B6080 in Sheffield, South Yorkshire.

In order to gain information on the effectiveness of the repair materials in developing an efficient composite action with the substrate concrete, vibrating wire strain gauges were attached to the substrate concrete and steel reinforcement after the deteriorated concrete was removed. Embedment and surface gauges were installed in the repair patches either during or after repair material was applied.

Laboratory investigations consisted of repairs to simply supported reinforced concrete beams. Repair patches were applied centrally at mid-span to beams which were subjected to two point loading at one-third span points. The interaction between the repair materials, steel reinforcement and concrete substrates were monitored by a combination of a demec extensometer and electrical resistance strain gauges.

A theory is presented which predicts the long term interaction between the concrete substrate and repair materials to unpropped compression members. The analysis is divided into two stages. The first part deals with the distribution of shrinkage strain within the repair patch; the second part deals with the redistribution of external load from the substrate concrete into the repair patch. The distribution of shrinkage strain in the repair patch is based on the analogy of a bi-metallic strip contracting due to a

drop in temperature (similar to a repair material contracting due to shrinkage). It has been observed that a repair material with an elastic modulus greater than the elastic modulus of the substrate concrete is able to transfer some shrinkage strain to the substrate concrete. This analysis, therefore, enables the tensile stress in the repair material, due to the partial restraint to shrinkage provided by the substrate concrete, to be predicted. Similarly, the restrained shrinkage strain that is transferred to the substrate concrete is also predicted as an increase in compressive stress in the substrate concrete. The transfer of external load into the repair patch is based on analysing the distribution of stress in a compound member when subjected to an axial force. The compound member consists of two different materials - the substrate concrete and repair material. The analytical expressions require basic properties of the repair material (elastic modulus, shrinkage and creep) and substrate concrete (elastic modulus) to enable a prediction of the stress across the repair patch in the long term to be made. The validity of the model is verified on the basis of the field data from the spray applied repair materials on two of the highway structures (Lawns Lane Bridge and Gunthorpe Bridge).

Declaration

I hereby declare that no portion of the work referred to in this thesis has been submitted in support of an application for another degree or qualification of this or any other University or other institution of learning. All sources of information have been duly acknowledged.

Finbarr J. O'Flaherty

March 1998

Acknowledgements

The author wishes foremost to express his sincere appreciation to Professor P.S. Mangat of the School of Construction, Sheffield Hallam University, for his guidance, invaluable advice and support throughout this research project.

The author also gratefully acknowledges the contributions of Dr. F. Al-Shawi of the School of Construction, Sheffield Hallam University.

The author wishes to express his gratitude to the LINK TIO Programme and the Department of Transport for funding this research project. The author is also grateful for the financial and technical contribution to the project made by the following companies:

V.A. Crookes (Contracts) Ltd.

M.J. Gleeson Group plc.

Flexcrete Ltd.

The author gratefully acknowledge the support of Nottinghamshire County Council, The Highways Agency and Sheffield City Council for the project and in particular their co-operation in the field investigations.

The author is indebted to the following individuals for their important contributions to the research:

Mr. Ian Hawthorne (Department of Transport), Mr. Howard Wyborn (LINK TIO Co-ordinator), Mr. Peter Brown and Mr. John Seaton (M.J. Gleeson Group plc), Mr Paul Bennison and Mr. John Bailey (Flexcrete Ltd.) and Mr. Martin Crookes (V.A. Crookes (Contracts) Ltd.

The support provided both in the field and in the laboratory by the technical staff, especially Mr. Bob Skelton and Mr. Geoff Harwood, at the School of Construction, Sheffield Hallam University, is also appreciated.

CONTENTS

NOTATION

A_{rm} is the cross sectional area of the repair material

$A_{rm(trans)}$ is the transformed area of the repair material

$= A_{rm} + m_{st}A_{st}$

A_{st} is the area of the steel reinforcement in the repair patch

A_{sub} is the cross sectional area of the zone of influence in the substrate concrete

$= bmd_{rm}$

b is the breadth of the repair patch or zone of influence in the substrate concrete

d_{rm} is the depth of the repair material

$d_{rm(trans)}$ is the transformed depth of the repair material

d_{sub} is the depth of the zone of influence in the substrate concrete

E_{rm} is the 28 day elastic modulus of the repair material

$E_{rm(eff)}$ is the effective elastic modulus of the repair material after creep in the repair material has taken place

$= E_{rm} / (1+\phi)$

E_{sub} is the elastic modulus of the substrate concrete

F is the virtual force in the repair material causing a displacement equivalent to $(\varepsilon_{shr(free)} L)$

$F_{rm(ELT)}$ is the compressive force in the repair material after external load transfer from the substrate concrete

$F_{rm(shr)}$ is the virtual tensile force in the repair patch due to the restraint to shrinkage provided by the substrate concrete

$F_{rm(U)}$ is the virtual compressive force applied to the repair material to cause a strain equivalent to $\varepsilon_{rm(shr)}$, the dissipated strain energy

F_{shr} is the virtual force in the substrate concrete, due to transfer of shrinkage from the repair material, or in the repair material due to restraint to shrinkage provided by the substrate concrete

$= F_{sub(shr)}$ or $F_{rm(shr)}$

$F_{sub(ELT)}$	is the compressive force in the substrate concrete after external load transfer to the repair patch
$F_{sub(ext)}$	is the compressive force in the zone of influence in the substrate concrete due to external loading
$F_{sub(shr)}$	is the virtual compressive force in the substrate concrete due to distribution of shrinkage strain from the repair material
$F_{sub(U)}$	is the virtual compressive force in the substrate concrete due to transfer of dissipated strain energy from the repair material
f_{co}	is the core strength of the substrate concrete
f_{cu}	is the cube strength of the substrate concrete
$f_{rm(shr)}$	is the bending stress in the repair patch due to shrinkage in the repair material
$f_{sub(shr)}$	is the bending stress in the substrate concrete due to transfer of shrinkage strain from the repair material
f_1	is the datum frequency of the vibrating wire strain gauge (in Hertz)
f_2	is the frequency of subsequent readings of the vibrating wire strain gauge (in Hertz)
I_{rm}	is the second moment of area of the repair material $=b(d_{rm})^3/12$
I_{sub}	is the second moment of area of the zone of influence in the substrate concrete $=b(d_{sub})^3/12$
k	is the vibrating wire strain gauge constant
k_1	is a constant for volume/surface correction of the laboratory shrinkage data
k_2	is a constant for temperature correction of the laboratory shrinkage data
k_3	is a constant for relative humidity correction of the laboratory shrinkage data
k_4	is a constant for the efficiency of the curing compounds on the shrinkage of the repair materials in the field

L is the length of the repair patch or zone of influence in the substrate concrete

$M_{rm(shr)}$ is the moment in the repair material due to bending caused by restraint to shrinkage in the repair material

$M_{rm(U)}$ is the virtual moment applied to the repair material to cause a strain equivalent to $\varepsilon_{sub(shr)}$, the dissipated strain energy

$M_{sub(shr)}$ is the moment in the substrate concrete due to bending caused by transfer of shrinkage from the repair material

$M_{sub(U)}$ is the moment in the substrate concrete due to transfer of dissipated strain energy from the repair material

m is the modular ratio between the repair material and the substrate concrete

$= E_{rm} / E_{sub}$

m_{st} is the modular ratio between the steel reinforcement and repair material

$= E_{st} / E_{rm}$

R is the radius of curvature of the repair patch and substrate concrete due to distribution of shrinkage strain in the repair material

$U_{rm(axial)}$ is the strain energy in the repair material due to the application of a virtual force

$U_{rm(bend)}$ is the strain energy in the repair material due to the application of a virtual moment

$U_{rm(total)}$ is the total strain energy in the repair material due to the application of a virtual force and moment

$= U_{rm(axial)} + U_{rm(bend)}$

$U_{sub(total)}$ is the total strain energy transferred to the substrate concrete due to the dissipation of strain energy in the repair material

y_{rm} is the distance from the centroidal axis in the repair material to the point under consideration

y_{sub} is the distance from the centroidal axis in the zone of influence, in the substrate concrete, to the point under consideration

α is the ratio of the stress in the substrate concrete to the ultimate strength of the substrate concrete

Δ is the displacement due to dissipation of strain energy in the repair material

$= \varepsilon_{rm(shr)} L$

$\varepsilon_{rm(bend)}$ is the strain in the repair material due to bending caused by restraint to shrinkage

$\varepsilon_{rm(creep)}$ is the strain due to creep in the repair material

$\varepsilon_{rm(elast)}$ is the instantaneous elastic strain in the repair material immediately after loading

$\varepsilon_{rm(ELT)}$ is the strain in the repair material due to external load transfer from the substrate concrete

$\varepsilon_{rm(shr)}$ is the restrained shrinkage strain in the repair material

$= \varepsilon_{sub(shr)}$ at the interface

$\varepsilon_{rm(tens)}$ is the virtual tensile strain in the repair material due to restraint to shrinkage provided by the substrate concrete or steel reinforcement

$\varepsilon_{shr(free)}$ is the modified free shrinkage strain in the repair material

$= k_1 k_2 k_3 k_4 (\varepsilon_{shr(lab)})$

$\varepsilon_{shr(lab)}$ is the shrinkage of the repair materials measured in the laboratory

$\varepsilon_{sub(bend)}$ is the strain due to bending in the substrate concrete due to transfer of shrinkage strain from the repair material

$\varepsilon_{sub(ELT)}$ is the strain in the substrate concrete after external load transfer to the repair material

$\varepsilon_{sub(shr)}$ is the strain in the substrate concrete due to distribution of shrinkage strain from the repair material

$= \varepsilon_{rm(shr)}$ at the interface (strain compatibility)

λ is the percentage of shrinkage strain transferred to the substrate concrete, divided by the free shrinkage of the repair material

$$= \frac{\varepsilon_{sub(shr)}}{\varepsilon_{shr(free)}}$$

ϕ is the creep coefficient of the repair material

$= \varepsilon_{rm(creep)} / \varepsilon_{rm(elast)}$

$\sigma_{rm(ELT)}$ is the stress in the repair material due to external load transfer from the substrate concrete

$\sigma_{rm(U)}$ is the stress in the repair material due to application of an axial force and moment equivalent to the dissipated strain $\varepsilon_{rm(shr)}$

$\sigma_{rm(wk60)}$ is the total stress in the repair material at the end of the monitoring period (week 60)

$\sigma_{sub(ELT)}$ is the stress in the substrate concrete after external load transfer to the repair material

$\sigma_{sub(ext)}$ is the stress in the substrate concrete due to external loading

$\sigma_{sub(shr)}$ is the stress in the substrate concrete due to transfer of shrinkage from the repair patch

$\sigma_{sub(wk60)}$ is the total stress in the substrate concrete at the end of the monitoring period (week 60)

LIST OF FIGURES

LIST OF TABLES

CHAPTER 1

INTRODUCTION

1.1 INTRODUCTION

In recent years, concrete deterioration due to corrosion of the steel reinforcement has become a major problem world-wide. Undoubtedly, prevention is the best cure for the problem, but a large number of structures which are already contaminated with chlorides or have undergone carbonation require urgent repair. The most common form of rehabilitation for a deteriorated structure is to remove the damaged concrete and replace it with a new material, thus increasing the design life of the structure. At present, numerous repair materials exist for this purpose, each one possessing different mechanical properties.

The current standard for repair of concrete highway structures in the UK [1] does not take into account, in any significant quantitative manner, the mismatch in basic material properties such as elastic modulus, shrinkage and creep and particularly the effect of this mismatch on long term performance. Emphasis is normally given to short term properties such as 28 day cube strength, bond and early age shrinkage/expansion etc. Early age material properties, even though important in their own right, do not give a reliable indication of the long term performance of the repair with respect to the durability and efficiency of the composite action between the repair material and substrate concrete. The mechanics of concrete repair needs to be fully understood before a durable repair can be specified.

1.2 SCOPE OF RESEARCH

Patch repairs are an effective way of restoring the integrity of a structure damaged by reinforcement corrosion. Over £500 million is spent annually in the UK on refurbishment [2] as the tendency is to repair a structure to increase its design life rather than demolish and replace. There is widespread research in the broad area of concrete repair, but very little information exists on the long term effects that shrinkage and creep of the repair material will have on the in-service performance of the repair patch. Mismatching the elastic modulus of the repair material and substrate concrete may affect the performance of the repair, especially in the long term when the mismatch becomes more pronounced due to the effects of creep in the repair material. As a result, there is a need to evaluate the long term redistribution of shrinkage and creep strains in the repair patch and determine the effect of mismatching material properties on the performance of the repair. Also, the transfer of service load from the substrate concrete to the repair patch in the long term and its relationship to property mismatch i.e. elastic modulus, shrinkage and creep needs to be investigated.

Understanding the interaction between the repair material and substrate concrete and combining the knowledge with the basic material properties will allow more durable repairs to be specified. At present, there is an inadequate understanding of this interaction. Analytical models which determine this interaction and predict the long term performance of a patch repair are required.

1.3 SCOPE OF PRESENT INVESTIGATION

The long term structural interaction between a repair patch and substrate concrete as introduced in Section 1.2 was investigated in this project in order to determine the in-service performance of a number of generic repair systems currently employed on repairs to highway structures. Repair and maintenance methods and strategies used in current practice for the restoration and improvement of structural capacity were considered. Analytical derivations based on experimental and field data were used to correlate the long term structural interaction between the repair patch and substrate concrete to basic material properties such as elastic modulus, shrinkage and creep. The research project was funded by the LINK TIO Programme. The project team comprised three industrial partners (Flexcrete Ltd., V.A. Crookes (Contracts) Ltd., and M.J. Gleeson Group PLC) and the research team from Sheffield Hallam University which conducted all the scientific research.

Three highway bridge structures were selected for repair as part of the project, namely Gunthorpe Bridge in Nottinghamshire, Lawns Lane Bridge in West Yorkshire and Sutherland Street Bridge in Sheffield. Deteriorated concrete was removed from each bridge and replaced with commercially available generic repair materials. The main variables of the properties of repair materials were elastic modulus, shrinkage and creep. Three repair application techniques were used: hand applied, sprayed and flowing. Both hand and spray applied repair materials were used at Gunthorpe Bridge. Spray applied repair materials were used at Lawns Lane Bridge due to the large volume of repair patch. Flowing repair materials were applied at Sutherland Street Bridge.

The interaction between the repair patch and the substrate concrete, in the field studies was monitored by placing vibrating wire strain gauges within the repair patch. Gauges were attached to the cut-back substrate concrete, steel reinforcement and embedded in the repair material to monitor long term strains. As a result, the redistribution of strain in repair patches and the efficiency of composite action between repair and substrate concrete as affected by their material properties were determined.

The in-service performance of concrete repair to simply supported reinforced concrete beams was also investigated in the laboratory. Different repair materials were hand applied in patches in the tensile zone of the beams. Strain measuring instrumentation, such as electrical resistance and demec gauges were used to monitor the distribution of strain within the repair patch. The performance of the repair was related to the repair material properties.

The overall aims of the research reported in this thesis, therefore were:

- to determine the long term structural performance and efficiency of composite action between the repair material and substrate concrete after repair has been carried out.
- to investigate the mechanical and deformation properties of different repair materials, which are responsible for the interaction between the repair materials and substrate concrete.
- to relate the long term structural interaction between the substrate concrete and repair material to basic properties such as elastic modulus, shrinkage and creep of the repair material.

- to derive analytical models which predict the redistribution of strain between the repair material, substrate concrete and steel reinforcement.
- develop guidelines for the selection of optimum repair materials which lead to satisfactory long term structural performance of repair
- lead to innovation resulting in improved repair materials

1.4 THESIS LAYOUT

The thesis is divided into 13 chapters. It presents a comprehensive literature review on the subject in chapters 8, 9 and 11. An introduction to the thesis is given in Chapter 1.

Details of the experimental programme are given in Chapter 2. The methodology adopted to monitor the performance of concrete repairs in three field structures (highway bridges) and in the laboratory investigations is outlined.

The equipment and instrumentation used to monitor the distribution of strain within the repair patches in both the field and laboratory studies are detailed in Chapter 3. It consists of vibrating wire, electrical resistance and demec strain gauges. Details of strain recording devices used to monitor the strain gauges (data loggers and digital strain indicator) are also given in Chapter 3.

A description of the repair methods used and the installation of the equipment to monitor the distribution of strain within the repair patches in the field studies is presented in Chapter 4 (Gunthorpe Bridge), Chapter 5 (Lawns Lane Bridge) and

Chapter 6 (Sutherland Street Bridge). Information on the properties of repair materials used in each bridge is given in the chapters. The location of repair patches on each bridge and position of strain gauges within the repair patches are also detailed.

Details of repairs applied to simply supported reinforced concrete beams in the laboratory are given in Chapter 7. Repair material patches were applied to both propped and unpropped beams and the distribution of strain within the repair patch was monitored with strain gauges. The performance of the materials was also monitored when the depth of repair patch behind the steel reinforcement was increased. The repaired beams were stored in a controlled environment (20°C and 55% RH) throughout the monitoring period.

Chapter 8 deals with the properties of repair materials which influence the long term performance of concrete repair (shrinkage, creep and elastic modulus). Shrinkage was determined on specimens which were stored in controlled environments (in air at 20°C and 55% RH and in water at 20°C for the first 28 days) throughout the duration of the tests. Shrinkage tests were carried out on 500 x 100 x 100mm prism specimens and strains were measured from the age of 24 hours to 100 days for specimens stored in air, and from 28 days for specimens initially stored in water. Creep was determined on specimens which were cured in water for the first 28 days and then loaded in compression in custom built creep rigs. Creep of the repair materials was obtained by applying a constant load (30% stress/strength ratio) to a pair of specimens in series for 70 days. The creep recovery upon unloading was subsequently monitored for 30 days.

The elastic modulus of the repair materials was obtained by testing 200 x 100mm diameter cylinders in accordance with BS 1881 Part 121 [3] at 28 days of age.

Extensive field data which describes the in-service performance of the concrete repairs to the three highway bridges and the laboratory data on repaired beams is given in Chapter 9. The monitoring period lasted for approximately 60 weeks. The in-service performance of the repairs is related to the basic properties (shrinkage, creep and elastic modulus) of the repair materials.

Chapter 10 presents the stress distribution across the repaired section for spray applied repair materials to unpropped compression members. Stresses occur as a result of the restraint to shrinkage in the early ages (tensile) and as a result of external load transfer into the repair patch (compressive). These stresses are related to material properties.

Analytical models are derived in Chapter 11, which predict the long term in-service performance of concrete repair in highway structures. Basic properties such as elastic modulus, shrinkage and creep of the repair material and elastic modulus of the substrate concrete (shrinkage and creep will be negligible in the substrate concrete at the time of repair) are the main variables of the analytical models.

Conclusions and recommendations for future research are given in Chapter 12. Previous research referred to in this thesis is listed in Chapter 13. Publications to date arising from the results of this research programme are given at the end of the thesis.

CHAPTER 2

EXPERIMENTAL PROGRAMME

2.1 INTRODUCTION

In recent years, deterioration of reinforced concrete in highway structures has led to the premature failure of many structural elements. This is mainly due to the corrosion of the steel reinforcement within the concrete which has become subjected to a very harsh environment containing chlorides and carbon dioxide. Restoration of structural performance is achieved by removing the damaged concrete to arrest the deterioration and replacing it with a new material. Specification of repair materials at present is based on an inadequate understanding of the interaction between the substrate concrete and repair material. Basic material properties such as elastic modulus, shrinkage and creep are primarily responsible for this interaction. A mismatch in stiffness between the repair material and substrate concrete can effect the distribution of stress between the two mediums. Drying shrinkage may induce tensile stress in the repair material which could have serious durability consequences if the material cracks. Compressive creep of the material under sustained stress may render the load sharing capabilities of the material less effective, although tensile creep may have an advantageous role in helping to alleviate the tensile stress induced due to restrained shrinkage.

The aim of the experimental programme was to determine the in-service performance of different repair materials and different techniques of repair application in actual highway structures and in laboratory based concrete repairs.

2.2 OBJECTIVES OF THE INVESTIGATION

The main objectives of the investigation were:

1. To select monitoring equipment which could be used to measure the redistribution of strain within a repair patch both in field structures and in structural elements in the laboratory.
2. To carry out repairs to actual highway bridges using different repair techniques and different repair materials representing a range of material properties. To monitor these repairs in order to gain an understanding of the efficiency of the composite action between the substrate and repair material under service conditions.
3. To simulate repaired structural elements (beams) in the laboratory. To monitor the in-service performance of the repair patch in order to gain an understanding of the structural interaction between the repair material and substrate concrete.
4. To investigate the properties of repair materials which influence the long term performance of concrete repair i.e. elastic modulus, shrinkage and creep.

2.3 DETAILS OF THE EXPERIMENTAL PROGRAMME

2.3.1 Strain monitoring equipment

Vibrating wire strain gauges were used for measuring strains in the field structures due to their long term reliability and ease of application. Two different types of strain gauges were used, type TSR/SWP/5.5 for surface mounting and type TES/SWP/5.5 for embedding in the repair materials. The strains from these gauges were automatically recorded and stored on site in a data logger which was compatible with vibrating wire strain gauges.

Strain distribution within the repair patches in the laboratory based investigation was measured with foil-backed electrical resistance strain gauges which were attached to the steel reinforcement and with electrical resistance strain gauges protected in a polyester mould which were embedded in the repair material. A digital strain indicator was used to monitor and record deformation in the gauges.

Demec extensometer gauges, with a gauge length of 100mm, were used in the study to monitor surface strains.

Details of the monitoring equipment used in the investigation are given in Chapter 3.

2.3.2 Highway structures

Three deteriorating highway structures of different forms of construction were used to monitor the performance of concrete repairs. These were Gunthorpe Bridge carrying the A6097 in Nottinghamshire, Lawns Lane Bridge, near Wakefield, in West Yorkshire carrying part of the M1 just south of junction 42, and Sutherland Street Bridge carrying the B6080 in Sheffield.

Gunthorpe Bridge is a three span, reinforced concrete arch bridge spanning the River Trent at Gunthorpe, Nottinghamshire. It was built in 1927 to replace an old iron toll-bridge due to an increase in heavy traffic using the bridge. The central arch in the bridge spans 38.1m, while the two side arches span 30.9m. Each of these three arches contain four ribs.

Two different repair application techniques were employed at Gunthorpe Bridge, namely hand applied and spray applied. Three generic repair materials were hand applied to the lateral beams spanning the arch ribs. Three spray applied repair materials were used in parts of the south abutment.

Lawns Lane Bridge is a three span reinforced concrete bridge which carries part of the M1 between junctions 41 and 42 in West Yorkshire. It was built in the mid 1960's and consists of in-situ deck panels supported by prestressed beams, all of which are carried by reinforced concrete piers and abutments. Five different repair materials were monitored at Lawns Lane Bridge. Repairs were applied to the concrete piers and abutments by the dry spray process due to the large volume of the repair patches.

Sutherland Street Bridge in Burngreave, Sheffield, carries the B6080 over an access road which once linked steel industries together. The superstructure of this bridge consists of an in-situ bridge deck supported by prestressed beams. The prestressed beams are supported on a reinforced concrete substructure which has a portal frame configuration. Repairs were applied to the portal frame substructure using the flowing technique of repair and suitable materials for this technique. Four different repair materials were monitored at Sutherland Street Bridge.

Details of the field studies on each bridge are given in Chapter 4 (Gunthorpe Bridge), Chapter 5 (Lawns Lane Bridge) and Chapter 6 (Sutherland Street Bridge).

2.3.3 Laboratory investigation

Eight reinforced concrete beams measuring 2700mm x 100mm x 200mm were repaired with different repair materials. The beams were reinforced in the tension zone with two 16mm diameter high yield steel bars. Shear reinforcement consisted of 6mm diameter mild steel links at 110 mm centres in the shear zones. The shear reinforcement links were supported by 6mm diameter mild steel hanger bars in the compression zone.

Voids were inserted in the beams at the casting stage which were later filled with different hand applied repair materials. The strains in the longitudinal steel reinforcement were monitored by means of foil-backed electrical resistance strain gauges (type CEA-06-250UN-120). The strain in the repair material was monitored by means of embedded electrical resistance strain gauges which were protected by a

polyester mould (type PML-30). Demec points were attached across a gauge length of 100mm on opposite faces of the beam at different depths from the soffit to determine the strain diagram and the depth of the neutral axis. The beams were loaded under four-point bending to monitor deformation under long term service loading. Two service loads were applied at one-third of the span. This loading arrangement provided a pure bending moment zone (with zero shear force) in the middle third of the beam where the repair patch was applied. The laboratory tests investigated the long term distribution of strain in the substrate concrete and repair patches comprising of different repair materials. The depth of repair material behind the steel reinforcement was extended incrementally to study the effect of increased depth on structural interaction. The effect of carrying out repair on the beams in a propped and unpropped state on long term structural interaction (strain redistribution) was also studied.

Details of this series of experiments are given in Chapter 7

2.3.4 Properties of repair materials

The properties of repair materials which govern interaction of repair patches with the substrate concrete, such as elastic modulus, shrinkage and creep, were determined for all the repair materials used in the research. The elastic modulus of the concrete substrates from the three highway bridges and the laboratory beams was also determined.

The elastic modulus was determined for both the repair materials and concrete substrates using cylinders/cores of similar size (approximately 200mm x 100mm

diameter). Cylindrical specimens were cast in the laboratory for each repair material whereas cores of similar size were extracted from areas of sound substrate concrete on site.

Drying shrinkage of the repair materials was determined from prism specimens of dimensions 500 x 100 x 100mm. Deformation was monitored by means of a demec extensometer over a gauge length of 200mm. Datum readings for air cured specimens were taken 24 hours after casting and monitoring continued for 100 days. Datum readings for water cured specimens were taken at 28 days and monitoring continued for 100 days. Air cured specimens were stored in a temperature controlled environment (20°C and 55% RH) throughout the duration of the test. Water cured specimens were initially submerged for 28 days and subsequently stored in a temperature controlled environment (20°C and 55% RH) for the remainder of the test.

Creep tests on each repair material were based on two 500mm x 100mm x 100mm prism specimens which were cured in water at 20°C for 28 days prior to loading. Two prisms of each repair material were loaded in series in a standard creep rig for a period of 70 days to determine the creep characteristics. A stress/strength ratio of 0.30 was applied. Upon unloading, the creep recovery in each repair material was monitored for a period of 30 days. Shrinkage was monitored on two identical prisms which were cured and stored under the same conditions. Shrinkage strains were subtracted from the total strain measured on the prisms in the creep rigs in order to determine the net creep strain.

The results show that the shrinkage of the different generic repair materials varied from 325 to 1311 microstrain at 100 days. Shrinkage of a basic sand/cement mortar, which can be used as a control material to compare the shrinkage of the repair materials, was 717 microstrain. Creep of the repair materials varied from 421 to 1411 microstrain at 70 days. In comparison, creep of the sand/cement material was 938 microstrain.

Details of this series of experiments are given in Chapter 8.

2.3.5 In-service performance of repair materials

The long term performance of repair patches loaded under service conditions was determined from repairs to Gunthorpe Bridge, Lawns Lane Bridge and Sutherland Street Bridge and to structural elements in the laboratory. The application of repair was made using three methods: spray applied (Gunthorpe Bridge and Lawns Lane Bridge), hand applied (Gunthorpe Bridge and laboratory elements) and flowing repair (Sutherland Street Bridge).

The performance of the repair was related to the basic properties of the repair materials (elastic modulus, shrinkage and creep). The results show that for optimal repair, the elastic modulus of the repair material should be greater than the elastic modulus of the substrate concrete to enable distribution of shrinkage strains from the repair material to the substrate concrete and steel reinforcement. This results in a lower restrained shrinkage stress in the repair material. Also, the results show that a repair material that

is stiffer than the substrate concrete will attract external applied load more effectively into the repair patch.

Full details of the in-service performance of repair patches are given in Chapter 9.

2.3.6 Stress distribution across a repaired section

In the early ages after application, the repair material is prevented from shrinking freely due to the partial restraint provided to shrinkage by the substrate concrete and steel reinforcement. Although a repair material with a high elastic modulus will transfer a portion of the shrinkage strain to the less stiff substrate concrete, nevertheless tensile stress is induced in the repair material during the shrinkage period (weeks 0 to 11) due to the restraint. The magnitude of the tensile stress varies from material to material since it is dependant upon the properties of the repair material (elastic modulus, shrinkage and creep) and substrate concrete (elastic modulus). In the long term (weeks 25 to 47), it is shown that external load is attracted into the repair patch. This induces compressive stress in the repair material. This compressive stress reduces or neutralises the tensile stress that remains in the repair material from the shrinkage period. This is crucial for the long term performance of the repair material, as it is shown that the tensile strength of the repair material reduces with time.

Full details of the stresses in the repaired sections are given in Chapter 10.

2.3.7 Long term structural interaction

An analytical model to predict the structural interaction between the repair material and substrate concrete is derived from elementary structural analysis. The analytical model consists of two parts - the first part predicts the transfer of shrinkage strain from the repair material to the substrate concrete, the second part predicts the transfer of external load from the substrate concrete into the repair material. Prediction of the transfer of shrinkage strain from the repair material to the substrate concrete is based on the analogy of a bi-metallic strip undergoing contraction due to a drop in temperature. When the temperature of the bi-metallic strip is decreased, contraction will occur and both metals will exhibit the same strain at their interface even though their coefficients of thermal expansion will be different. As a result, compression will be forced on one of the metals and tension will be induced in the other. A similar situation occurs when a shrinking repair material is applied to the substrate concrete. Some shrinkage strain is transferred from the stiffer repair material to the weaker substrate concrete (giving strain compatibility at the interface due to interfacial bond). This transfer of shrinkage strain will induce a compressive stress in the substrate concrete. The partial restraint to shrinkage provided by the substrate concrete will induce tension in the repair material.

Prediction of the transfer of external stress from the substrate concrete into the repair patch is based on the distribution of stress across a compound section. The compound section consists of two different materials - substrate concrete and repair material. The substrate concrete is assumed to exhibit a permissible stress due to external loading. Since the repair material is stiffer than the substrate concrete, the repair material attracts a portion of the external stress from the substrate concrete. The proportion of stress

attracted into the repair patch is calculated from compatibility equations involving properties of the substrate concrete and repair material.

Details of the analytical models are given in Chapter 11.

2.4 MATERIALS

2.4.1 Introduction

Information on the different repair materials used at Gunthorpe Bridge, Lawns Lane Bridge, Sutherland Street Bridge and in the laboratory investigation is given in Chapters 4, 5, 6 and 7 respectively. This chapter outlines details of only the concrete materials which were used in the laboratory investigation.

2.4.2 Cement

Ordinary Portland cement was supplied by Castle Cement Ltd., Stamford, Lincolnshire. The chemical composition of the cement, tested in accordance with BS 12 [4] is given in Table 2.1.

2.4.3 Aggregates

The aggregates used in the laboratory tests were supplied by Tarmac Roadstone Ltd., Nottingham. Coarse aggregates consisted of 20-5 mm graded quartzite whereas the fine aggregate consisted of a medium grade sand. Grading curves of the aggregates are given in Figures 2.1 and 2.2. These were determined in accordance with BS 882 [5].

Table 2.1 Chemical composition of Portland cement

	%
CaO	64.50
SiO_2	21.00
Al_2O_3	5.00
Fe_2O_3	3.00
SO_3	3.10
MgO	1.10
K_2O	0.67
Na_2O	0.13
Cl	0.03
Loss on ignition	1.00
Non detected	0.47
	Total 100.00
Cement compounds	
Tricalcium Silicate (C_3S)	52.00
Dicalcium Silicate (C_2S)	21.00
Tetracalcium Aluminoferrite (C_4AF)	8.10
Tricalcium Aluminate (C_3A)	9.10

2.4.4 Steel reinforcement

Deformed high yield steel bars of grade 460 were used as reinforcement in the experimental investigation described in Chapter 7. The steel was supplied by Derim Steels Ltd., Chesterfield, Derbyshire. The yield point, obtained from laboratory tests, was 492 N/mm^2. The elastic modulus was 194 kN/mm^2. A graph showing the stress/strain curve of the steel reinforcement to yield point is given in Figure 2.3.

References Ch 2

4 British Standards Institution. (1978). *Specification for ordinary and rapid hardening Portland cement,* BSI, London, 1978. BS 12.

5 British Standards Institution. (1983). *Specification for aggregates from natural sources for concrete,* BSI, London, 1983. BS 882.

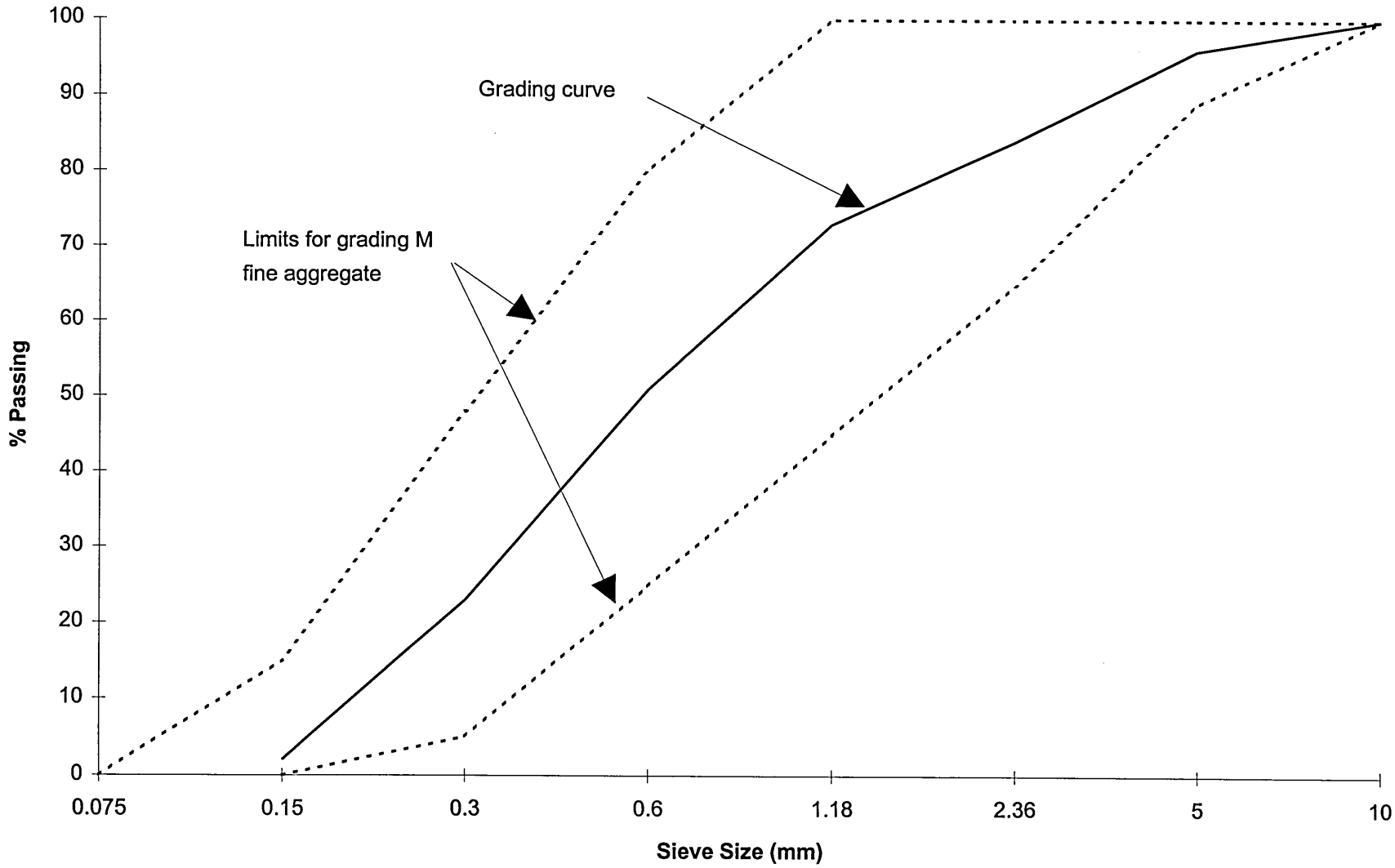

Figure 2.1 Grading curve for fine aggregate

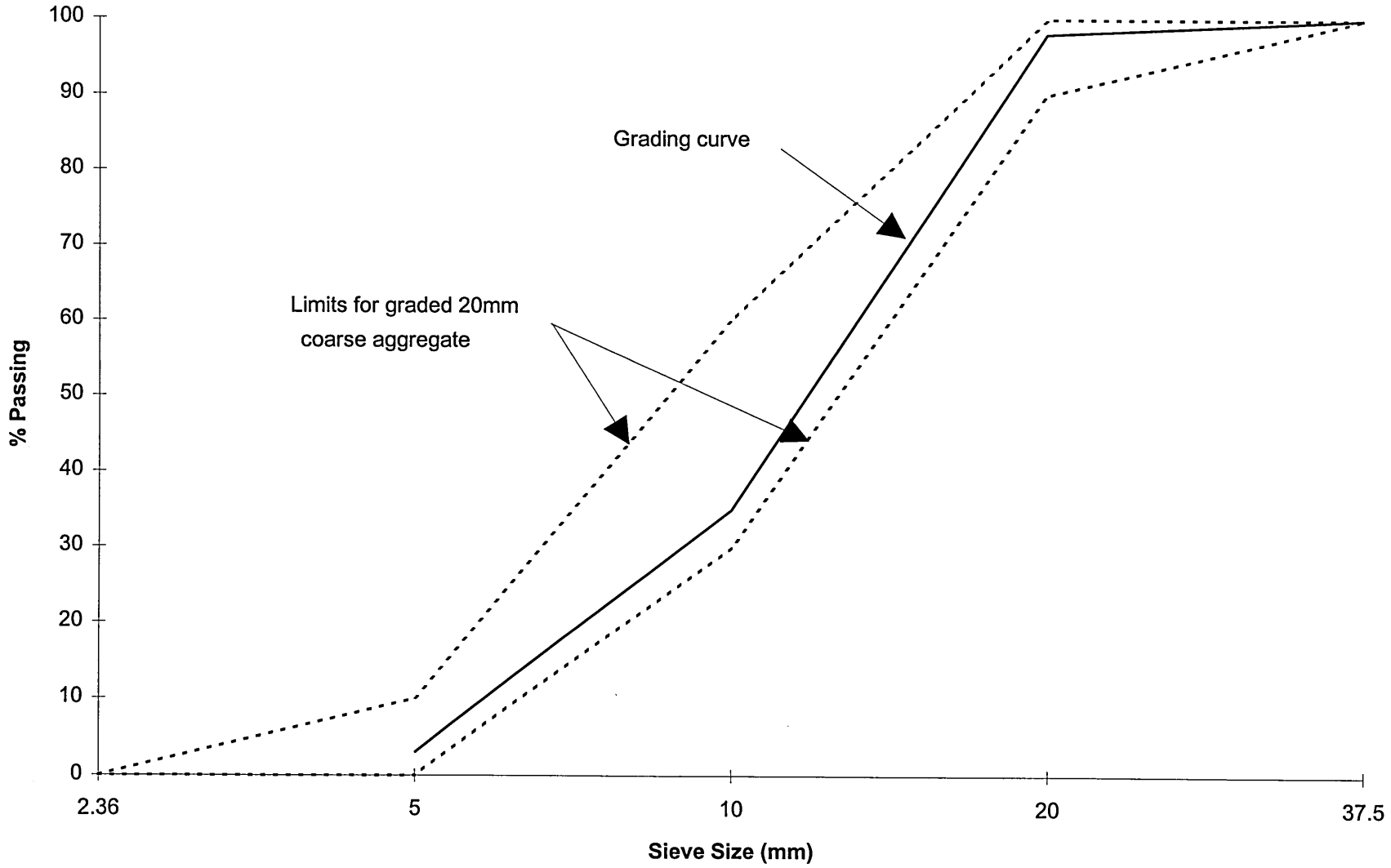

Figure 2.2 Grading curve for coarse aggregate

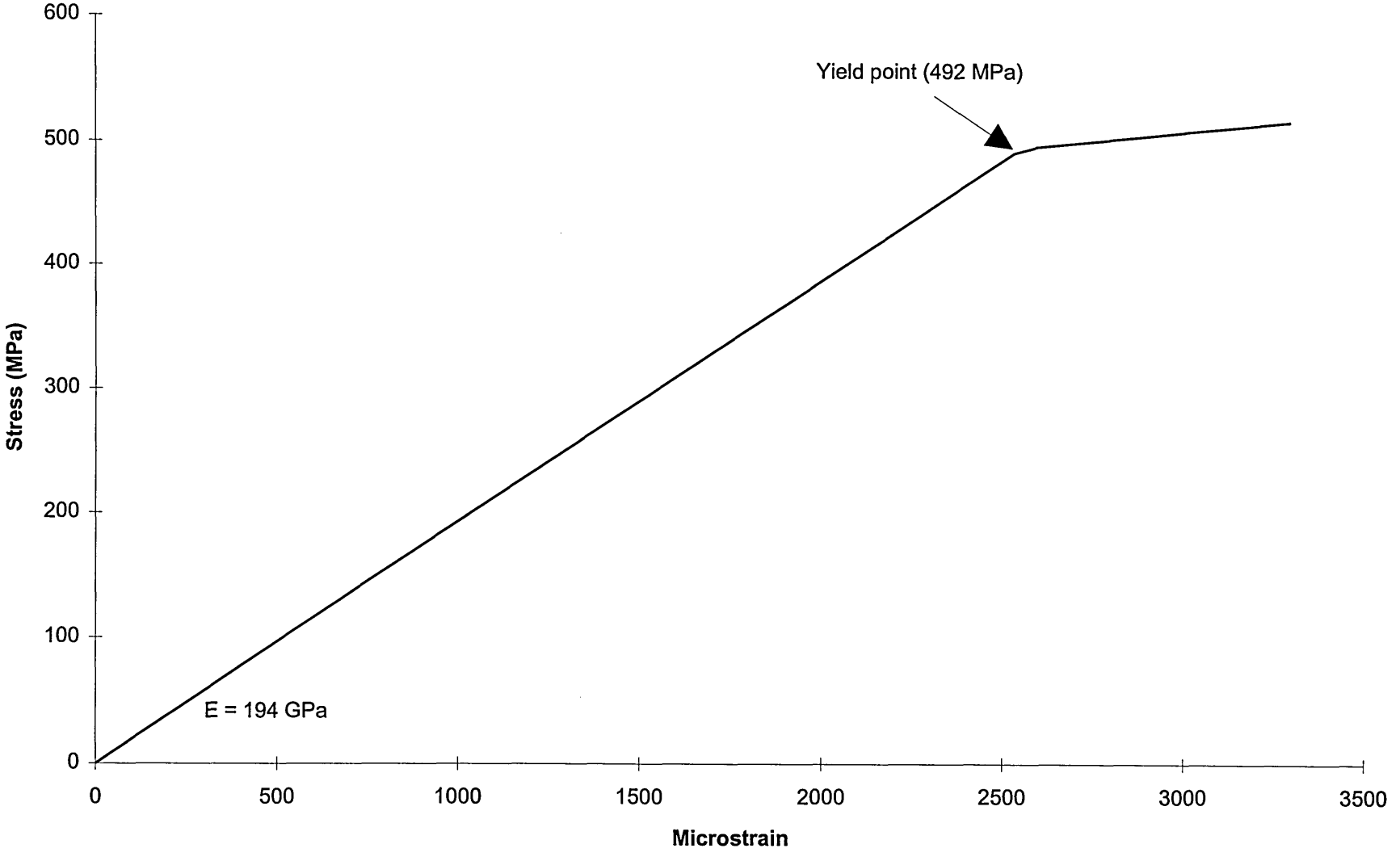

Figure 2.3 Stress-strain curve to yield point for the longitudinal steel reinforcement

CHAPTER 3

DETAILS OF MONITORING EQUIPMENT

3.1 INTRODUCTION

The effectiveness of a repair patch in developing an efficient composite action with the original concrete can be determined by measuring the redistribution of stress between the repair material, steel reinforcement and substrate concrete. The redistribution of stress in a repair situation is primarily due to the deformation (shrinkage) of the repair material. Redistribution of externally applied loads may also be evident. Stress redistribution to either the repair material, steel reinforcement or concrete substrate can be obtained by measuring the strain and applying Hooke's Law to find the stress. Strain can be measured by one of the many types of strain gauges available - vibrating wire, electrical resistance and demec extensometer gauges were employed in this study.

Vibrating wire strain gauges, even though more expensive than the other conventional strain measuring devices, were selected for site monitoring because of their reliability over a long period, ease of application and their ability to yield results from even the remotest locations. Readings can be taken automatically with a logging device or manually with a hand held instrument. In this instance, readings were stored in a data logger on site.

Two types of electrical resistance gauges were employed in laboratory tests to monitor the deformation in steel reinforcement and repair materials. The performance of the electrical resistance gauges installed under laboratory conditions could be guaranteed as opposed to the uncertainty which surrounds installation under field conditions. Electrical resistance strain gauges must be clinically clean at installation; this would be impossible to achieve in the field. Strain readings from the gauges were taken by a digital strain indicator.

Demec extensometer gauges were employed in the laboratory to measure surface strain only.

3.2 DETAILS OF FIELD MONITORING EQUIPMENT

3.2.1 Introduction to vibrating wire strain gauges

An introduction to the vibrating wire strain gauge is given by Hornby [6]. The vibrating wire principle of strain measurement has been known for many years and reports of its use have appeared as far back as 1928 in a paper by Davidenkoff [7]. This was followed by papers in France, Germany and the UK. The initial experiences in the UK were gained at the Building Research Station (BRS) [8, 9] and then later by the Road Research Laboratories [10].

The vibrating wire strain gauge consists of a thin steel wire held in tension between two anchorages (Figure 3.1, [6]). The wire is set into transverse vibration by exciting it with

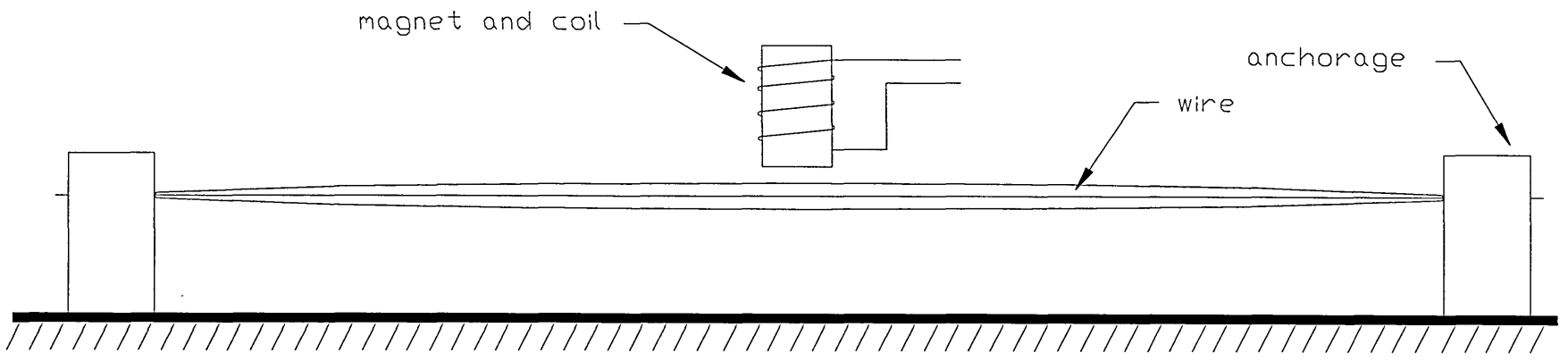

Figure 3.1 Vibrating wire string and electromagnet [6]

a short pulse of current passed through the coil of an electromagnet positioned near the mid point of the wire. The same coil is then used to detect the frequency of the vibrating wire. When the distance between the anchorages changes, the tension of the wire and consequently its natural frequency also change. This form of gauge has been shown to be stable over periods exceeding 15 years and it has the advantage that its frequency is not changed by the resistance or length of the leads [6]. Gauges of this design are used for measuring strain from a variety of materials and structures but it has been found ideally suited to casting or embedding into concrete.

3.2.2 Details of vibrating wire strain gauges used in this study

The vibrating wire strain gauges which were used on the three bridges under observation were supplied by Gage Technique Ltd., a company which specialises in the design of monitoring equipment for structural assessment. Waterproof vibrating wire strain gauges, type TSR/5.5/SWP for surface mounting and TES/5.5/WP for embedment were used for strain monitoring. Types TSR/5.5/SWP/T and TES/5.5/T accommodate both strain and temperature measurements. The gauges were of all metal construction and have been developed from the standard strain gauges designed by the Transport and Road Research Laboratory since 1969. Gauges were supplied with cable attached which could easily be extended or shortened as required.

The surface gauges (type TSR/5.5/SWP) are tensioned to a datum frequency of approximately 800 Hertz at installation. The embedment gauges (type TES/5.5/SWP)

are delivered pre-tensioned to approximately the same frequency. When the tension of the wire is increased in a vibrating wire strain gauge (i.e. as on a member with an increasing tensile stress), the frequency of the wire increases; alternatively it decreases in compression. Hence the change in strain can be calculated using the gauge equation:

$$\delta\varepsilon = k (f_1^2 - f_2^2)$$

Equation 3. 1

where $\delta\varepsilon$ is the strain change

k is the gauge constant (3×10^{-3})

f_1 is the datum frequency in Hertz

f_2 is the frequency of subsequent readings in Hertz

(Note: Positive sign indicates *compressive* strain; negative sign indicate *tensile* strain)

3.2.2.1 Measurement of substrate concrete strain in the field

In order to facilitate the measuring of strain in the concrete substrate, a vibrating wire surface strain gauge, type TSR/5.5/SWP, was attached to the cut back substrate as shown in Figure 3.2. The "bolted mounted plate" method of installation was used to securely fasten the gauge to the concrete surface. This method is for long term fixing of surface gauges to concrete. A pair of small mounting plates were screwed and bonded to the structure. The gauge was then bolted to the mounting plates. A description of this method is as follows:

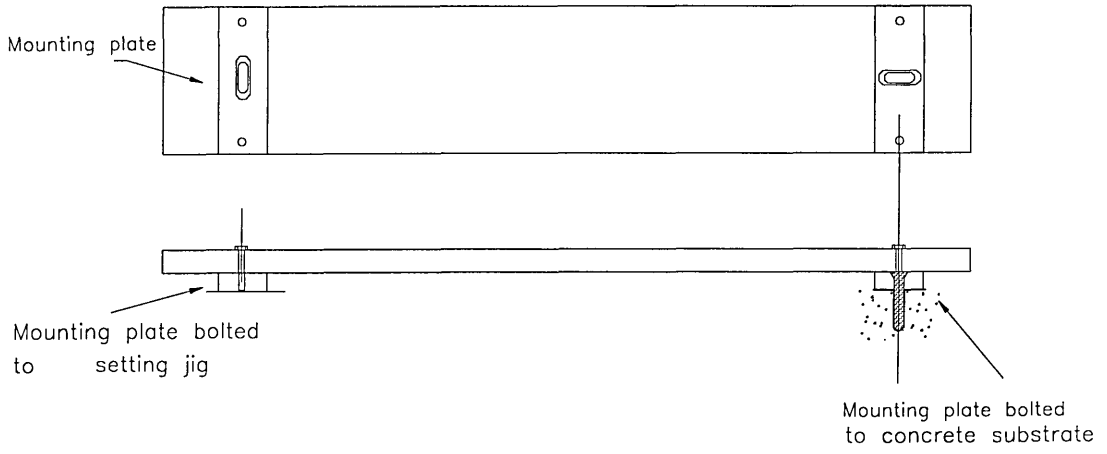

(a)

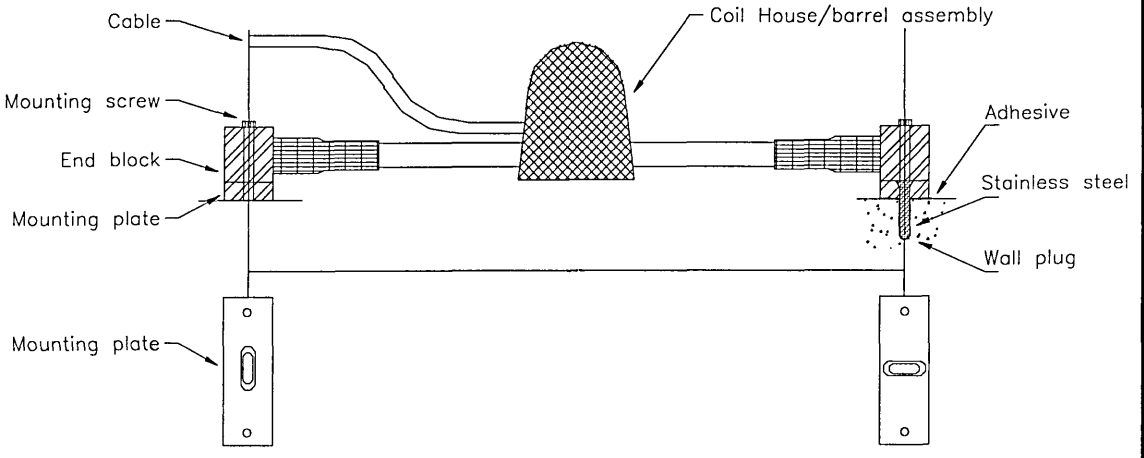

(b)

Figure 3.2 Vibrating wire surface gauge (type TSR/5.5/SWP) with bolted connections (a) Setting jig (b) Gauge in position

(i) The position and orientation of the gauge was marked on the substrate concrete. A scabbling bit was used to remove the irregularities on the substrate concrete to give a smooth surface onto which the mounting plates were attached.

(ii) The position of one hole was marked on the substrate concrete and a 6mm diameter hole was drilled to a depth of 25mm. A wall plug was then inserted in the drilled hole and a drilling jig was fixed securely by means of a woodscrew. The drilling jig was used to accurately locate the position of the second drilled hole.

(iii) A second hole was then drilled through the bushed hole in the free end of the drilling jig.

(iv) The drilling jig was removed and a wall plug was inserted into the second hole.

(v) A pair of mounting plates was fitted to a setting jig [see Figure 3.2 (a)] with M5 screws. The plates were cleaned and degreased. An adhesive was then applied to the surface of the plates and around the wall plugs in the substrate concrete.

(vi) The mounting plates were then fixed to the substrate with two stainless screws. Once the adhesive had cured, the setting jig was removed.

(vii) The vibrating wire surface gauge was then removed from its transport plate and loosely fixed to the mounting plates. The gauge cable was attached to a portable strain meter to monitor the gauge throughout the fixing operation. Both cap screws in one end block were progressively tightened, ensuring that the gauge barrel assembly rotates freely in the end blocks.

(viii) The second end block was gently pulled and set to the required datum reading. The second two mounting screws were then tightened, again ensuring that the gauge barrel assembly is free to rotate in the end blocks. It was important that

the tone of the vibrating wire was pure and sustained at this stage and the gauge reading returned to an acceptable datum reading [see Figure 3.2 (b)].

(ix) The gauge cable was then protected with armoured trunking to enable the cable to safely exit the repair patch without the risk of damage. The cable was then carried along the main trunking to the data logger which scanned the gauges at regular intervals and stored the readings in the field.

(x) The substrate gauge was then covered with a stiff polystyrene cover to isolate the substrate concrete gauge from the repair material. Polystyrene was used since a stiffer material would restrict the substrate concrete from deforming freely.

3.2.2.2 Measurement of steel reinforcement strain in the field

The redistribution of strain to the steel reinforcement was also monitored by means of a surface strain gauge, type TSR/5.5/SWP, securely fastened to the reinforcement by welding custom made mounting plates to the reinforcement, as shown in Figures 3.3 (a) and (b).

The gauge was tensioned to a datum frequency during the bolting operation to the mounting plates, as shown in Figure 3.3 (c). Any deformation in the steel reinforcement results in a change in the frequency of the wire thus enabling the strain in the steel to be obtained. An end view of a typical gauge attached to the steel reinforcement is given in Figure 3.3 (d). A full description of this procedure is as follows:

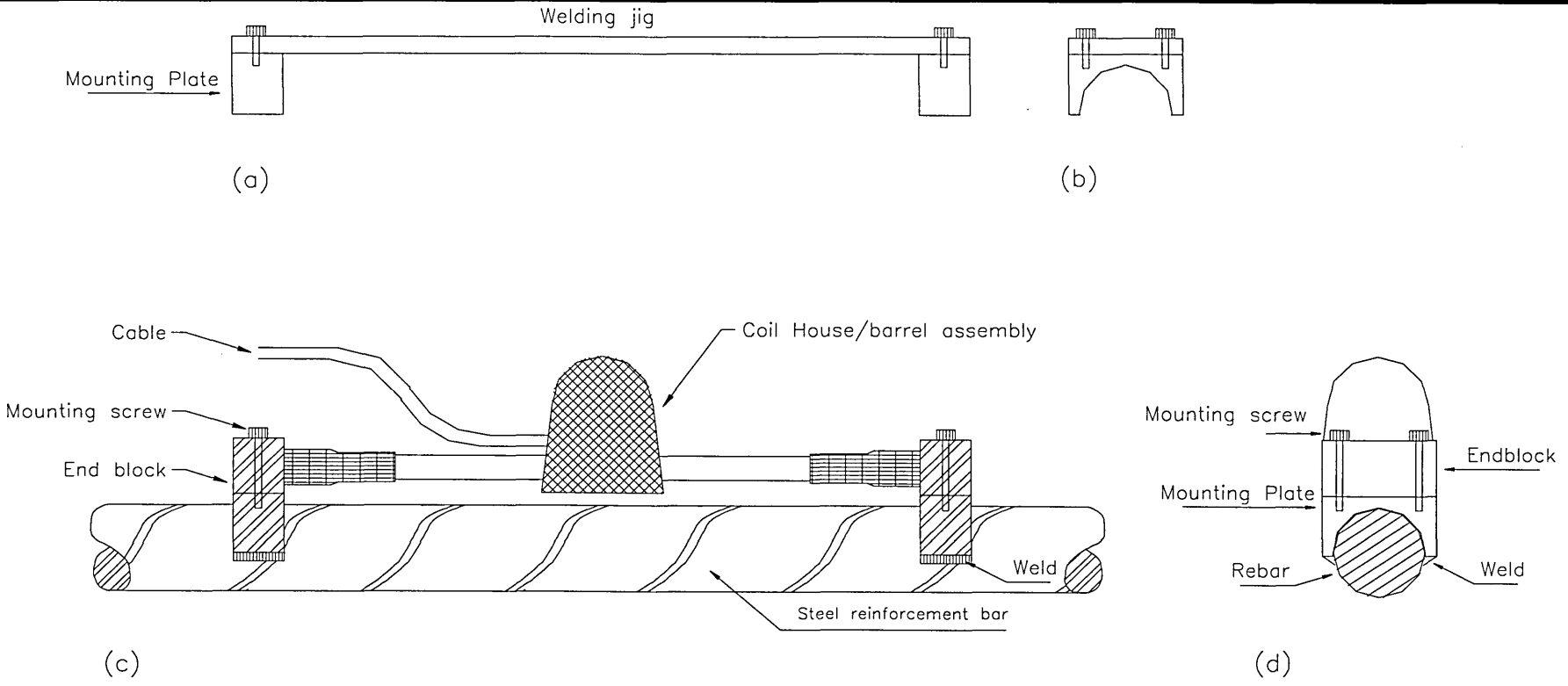

Fig. 3.3 Measuring of steel reinforcement strain

(a) Elevation and (b) end view of welding jig with mounting plates

(c) Elevation and (d) end view of gauge attached to steel reinforcing bar

(i) The steel was cleaned and the position of the gauge was marked on the reinforcement

(ii) Two custom made mounting plates were bolted to a welded jig [see Figure 3.3 (a)] which accurately spaces the plates apart. The welding jig was then securely fastened to the steel reinforcement by means of some cable ties.

(iii) The mounting plates were then spot welded to the steel reinforcement. The cable ties and welding jig were then removed.

(iv) The gauge was then fitted to the mounting plates as described in section 3.2.2.1 (vii) to (ix) [see Figure 3.3 (c) and (d)].

3.2.2.3 Measurement of repair material strain in the field

The strain in the repair material was measured by means of an embedment gauge, type TES/5.5/SWP. Gauges of this description are supplied pre-tensioned, hence they do not need to be set to the datum frequency at installation. These gauges were located in the body of the repair material between the steel reinforcement. As before, any deformation in the repair material resulted in a change in the pre-set frequency of the gauge wire, therefore, the strain can be obtained from Equation 3. 1. A full description of application technique is as follows:

(i) The position and orientation of the gauge was marked on the adjacent steel reinforcement

(ii) Two support bars were tied to the steel reinforcement parallel to each other and spaced approximately 85mm apart (see Figure 3.4). These support bars were

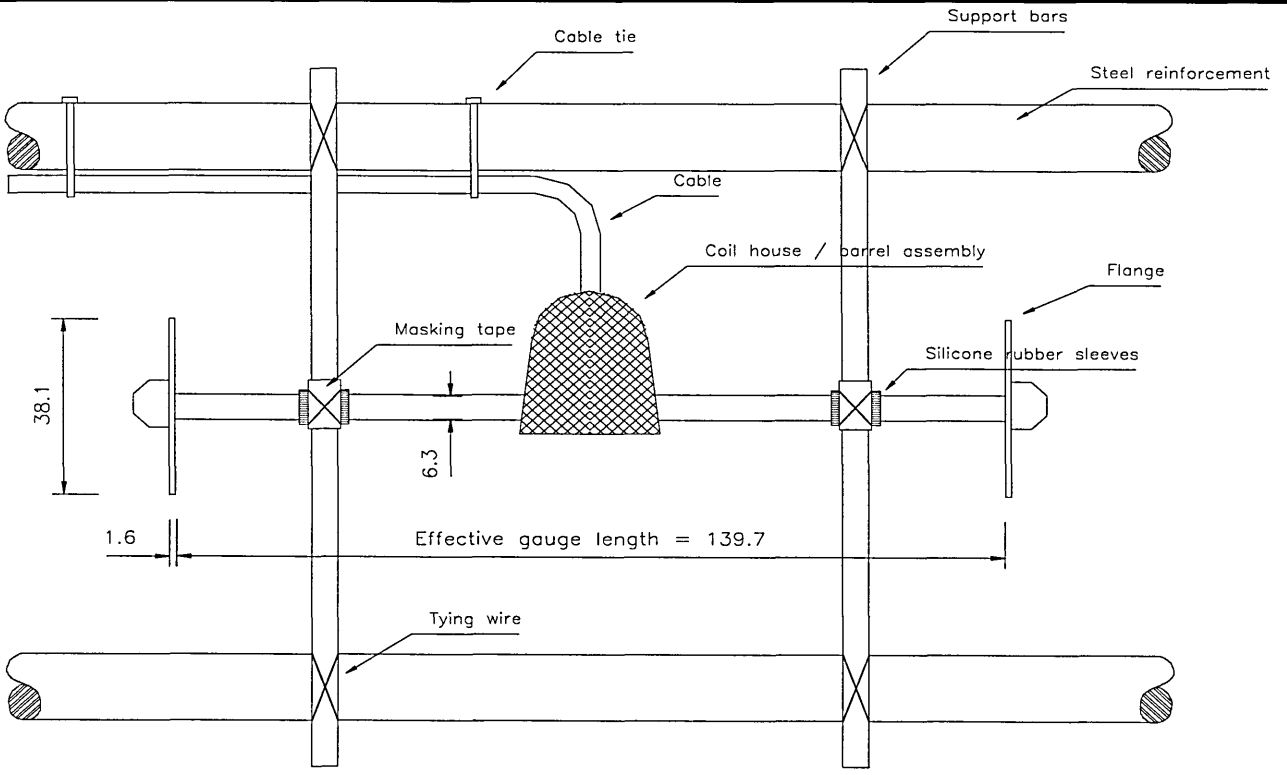

Figure 3.4 Measuring of repair material strain: embedment gauge attached parallel to the steel reinforcement

placed at right angles to the gauge to support it in the correct position and orientation

(iii) The gauge was then placed against the support bars. The flanges at each end of the gauges were kept clear of obstructions.

(iv) Masking tape was then wrapped around the support bars where the gauge barrel touches. The gauge barrel itself was fitted with silicone rubber to cushion the gauge barrel when it was tied to the support bars.

(v) The gauge was then securely fixed to the support bars by means of soft tying wire so that it could not alter during application of the repair material. The gauge reading was monitored throughout the fixing operation by means of a portable strain meter.

(vi) The gauge cables within the repair patch were fastened parallel with the steel reinforcement for protection. Armoured cable was then attached to the cable to protect it at the exit point of the repair patch.

3.2.3 Details of the data logging equipment in the field

Strain readings from the vibrating wire strain gauges were automatically recorded in the field at a central location. This was achieved using a GT1192 Universal Data Logger, supplied by Gage Technique Ltd. This instrument can monitor and store data from a wide range of transducers including the vibrating wire strain gauge. Data was stored in the internal memory of the logger, or in optional (or backup) replaceable memory cards.

A compatible PC was used to program the data logger, after which the computer link was removed. The logger then monitored the gauges and stored the data in the field, with power being supplied by an external 12 volt battery. The logger could accommodate up to ten differential connections, i.e. strain and temperature measurements, or thirty single ended connections (strain measurements only), or a combination of both. The number of gauges being recorded could be increased by attaching a maximum of three expansion modules to the data logger, each expansion module having the same capacity as the data logger (ten differential or thirty single ended connections). The data logger, expansion module and accessories in position in the field are shown in Figure 3.5. The downloading of stored data from the data logger is shown in Figure 3.6.

The logger could record data at any time by programming the frequency of monitoring, the channel and the sensor to be read. Scan rates and channel selection could be altered automatically during periods of particular interest. The internal memory capacity was 11,000 readings, but was expanded using a memory card, allowing up to a further 256,000 readings to be stored. The readings were downloaded to a computer and analysed, as the data logger is compatible with spreadsheet and graphical application packages. The logger was housed in a steel container to protect it from the environment. Extra protective covers were provided in locations where the logger was particularly vulnerable.

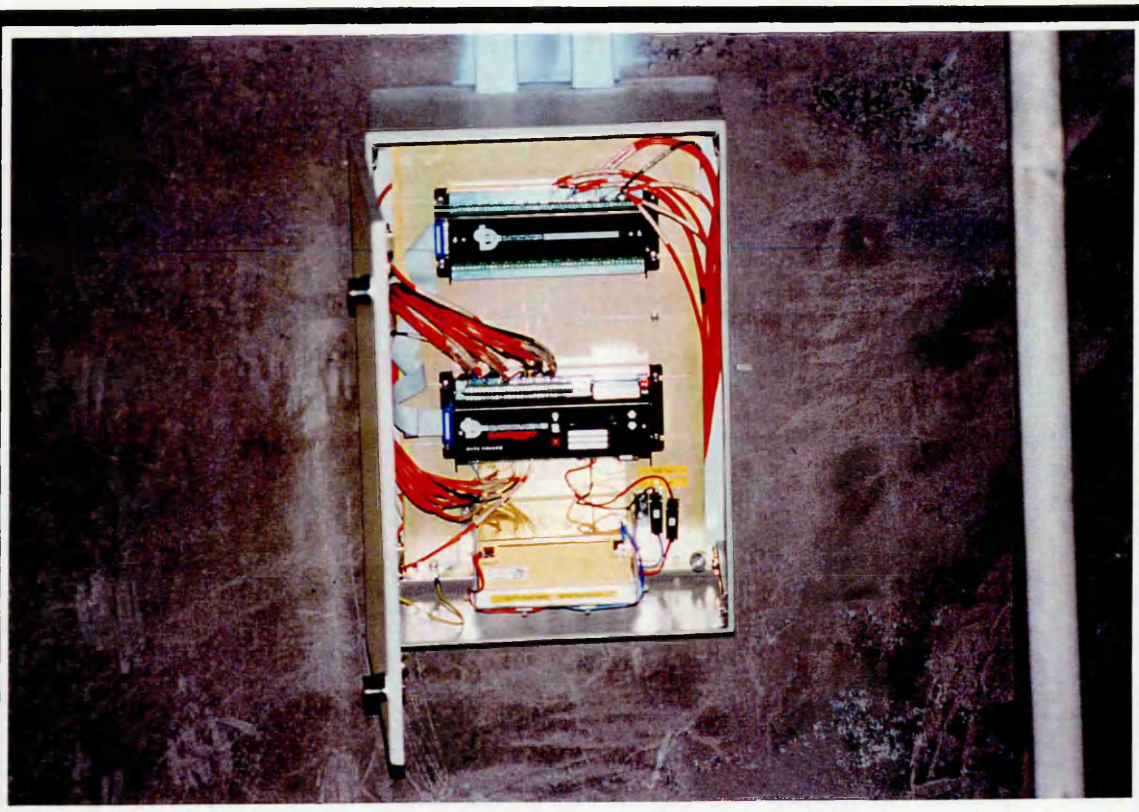

Figure 3.5 View of (from top) expansion module, data logger and 12 volt battery installed in a protective container on site (Location: Lawns Lane Bridge)

Figure 3.6 Downloading of stored information from data logger using a laptop computer (Location: Sutherland Street Bridge)

3.3 DETAILS OF LABORATORY MONITORING EQUIPMENT

3.3.1 Electrical resistance strain gauges

A brief history of the electrical resistance strain gauge is given by Chalmers [11]. In 1856 it was first discovered that the resistance of an electrical conductor changed when it was stretched, but it was not until the late 1930's that the principle was applied by using a grid of fine wire bonded to a test surface as a means of measuring strain. Electrically conductive materials posses a strain/resistance relationship defined as the relative electrical resistance change of the conductor to the relative change in its length. This strain sensitivity is a function of the dimensional changes which take place when the conductor is deformed elastically.

Two different types of electrical resistance gauges were employed in the laboratory on repaired reinforced concrete beams. The strain in the steel reinforcement was measured by means of a 6mm long foil backed strain gauge which was attached to the steel reinforcement with an adhesive. The strain in the repair material was measured by means of an 30mm gauge embedded in the material (see Chapter 7). The deformation in both of these gauges was measured by means of a digital strain indicator.

3.3.1.1 Measurement of strain in steel reinforcement

Type CEA-06-250UN-120 electrical resistance strain gauges, supplied by Micro Measurements Group, USA, were used to monitor the redistribution of stress to the steel reinforcement. These are general purpose strain gauges which are particularly suited to

long term installation. A full description of the installation procedures is given below [12].

(i) The position of the gauges on the steel was marked and any irregularities on the surface of the steel were removed with a smooth file. The final finish was then achieved by use of 220-400 grit emery paper.

(ii) The position of the gauge was accurately marked and the gauged area was clinically cleaned with cotton tipped applicators and a degreaser.

(iii) The gauge to be installed was placed on a clean glass surface. Cellophane tape was tacked to the glass behind the gauge and wiped forward onto the gauge. The tape was then lifted at a shallow angle (about 45 degrees to the glass surface) bringing the gauge with it.

(iv) The gauge/tape assembly was positioned so that the alignment marks on the gauge were over the layout lines. Once alignment was correct, one end of the tape was firmly fixed down.

(v) The free end of the tape was then lifted at a shallow angle until the gauge was free of the surface. Both the gauging area and back of gauge were coated with an adhesive.

(vi) The gauge/tape assembly was then wiped over the adhesive in a single stroke, with care being taken exude as much of the adhesive as possible.

(vii) A silicone gum pad was placed over the gauge and a clamping pressure of approximately 85 kN/m^2 was applied for 24 hours.

(viii) The lead wires were then soldered to the gauge terminals and the resistance of the gauge monitored to ensure full contact. A protective coating was then applied to the gauge.

The location of the gauges on the steel reinforcement within the repair patch (along with the abbreviations used) are given in Chapter 7, Section 7.2.3.1.

3.3.1.2 Measurement of repair material strain

Type PML-30 electrical resistance strain gauges, supplied by Tokyo Sokki Kenkyujo Co., Japan, were used to monitor the strain within the repair materials. This gauge has been especially designed for the measurement of interior strains in concrete (or repair materials) by simply embedding the gauge. It consists of a standard wire gauge, to which 2 metres of vinyl lead wires are attached. The gauge and lead wires are hermetically sealed between thin resin plates, completely waterproofing the unit. The gauge is coated with a coarse grit to eliminate bond failure with the repair material [13]. The gauge length is 30mm and the gauge factor (or strain sensitivity) is approximately 2.10.

The gauges were placed centrally at mid-span in the repair patch as the work progressed at three levels - (i) at the concrete substrate/repair material interface, (ii) at the steel reinforcement level and (iii) at the soffit of the repair.

Full details of these gauges along with the abbreviations used are given in Chapter 7, Section 7.2.3.2.

3.3.2 Digital strain indicator

The digital strain indicator (Model P-3500) supplied by Micro Measurements Group, USA is a portable, battery-powered precision instrument for use with electrical resistance strain gauges. The P-3500 accepts full, half and quarter bridge inputs. The digital strain indicator was connected to an SB-10 switch and balance unit which provided an output from ten channels of strain gauge information from one digital strain indicator. This equipment allowed strain readings to be obtained from both types of electrical resistance strain gauges used in the laboratory study, type CEA-06-250UN-120 on the steel reinforcement and type PML-30 embedded in the repair material.

These gauges were monitored on quarter bridge inputs. The output was directly in microstrain.

3.3.3 Extensometer gauges

Demec extensometer of gauge length 100mm was used to measure the surface strain on the substrate concrete. Demec points were accurately positioned on both faces of the beam by means of a 100mm setting bar.

Full details of this monitoring equipment are given in Chapter 7, Section 7.2.3.3.

CHAPTER 4

REPAIR AND INSTRUMENTATION OF GUNTHORPE BRIDGE

4.1 INTRODUCTION

Gunthorpe Bridge is a three span, reinforced concrete arch bridge spanning the River Trent at Gunthorpe, Nottinghamshire. It was built in 1927 to replace an old iron toll-bridge due to an increase in heavy traffic using the bridge. The central arch in the bridge spans 38.1m, while the two side arches spans 30.9m. Each of these three arches contain four ribs. A view of Gunthorpe Bridge is shown in Figure 4.1.

Over the past number of years, the lateral beams spanning between the arch ribs began to show considerable signs of reinforcement corrosion (see Figure 4.2). The scale of deterioration made this bridge suitable for the LINK project, hence permission was obtained from Nottinghamshire County Council to use Gunthorpe Bridge for research purposes. Repairs carried out at this site were confined to half of the south span (flood plain side) and the south abutment (Figure 4.3). Attention was concentrated on the deteriorating beams and the south abutment; no repairs were carried out on the bridge deck and arch ribs.

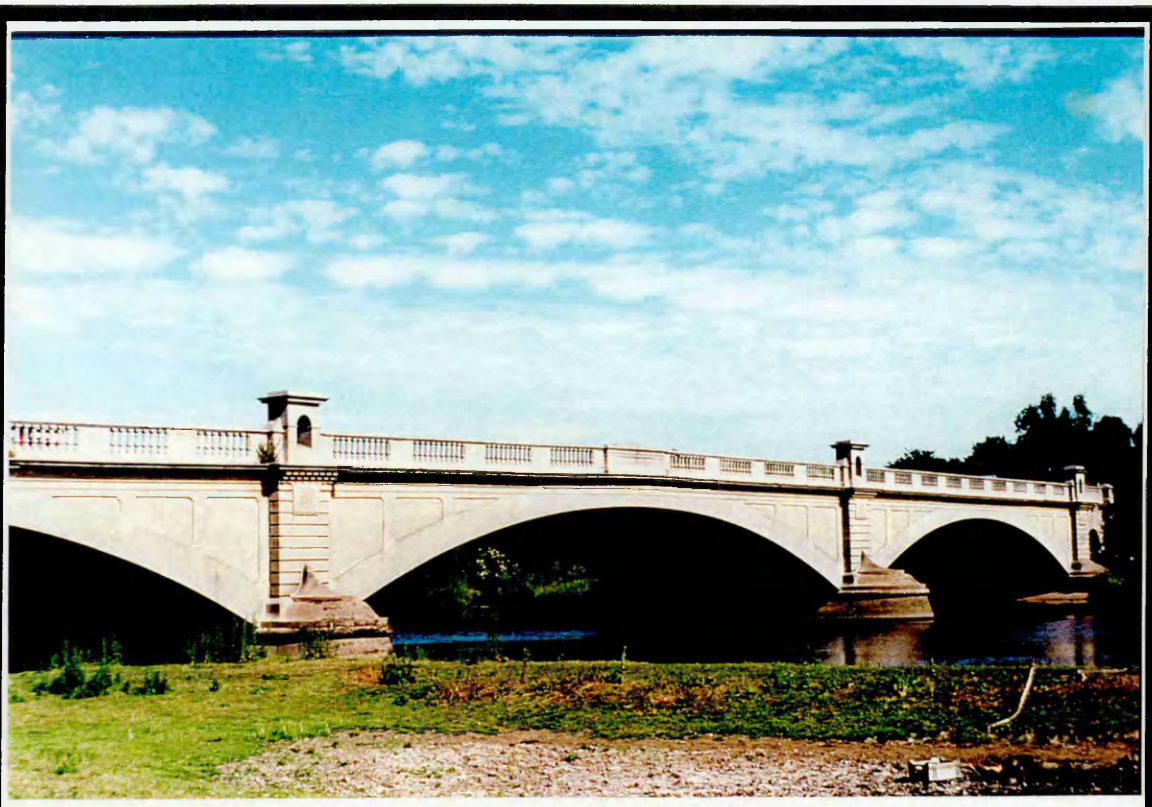

Figure 4.1 Gunthorpe Bridge, Nottinghamshire

Figure 4.2 Typical deteriorating lateral beam at Gunthorpe Bridge

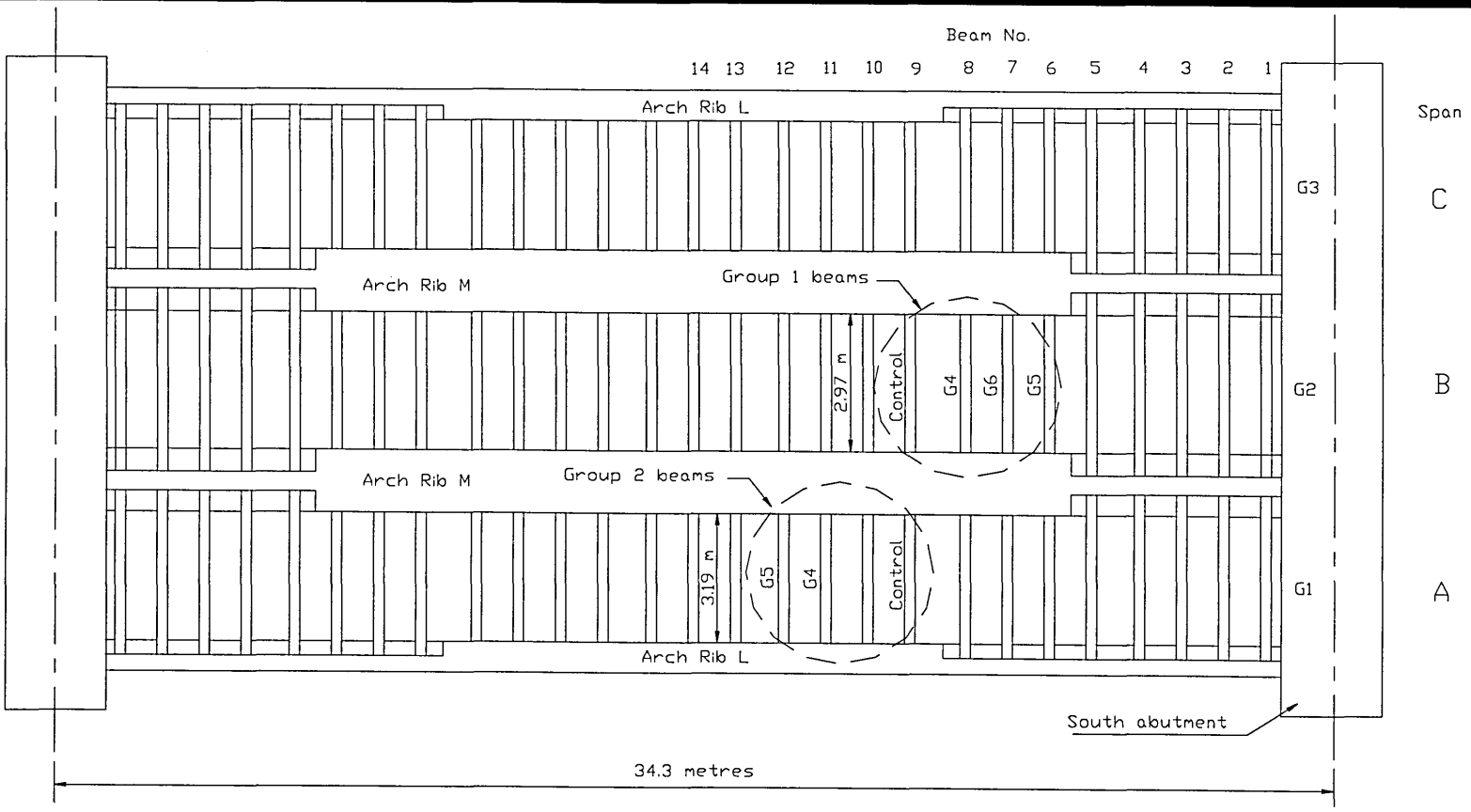

Figure 4.3 Location of instrumented repairs on south span at Gunthorpe Bridge
Group 1 - beams B6, B7, B8, and B9 (materials G5, G6, G4 and control respectively)
Group 2 - beams A9, A11 and A12 (control, materials G4 and G5 respectively)

4.2 DETAILS OF CONCRETE REPAIRS AT GUNTHORPE BRIDGE

4.2.1 Initial surveys

A photographic survey of typical deteriorated elements was taken prior to any work starting on the bridge, to record the state of the bridge before repair. Other initial surveys which were carried out by UK Analytical Ltd. included a half cell potential survey and a visual defects survey on the elements selected for detailed investigations. Drilling of the same elements for chloride analysis was carried out by V.A. Crookes (Contracts) Ltd. and analysed by UK Analytical Ltd. A specialist coring company, D Drill Ltd., was employed for coring of selected elements. The cores were tested in the laboratory to determine the elastic modulus of the substrate concrete.

4.2.2 Installation of monitoring equipment and application of repair in the south abutment

4.2.2.1 Preparation of the south abutment

Three similar areas on the abutment were selected for repair, as shown in Figure 4.4. Each repair area was approximately 2.3m x 1.8m in elevation. Repairs were carried out in these locations to determine the long term performance of different spray applied repair materials to unpropped compression members.

The extent of each area was determined from the results of the half cell survey and marked with a saw cut on the abutment. Removal of deteriorated concrete was carried out by V.A. Crookes (Contracts) Ltd. using mechanical equipment. The average depth

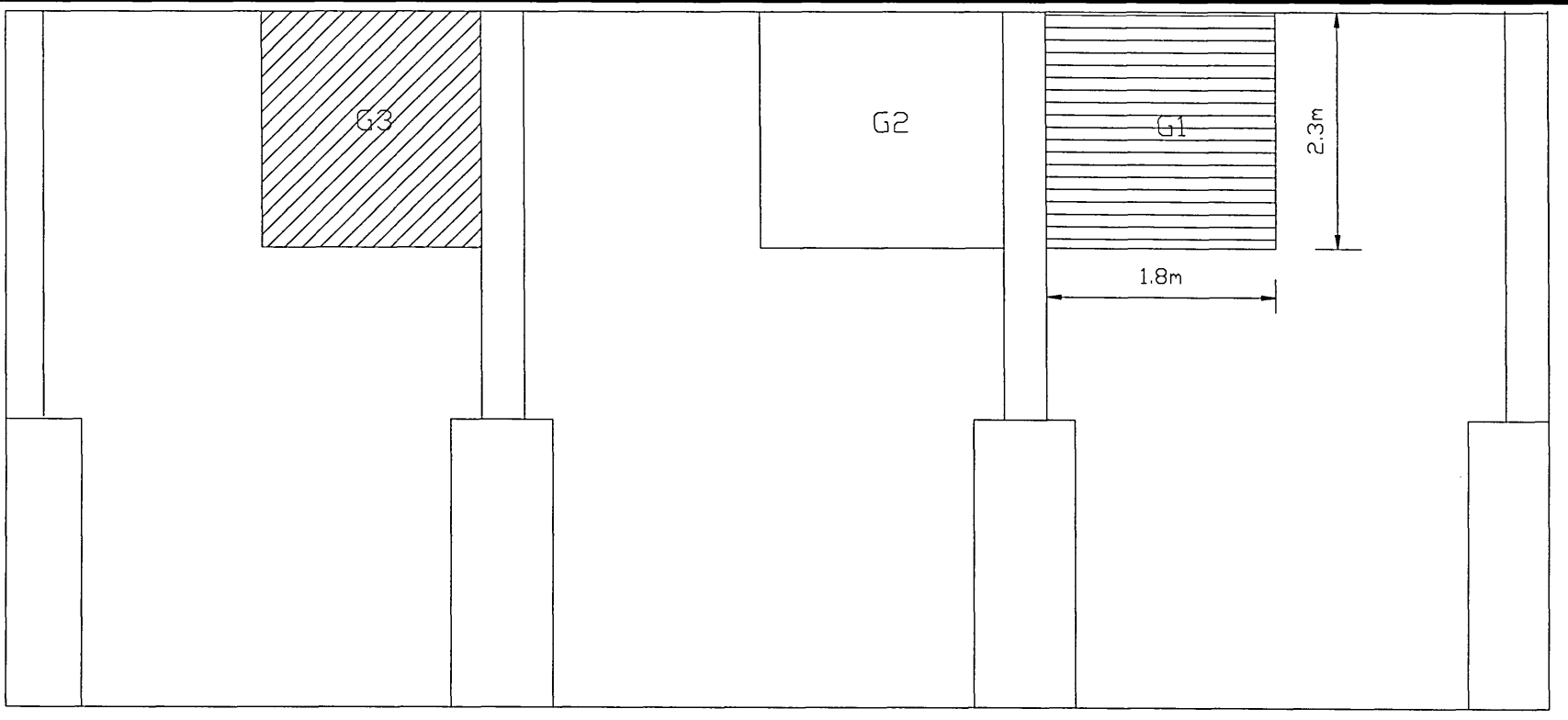

Figure 4.4 Elevation of south abutment at Gunthorpe Bridge showing areas selected for repair

of each repair was 140mm. Depth of carbonation was also monitored as the work progressed.

Two of the repair materials applied on the south abutment at Gunthorpe Bridge were supplied by SBD Ltd. and Flexcrete Ltd., whereas the third material consisted of a conventional sand and cement mixture (see Section 4.3.1 for a full description).

All exposed steel was grit blasted to remove any loose rust before a primer was applied. A steel reinforcement protector supplied by Flexcrete Ltd. was used as primer. This was a two component material consisting of a cementitious powder and a polymer dispersion which react together to passivate the steel. All the grit blasted steel received two coats of the primer.

The vibrating wire strain gauges were then installed as shown in Figure 4.5. Mounting plates, onto which the gauges would be fixed, were attached to the cut-back substrate surface and the adjacent concrete surface as described in Section 3.2.2.1. Mounting plates were also welded to the steel reinforcement to accommodate gauges for measuring steel reinforcement strain, as described in Section 3.2.2.2. Finally, the support bars required to attach the embedment gauge were also installed, as described in Section 3.2.2.3.

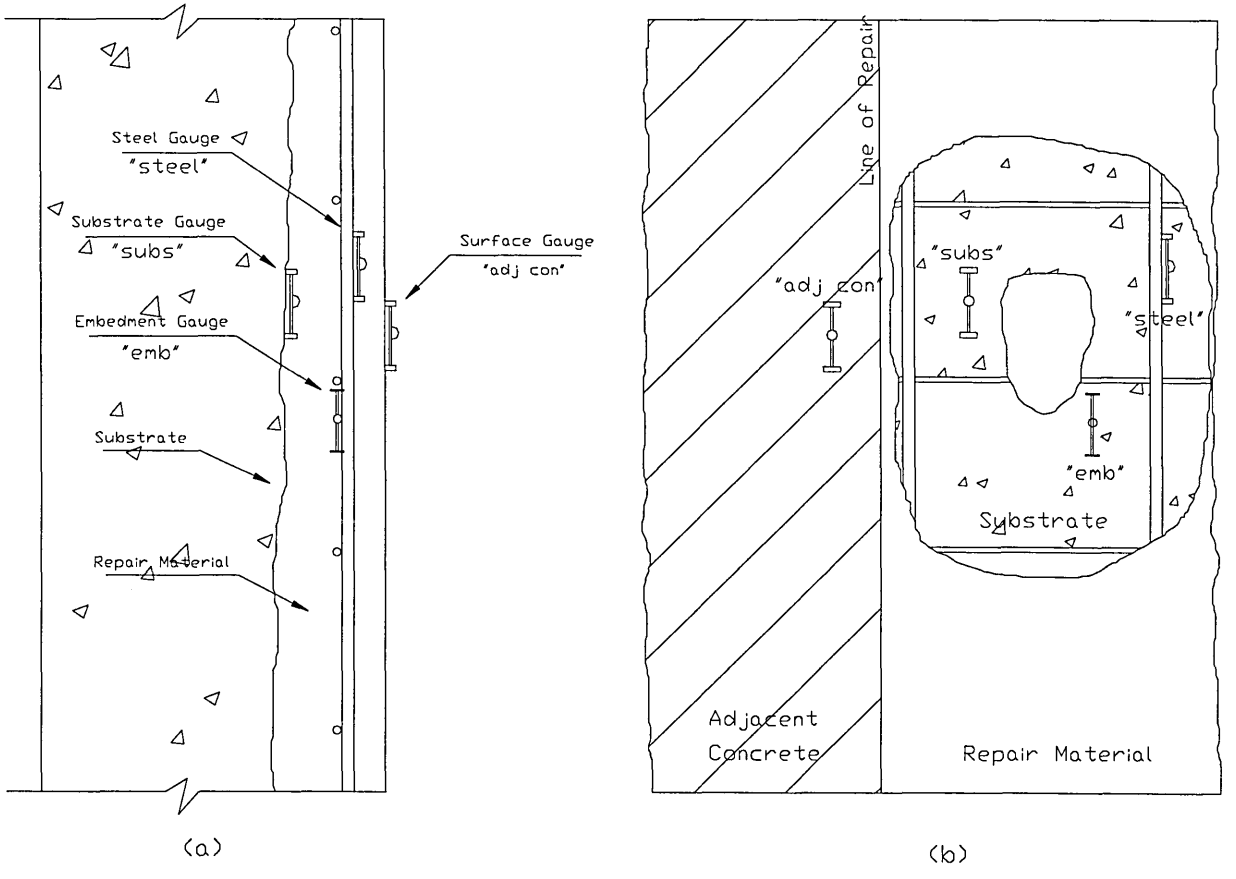

Figure 4.5 Position of gauges within a typical repair patch at Gunthorpe Bridge
(a) cross-section through abutment and
(b) elevation of repair material and adjacent concrete

4.2.2.2 Details of instrumentation and repair patches in the south abutment

Three vibrating wire strain gauges were installed in each of the repair material patches in the south abutment. One gauge each was attached on the cut-back substrate surface, steel reinforcement and repair material, as described in the previous section. The repairs were instrumented in such a way that information could be obtained on the redistribution of stress within the repair patch. A fourth gauge was installed on the surface of the adjacent concrete to monitor any redistribution of strain which may occur to that area. Figure 4.5 (a) shows a cross section through a typical repair indicating the location of the gauges within the repair. Each gauge (for reference purposes) was identified by an abbreviation of the position of the gauge in or adjacent to the repair patch, i.e. the gauge on the cut back concrete substrate surface was identified as "subs", the gauge on the steel reinforcement was identified as "steel", the gauge embedded within the repair material was identified as "emb" and finally, the gauge on the adjacent concrete was identified as "adj con". Figure 4.5 (b) shows an elevation of the repair, again showing the position of the gauges within the repair and on the adjacent concrete. The three internal gauges (i.e. attached to the substrate concrete, steel reinforcement and eventually embedded in the repair patch after application of the repair material) are also shown in Figure 4.6.

Application of sprayed (gunite) repairs on the abutment were carried out by Axiom Ltd., an independent specialist in the application of sprayed materials, as shown in Figure 4.7. The concrete substrate was saturated before the repairs were applied to reduce the

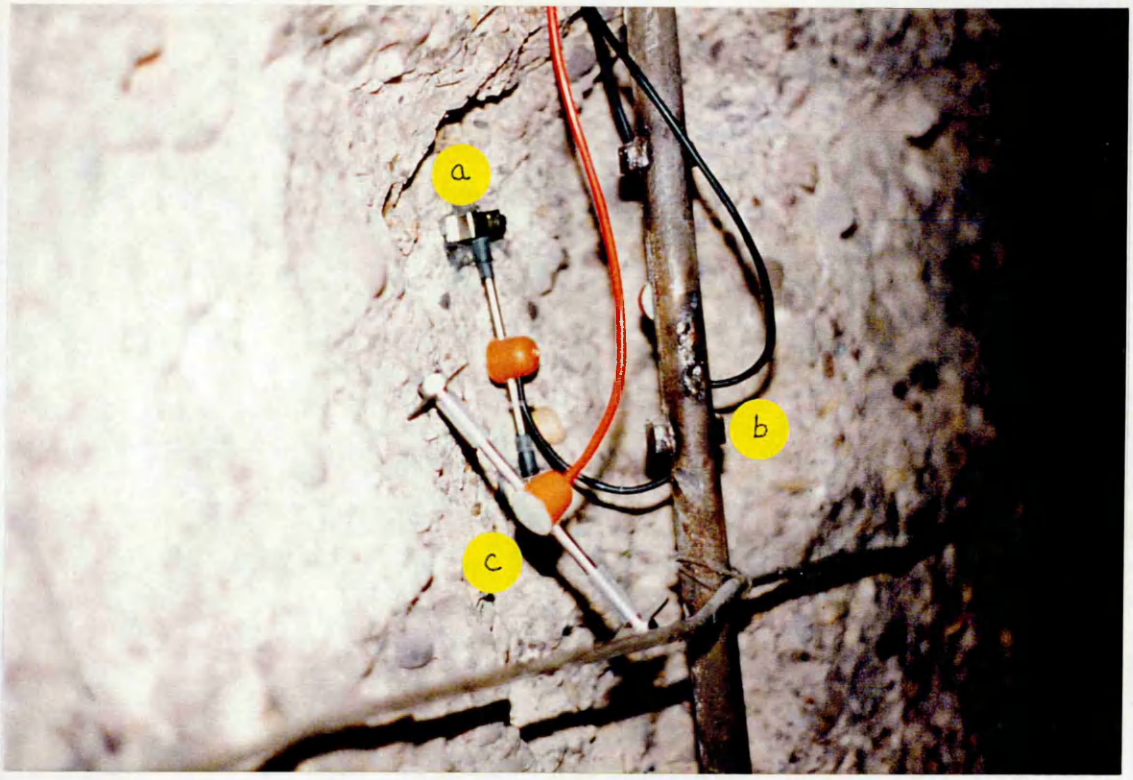

Figure 4.6 Configuration of vibrating wire strain gauges within a typical spray applied repair patch at Gunthorpe Bridge: (a) gauge attached to substrate concrete; (b) gauge attached to steel reinforcement; (c) gauge embedded in repair material (still to be permanently fixed)

Figure 4.7 Application of a spray applied repair patch (material G1) on the south abutment at Gunthorpe Bridge

absorption of free water from the repair material into the substrate. In order to minimise the risk of trapping rebound material, the spray was applied upwards starting from the bottom of the repair patch. The repair was built steadily in incremental thickness to the final required depth. A flash coat, which is the final coat with increased water content to increase workability, was then applied to assist with the finishing operations.

Repair materials G1 and G3 (see Section 4.3.1) were finished by levelling the flash coat with a wooden float and smoothening with a damp sponge. Floating was not possible for material G2 (see Section 4.3.1) due to its very low workability immediately after application. Material G2 was trimmed instead using a wooden float to obtain a level surface.

The abutment was kept in an unpropped state during the application of repairs.

4.2.3 Installation of monitoring equipment and application of repair in the lateral beams

4.2.3.1 Preparation of the lateral beams

Figure 4.3 shows the locations of the lateral beams spanning between the arch ribs at Gunthorpe Bridge. Five beams were repaired with hand applied materials to enable data on the long term performance of hand applied repairs to unpropped flexural members to be obtained.

Breaking out of deteriorated concrete on the lateral beams was again carried out by V.A. Crookes (Contracts) Ltd. using mechanical means. Deteriorated concrete was removed along the full length of the beams under test and to a depth of at least 25mm behind the steel (130-140mm total depth). The exposed steel was grit blasted to remove any loose rust and then primed as described in Section 4.2.2.1.

Custom-made mounting plates were welded to one steel reinforcing bar in each of the repair patches, as described in Section 3.2.2.2. Where applicable, support bars were also placed to assist in the installation of an embedment gauge, as described in section 3.2.2.3. Preparation and drilling for other gauges on the web of the beams and for protective covers to the gauges was also done at this stage. The majority of the strain gauges, however, were applied on the surface (web) of the beams, these were installed after the repairs were carried out.

4.2.3.2 Details of instrumentation and repair patches on the lateral beams

The location of the monitored beams on the south span at Gunthorpe Bridge is shown in Figure 4.3. A total of seven lateral beams were instrumented with vibrating wire strain gauges. They were classified into two groups; group one consisted of four monitored beams [a control (unrepaired) beam and three repaired beams]. Group 2 consisted of three monitored beams [one control (unrepaired) beam and two repaired beams]. Group 2 was restricted to three monitored beams due to a limit of 20 channels on the data logger/expansion module. Generic repair materials from the Flexcrete range

of hand applied repair products were used on the lateral beams at Gunthorpe Bridge (details of the repair materials are given in Section 4.3.2).

The selected positions of the strain gauges on the beams were influenced by the shape of the bending moment diagram of an encastre beam. Strains were measured centrally on the web and soffit of the beam together with the steel reinforcement in the tension zone of the beam. Figure 4.8 shows an enlarged elevation and section through one of the beams. Four surface gauges (type TSR/5.5/SWP) were installed along the web of the beams to give a strain profile. One of the gauges also monitored the atmospheric temperature. Two of the surface gauges were strategically positioned at the substrate/repair material interface to record the strain at that point. A fifth strain gauge (type TSR/5.5/SWP) was positioned on the soffit of the beams to measure the extreme fibre strains. The steel reinforcement strain was measured on one reinforcing bar only (again due to a maximum of twenty channels being available). Strain gauges of similar construction to those used for surface mounting were used.

The patch repairs on the lateral beams were carried out by V.A. Crookes (Contracts) Ltd. Repair materials G4-G6 (see section 4.3.2) were mixed on site using a Pennine barrel mixer until the required consistency was obtained. These materials were then applied by hand (see Figure 4.9) to a depth of approximately 10mm from the finished surface. The final coat was applied a few hours later when the original material had set slightly. The finished surface was obtained by levelling with a wooden float and screeding with a damp sponge. Shuttering was only used along the soffit of the beams, thus making these repairs very economical for small volume patches. Figure 4.10

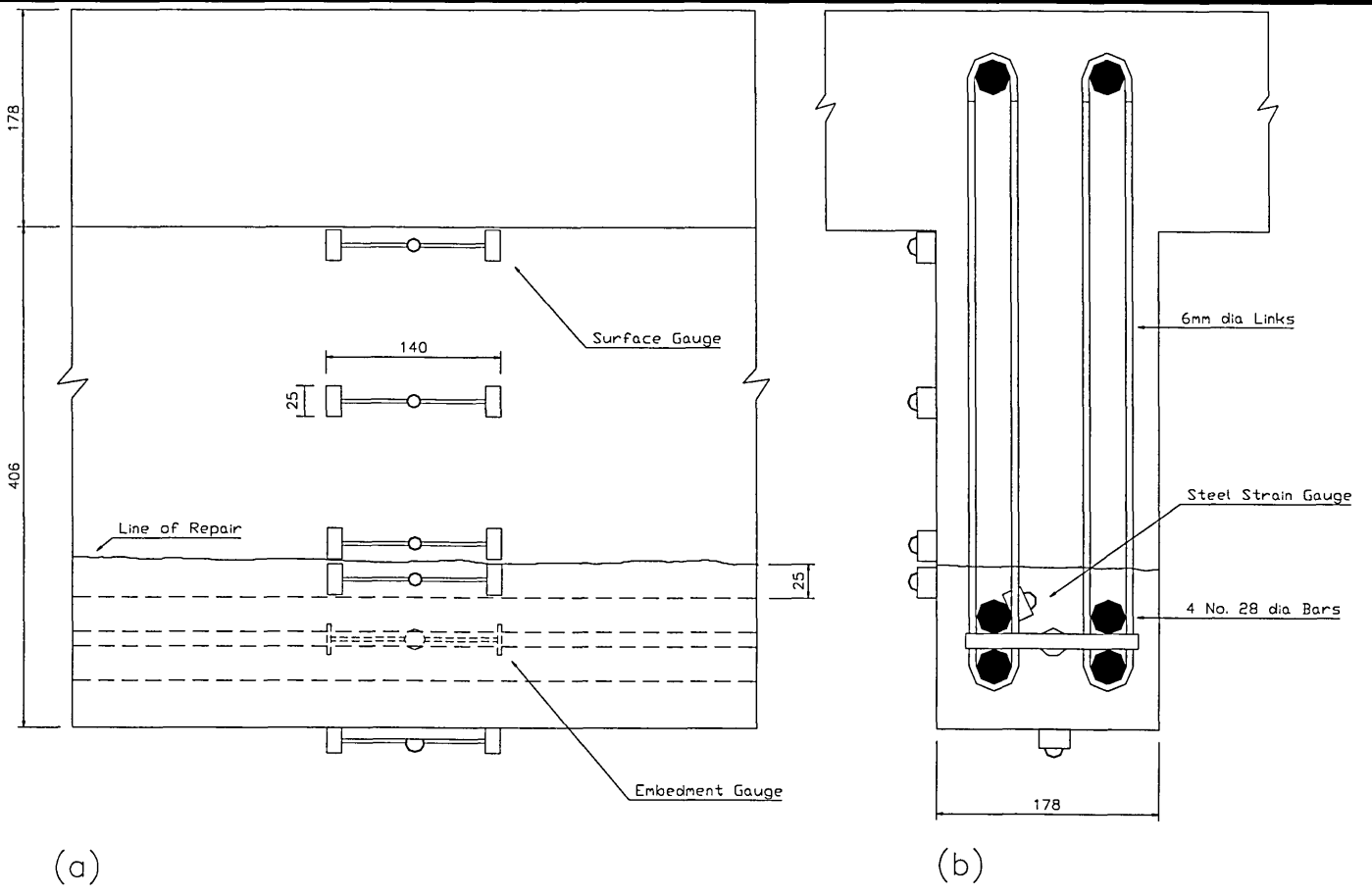

Figure 4.8 Position of gauges on a lateral beam at Gunthorpe Bridge (a) elevation and (b) cross-section

Figure 4.9 Application of hand applied repair material G4 on beam A11 at Gunthorpe Bridge

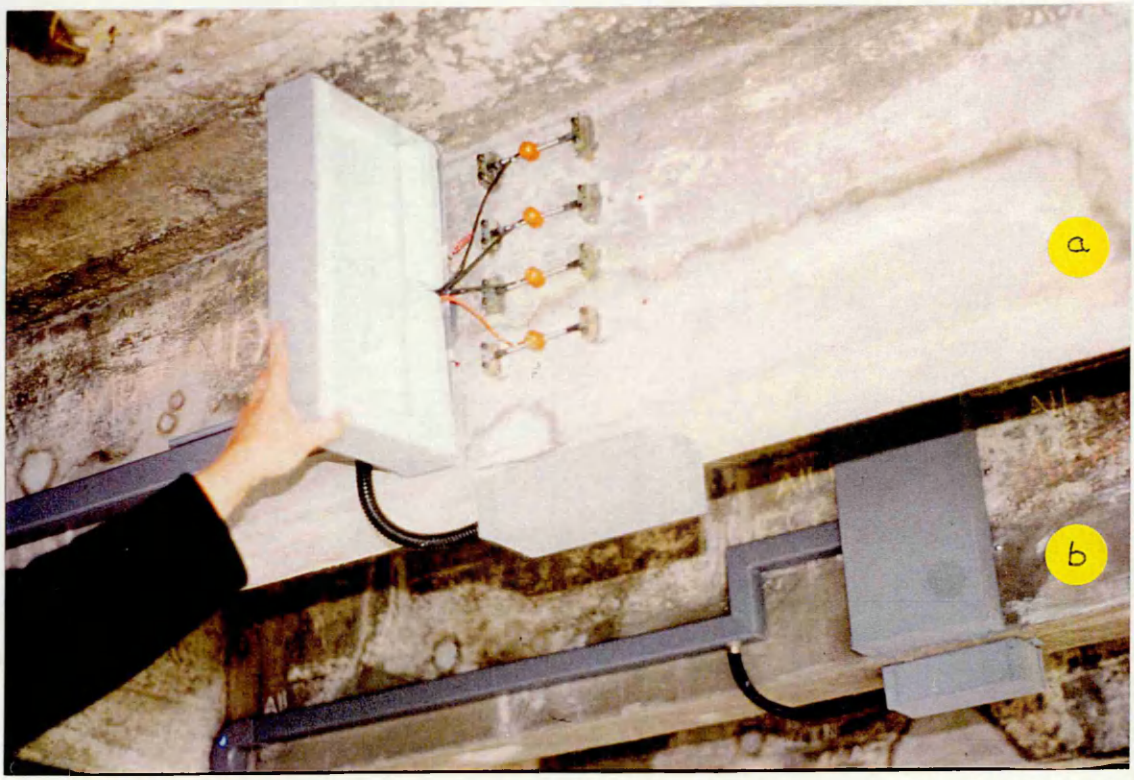

Figure 4.10 View of completed repairs to lateral beams, monitoring equipment and protective covers: (a) material G5, (b) material G4

shows a view of the repairs complete with monitoring equipment, trunking and protective covers. PVC trunking carried the gauge cables to the central logging system where the gauges were automatically scanned at regular intervals.

4.3 DETAILS OF REPAIR MATERIALS

4.3.1 Spray applied repair materials

Three materials (labelled G1, G2 and G3) for spray repairs were used at Gunthorpe Bridge. All materials vary in composition. Two of the materials (G1 and G2) are commercially available, whereas material G3 is a mixture of conventional sand and cement, also applied by the dry spray process. Spray repairs were applied by an independent specialist contractor. A detailed description of the materials is given below.

Material G1 is a single component polymer modified cement based concrete mix, supplied by SBD Ltd [14]. It contains inert limestone aggregates and dust suppressants. The formulation has been designed specially for dry process spray application to give high early strength, reduce rebound and maximise application thickness. The material consists of rapid hardening Portland cement [4] (minimum cement content of 400 kg/m^3) and 5mm maximum sized graded limestone aggregate (clause 1702 of DoT Specification for Highway Works, Part 5). Microsilica and a copolymer are also incorporated in the mix.

This material achieves a 28 day compressive strength of 60 N/mm^2. It has a dry density of 2250 kg/m^3 and modulus of elasticity of 31.1 kN/mm^2.

Material G2, supplied by Flexcrete Ltd. [15], is a special blend of rapid hardening Portland cement [4], microsilica, fibres, chloride-free admixtures and the latest generation spray dried styrene acrylic copolymer which, when blended with a sharp washed medium grade concrete sand in accordance with BS 882 (1984) [5] produces a gunite for machine application using the dry process with physical characteristics similar to the base concrete.

Based on a gunite:sand ratio of 1:4 by weight and a water:cement ratio of 0.35-0.40, a compressive strength of 56.5 N/mm^2 is obtained at 28 days. The modulus of elasticity is 17.6 kN/mm^2. The density lies in the range 2200-2300 kg/m^3.

Material G3 is a laboratory designed mix comprising of ordinary Portland cement in accordance with BS 12 [4] and a medium grade sand in accordance with BS 882 (1984) [5]. It is used solely for the purpose of research to compare the performance of ordinary mortar mixes with commercial repair materials. The material was applied using the dry spray process, the water:cement ratio being controlled at the nozzle by an experienced operator.

4.3.2 Hand applied repair materials

Three different hand applied repair materials, all supplied by Flexcrete Ltd, were instrumented at Gunthorpe Bridge to determine their long term service performance in highway structures. Material G4 is a pre-packed three component system which only requires mixing on site. The other two materials (G5 and G6) are supplied as single component materials. These require only the addition of clean water on site. Details of these hand applied materials are as follows:

Material G4 is a three component heavy duty repair mortar. Part A comprises of a liquid dispersion of a styrene acrylic copolymer and admixtures (including a waterproofing agent). Part B, the powder constituent, is made up of ordinary Portland cement, fibres and 6mm down graded aggregate. Part C comprises of a 10mm size granite aggregate. The material achieves a compressive strength of 50 N/mm^2 and a modulus of elasticity of 24 kN/mm^2 at 28 days. The fresh density of the mixture is 2100 kg/m^3 [15].

Material G5 is a single component cementitious mortar - the powder being mixed with water on site. It consists of a spray dried styrene acrylic copolymer which complies with the Department Of Transport standard BD 27/86 [1] for the repair of highway structures. It incorporates the latest cement chemistry and consists of finely ground Portland cement with inclusions of sulphoaluminate cement, microsilica, fibres and other pozzolanic materials. It is, therefore, shrinkage compensated whilst the density is substantially lower than traditional concrete (approximately 1750 kg/m^3) at a recommended water:powder ratio is 0.14. It is a structural repair material achieving a

28 day compressive strength of 50 N/mm^2. The modulus of elasticity is 19.6 kN/mm^2 [15].

Material G6 is a single component, cementitious mortar requiring only the addition of clean water on site. It incorporates advanced cement chemistry, microsilica, fibre and styrene acrylic copolymer technology. This results in a rapid hardening mortar with enhanced polymeric properties. It has a low density of approximately 1250 kg/m^3 at a recommended water:powder ratio of 0.16. Material G6 has a compressive strength of 30 N/mm^2 and a modulus of elasticity of 11.5 kN/mm^2 at 28 days [15]

CHAPTER 5

REPAIR AND INSTRUMENTATION OF LAWNS LANE BRIDGE

5.1 INTRODUCTION

Lawns Lane Bridge is a three span reinforced concrete bridge which carries part of the M1 between junctions 41 and 42 in West Yorkshire. It was built in the mid 1960's and consists of insitu deck panels supported by prestressed beams, all of which are carried by reinforced concrete piers and abutments. Views of Lawns Lane Bridge are given in Figure 5.1.

A detailed investigation carried out by Harry Stanger, Consulting Materials Engineers, on behalf of the client, The Highways Agency, revealed that Lawns Lane Bridge was in need of substantial concrete repairs. The south piers needed to be demolished and were reconstructed, whereas the south and north abutments and the north piers required repair. This repair contract was awarded to M.J. Gleeson Group plc. The repairs were instrumented and monitored to gain an understanding of the interaction between the repair material and substrate as part of the LINK project.

A total of five different repair materials were applied at Lawns Lane Bridge using the dry spray process. The materials were applied by a specialist contractor.

(a)

(b)

Figure 5.1 Views of Lawns Lane Bridge, West Yorkshire: (a) east elevation and (b) south east elevation

5.2 DETAILS OF CONCRETE REPAIRS AT LAWNS LANE BRIDGE

5.2.1 Initial surveys

Lawns Lane Bridge underwent a full durability survey as part of the M1 Bridges Investigation commissioned by the Highways Agency. Among the surveys completed was a visual defects survey, a half-cell potential survey, depth of cover survey and depth of carbonation measurements. Chloride ion content in the concrete and electrical resistance of the concrete were also determined. 100mm diameter cores were also extracted from areas of sound concrete to enable the stiffness of the substrate concrete to be determined.

The results of these surveys were used to determine the areas of the bridge that needed repairs.

5.2.2 Installation of monitoring equipment and application of repair in the north piers and north abutment

5.2.2.1 Preparation of repair areas on the north piers and north abutment

Figure 5.2 and Figure 5.3 show the locations of the repair patches on the north piers and north abutment at Lawns Lane Bridge. These repairs were instrumented to

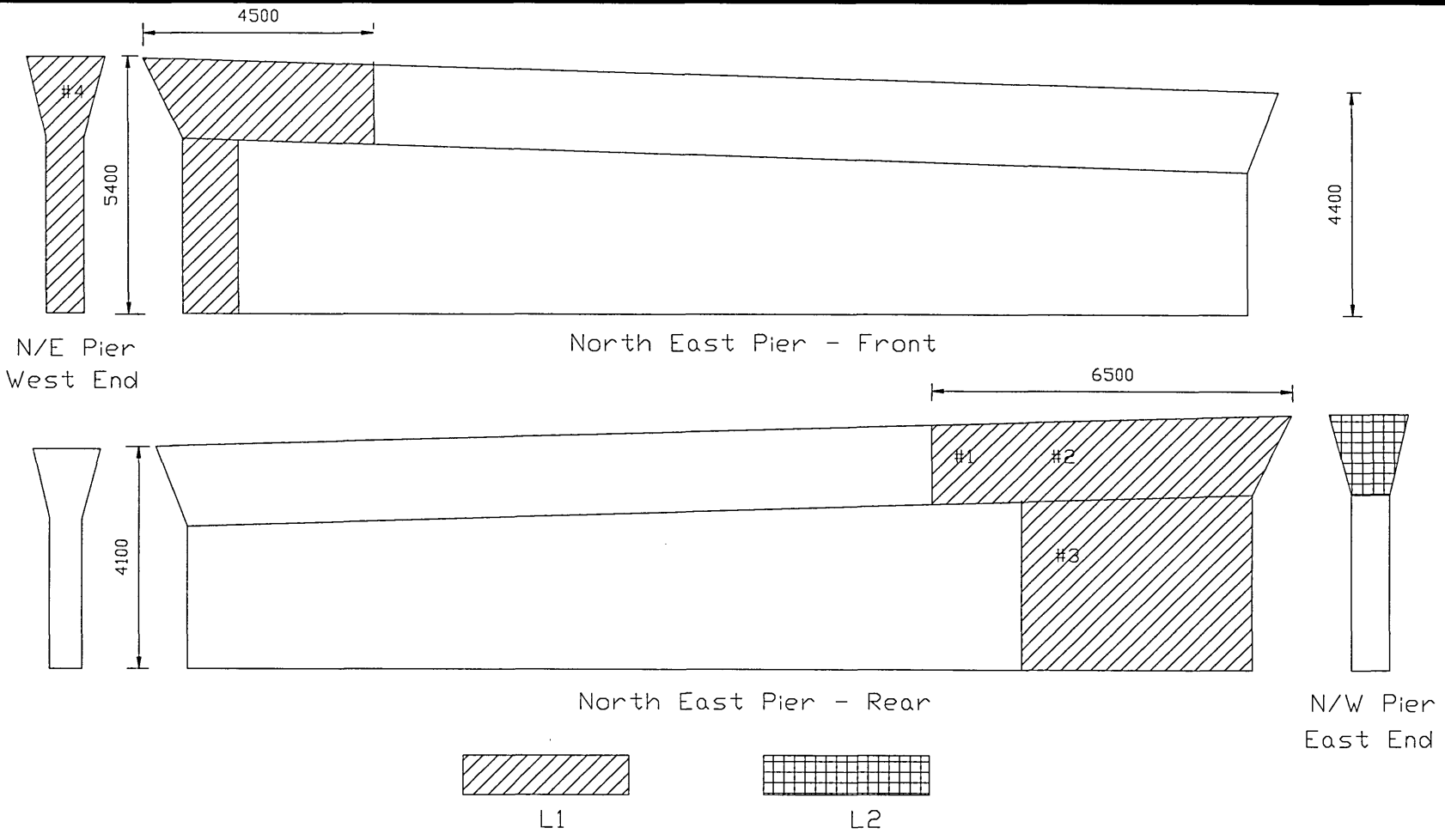

Figure 5.2 Location of instrumented materials on north piers at Lawns Lane Bridge

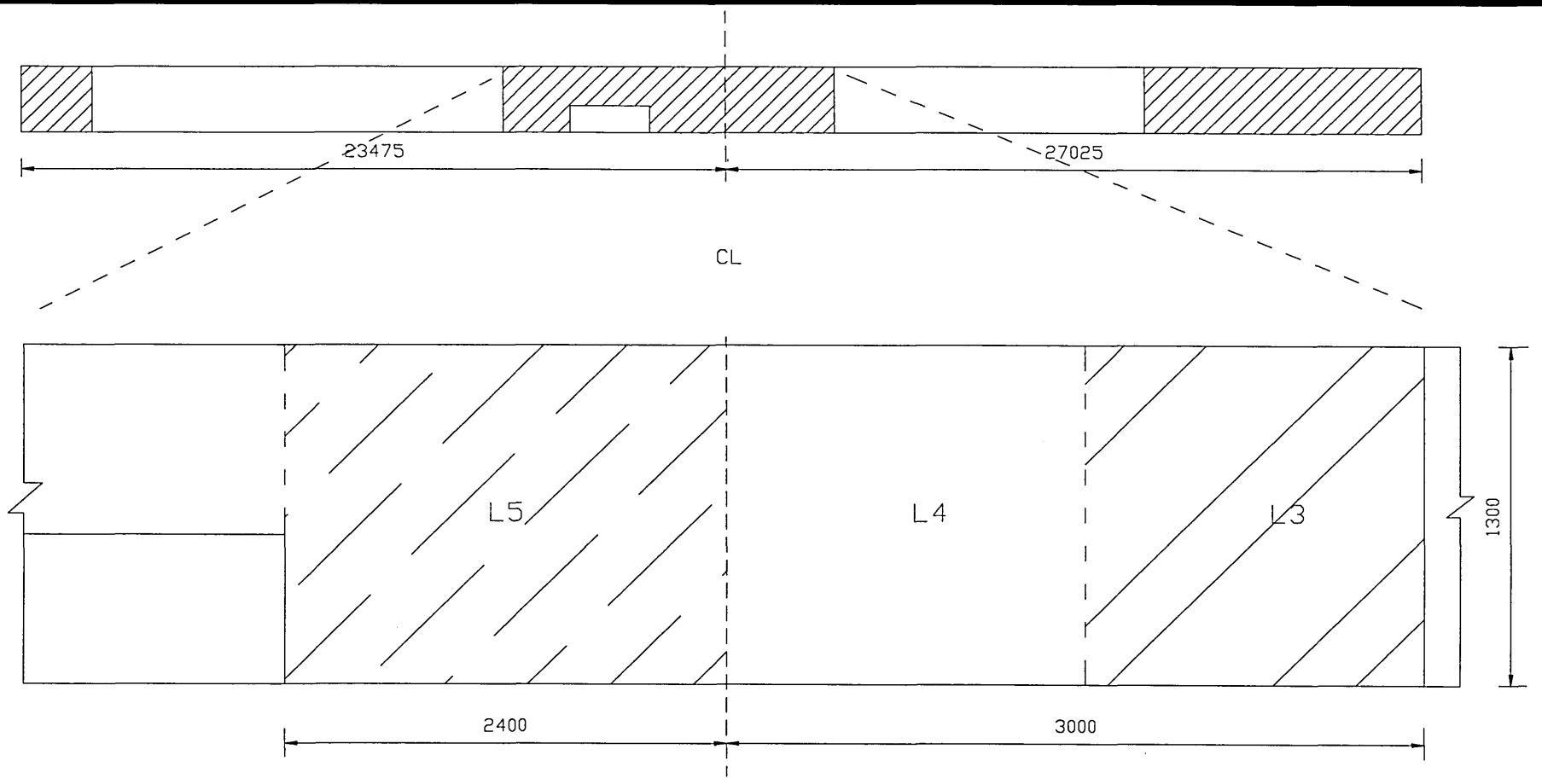

Figure 5.3 Location of instrumented materials on north abutment at Lawns Lane Bridge

determine the long term performance of spray applied repair materials to unpropped compression members. The extent of the deteriorated concrete determined from the results of the half cell survey was marked on the structure. A saw cut was then applied along the marked lines to envelope the repair areas. Removal of the deteriorated concrete was by pressurised water jet. Exposed steel was grit blasted to remove any loose rust and primed using Flexcrete FCR 841 steel reinforcement protector. The average depth of repair was approximately 140mm.

Two repair materials were applied to the north east and north west piers as shown Figure 5.2. Material L1 was applied mainly to the north east pier whereas material L2 was applied to the north west pier. Material L1 was selected by the Resident Engineer since it conformed fully with the Highways Agency specifications. This forms the main material for repair at Lawns Lane Bridge. Material L2 was selected by the research team, although it did not meet the specifications of the Highways Agency (details of repair materials are given in Section 5.3.1).

Figure 5.3 shows the position of the repair areas on the north abutment at Lawns Lane Bridge. Three different repair materials were applied and monitored at this location, namely L3, L4 and L5.

5.2.2.2 Details of instrumentation and repair patches in the north piers and north abutment

The position of the gauges in the repair materials at Lawns Lane Bridge followed a similar pattern to the gauges in the spray applied materials in the abutment at Gunthorpe Bridge (i.e. a gauge on the cut back substrate, one welded to the steel reinforcement and one embedded in the body of the repair material, as described in Sections 3.2.2.1, 3.2.2.2 and 3.2.2.3. respectively).

Due to the large volume of material L1 applied at Lawns Lane Bridge, four sets of gauges were installed in the material, labelled #1 to #4 in Figure 5.2.

Figure 5.4 (a) shows a section through a typical repair and the position of the gauges within the repair at Lawns Lane Bridge. Figure 5.4 (b) shows the elevation of a typical repair, again showing the position of the gauges within the repair. In some instances, a gauge was attached to the adjacent concrete to monitor the redistribution of stress to that area from the repair patch. Figure 5.5 shows a set of gauges in material L5 on the north abutment at Lawns Lane Bridge, whereas Figure 5.6 shows the three sets of gauges in position before material L3, L4 and L5 were applied at the north abutment.

The substrate was saturated before the repairs were applied, to minimise the absorption of free water from the repair materials. The dry spray process was used for all materials. The materials were applied starting at the bottom of the repair patch and gradually moving upwards to reduce the risk of trapping rebound material. A flash coat was applied to the surface to aid the finishing operations. This was then removed with a

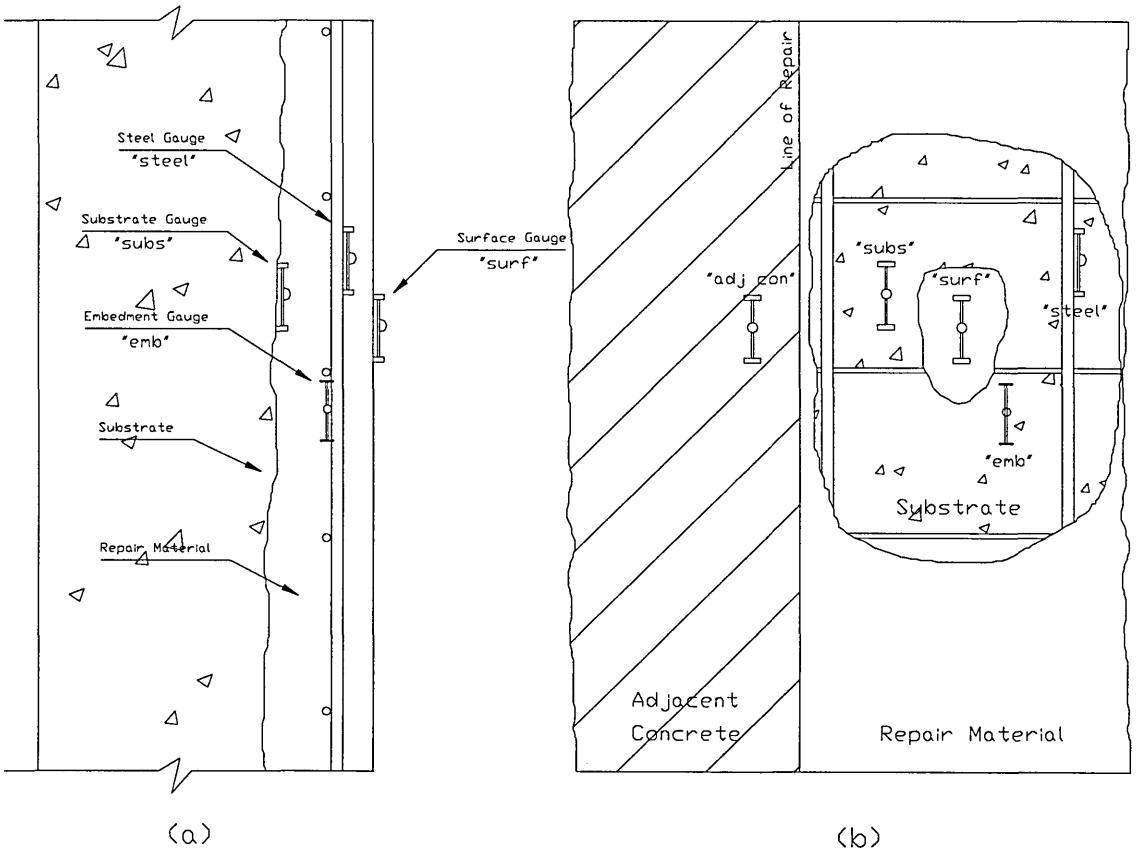

Figure 5.4 Location of gauges within a typical repair (pier and abutment) at Lawns Lane Bridge:
(a) section through a typical repair, (b) elevation of a typical repair

Figure 5.5 View of vibrating wire strain gauges within material L5 at Lawns Lane Bridge (north abutment), from left, steel reinforcement, substrate concrete and embedment gauges

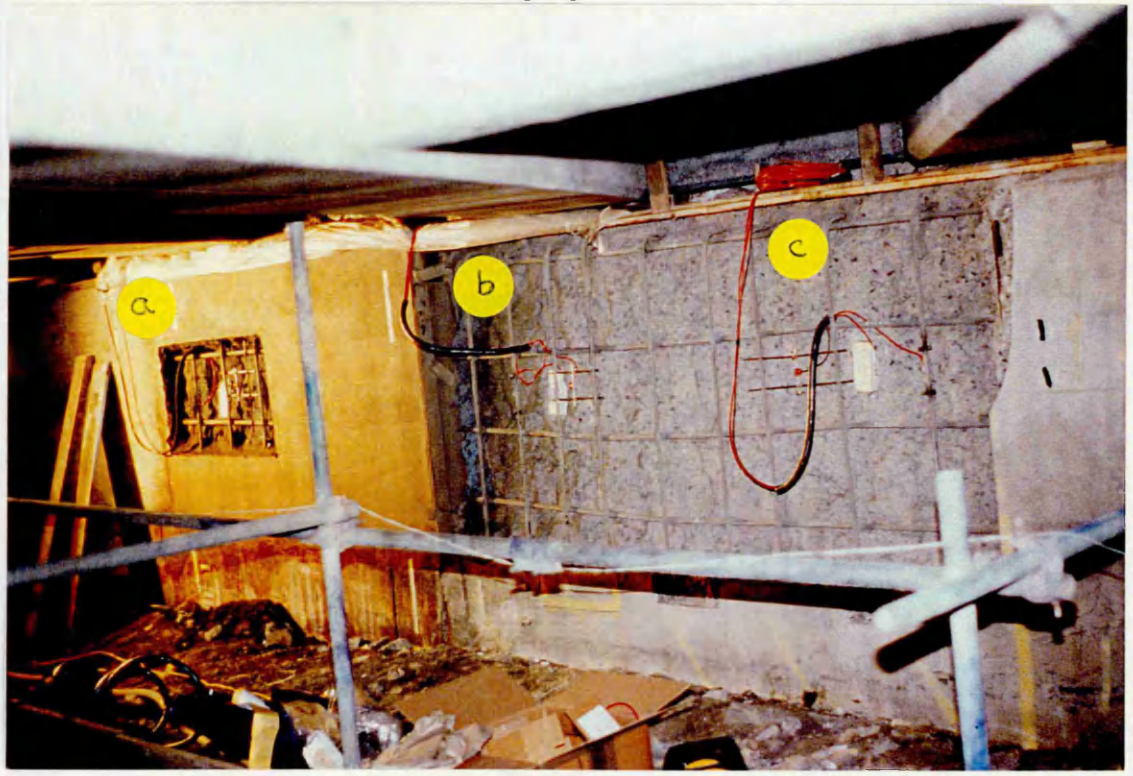

Figure 5.6 View of instrumented north abutment at Lawns Lane Bridge before application of repair materials: (a) material L5, (b) material L4 and (c) material L3

wooden screeding board. The final surface was obtained by floating with a steel float. Figure 5.7 shows material L4 being applied to the north abutment at Lawns Lane Bridge. Figure 5.8 shows materials L3, L4 and L5 in the north abutment after application with strain gauges attached to the surface of the repair materials and adjacent concrete. A curing compound was applied to the surface of all the materials. This was further complimented by covering the repair with polythene sheeting. The gauge on the new surface was installed on the day after the application of the repair. The surface gauges were covered with steel boxes to protect them from damage.

Trunking was installed on the bridge to protect the cables running from the gauges to the data logger. This consisted of 50mm square uPVC bolted to the concrete and the cables were placed inside through an open face. A cover was then fitted to keep the cables in place. In locations where the trunking (and the steel boxes covering the gauges) were particularly vulnerable to vandalism, extra protection was supplied in the form of solid mild steel covers

The gauge cables were threaded through the 50mm trunking to a central location where the data logger was stored. Cables were attached to the various channels on the data logger which was programmed to scan at pre-set intervals using a laptop computer.

Figure 5.7 Application of a repair patch (material L4) on the north abutment at Lawns Lane Bridge using the dry spray process

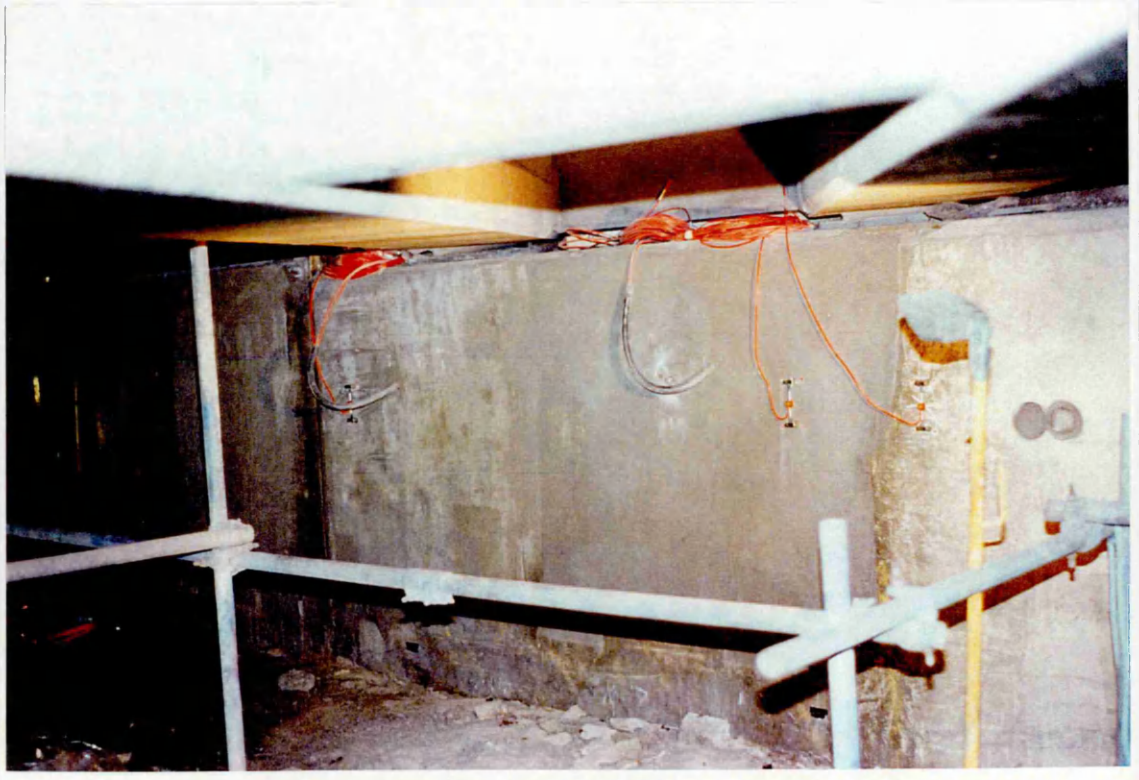

Figure 5.8 Completed repairs on the north abutment at Lawns Lane Bridge with strain gauges attached to the surface of the repair materials and adjacent concrete

5.3 DETAILS OF REPAIR MATERIALS

5.3.1 Spray applied repair materials

Five repair materials (labelled L1-L5) were instrumented at Lawns Lane Bridge. Spray applied materials were used due to the large volume of repairs. All the materials were applied by Concrete Repairs Ltd., who are part of M.J. Gleeson Group plc. Material L1 was the only material which fully complied with the requirements of the Highways Agency Repair Specification, BD 27/86 [1]. A detailed description of the repair materials is given below.

Material L1 was supplied by Proton Group Limited [16]. It is a blend of low alkali Portland cements, microsilica and high purity limestone aggregates together with a system of compatible admixtures. This powder, when mixed with water, produces a non-shrink (according to manufacturers literature), homogeneous microconcrete that produces no-slump, has excellent adhesion and very low permeability. It is designed to meet the Department of Transport requirements for sprayed concrete as detailed in BD 27/86 [1] and clause 29F (Midlands Links Specification). The maximum aggregate size is 3mm. This material was selected by the Resident Engineer as the main material at Lawns Lane Bridge since it fully complied with the current repair specification, BD 27/86 [1].

When mixed at a water:powder ratio of 0.12, material L1 has a density of 2210 kg/m^3, modulus of elasticity of 22.7 kN/mm^2 and a 28 day compressive strength of 60 N/mm^2.

Material L2 was supplied by Nufins Limited [17]. It is a prepacked, single component polymer modified repair mortar, requiring only the addition of clean water on site. It has been designed for machine applications using the dry spray process and is particularly suitable on large repairs to reinforced concrete structures which have been damaged due to reinforcement corrosion or frost attack.

Typical properties of material L2 include a 28 day compressive strength of 60-65 N/mm^2 and a density of between 2050-2150 kg/m^3. The modulus of elasticity is 30.3 kN/mm^2.

Material L3 was supplied by Fosroc Expandite Limited [18]. It is a ready to use blend of dry powders which requires only the addition of clean water on site to produce a highly consistent, shrinkage compensated medium-weight repair mortar for general purpose use. It can be applied by the wet or dry spray process. The material is based on Portland cement [4], graded aggregates [5], special fillers and chemical additives to provide a mortar with good handling characteristics, while minimising water demand. The product exhibits excellent thermal compatibility with concrete and good water repellent properties. The low water requirement ensures fast strength gain and long-term durability.

At a typical water:cement ratio of 0.18, material L3 obtains a 28 day compressive strength of 28 N/mm^2. The fresh wet density is approximately 1850 kg/m^3. The elastic modulus of this material is 27.4 kN/mm^2.

Material L4, supplied by Pozament Limited [19], is a factory blended dry spray gunite for the repair, strengthening or new construction of concrete structures. It consists of an intimate blend of Portland cement [4], silica sand and admixtures including plastic fibres. The maximum aggregate size of the sand is 5mm. The inclusion of suitable additives gives reduced rebound characteristics.

This material is designed to give a minimum 28 day compressive strength of 40 N/mm^2 when sprayed at a maximum water to cement ratio of 0.35. The modulus of elasticity, when tested in accordance with BS1881:Part 121:1983 [3] was 29.1 kN/mm^2.

Material L5, supplied by Pozament Limited [19], is a factory blended fibrous dry spray gunite for repair, strengthening or new construction of concrete structures. The inclusion of fibres controls early age shrinkage cracking and gives additional benefits particularly with respect to flexural strength, abrasion resistance and impact resistance. The properties of material L5 are very similar to those of material L4.

CHAPTER 6

REPAIR AND INSTRUMENTATION OF SUTHERLAND STREET BRIDGE

6.1 INTRODUCTION

Sutherland Street Bridge in Burngreave, Sheffield, carries the B6080 over an access road which once linked steel industries together. The superstructure of this bridge consists of an in situ bridge deck supported by prestressed beams. The substructure consists of reinforced concrete beams, supporting the prestressed beams, and columns in a portal frame (trestle) configuration. Elevations of Sutherland Street Bridge are given in Figures 6.1 and 6.2.

The bridge was substantially rebuilt in 1963. The decks were renewed along with new trestle piers. A capping beam was also provided on the existing masonry abutments.

Repairs at Sutherland Street Bridge were confined to the beams and columns of the north and south frames (see Figure 6.1). A total of four different repair materials were applied using the flowing method of application.

6.2 DETAILS OF CONCRETE REPAIRS AT SUTHERLAND STREET BRIDGE

6.2.1 Initial surveys

The substructure of Sutherland Street Bridge underwent a full durability survey, including a half-cell potential and covermeter surveys. 100mm diameter cores (see Figure 6.3) were extracted from selected parts of the bridge to determine the elastic

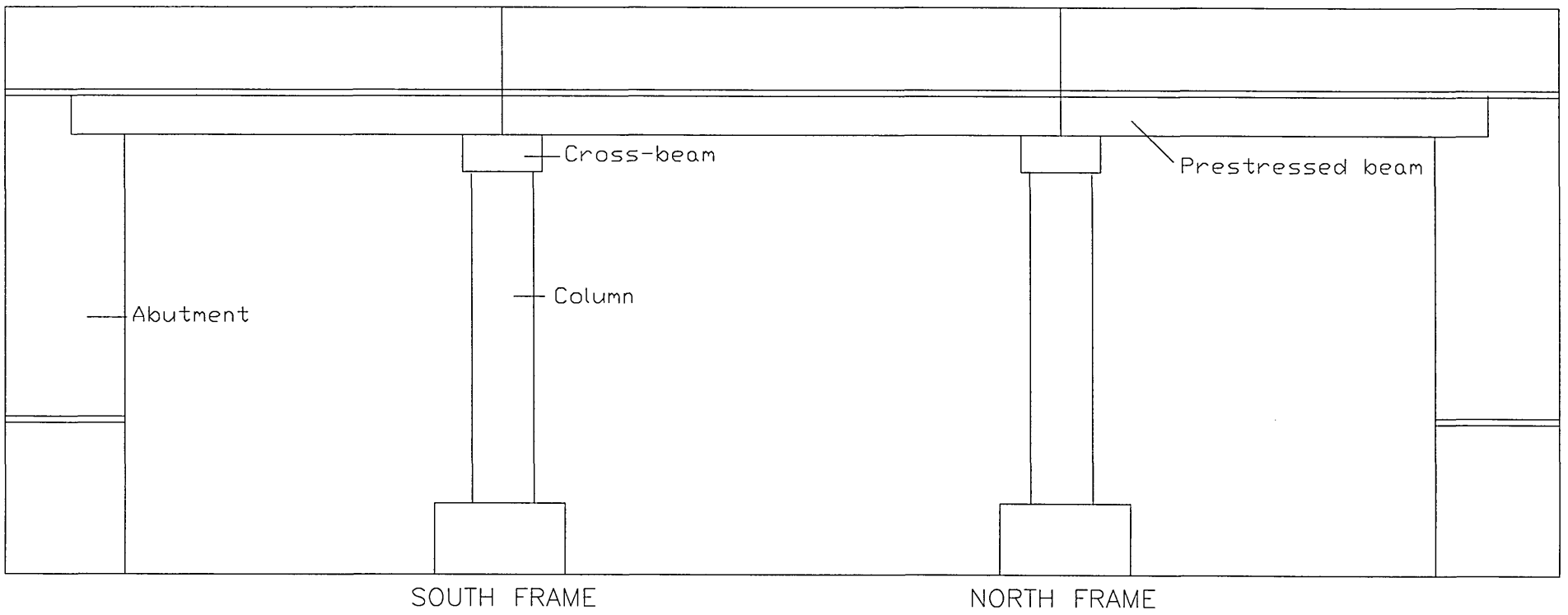

Figure 6.1 Elevation of Sutherland Street Bridge

Figure 6.2 East elevation of Sutherland Street Bridge, Sheffield.

Figure 6.3 Coring at Sutherland Street Bridge to determine the elastic modulus of the substrate concrete

modulus of the substrate concrete. Concrete dust samples were taken for chloride ion analysis.

6.2.2 Installation of the monitoring equipment and application of repair on the north and south frames

6.2.2.1 Preparation of the repair areas on the north and south frames

Figure 6.4 shows the positions of the repair patches on the substructure at Sutherland Street Bridge. These repairs were carried out to investigate five different parameters at Sutherland Street Bridge. These are (i) performance of repair patches in compression members, (ii) performance of the repair patches in tension zones, (iii) effect of the volume of the repair patches on the structural interaction with the substrate, (iv) performance of the repair when the depth of concrete removed behind the steel is increased and (v) propped and unpropped repairs, to establish the effect of propping prior to applying the repair on structural interaction.

Propping of the south frame and half of the north frame, to enable comparisons between propped and unpropped repairs, was carried out by Mabey Support Systems Ltd. Every second prestressed beam which make up the bridge deck was supported by steel props.

Removal of deteriorated concrete was achieved by using both water jetting equipment and mechanical means by V.A. Crookes (Contracts) Ltd. Concrete was removed to a depth of 25mm behind the steel, except in some instances when it was removed to a

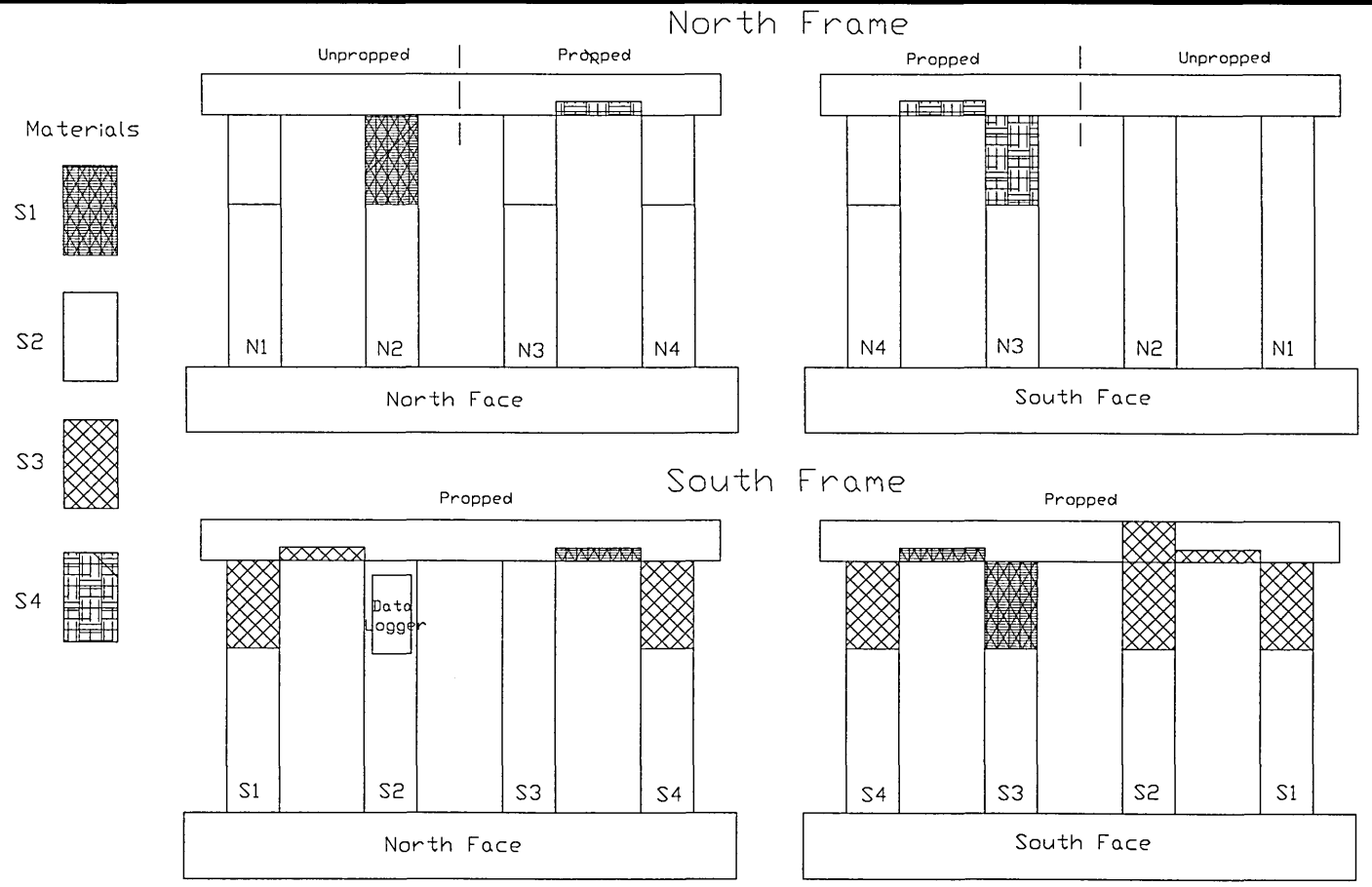

Figure 6.4 Sections of Sutherland Street Bridge showing the column and beam support system and positions of repair patches

depth of 60mm when information on the performance of the repair with increased depth was required. All the exposed steel was grit blasted and primed using Flexcrete Steel Reinforcement Protector (FCR 841). This is a two component material consisting of cementitious powder and a polymer dispersion which react together to passivate the steel.

The configuration of the gauges in the repair materials at Sutherland Street Bridge was similar to that applied in the other bridges. Mounting plates were attached to the cut back substrate and welded to the steel reinforcement. Support bars, onto which the embedment gauge would be attached with tying wire, were also fitted across the main steel reinforcement.

6.2.2.2 Details of instrumentation and repair patches on the north and south frames

The positions of the gauges are shown in Figure 6.5 (a and b) for the columns at Sutherland Street Bridge. Figure 6.5 (a) shows the cross section through a typical column repair whereas Figure 6.5 (b) shows an elevation of a column repair. Gauges are installed on the substrate surface, steel surface, embedded in the repair material and on the surface of the repair material. A similar configuration was employed on the soffits of the beams at Sutherland Street Bridge, as shown in Figure 6.5 (c and d). Figure 6.5 (c) shows a cross section through a beam repair whereas Figure 6.5 (d) shows the soffit of a typical beam repair. The gauges were installed as described in Sections 3.2.2.1 (substrate concrete gauge), 3.2.2.2 (steel reinforcement gauge) and 3.2.2.3

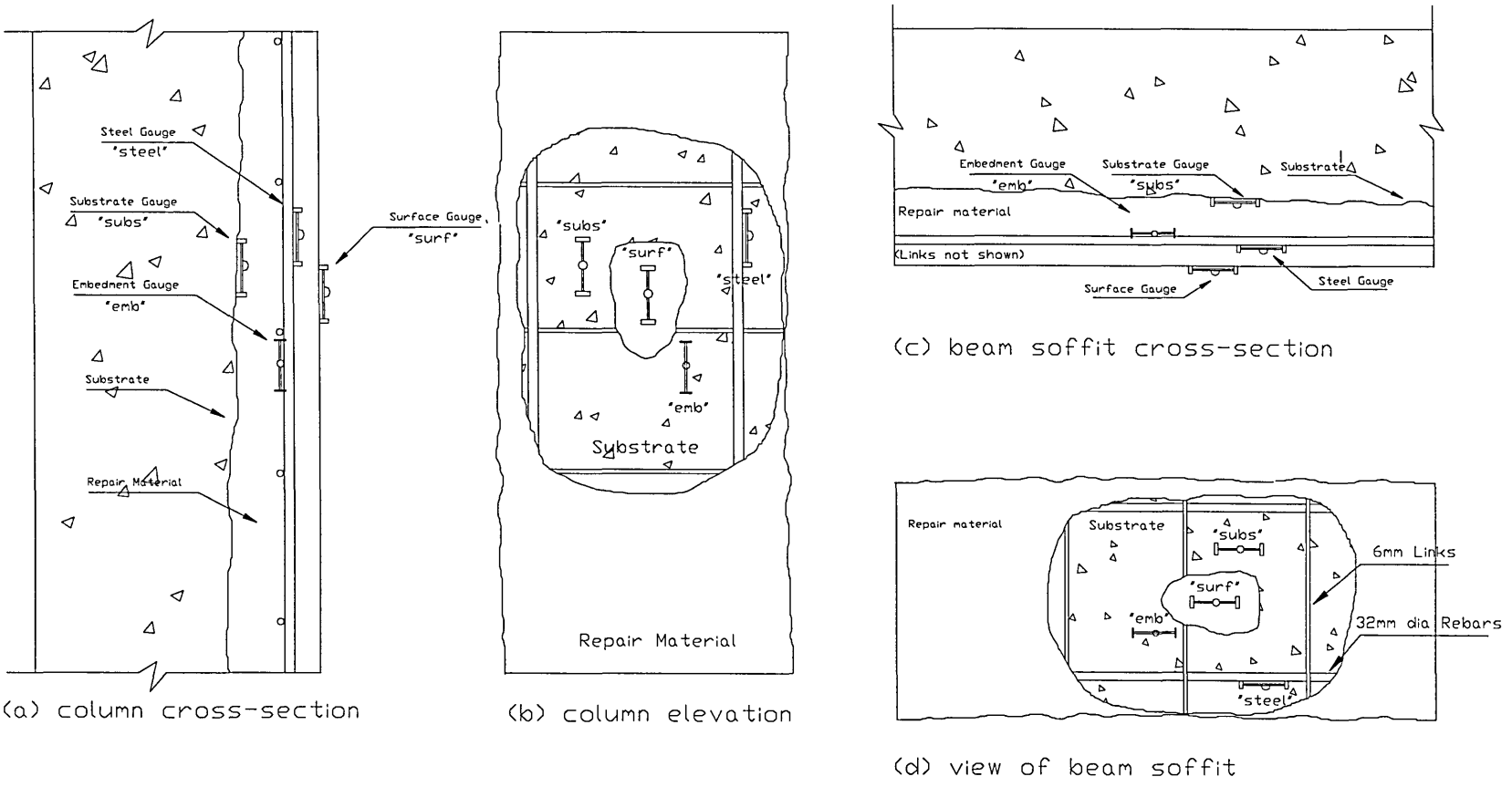

Figure 6.5 Position of gauges in the repair patches on the beams and columns at Sutherland Street Bridge

(embedded in the repair material). A view of the vibrating wire strain gauges (attached to substrate concrete, steel reinforcement and embedded in the repair material) in position on one of the columns at Sutherland Street Bridge is given in Figure 6.6

Shuttering for the flowing repairs consisted of plywood faced timber formwork, custom made for the repairs at Sutherland Street. The repetitiveness of the repairs allowed the column formwork and the soffit formwork to be used more than once.

The substrate concrete was saturated by filling the shuttering with water and leaving in place overnight. This was to reduce the absorption of water from the repair material into the substrate concrete.

The repair materials were mixed in accordance with the manufacturers instructions in a Pennine barrel mixer. The materials were either pumped into the shuttering or poured from a bucket (see Figure 6.7). Compaction of the flowing material was provided by firmly tapping the shuttering with a hammer at regular frequency, as the material was placed by pouring.

Shuttering was left in place for at least three days after the pour to assist with curing. When the shuttering was removed, some of the materials received a thin coat of cementitious material when the original surface finish was poor. Surface strain gauges were subsequently attached together with steel covers for protection (see Figure 6.8). The gauge cables travelled via 50mm uPVC trunking to the south frame where they were attached to the data logger (see Figure 6.9).

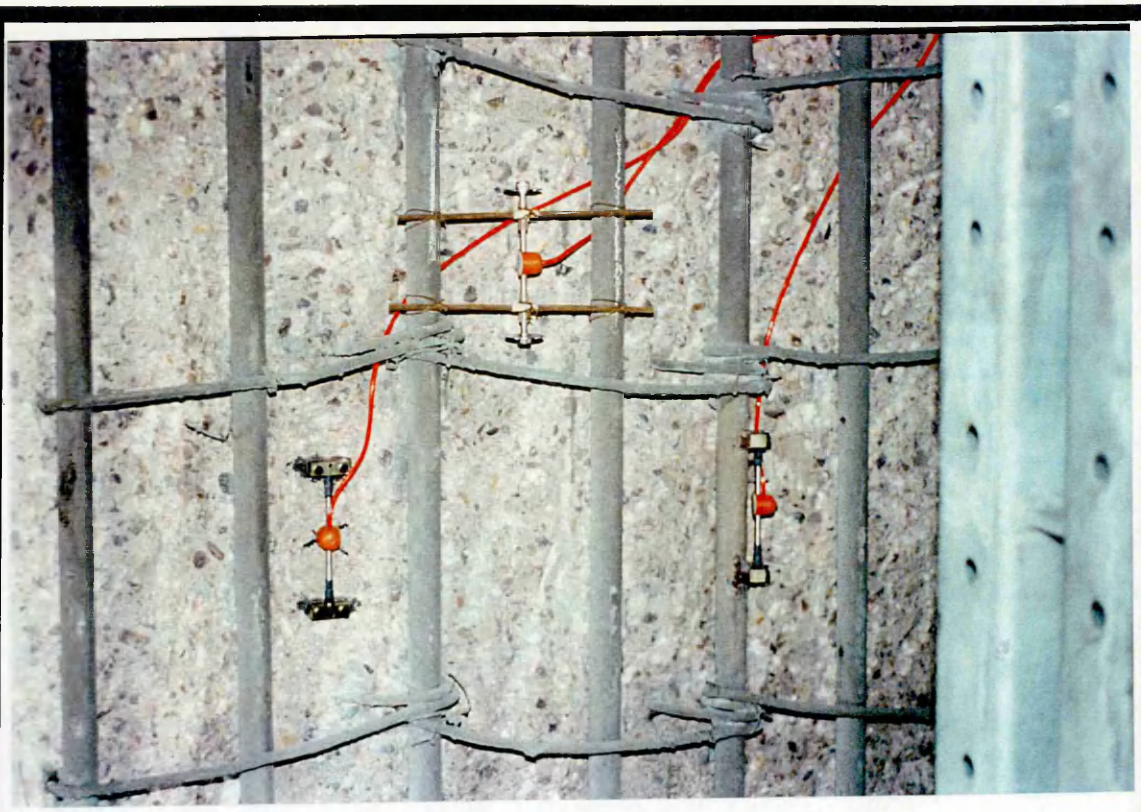

Figure 6.6 Position of gauges within a typical column repair at Sutherland Street Bridge, from left, substrate concrete gauge, embedment gauge and steel reinforcement gauge

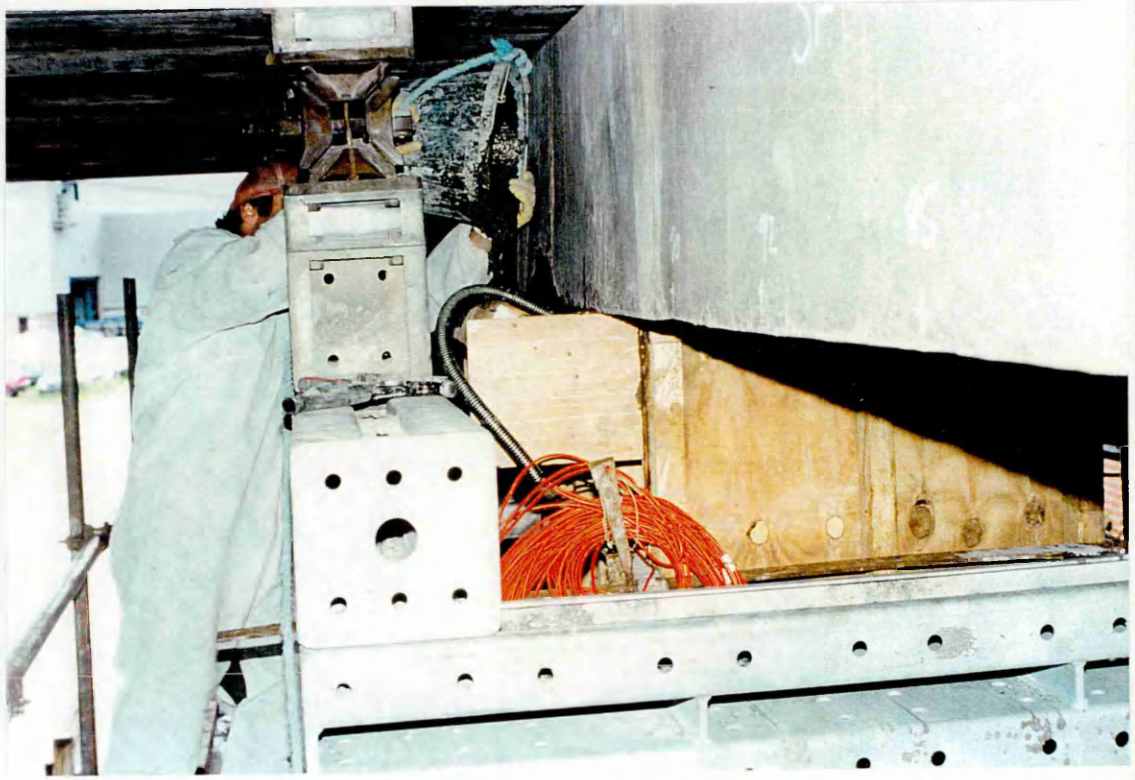

Figure 6.7 Application of material S2 by pouring into a compression member repair at Sutherland Street Bridge

Figure 6.8 View of the completed repairs on the north frame at Sutherland Street Bridge and the protective steel covers on the surface strain gauges (columns on the left and second from left).

Figure 6.9 Positioning the gauge cables in the trunking which travel to the data logger on the south frame at Sutherland Street Bridge.

Propping to the south frame and half of the north frame remained in place until the repair materials had cured sufficiently. Upon completion of the curing period, the load was reapplied to the structure. This occurred when the repair materials reached the design strength of the bridge members, or were in situ for 28 days.

6.3 DETAILS OF REPAIR MATERIALS

6.3.1 Flowing repair materials

Repairs to Sutherland Street Bridge incorporated flowing materials as a repair technique. Four materials are monitored in total, three of which are commercially available materials, labelled S1-S3. The fourth material, S4, is a laboratory designed conventional flowing concrete, used solely for the purpose of research to compare the performance of conventional materials with commercial repair products. A detailed description of the materials is given below.

Material S1, supplied by SBD Limited [15], is a single component, pre-blended cementitious repair material simply requiring the addition of clean water on site to produce a repair concrete which complies with the model requirements for replacement concrete as outlined in BD 27/86 Part 4 [1]. This material contains 5mm maximum sized graded aggregate, additives and shrinkage compensating agents. The cement content is 500 kg/m^3.

At the recommended water/cement ratio of 0.37, this material has a density of 2250 kg/m^3, compressive strength of 65 N/mm^2 at 28 days and a flow of 750mm when tested using the DoT flow trough [1]. The modulus of elasticity is 24.2 kN/mm^2.

Material S2 from Fosroc Expandite Limited [18] comprises of a blend of dry powders which require only the addition of clean water on site. It is based on Portland cement [4], graded aggregates [5] and additives which produce a free flowing, shrinkage compensated concrete for large volume concrete repairs. The recommended water:powder ratio of 0.13 achieves a compressive strength of 60 N/mm^2 (BS 1881 Pt 116 - restrained [20]), a fresh density of 2270 kg m^3 and a flow of 750mm within 10 seconds. The modulus of elasticity is 32.2 kN/mm^2 at 28 days (BS 1881 Pt 121 [3]).

Material S3, supplied by Flexcrete Limited [14], is a rapid hardening, high strength, non-shrink material which incorporates the most advanced cement chemistry, microsilica, shrinkage compensating admixtures and styrene acrylic copolymer technology. It is supplied as a single component material for on-site mixing with clean water. This material also includes a 6mm aggregate for depths of repairs greater than 50mm. Typical properties are a compressive strength in excess of 70 N/mm^2 at 28 days and a fresh density of 2250 kg/m^3. The modulus of elasticity is 31.9 kN/mm^2.

Material S4 comprises of conventional concrete materials to produce a flowing concrete. It consists of Portland Cement, complying with BS 12 [4], 10mm rounded aggregate and a medium grade sand complying with BS 882 [5], pulverised fuel ash, complying with BS 3892 Pt 1 [21], superplasticiser, complying with BS 5075 Pt 3 [22]

and polypropylene fibres to control shrinkage cracks. A water:cement ratio of 0.48 is used, which results in a compressive strength of 45-50 N/mm^2 at 28 days. The mix proportions are given in Table 6.1.

Table 6.1 Mix proportions for material S4

Constituent	*Quantity (kg/m^3)*	*Type/source*
Total cementitious	**400**	
Cement	340	Portland
PFA	60	Pozzolan Ltd.
Total aggregate	**1820**	
Coarse	1092	10mm rounded
Fine	728	Grade M sand
Water	180	Yorkshire Water
Superplasticiser	2.25% / weight of cementitious	Melment F10
Fibres	910 g/m^3	Polypropylene

Mix ratios:

Cementitious:sand:aggregate	1:1.8:2.7
Water:cementitious	0.45

CHAPTER 7

LABORATORY INVESTIGATION: REPAIR AND INSTRUMENTATION OF REINFORCED CONCRETE BEAMS

7.1 INTRODUCTION

A hand-applied patch repair is an effective restoration technique when a structural element, such as a reinforced concrete beam, requires low volume repairs. This is due to the fact that most of the deterioration will have taken place in the tensile cover zone only due to the corrosion of the main steel reinforcement and stirrup reinforcement. To enable the member to return to its original strength, a repair material must be selected that will enable the full tensile moment of resistance to be developed. Therefore, the applied repair material must posses adequate tensile properties. The material must first be able to withstand the tensile stress induced due to restrained shrinkage and then interact with the steel reinforcement and the substrate concrete to redevelop the tensile moment of resistance

A laboratory investigation was carried out to determine the in-service performance of different hand-applied repair materials. Eight reinforced concrete beams (see Table 7.1) with deterioration simulating actual field conditions were repaired in the laboratory with a total of four different hand applied materials [L3(L), G4(L), G5(L) and G6(L) - see

Table 7.1] with varying mechanical properties. The investigation examined the performance of the different repair materials when repairs were applied to the beams. The repaired beams were kept under serviceability flexural load over a long period of time. The following parameters of beam repair were considered in the investigation:

- repairs to unpropped flexural members (the load remained in place during application of the repair patch, Table 7.1)
- repairs to propped flexural members (the load was removed during application of the repair patch, Table 7.1)
- an incremental increase in depth of repair [patches extended 25mm (total patch depth: 71mm) and 50mm (total patch depth: 96mm) behind the steel reinforcement, Table 7.1]

Table 7.1 Laboratory repairs to reinforced concrete beams

Beam Number	*Repair material*	*State of loading during repair*	*Depth behind steel reinforcement (mm)*
1	G6(L)	Unpropped	25
2	G4(L)	Unpropped	25
3	G5(L)	Unpropped	25
4	G5(L)	Unpropped	50
5	L3(L)	Unpropped	25
6	G5(L)	Propped	25
7	L3(L)	Propped	25
8	L3(L)	Unpropped	50

7.2 DETAILS OF LABORATORY CONCRETE REPAIRS

7.2.1 Reinforced concrete beams

A total of eight reinforced concrete beams measuring 2740 x 100 x 200mm were cast in steel moulds in the laboratory. Two 100 x 100 x 100mm cube specimens and two 200 x 100mm diameter cylinder specimens were cast simultaneously for each beam to enable the compressive strength and elastic modulus of the concrete in each beam to be obtained.

All concrete beams were reinforced with two 16mm diameter high tensile steel bars. The cover to each bar was 30mm based on the very severe condition of exposure from Table 3.4, BS 8110 [23]. 6mm diameter mild steel links at 110mm centres were provided in the shear zones and they were supported with 6mm diameter mild steel hanger bars in the compression zone [see Figure 7.1 (a)].

To simulate a repair situation where deteriorated concrete has been removed, voids measuring 640mm long by 71 or 96mm deep (depending on which parameter was being investigated) were inserted centrally at the casting stage, as shown in Figure 7.1 (b). Sections through a typical beam are given in Figures 7.1 (c) and (d).

The loading arrangement on a typical beam is given in Figure 7.2 (a). A two point loading configuration at third span intervals was used. This loading arrangement was employed so as to simplify the stresses induced in the repair material. This negated the need for shear reinforcement in the central third due to the absence of shear stresses [see

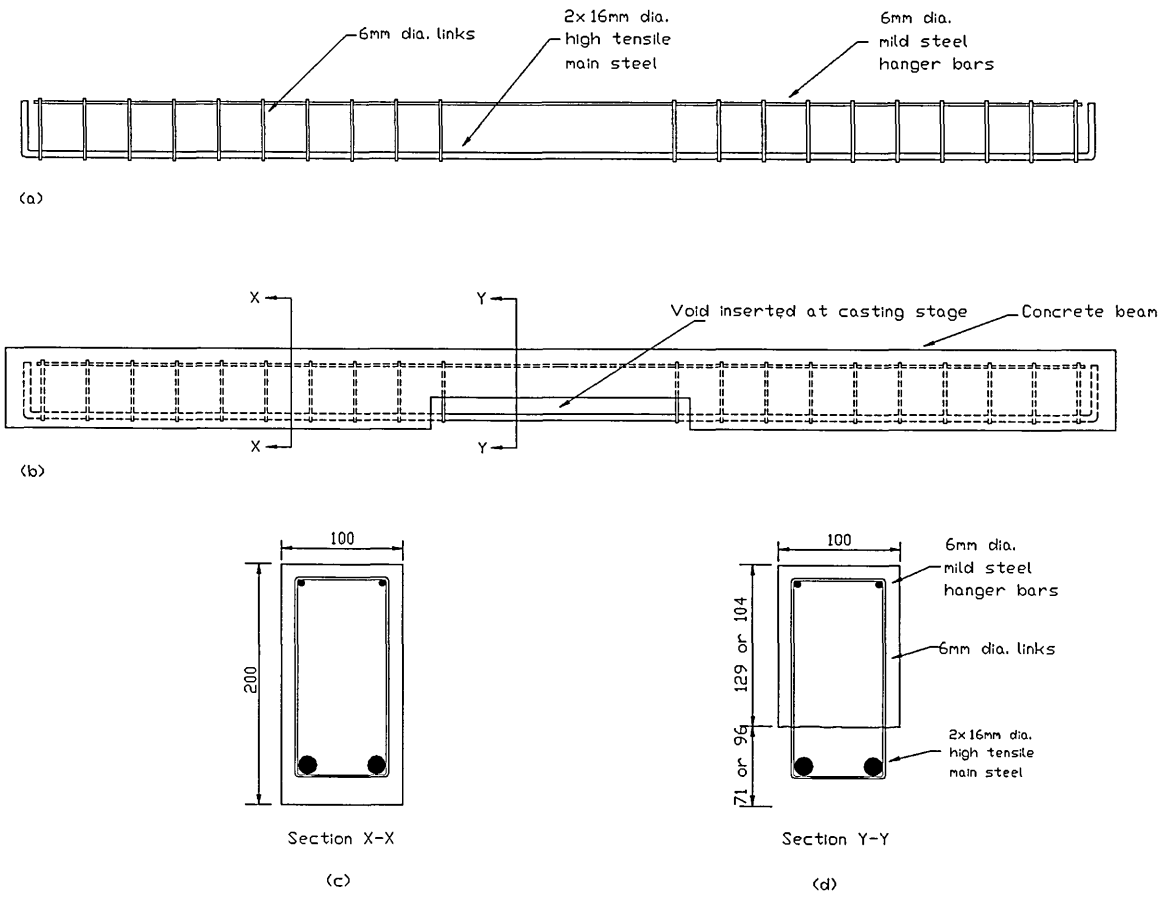

Figure 7.1 Reinforcement details of repaired beams: (a) steel fabricated and (b) reinforced concrete beam (c) and (d) sections through reinforced concrete beam

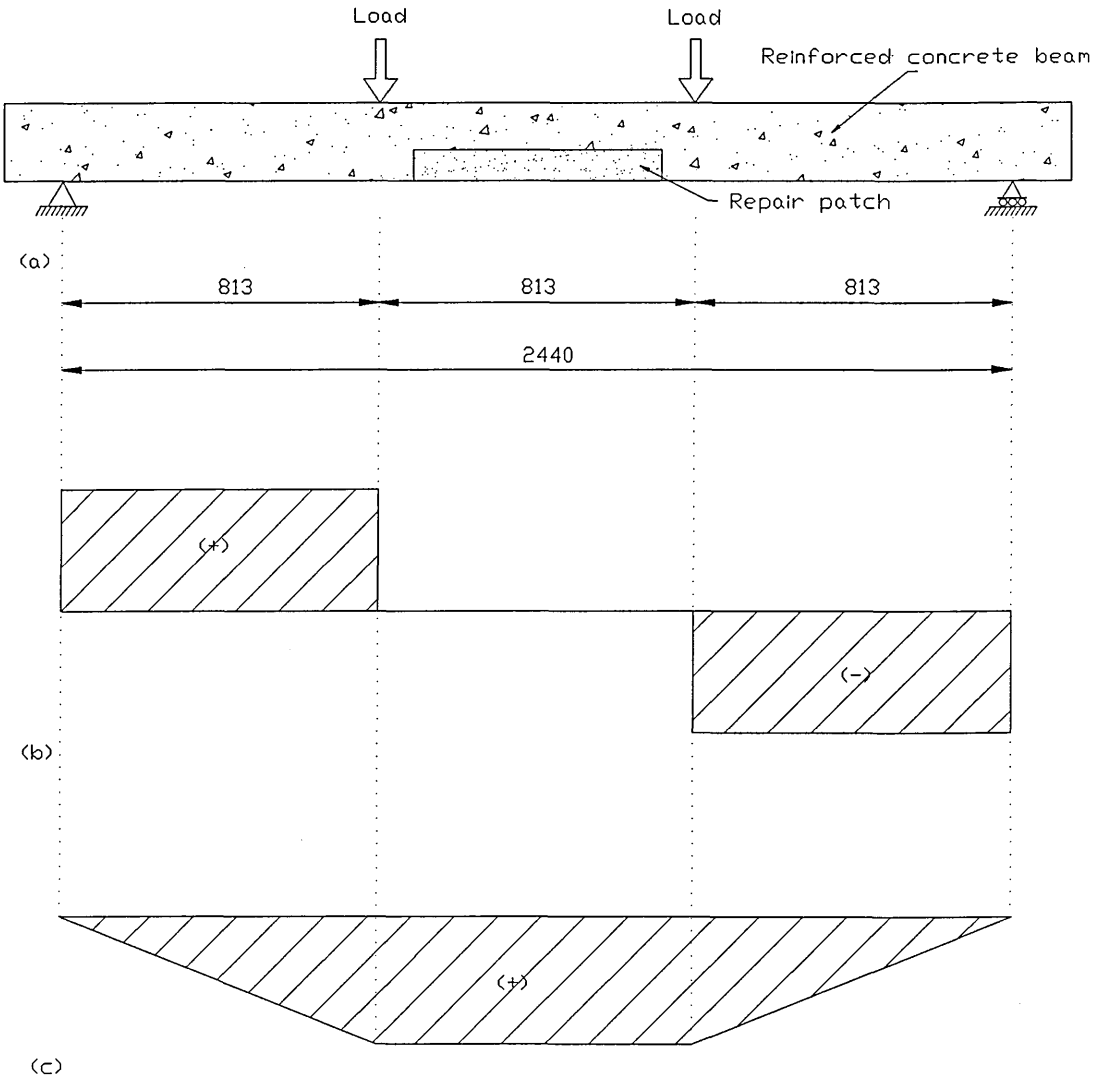

Figure 7.2 Schematic representation of stress due to external loading (a) loading configuration (b) shear force diagram and (c) bending moment diagram

Figure 7.2 (b)] and ensured that the material was in the constant bending moment zone, as shown in Figure 7.2 (c).

7.2.2 Creep rig

Custom built creep rigs, as shown in Figure 7.3 (a), were used to apply a constant load on the repaired reinforced concrete beams. The rig consists of a 203 x 102 x 23 kg/m universal beam and a loading arrangement which applies the load at one-third span points along the beam. A service load of 22 kN (2 x 11 kN at one-third span points), approximately 40% of the ultimate load, was applied on the reinforced concrete beam.

The loading apparatus was designed so as to allow the service load to be applied without having to incorporate a load cell in each rig. This was done by calibrating a torque wrench to 22 kN (accuracy +/- 3%) for this purpose and applying the load via a loading bolt in the top platen of the rig [see Figure 7.3 (b)]. The calibration of the torque wrench was frequently re-checked throughout the loading operations.

7.2.3 Strain measurement

7.2.3.1 Strain gauges on the steel reinforcement

To facilitate the measuring of the steel reinforcement strain, three CEA-06-250UN-120 electrical resistance strain gauges were attached to one steel reinforcing bar as described in section 3.3.1.1. Figure 7.4 (a) shows an elevation of a typical beam under load along.

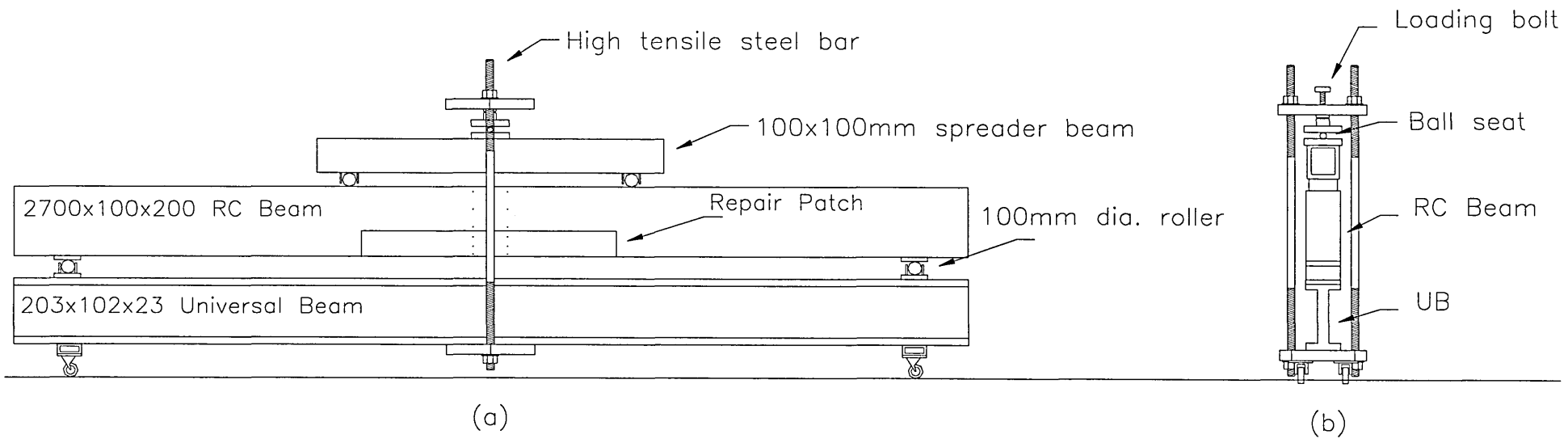

Figure 7.3 Repaired reinforced concrete beam under load: (a) elevation and (b) end view

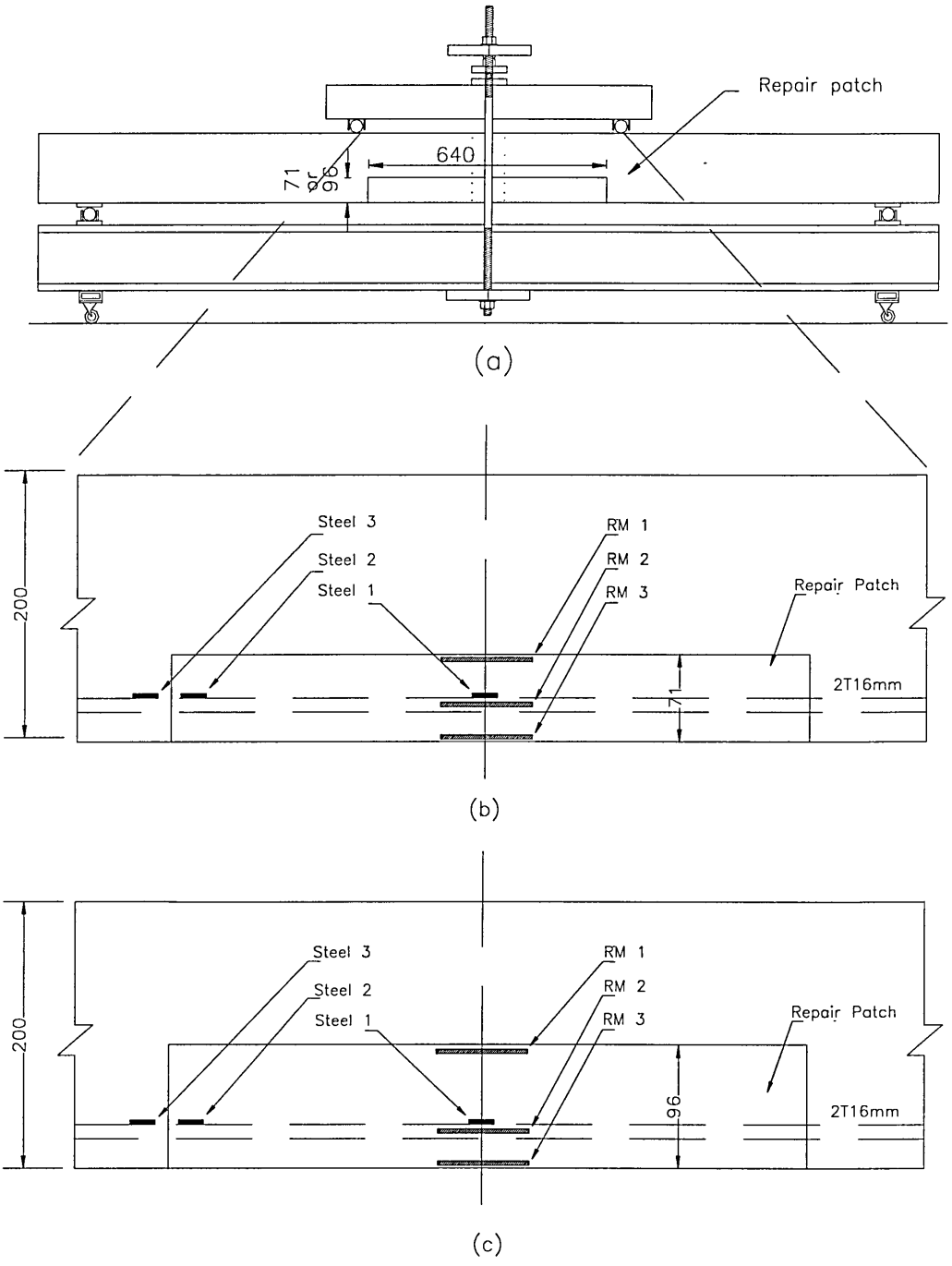

Figure 7.4 Position of electrical resistance gauges within the repair
(a) Elevation of repaired beam under load
(b) Position of gauges within a 71mm deep repair
(c) Position of gauges within a 96mm deep repair

with the position of the repair patch. Figure 7.4 (b) shows an enlarged elevation of the steel reinforcement within the repair patch and the positions of the gauges on the steel Gauge "Steel 1" [see Figure 7.4 (b)] is positioned centrally on the steel reinforcement (at mid-span) whereas "Steel 2" and "Steel 3" are positioned on either side of the repair material/substrate interface. The strain data from these gauges are obtained by attaching them to a digital strain indicator, as described in Section 3.3.2.

7.2.3.2 Strain gauges in the repair materials

Three PML-30 electrical resistance strain gauges were embedded in the repair material during repair of the beam, as described in Section 3.3.1.2. The position of the repair material in the beam is shown in Figure 7.4 (a). A gauge length of 40mm is used. The gauges were protected by 85 x 14 x 4mm resin plates, which were hermetically sealed to waterproof the gauge. The gauges, positioned at mid-span, are shown in Figure 7.4 (b) and (c). Gauge "RM 1" is placed at the repair material/substrate interface level, gauge "RM 2" is placed at the steel reinforcement level whereas "RM 3" is placed at the soffit of the repair. The strain from the PML-30 strain gauges is obtained by connecting to a digital strain indicator, as described in Section 3.3.2.

7.2.3.3 Strain gauges on the substrate concrete

Figure 7.5 (a) shows an elevation of a typical beam under load along with the position of the repair patch on the beam. The strain in the substrate concrete was measured by attaching demec points (gauge length 100mm) to the vertical faces at mid-span of the

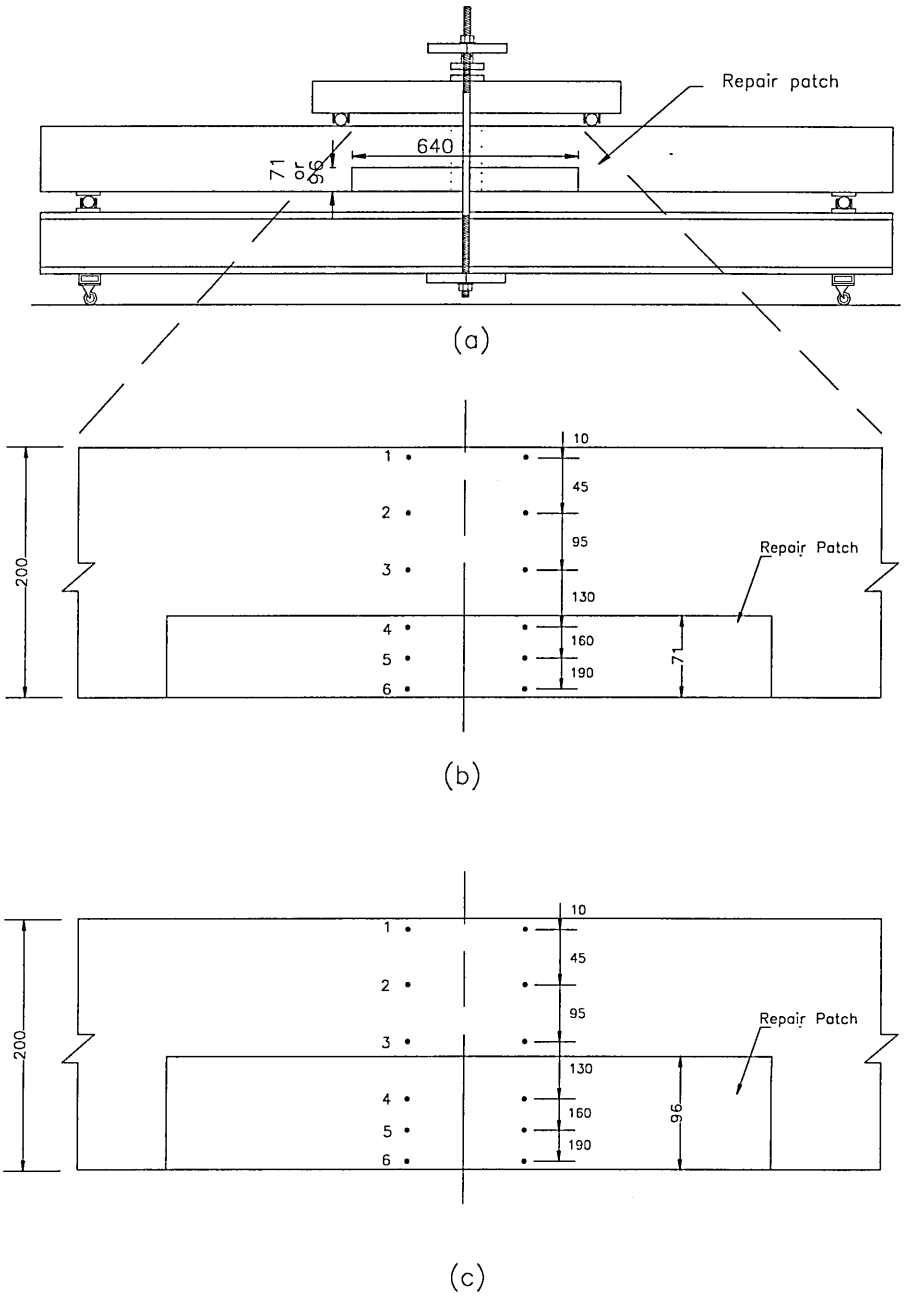

Figure 7.5 Position of demec points on the face of a repaired beam

(a) Elevation of repaired bean under load

(b) Position of demec points on the face of a 71mm deep repair

(c) Position of demec points on the face of a 96mm deep repair

beam as shown in Figure 7.5 (b) and (c). Demecs 1, 2 and 3 were positioned along both vertical faces of the substrate concrete whereas demecs 4, 5 and 6 were positioned on both vertical faces of the repair material. A demec extensometer of gauge length 100mm was used to measure the deformation.

7.2.4 Details of concrete mix and repair materials

Details of the concrete mix, which formed the substrate beam, and the repair materials are given in Table 7.2. Concrete mix proportions (by weight) of 1:1.8:2.9 with a water:cementitious ratio of 0.45 were used throughout. The cementitious content was 400 kg/m^3 which included 15% (60 kg/m^3) pulverised fuel ash. The mix was designed to give a 28 day cube strength of 45 N/mm^2 and a slump of 30-60mm.

Three of the four repair materials used in the laboratory [G4(L), G5(L) and G6(L)] were the same as the three hand applied materials used at Gunthorpe Bridge [G4, G5 and G6 respectively], whereas material L3(L) in the laboratory was the same as material L3 at Lawns Lane Bridge, except that it was applied by hand instead of spray application. A full description of the materials is given is Sections 4.3.2 and 5.3.1.

7.2.5 Casting and curing

In order to simulate a repair situation where deteriorated concrete has been removed due to steel reinforcement corrosion, pieces of stiff polystyrene were inserted centrally around the reinforcement cage to create a void measuring 640 x 100 x 71 or 96 mm

deep. All joints were then sealed with silicone rubber to stop moisture from the concrete mix entering the void.

Prior to casting, the moulds were lightly oiled with mould oil to ensure easy removal of

Table 7.2 Details of concrete mix and repair materials

Mix	*Materials and Description*	*Quantity (kg/m^3)*	*Water/Cementitious Ratio*
Concrete	Portland Cement	340	
	PFA	60	
	Fine aggregate (grade M)	720	0.45
	Coarse aggregate (20-5mm graded)	1160	
Repair Material	*Description*	*Density of fresh material*	*Water Content*
L3(L)	Single component, medium weight cementitious mortar	1850	4.5 litres per 25 kg pack
G4(L)	Three component, fibre reinforced, polymer modified cementitious mortar	2100	Pre-packed polymer
G5(L)	Single component, polymer modified cementitious mortar	1725	3.5 litres per 25kg pack
G6(L)	Lightweight, single component cementitious mortar		5.0 litres per 30 kg pack

the concrete beam. The reinforcement cage was then positioned in the mould, care being taken not to damage the wires from the gauges on the steel reinforcement. Concrete was mixed dry in a forced action pan mixer for 2 minutes before the water was added. Mixing continued until the concrete was mixed thoroughly. All beams were cast horizontally in three layers, each layer was adequately compacted with a poker vibrator. The top surface of the concrete was levelled off and covered with polythene sheeting. The beams remained in the mould under laboratory conditions of temperature and humidity for four days before demoulding. Afterwards, they were stored under laboratory conditions of temperature and humidity for 28 days before loading. Prior to loading, the polystyrene was removed from the beam, leaving a void which would be repaired at a later stage. The surfaces of the void which would later form the substrate/repair material interface were roughened by a hammer and chisel to simulate actual site conditions for enhancing bond.

7.2.6 Repair of reinforced concrete beams

Deterioration processes in reinforced concrete structures are long term phenomena and the need for repair normally occurs after a structure has been in service for many years. As a result, the creep and shrinkage effects on the concrete have stabilised and reached negligible levels when repairs normally take place. In order to simulate field conditions where shrinkage and creep of the parent concrete is negligible at the time of repair application, the reinforced concrete beams with the void as described above were loaded for approximately 6-8 weeks prior to the application of repair to eliminate the effects of creep. A load of 22 kN (2 x 11 kN at one-third span points) was applied to

each beam as described in section 7.2.2 and loaded members were stored at 20°C and 55% RH in an environmentally controlled room. During this loading period, the load was frequently topped-up to allow for any drop-off in load due to the creep of concrete.

Repair of the reinforced concrete beams was then carried out while still under load (unpropped state) by placing timber formwork on the soffit of the beam and supporting it with packing/wedges built up from the top flange of the creep rig. This allowed the repair material to be inserted from either side (vertical face) of the beam. Embedment gauges within the repair material were also inserted as the repair progressed (see Figure 7.6). Each material used for repair was mixed in accordance with the manufacturers' instructions. The material was built to within 10mm of the finished surface before a final coat was applied and smoothened with a steel float. The repair operation was carried out under laboratory conditions of temperature and humidity. Upon completion of the repair, the fresh material was covered with polythene sheeting. After 24 hours of curing, demec points were attached to the surface of the repair patch at a gauge length of 100mm in order to measure longitudinal strain at different sections parallel to the neutral axis of the beam. After three days, the polythene sheeting and formwork were removed (see Figure 7.7).

Out of a total of eight beams, six were repaired in an unpropped state as described above. The remaining two beams were repaired in a propped state. The repair of the propped beams differed from the repair of the unpropped beams in that the service load on the latter beam was released during repair (see Figure 7.8). The load was reapplied when the cube strength of the repair material reached the cube strength of the reinforced concrete beam or at 28 days, whichever was sooner (see Figure 7.9).

Figure 7.6 Application of a hand applied repair material and installation of embedment strain gauges to an unpropped flexural member in the laboratory

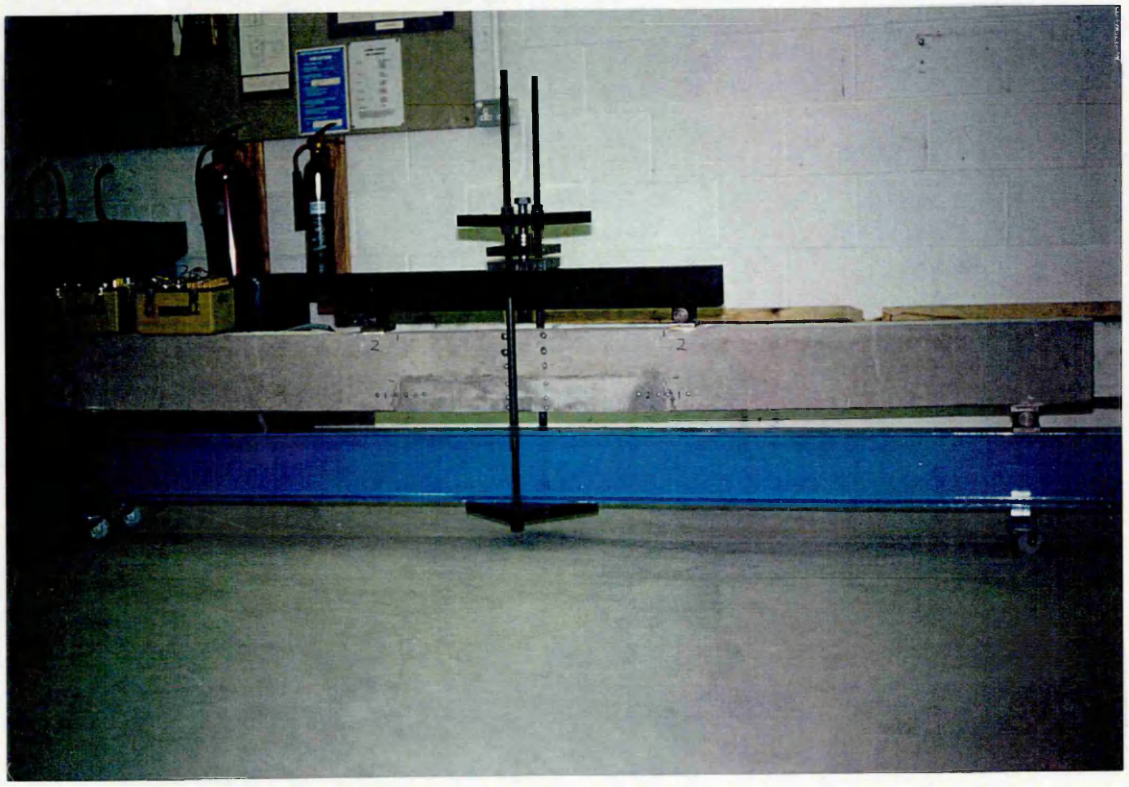

Figure 7.7 View of completed hand applied repair to an unpropped flexural member in the laboratory

Figure 7.8 Application of a hand applied repair material to a propped flexural member in the laboratory

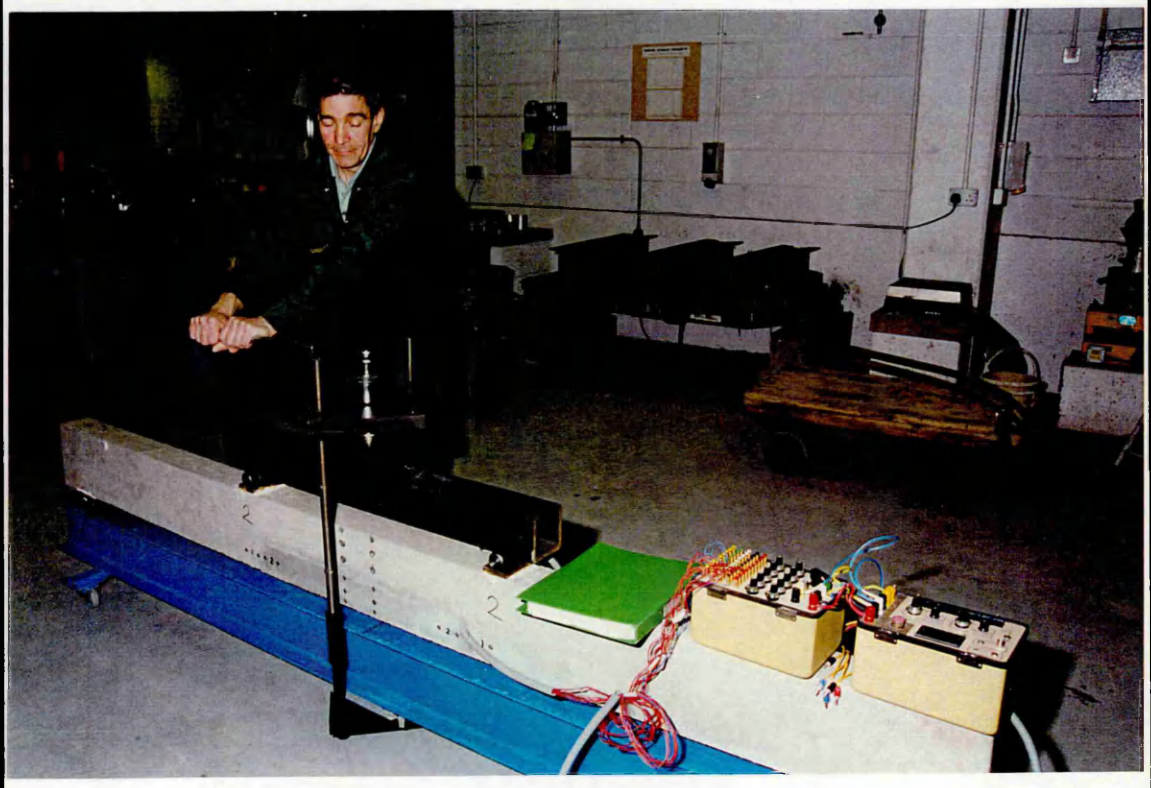

Figure 7.9 Reloading a beam at 28 days after the application of the repair patch (the load was removed during application of the repair)

Upon completion of the repairs, the flexural members were stored under load in a controlled environment throughout the duration of the monitoring period (20°C and 55% RH, see Figure 7.10), Strain readings from the steel reinforcement, repair material and substrate concrete were taken every day for the first 6 days after repair and once a week thereafter (a view of the digital strain indicator which monitors the electrical resistance strain gauges is given in Figure 7.11).

Figure 7.10 Repaired reinforced concrete beams under load in a controlled environment (20°C and 55% RH)

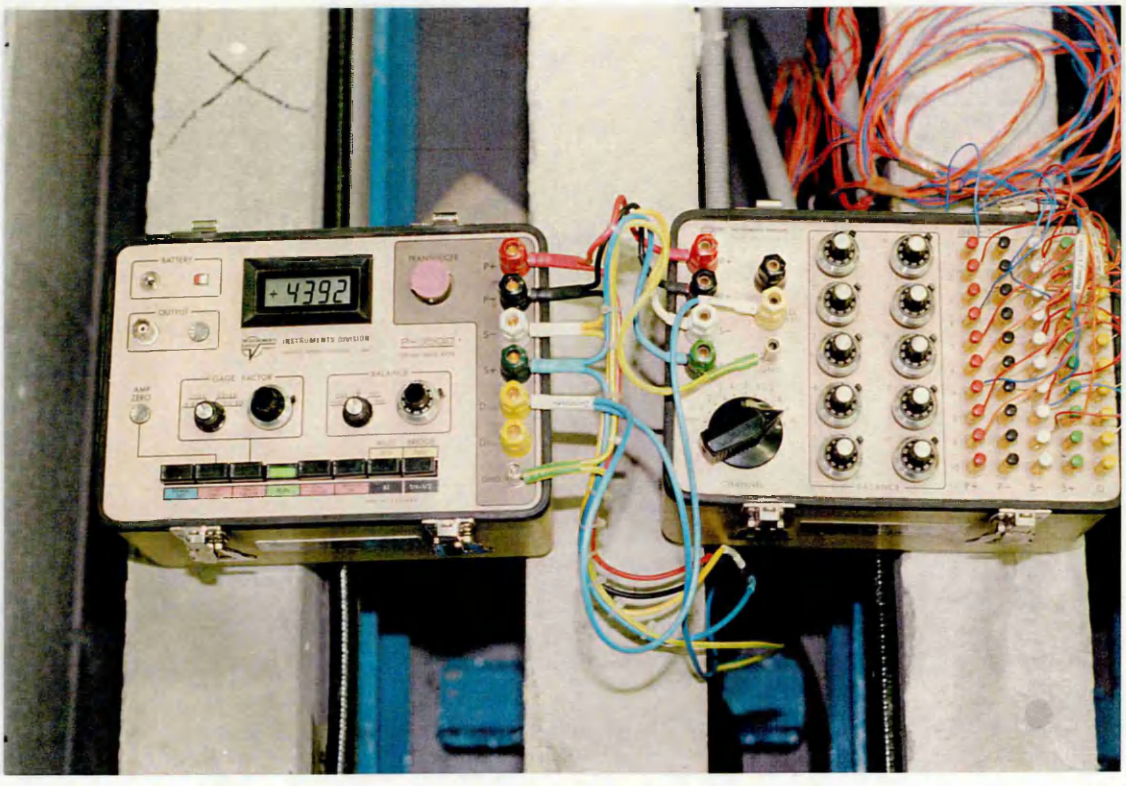

Figure 7.11 Digital strain indicator (left) and switch and balance unit (right) which were used to monitor the electrical resistance strain gauges

CHAPTER 8

PROPERTIES OF REPAIR MATERIALS WHICH INFLUENCE THE LONG TERM PERFORMANCE OF CONCRETE REPAIR

8.1 INTRODUCTION

When a concrete structure exhibits signs of distress, such as spalling of concrete cover, delaminations or rust staining, the service life can be extended by the application of a new material in place of the damaged concrete. This method of rehabilitation can only prove to be successful if the new material interacts well with the parent concrete and forms a durable barrier against ingress of carbon dioxide and chlorides. Problems may arise since a dimensionally unstable repair material is placed against a dimensionally stable substrate concrete, as any significant drying shrinkage and creep will no longer exist in the substrate concrete due to its long term exposure to the environment and the service loading. Internal stresses will be generated due to shrinkage and creep in the repair material which need to be evaluated before a durable repair can be specified.

Tensile shrinkage stress will be induced in the repair patch due to the restraint provided by the substrate concrete. To reduce the restrained tensile stress in the material, it is best to specify a repair material with low shrinkage characteristics. Moreover, a repair material with a high tensile strain capacity will be very beneficial if the tensile stress is

high. Furthermore, a repair material which expands slightly in the early stages may cancel or reduce the final net shrinkage strain in the material.

Creep is a phenomenon which occurs in cement based materials when subjected to a sustained stress, either in compression or tension. The magnitude of creep varies in different materials and is dependant upon the magnitude of load applied and the different constituents and composition of the material. Compressive creep may render the load sharing capacity of a repair patch less effective with time, whereas tensile creep may help alleviate the high tension induced due to restrained shrinkage [24].

The stiffness (elastic modulus) of the repair material is also an important material property, as a material which is stiffer than the substrate concrete is able to attract more stress into the repair patch, whereas the opposite is true for a material which is less stiff than the concrete substrate [25]

The results of the shrinkage, creep, elastic modulus and modulus of rupture tests carried out on the repair materials used in the research will be presented in this chapter, but first a brief literature review will be presented.

8.2 LITERATURE REVIEW

8.2.1 Shrinkage deformation

8.2.1.1 Free shrinkage

Over the past number of years, the number of researchers investigating the properties of repair materials has increased considerably. Arguably the most frequently investigated

repair material property is drying shrinkage, or more correctly, volume change, as some repair materials have a tendency to expand as well as shrink. Emmons *et al* [26] report that shrinkage in the repair material can effect the durability of the repair patch along with the load carrying capacity of the repair patch. Shrinkage cracking on the surface of a repair material greatly affects the appearance of the repair patch. When cracking occurs in a repair material, remedial works may be required to seal the cracks to restrict the ingress of chlorides and carbon dioxide to the steel reinforcement level. This occurred with some repair materials monitored in the field studies of the present investigation.

The results of shrinkage tests carried out on 46 different proprietary repair materials in Canada [27] are presented by Morgan [28]. The tests were carried out using the ASTM C157 test method. One of the materials showed a slight expansion at 30 days, whereas the rest exhibited varying amounts of free shrinkage. A typical structural concrete tested in the same manner displayed a drying shrinkage of 0.05%. Only 15% of the materials tested displayed a shrinkage which was less than this figure. Over 50% of the materials had shrinkage strains twice as great as the plain concrete, despite the manufacturers' claims that they were expansive, non-shrinking or shrinkage compensated. The free shrinkage of a structural concrete tested in a previous study at Sheffield Hallam University [24] was 450 microstrain at 90 days (storage conditions: 20°C and 55% RH). Only two of the thirteen commercially available repair materials (i.e. 15%, similar to the ratio presented by Morgan [28]) tested for shrinkage in the current research exhibited shrinkage strains lower than 450 microstrain, again despite the manufacturers' claims that they were shrinkage compensated (storage conditions and

specimen size were identical to the previous study [24]). 23% of the repair materials (as opposed to 50% presented by Morgan [28]) had shrinkage strains twice as great as the structural concrete. High shrinkage strains in repair materials were also found by Mangat and Limbachiya [29, 30]

Dector and Lambe [31] report on the Hong Kong Housing Authority (HKHA) specifications for repair mortars. Mortars are classified on the basis of their compressive strength, but other material properties which are equally important are also specified (see Table 8.1) [31]. The drying shrinkage, as shown in TM8 (Test Method 8) Table 8.1, is limited to 300 microstrain at 7 days for each class of mortar. The specimen size is 25 x 25 x 285mm (surface/volume ratio = 0.17) and storage conditions are 27°C and 55% RH - the effect of specimen size and curing conditions on free shrinkage is considered in section 8.2.1.4. Another requirement is that no cracks shall be evident at 28 days when the repair material is cast in the Coutinho ring (the Coutinho ring made of steel restrains mortar from shrinkage which induces tension in the repair material - see Section 8.2.1.2).

The strict requirements of the specifications in Table 8.1 have undergone amendments and the four main classes have now been reduced to three broader classes (see Table 8.2). TM8, for drying shrinkage, is also temporarily removed from the revised specification in Table 8.2 and is under review as few materials were found to have drying shrinkage less than 300 microstrain at 7 days as specified in Table 8.1. 50% of the materials tested in the current study exhibited free shrinkage which was less than

Table 8.1 Technical specifications for repair mortars* [31]

1.	Characteristics of repair mortar				
Characteristics		*Mortar class*			
		60	*40*	*25*	*15*
TM1	Range of compressive strength at 28 days, N/mm^2	40-80	25-55	15-35	10-20
TM2	Flexural strength	no specific requirements			
TM3	Minimum tensile strength at 7 days, N/mm^2	2.5	2.0	1.5	1.0
TM4	Range of modulus of elasticity at 28 days, kN/mm^2	20-30	13-20	8-13	5-8
TM5	Minimum bond strength at 7 days, N/mm^2	2.5	2.0	1.5	1.0
TM6	Cracking in Coutinho Ring test at 28 days	nil	nil	nil	nil
TM7	Minimum Figg air permeability, seconds	250	200	150	100
TM8	Maximum drying shrinkage at 7 days, microstrain	300	300	300	300
	Minimum pull off stress at 7 days, N/mm^2	1/4 x minimum bond strength at 7 days			

* *Taken from Hong Kong Housing Department Manual of Structural Maintenance*

300 microstrain at 7 days, but the larger specimen size of 100 x 100 x 500mm (which gives a lower surface/volume ratio of 0.04) and storage conditions of 20°C and 55% RH differ to the HKHA (Hong Kong Housing Authority) test conditions. These would result in lower free shrinkage in the repair materials compared with tests carried out according to HKHA conditions (surface/volume ratio 0.17, 27°C and 55% RH).

Table 8.2 Amended version of Hong Kong Housing Authority specification, April 1991 [31]

1. Characteristics of repair mortar				
Characteristics		*Required Values*		
		Class 40	*Class 25*	*Class 15*
TM1	Range of compressive strength at 28 days, N/mm^2	30-60	20-40	10-30
TM3	Minimum tensile strength at 7 days, N/mm^2	2.0	1.5	1.0
TM4	Range of modulus of elasticity at 28 days, kN/mm^2	15-25	9-15	5-9
TM5	Minimum bond strength at 7 days,	2.0	1.5	1.0
TM6	Cracking in Coutinho Ring test at 28 days	0	0	0
TM7	Minimum Figg air permeability, seconds	200	150	100

The Australian standard for testing concrete, AS 1012, Part 3 [32] also takes an interest in drying shrinkage [31]. A drying shrinkage of not greater than 450 microstrain at 28 days has been put forward. The specimen size is 75 x 75 x 285mm (surface/volume ratio = 0.06) and storage conditions are 23°C and 50% RH. 33% of the repair materials tested in the current study exhibited free shrinkage which was less than 450 microstrain at 28 days. The surface/volume ratio of 0.06 was similar to the Australian standard, but the storage conditions of 20°C and 55% RH would result in lower free shrinkage in the repair materials compared to tests carried out according to Australian conditions (23°C and 50% RH).

The UK Department of Transport's 1987/88 maintenance programme included the use of shrinkage-compensated flowable concretes on two concurrent trial repair contracts on the Midland Links Motorway viaducts. The repair materials were based on their specifications document, BD 27/86 [1]. With regards to the shrinkage of the repair materials, the *New Civil Engineer* [33] argues that these materials should show no sign of cracking after 56 days. This is a stringent requirement of a repair material. However, it is helped by the fact that most of the total shrinkage in a flowing repair material occurs in the first 24 hours (see Section 8.2.1.3, Table 8.4) when the degree of restraint is low. Nevertheless, only 25% of the repair patches at Sutherland Street Bridge (flowing repairs) were crack-free at 56 days, but other influences such as steel covers on the surface of the repair patches to protect the gauges contributed significantly to the short-term performance of the repair materials (full details are given in Chapter 9).

8.2.1.2 Restrained shrinkage

Test methods used to examine the effect of restrained shrinkage in a repair material generally rely on cracking to occur in the mortar within a given time period [31]. The most widely used test method for restrained shrinkage is to cast a repair material in the Coutinho Ring [34] (steel ring) and monitor the performance of the repair material over 28 days. The Coutinho Ring serves a restraint for the shrinking mortar, therefore, tension is induced into the sample as the repair material tries to shrink. The repair material is assumed to have passed the restrained shrinkage test if no cracks are evident at 28 days. This test is included in the draft Department of Transport standard, BD /94 [35], which aims to supersede the current repair specification, BD 27/86 [1].

The German BAM Trough Test [36] also evaluates the performance of a mortar under restrained shrinkage conditions. The mortar is cast in a 1 metre long grit blasted steel trough which provides a restraint to shrinkage. The appearance of cracks (in this case, cracks which are greater than 0.02mm) are monitored for 90 days.

Figure 8.1 [37] shows the difference between unrestrained and restrained shrinkage for two concretes modified with Acrylic and SBR latexes. The ratio of the acrylic modified concrete was 10 : 0.45 : 0.85 : 5 [mortar powder : admixture : water : aggregate (10mm)] whereas the ratio of the SBR modified concrete was 10 : 1.8 : 5 [mortar powder : admixture : aggregate (10mm)].

The free shrinkage during the first 24 hours was measured in a mould made of perspex [38] and subsequently the change in length of the hardened mortars was measured for up to 28 days in accordance to the recommendations given by Brull *et al* [38]. The restrained shrinkage in the repair material was measured from two repaired sections (repairs were carried out on reinforced concrete beams measuring 5200 x 150 x 250mm deep). The repairs were in the tensile zone. Restrained shrinkage measurements were taken by means of a demec extensometer gauge 10mm above the soffit of the repair. It is clear from Figure 8.1 [37] that the repair mortars are restrained against shrinkage by the substrate concrete and steel reinforcement within the repair patch. The free shrinkage for both repair materials is higher than the restrained shrinkage, although the restrained expansion in the early ages in the SBR material is unusually higher than the free expansion (Figure 8.1). The 14 day restrained shrinkage of the acrylic modified repair material is approximately 48% of the free shrinkage; similarly, the 14 day

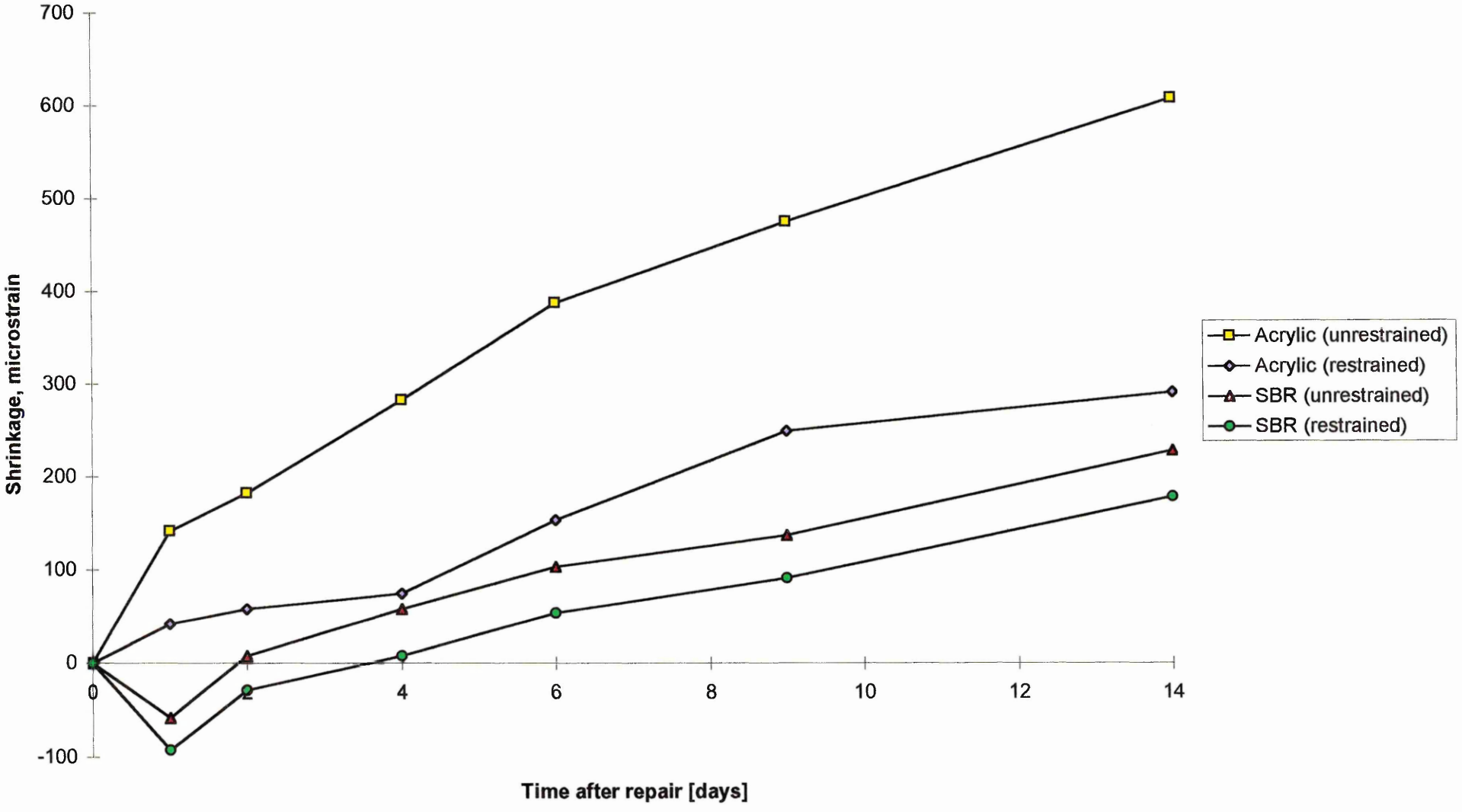

Figure 8.1 Comparison between free and restrained shrinkage for two repair mortars [37]

restrained shrinkage of the SBR modified repair material is approximately 78% of the free shrinkage (Figure 8.1).

8.2.1.3 Comparison between hardened and plastic shrinkage

Repair material manufacturers' generally quote the 28 day drying shrinkage in their product brochures. Possibly equally important is the short term drying shrinkage, i.e. when the materials are in a plastic state. This occurs when the material has a negligible elastic modulus and strength, hence the induced stress due to restraint will be lower but may be significant to cause cracking due to the lower shrinkage. This short term shrinkage may in fact make up a considerable part of the longer term shrinkage. Both of these properties were evaluated by Emberson and Mays [25]. One material from each of the categories listed in Table 8.3 was selected for monitoring. The early (0-24 hours) and long term shrinkage (24 hours-16 months) was evaluated for all the repair materials. An apparatus which was first developed by Staynes [37] was used to measure the early age shrinkage. The long term free shrinkage (24 hours to 16 months) was measured using unrestrained prisms of 40mm square by 160mm in length. Vibrating wire strain gauges were attached to two opposite faces of each specimen for this purpose. The results of these tests are given in Table 8.4.

Table 8.3 Categories of systems for concrete patch repair [25]

Resinous materials	*Polymer modified cementitious materials*	*Cementitious materials*
A: Epoxy mortar	*D*: SBR modified	*G*: OPC/sand mortar
B: Polyester mortar	*E*: Vinyl acetate modified	*H*: HAC mortar
C: Acrylic mortar	*F*: Magnesium phosphate modified	*I*: Flowing concrete

Table 8.4 Shrinkage strain results [25]

Repair material	*Category*	*Shrinkage*			
		0-24h	*24h-16 mths*	*0-16 mths*	$\frac{0-24hours}{0-16months}\%$
A	Epoxy	170	50	220	*77*
B	Polyester	4680	280	4960	*94*
C	Acrylic	80	360	440	*18*
D	SBR	920	740	1660	*55*
E	Vinyl acetate	2400	1060	3460	*69*
F	Mag. phosphate	-830	-700	-1530	*54 (expansion)*
G	OPC/sand	710	1140	1850	*38*
H	HAC	350	760	1110	*32*
I	Flowing	1120	650	1770	*69*

Note: Shrinkage strain (positive); expansion strain (negative)

A comparison of the early age shrinkage against the long term shrinkage is also given in Table 8.4. The modified repair mortars C, D & E, and the unmodified repair mortars G, H & I, show an early age shrinkage of between 18% and 69% of the total long term shrinkage. These mortars are similar to some of the repair materials tested in the current project. If most of the shrinkage occurs within the first 24 hours when the elastic modulus of the repair material is low and full bond to the substrate concrete and steel reinforcement is not yet achieved, the degree of restraint provided by the substrate concrete and steel reinforcement will be negligible. The repair material will therefore have some freedom of movement which will result in a low restrained shrinkage stress. Consequently, cracking in the repair material may be avoided. Repair materials most suitable for repair applications are likely to be the ones with low overall shrinkage and maximum proportion of the shrinkage occurring in the first 24 hours. On this basis the epoxy based material A is best (see Table 8.4). Material C is also suitable for repair

applications, since the long term shrinkage is relatively low (440 microstrain) even though the proportion of shrinkage occurring in the first 24 hours is also low (18% - see Table 8.4).

8.2.1.4 Influence of material constituents on shrinkage

8.2.1.4.1 Aggregates and cement

The material constituents that make up the mixture greatly affect the shrinkage in the repair material. Schrader [40] reports that shrinkage can be very different for various concretes and repair materials and pinpoints aggregate type as a major factor for influencing shrinkage. Mixtures with highly absorptive aggregates tend to shrink more and those with dense low absorptive aggregates tend to shrink less. Shrinkage increases whenever the cement content is increased, even if the water content is kept constant. Comparisons are also made between two commercial repair materials and typical concrete. Shrinkage was found to be greatest in the repair materials (2500 and 1000 microstrain versus 300 microstrain in the plain concrete) The only essential difference between the two repair materials was that the material with the lower shrinkage (1000 microstrain) contained more and larger aggregate. Consequently, it had less cement, less water and less shrinkage. A similar situation occurred in the present study, as repair materials with coarse aggregates in the mix exhibited lower free shrinkage than repair materials with fine aggregates. Elsewhere, investigations into the free shrinkage of commercially available repair materials [29, 30] also found that repair materials which contain coarse aggregate particles had less shrinkage than repair materials which did not contain coarse aggregate particles.

Tests were conducted by Lea [41] on plain concretes in which the aggregate/cement ratio and the water/cement ratio was varied to determine the effect of these parameters had on the shrinkage of mortar and concrete. The results (see Table 8.5) show that increasing the aggregate/cement ratio reduces the shrinkage of the mortar and concrete. However, an increase in water/cement ratio increases the shrinkage.

Another paper [42] recommended the use of higher strength concrete with low water-cement ratio and superplasticisers or the use expansive cements in order to reduce shrinkage in repair materials. Emmons *et al* [26], on the other hand, argued that high strength is achieved with high cement contents and consequently, these materials will have high drying shrinkage.

8.2.1.4.2 <u>*Admixtures*</u>

The effect that polymers have on the shrinkage of repair materials is studied by Pinelle [43]. His results showed that the free drying shrinkage of an acrylic copolymer

Table 8.5 Shrinkage of mortar and concrete, 127mm square in cross-section, stored at a relative humidity of 50% and 21°C [41]

Aggregate/cement ratio	*Shrinkage after 6 months (microstrain) for water/cement ratio of:*			
	0.4	*0.5*	*0.6*	*0.7*
3	800	1200	-	-
4	550	850	1050	-
5	400	600	750	850
6	300	400	550	650
7	200	300	400	500

modified mortar was reduced by approximately 20% compared to an unmodified mortar. However, a vinyl acetate modified mortar did not have a significantly different free drying shrinkage compared to the unmodified sample. In tests carried out by Mangat and Limbachiya [29,30] where three commercially available repair materials were tested for shrinkage, it was found that shrinkage was greatest in polymer modified repair materials despite the presence of some fibre additives. It was difficult to isolate the effect that polymers had on the free shrinkage of the repair materials in the present study, since the free shrinkage of the modified repair materials varied between 325 microstrain and 1311 microstrain, but it was generally found that the inclusion of coarse aggregates was more effective in reducing the shrinkage than the inclusion of polymers.

Dector and Lambe [31] compare the shrinkage of basic sand and cement mortar to cementitious repair materials to quantify the magnitude of drying shrinkage that repair materials exhibit (Figure 8.2). They report that technology has developed significantly which has led to a reduction in drying shrinkage of repair materials. Referring to Figure 8.2 [31], the free shrinkage of a basic sand:cement mortar is given along with the free shrinkage of typical repair materials manufactured in 1989 and 1992 with the advances in cement chemistry and copolymer technology of that era. Clearly, the repair materials manufactured in 1989 and 1992 exhibit lower free shrinkage than the sand:cement mortar, see Figure 8.2 [31]. This does not agree with the results of the current study and other studies [29, 30], as the results show that of the thirteen commercially available repair materials tested for free shrinkage, seven repair materials exhibited higher free shrinkage than a basic sand/cement mortar (ratio 3:1), whereas the other six exhibited free shrinkage that was lower than the reference sand/cement mortar.

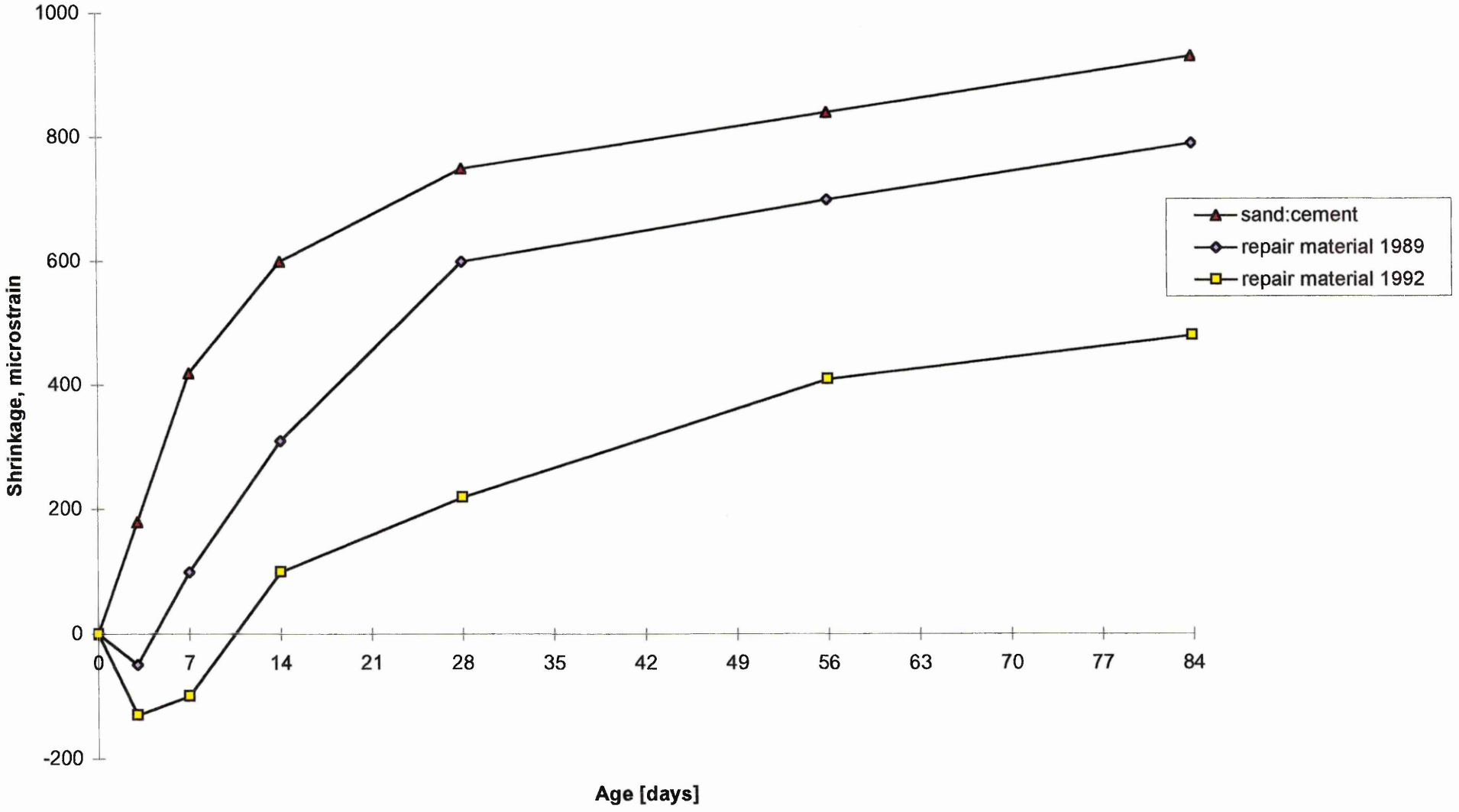

Figure 8.2 Comparison of free shrinkage in repair materials versus basic sand:cement mortar [31]

8.2.1.5 Influence of specimen size on the shrinkage of repair materials

Shrinkage of a repair material can be obtained by preparing samples and monitoring the deformation which occurs over a period of time. There are various standards world-wide for measuring shrinkage strains in concrete/repair materials, a list of some are given in Table 8.6 [31]. It can be seen from Table 8.6 that the specimen size and curing conditions vary from standard to standard. Shrinkage is very much affected by the specimen size and shape and storage conditions [29-31]. Figure 8.3 [31] shows the drying shrinkage results for a repair material tested under UK conditions (20°C, 65% RH), cast as a large prism (75 x 75 x 270mm, surface/volume ratio = 0.06) and HKHA conditions (27°C, 55% RH) cast as a small prism (25 x 25 x 285mm, surface/volume ratio = 0.17). The smaller prism specified by HKHA gives a much greater surface area to volume ratio (0.17 versus 0.06) which encourages more rapid drying of the specimen. Consequently, greater drying shrinkage occurs in both the early ages, which offsets the expansion in the repair material, and in the long term (see Figure 8.3). On the other hand, the lower surface/volume ratio of the UK specimens results in lower free shrinkage, hence, the benefit of having expansion in the repair material in the early ages is not lost. This is shown by comparing the initial expansion in the repair material tested under UK conditions (surface/volume = 0.06) with the shrinkage in the repair material tested under HKHA conditions (surface/volume = 0.17, Figure 8.3). Similarly, greater surface/volume ratios are also evident in USA (ASTM) and German (DIN) standards (see Table 8.6) Higher drying shrinkage will also be evident in repair materials which comply with the Hong Kong standard since the storage conditions of

Table 8.6: Drying shrinkage - Length change measurements [31]

Specification/ standard	*Conditions*	*Prism Dimensions (mm)*	*Surface / Volume ratio*
HKHA	27°C, 55% RH	25 x 25 x 285	0.17
Australian			
AS 1012 Part 3 - 1970	23°C, 50% RH	75 x 75 x 285	0.06
USA			
ASTM C157 - 1989	23°C, 50% RH	25 x 25 x 285	0.17
UK			
BS 1881 Part 5 - 1970	This standard does not relate to drying shrinkage therefore test conditions are not included here	75 x 75 x 270	0.06
Germany			
DIN 52450 - 1985	Various: 20°C, 65% RH 23°C, 50% RH 20°C, 45% RH 20°C, 95% RH min 20°C, Wet	40 x 40 x 60	0.13

relatively higher temperature (27°C) and lower relative humidity (55%) will increase the shrinkage in these specimens. In the current study, the test specimens measured 100 x 100 x 500mm (surface/volume ratio = 0.04) and were cured at 20°C and 55% RH. Therefore, this specimen size and curing condition will lead to lower free shrinkage compared with those tested under specifications listed in Table 8.6.

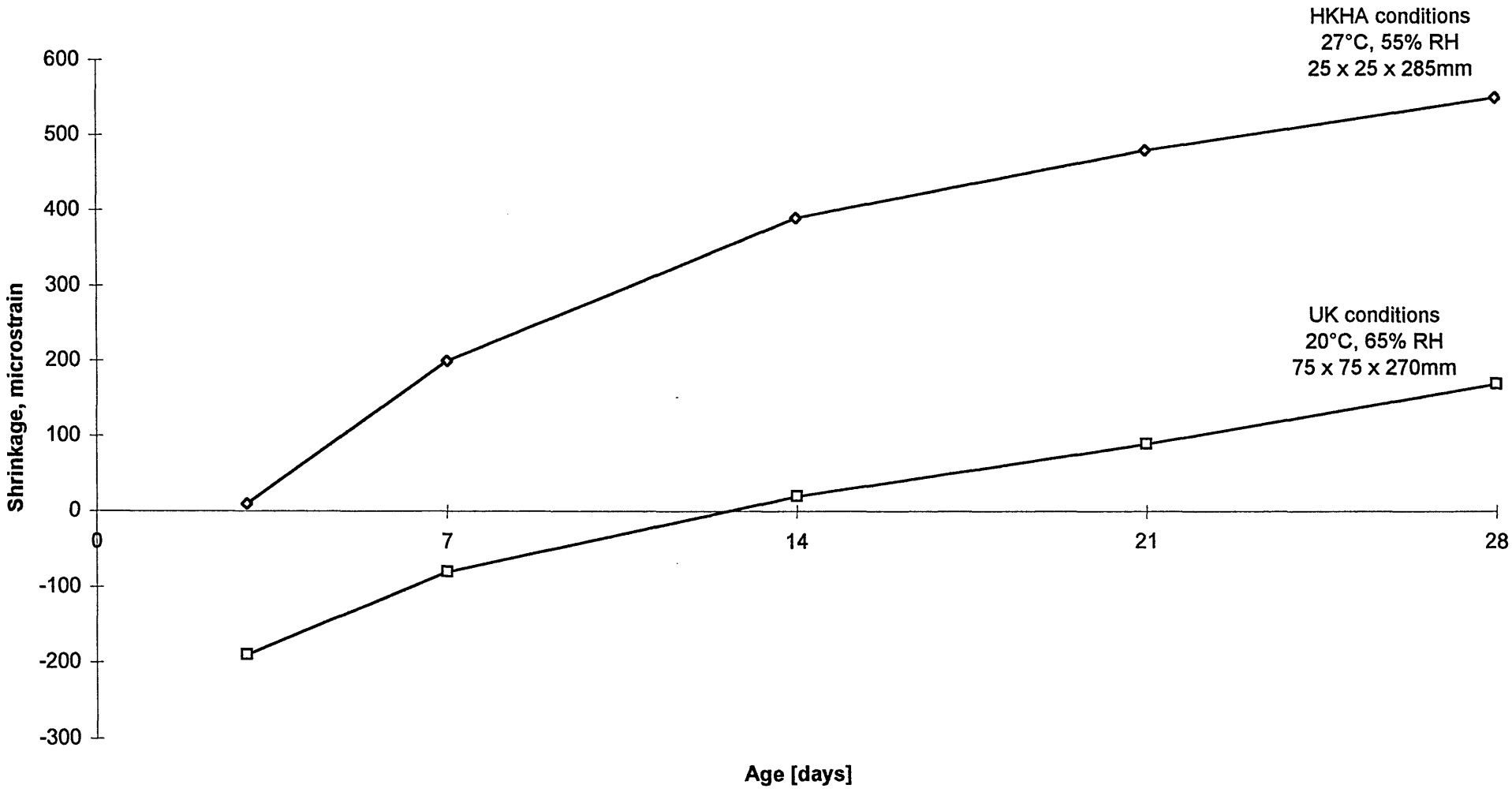

Figure 8.3 Comparison between UK conditions and HKHA conditions for measuring free shrinkage of a repair material [31]

8.2.2 Creep deformation

The effect that creep will have on the performance of a repair patch is widely reported [29, 30]. Cusson *et al* [44] report that creep is the continuous deformation of a member subjected to a sustained stress. It can result in reduced load bearing effectiveness in the repair material and also result in load transfer from the repair material to the substrate concrete. In the case of structural repairs loaded in compression, the repair material must posses very low creep potential in order to effectively attract load. On the other hand, in the case of repair patches which are in tension, creep can be beneficial, as it can reduce or cancel the adverse effect of shrinkage in the repair material [45]

8.2.2.1 Compressive creep

Compressive creep occurs in cementitious materials when subjected to a sustained stress in compression. The compressive creep strain can be divided conveniently into three components: elastic, delayed elastic and flow creep [46], as defined graphically in Figure 8.4 [46] for concrete under load between time t_1 and t_2. Immediately after application of the load at t_1, an instantaneous elastic strain is evident in the concrete. The concrete remains under load between t_1 and t_2, and exhibits a creep strain in the process, which includes a delayed elastic component. Upon removal of the load at t_2, an immediate elastic recovery is evident in the concrete. Creep recovery then occurs over a period of time which has two phases: rapid initially and slow in the later stages. The creep recovery is also evident as the delayed elastic creep. Creep strain can be defined as the sum of the flow and delayed elastic components (see Figure 8.4).

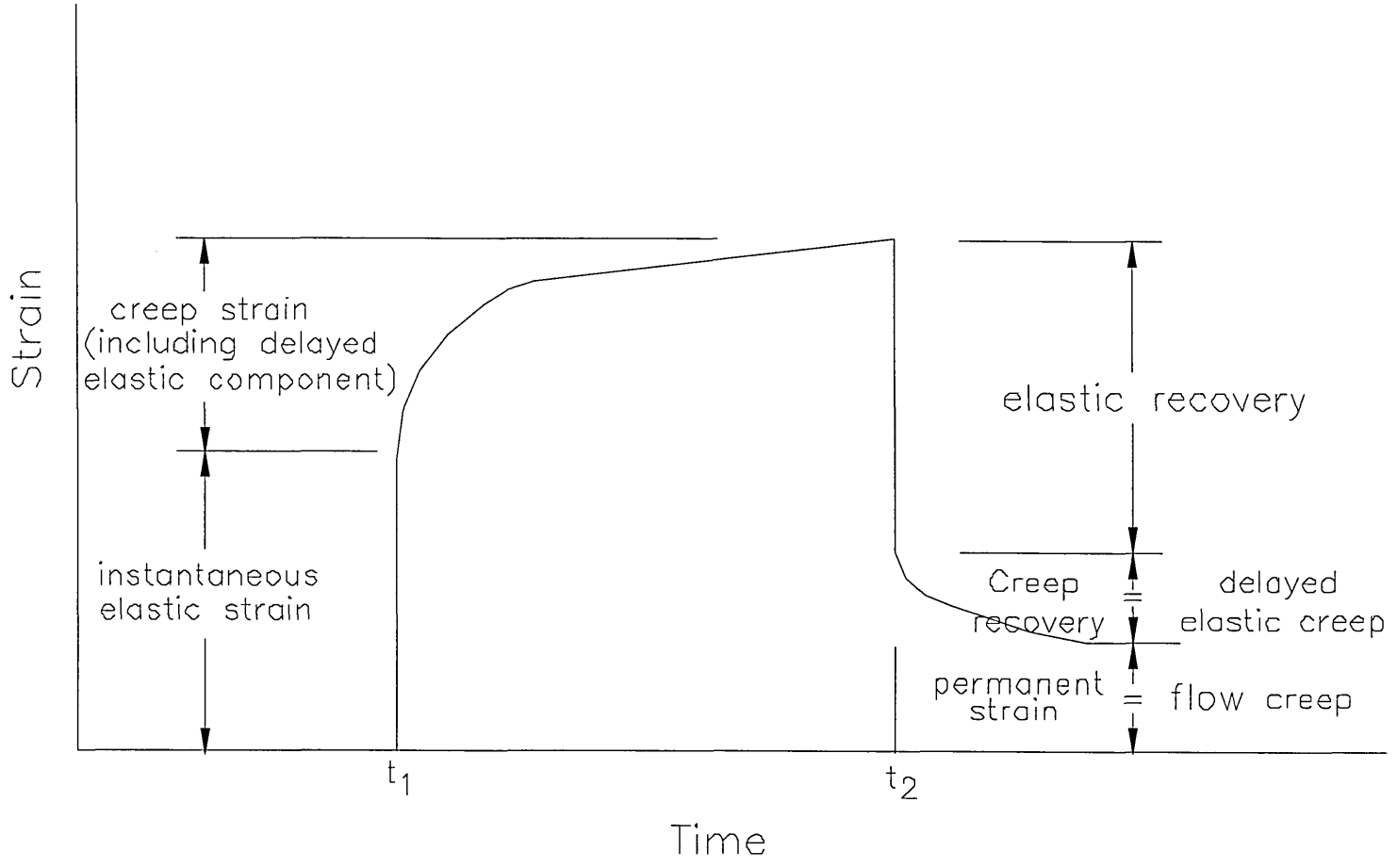

Figure 8.4 Components of compressive creep in concrete [46]

8.2.2.1.1 *Influence of material constituents on creep*

Emberson and Mays [25] tested nine different repair material categories, as listed in Table 8.3, to obtain information on the compressive creep characteristics of repair materials. The repair materials were loaded to a compressive stress of 10 N/mm^2 at an age of 28 days. The initial strain on loading and subsequent increases of strain were monitored using a pair of vibrating wire strain gauges attached to opposite faces of each specimen. Table 8.7 shows the gross and net creep strains in the repair materials. The net creep strains are obtained by subtracting the free shrinkage measured over the same time period on identical specimens from the gross creep strains. The net creep strains only are of interest in this section and these are discussed below.

The conclusions drawn from these results (net creep strains) are:

- material C, the acrylic resin mortar, has a very high creep strain (4110 microstrain) after 15 months

Table 8.7 Compressive creep strain results (microstrain) [25]

Repair material	*Category*	*Shrinkage 1-16 months*	*Gross creep 1-16 months*	*Net creep 1-16 months*
A	Epoxy	0	720	720
B	Polyester	10	1380	1370
C	Acrylic	100	4210	4110
D	SBR	200	430	230
E	Vinyl Acetate	420	2020	1600
F	Mag. Phosphate	320	330	10
G	OPC/Sand	440	840	400
H	HAC	280	1240	960
I	Flowing	210	790	580

- the vinyl acetate modified system (material E) also has a high creep strain (1600 microstrain)
- the lowest creep strains were exhibited by SBR modified and magnesium phosphate systems (materials D and F) (230 and 10 microstrain respectively)
- the net creep of the flowing system (material I, 580 microstrain) resembles more closely that of sand-cement mortar (400 microstrain).

Mangat and Limbachiya [29, 30] also found that compressive creep strains were greatest for repair materials which contained styrene acrylic copolymer, compared to other repair materials. Similar observations were encountered in the present study, as the repair materials with the highest creep strains were those modified with styrene acrylic. The creep strains of the sand/cement mortar and flowing materials resembled the creep strains of similar materials tested by Emberson and Mays [25].

8.2.2.1.2 *Creep coefficient*

Table 8.8 summarises the creep coefficient, ϕ (creep strain divided by instantaneous elastic strain) as observed by Emberson and Mays [25] for repair materials subjected to a sustained compressive stress. The net creep coefficient for materials C-E and G-I (similar to those tested in the current project) ranged from 0.9 to 8.6 (0.9 to 3.3 if the unusually high creep coefficient of material C is omitted). The range of creep coefficients of the repair materials tested in the current project ranged between 0.54 and 3.29 which are marginally lower to those tested previously [25] (with the exception of material C). The difference in creep coefficients between the study conducted by

Table 8.8 Creep coefficient, ϕ, at age 16 months (age of loading 28 days, stress 10 (N/mm^2) [25]

Repair Material	*A*	*B*	*C*	*D*	*E*	*F*	*G*	*H*	*I*
Net creep factor	1.4	3.3	8.6	0.9	2.8	0.1	1.1	3.1	2.2
Stress/strength	0.14	0.10	0.14	0.13	0.17	0.13	0.12	0.13	0.09

Emberson and Mays [25] and the present study may be due to factors such as (i) different repair material constituents, such as cement content and aggregate type/content, (ii) a constant stress of 10 N/mm^2 was applied to the repair materials tested previously whereas a stress/strength of 0.30 was applied to the repair materials in the present study, (iii) the curing and storage conditions may have differed to those of the present study (information on this is absent in the previous study) and (iv) the specimen size was 40 x 40 x 160mm previously compared to the specimen size of 100 x 100 x 500mm in the current investigation which may have an influence on the results.

Figure 8.5 [37] shows the development of creep coefficient of three repair concretes which were modified with acrylic, SBR and styrene acrylic. All concretes were loaded 14 days after casting. No information was given on the curing regimes adopted. Referring to Figure 8.5, the creep coefficient of the acrylic, SBR and styrene acrylic modified concretes was approximately 2.17, 1.73 and 1.2 respectively at 14 days. The creep coefficients of the acrylic and SBR modified mortars tested by Emberson and Mays [25] was 8.6 and 0.9 respectively, which differed significantly to the values obtained by Yuan and Marosszeky [37]. The differences were possibly due to the material constituents: Emberson and Mays [25] tested mortars whereas Yuan and Marosszeky [37] tested modified concretes. The styrene acrylic modified repair

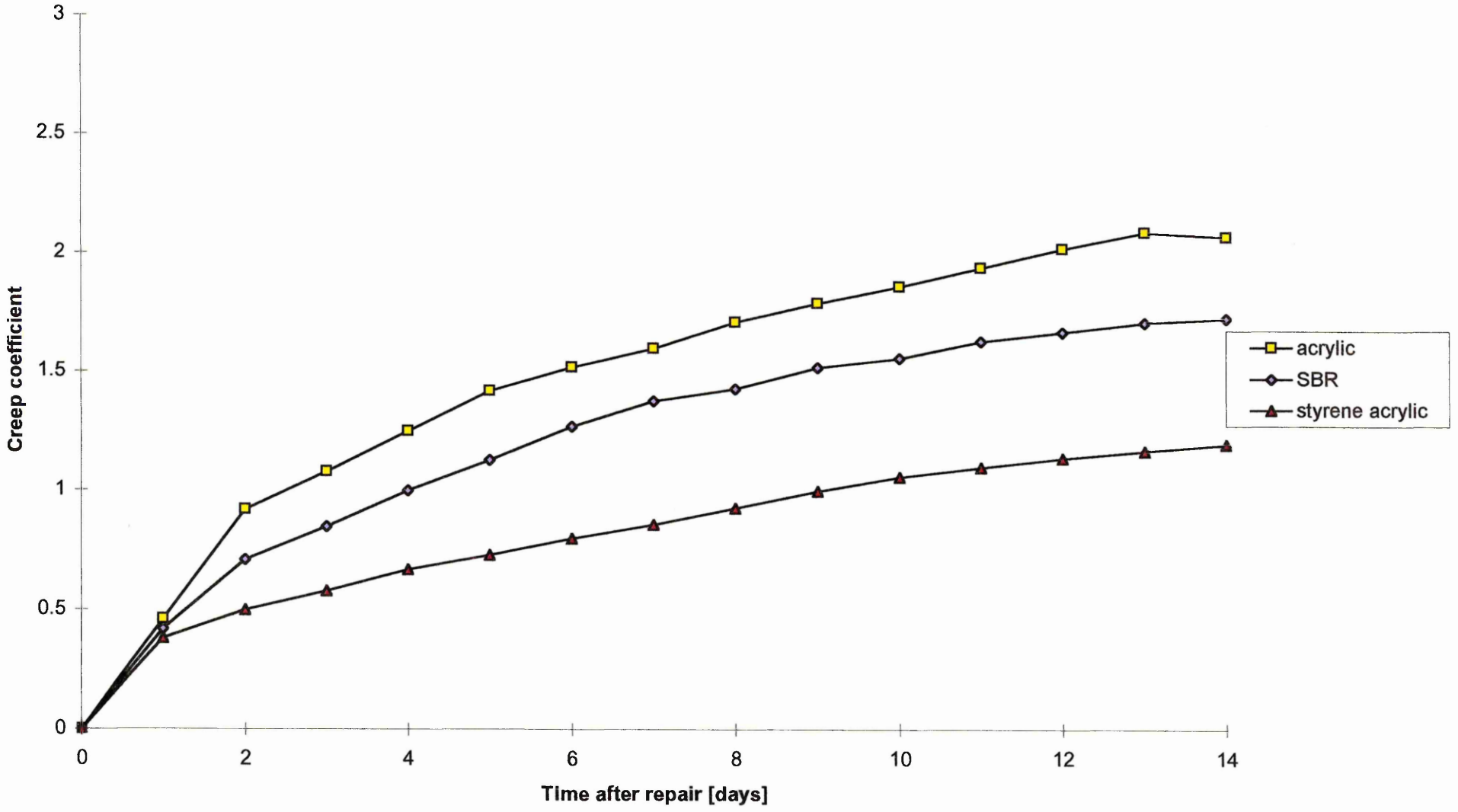

Figure 8.5 Development of creep coeffieient of three repair mortars loaded 14 days after casting [37]

materials in the current project exhibited creep coefficients ranging between 1.25 and 3.29, which encompass the coefficient of 1.73 found by Yuan and Marosszeky [37].

A high creep coefficient will result in a low effective elastic modulus, which will reduce the load bearing effectiveness of the repair material. On the other hand, it will allow significant stress relaxation which may prevent cracking in the repair material when high tensile stresses are induced due to restrained shrinkage.

Figure 8.6 [37] shows the development of creep coefficient of an SBR modified concrete for different ages of loading. The repair concrete was loaded at an age of 2, 4, 7, 14, and 28 days after casting. The creep coefficients up to 14 days are presented. A summary is given in Table 8.9. It is clear from Figure 8.6 that the creep coefficient is higher for materials loaded at earlier ages (compare the creep coefficient for t = 2 days with the creep coefficient for t = 28 days in Figure 8.6). The creep coefficient of the repair concrete loaded at 2 days after casting is 2.18 times greater than the creep coefficient of the repair concrete loaded 28 days after casting. This ratio decreases to

Table 8.9 Ratio of early age creep coefficient to 28 day creep coefficient for SBR modified concrete (from Figure 8.6 [37])

	Age t: (days)				
	2	*4*	*7*	*14*	*28*
Creep coefficient	2.49	2.10	1.81	1.19	1.14
Ratio $\left[\frac{t(days)}{28(days)}\right]$	2.18	1.84	1.59	1.04	1.00

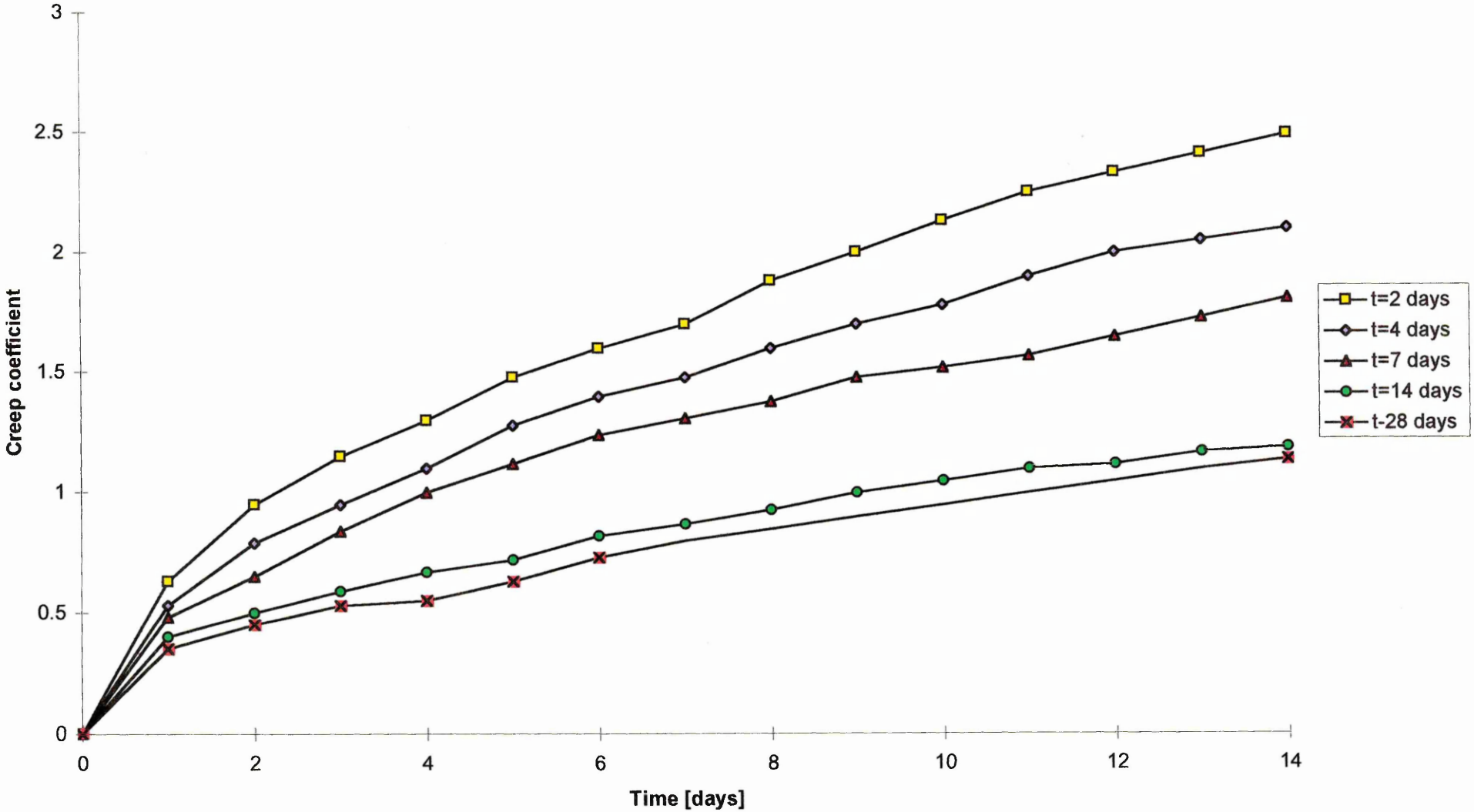

Figure 8.6 Development of creep coeffieient of SBR modified material for different ages of loading [37]

1.84, 1.59 and 1.04 for repair concretes loaded 4, 7 and 14 days respectively after casting. Based on the data given in Table 8.9, repair concretes loaded at early ages exhibit higher rates of creep.

8.2.2.2 Tensile creep

Most of the work on the creep of concrete (or repair materials) has been concerned with specimens under uniaxial compression [46]. However, it has also been recognised that time-dependent tensile deformations [47-51] are of great importance when the possibility of cracking has to be considered. This is particularly relevant to the performance of repair materials, as restrained shrinkage will induce tensile stress in the repair material. This will undoubtedly bring the durability of the repair material into question, but cracking may be avoided if stress relaxation occurs due to tensile creep in the repair material.

8.2.2.2.1 Mechanics of tensile creep

In an actual repair situation, shrinkage is restrained by the bond to the substrate concrete and steel reinforcement [43]. Under these restrained conditions, shrinkage of the material results in tensile stress. If the unrestrained shrinkage and tensile modulus of elasticity are known, then the resultant stress is calculable by: [43]

$$(\sigma_t)_t = (\varepsilon_{sh})_t (E_{\text{mod}})_t$$

Equation 8. 1

where

σ_t = tensile stress, MPa

ε_{sh} = free shrinkage strain, mm/mm

E_{mod} = tensile modulus of elasticity, MPa

$(\ )_t$ = value at time t, days

Equation 8. 1 assumes that the repair material is fully restrained from shrinking by the substrate concrete, therefore the tensile stress induced is a product of the free shrinkage strain and the tensile elastic modulus of the repair material. The current research has shown that this is not always the case, as stiffer repair materials are able to transfer some of the shrinkage strain to the less stiff substrate concrete, thus reducing the tensile stress induced [52].

When shrinkage occurs under restrained conditions, the strain can be absorbed by two mechanisms before the materials cracks [43]. These are elastic strain and creep strain in the repair patch in tension. Equation 8. 1 allows only for the elastic strain. However, the creep of the material must be taken into account to better represent the actual conditions [53-56]. When repair mortars are in a state of tension, tension creep serves as a kind of "relief valve" permitting restrained shrinkage to occur with a lower resultant stress [43] (also known as stress relaxation). This contribution of tensile creep may be substantial, and further, it is not necessarily predictable based on compressive creep data [57]. Assuming the drying shrinkage is completely restrained (current research has shown that this occurs when the elastic modulus of the repair material is less then the

elastic modulus of the substrate concrete), the tensile creep, when known, can be accounted for in general terms, by modifying Equation 8. 1 as follows: [43]

$$(\sigma_t)_t = (\varepsilon_{sh} - \varepsilon_{cr})_t (E_{\text{mod}})_t$$

Equation 8. 2

where

ε_{cr} = tensile creep at time, t, mm/mm

The existence of tensile creep, therefore, serves to reduce the tensile stress in the repair material. Cracking may be avoided as a result.

8.2.2.2.2 *Influence of material constituents on tensile creep*

Data on tensile creep of three repair mortars was obtained by Pinelle [43]. The test was first conducted on an unmodified mortar (cement:lime:sand = 1:0.14:1.7). The water:cement ratio was 0.45. A second sample was prepared by modifying the original mixture with an acrylic copolymer at a polymer:cement ratio of 0.10. A third sample was prepared by modifying the original mixture with a vinyl acetate/butyl acrylate combination, again at a polymer/cement ratio of 0.10. The water:cement ratios for the second and third mixtures also remained constant at 0.45.

A section through a typical briquette used in the tensile creep tests is given in Figure 8.7 [43]. The specimens (250 x 25 x 13mm) were cured in moulds for the first 24 hours at 20°C and 50% RH. Upon demoulding, 11.34 kg weights were applied to the briquettes,

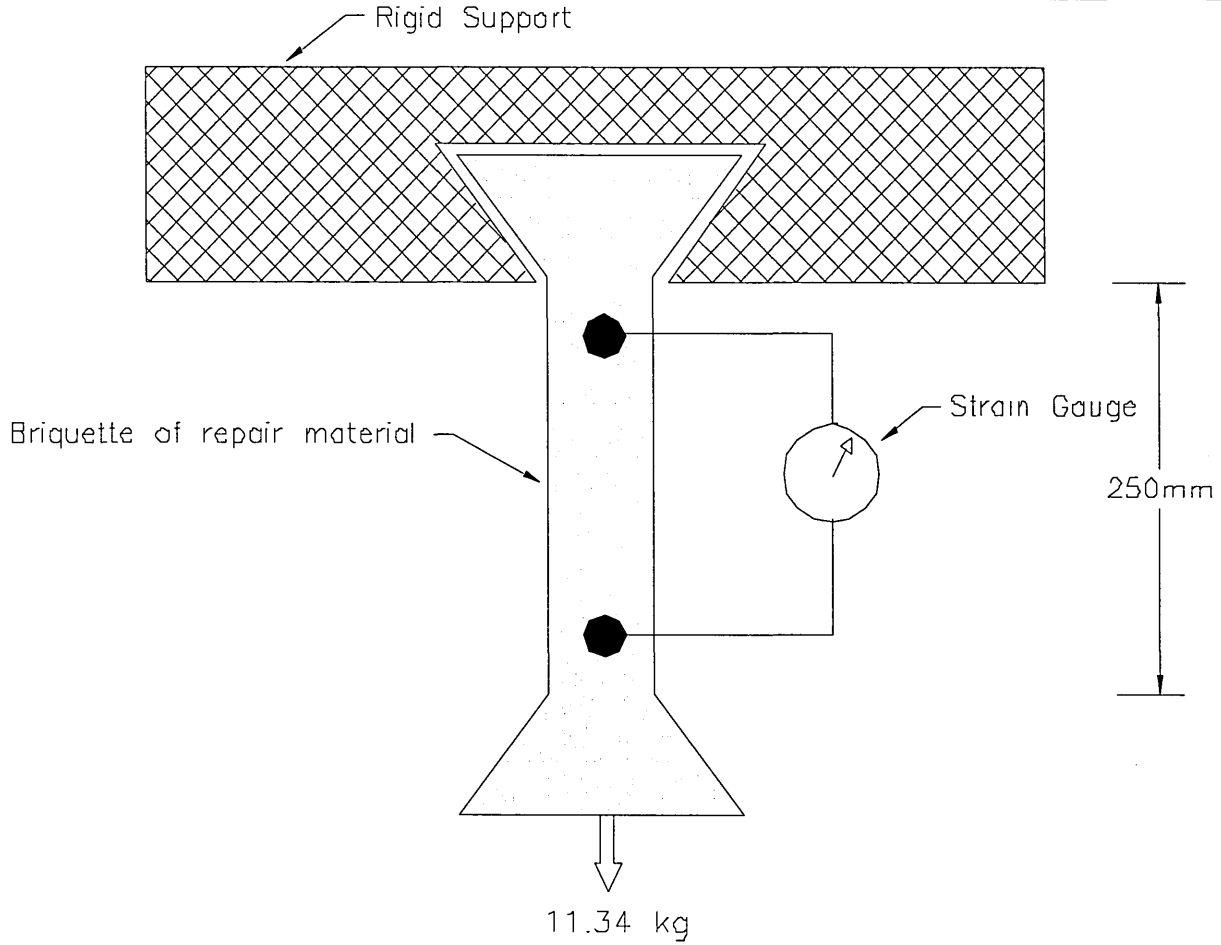

Figure 8.7 Test configuration used for tensile creep and tensile modulus of elasticity [43]

as shown in Figure 8.7 [43]. The stress/strength ratio was not given. Under the constant tensile load, the length change over time was measured using a mechanical strain gauge. Specimens of identical geometry were cast at the same time and the free shrinkage was monitored over the same time period. The shrinkage readings were then compared with the readings from the specimen under load. All specimens were stored at laboratory ambient conditions of 20°C and 50% RH during the duration of the study. The creep strain was calculated by

$$(\varepsilon_{cr})_t = \frac{(\Delta L_{loaded} - \Delta L_{unloaded})_t - (\Delta L_{elast})_{t=1}}{L}$$

Equation 8. 3

where

ΔL_{loaded} = length change at time t of loaded specimens,

$\Delta L_{unloaded}$ = length change at time t of specimens allowed to shrink freely,

ΔL_{elast} = elastic length change at time of loading (t = 1 day),

L = gauge length, mm

Figure 8.8 [43] shows a plot of specific tensile creep strain versus time for the three repair mortars. It shows that the acrylic copolymer lowered the tensile creep by approximately 35% relative to the unmodified mortar, whereas the vinyl acetate increased the tensile creep by approximately 60% compared to the tensile creep of the unmodified mortar.

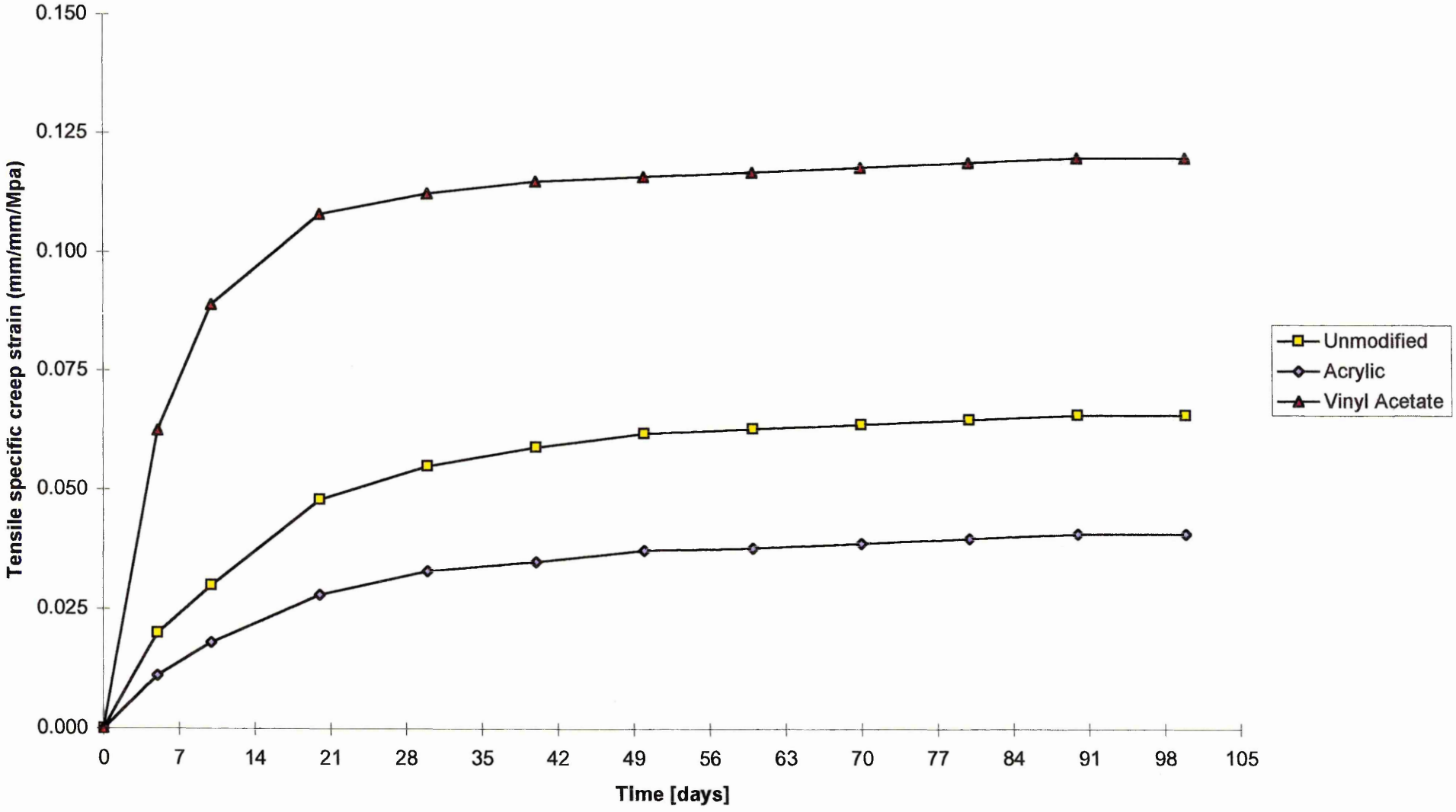

Figure 8.8 Plot of tensile creep strain versus time for three repair mortars [43]

8.2.2.3 Relationship between compressive and tensile creep

It is normally assumed that specific creep (of concrete) in tension is similar to the specific creep in compression [46, 58, 59]. However, research has also shown that specific compressive and tensile creep in cementitious materials may not be the same [60, 61]. Brooks *et al* [47] summarise a review into the creep of concrete which was carried out by Neville [62]. They state that for young concrete under numerically equal stresses and in the same environment, creep in tension is equal to or greater than creep in compression (the difference in percentage terms was not given). For example, with sealed concrete, there is little difference in the magnitude of tensile and compressive creep but, under saturated and drying conditions, tensile creep is greater than compressive creep. For older concrete stored in a drying environment, Illston [46] suggests that tensile creep may become less than compressive creep.

Based on the results of tests on the strain of concrete under sustained axial stress [46], it is reported that the strain of concrete in tension is similar to that in compression in the following respects:

- at stress greater than about 50% of ultimate, large plastic strains occur which are attributed to microcracking in the concrete
- creep reduces as the age of the concrete increases

Applying the above conclusions to the results obtained from the repair patches in the field, it is reasonable to assume that the compressive stress in the repair material will not exceed 50% of the ultimate compressive stress. However, the results of this project show that high tensile stresses do exist as a result of the restraint to shrinkage provided

by the substrate concrete and steel reinforcement which may in fact be greater than 50% of the ultimate tensile stress. Therefore, based on Illstons' conclusions [46], the creep in compression may not be the same as creep in tension for a repair material in situ.

Since the rate of creep diminishes with increasing age [46], it is an advantage, if possible, to delay the transfer of compressive stress to a repair material (i.e. application of an external compressive load). This would allow the repair material to mature and would result in lower creep when stressed. This conclusion was also observed by Yuan and Marosszeky (see Figure 8.6 [37]).

Differences between compressive and tensile strains also exist [46]:

- The initial rate of creep is higher in tension than in compression, but this position may be reversed later.

Finally, the strains under a cycle of compression stress are unaffected by a previous cycle of tensile stress [46]. This conclusion is very relevant to a repair material applied to an unpropped member in compression. A repair material will exhibit a tensile stress in the early stages after application due to the restraint to shrinkage provided by the substrate concrete. Assuming the repair material remains uncracked throughout this period (and the elastic modulus of the repair material is greater than that of the substrate concrete to begin with), the repair material will attract external load from the substrate concrete. This compressive load may not only neutralise the tensile stress in the repair patch, but may also cause a compressive stress to occur in the repair material. Therefore, although both tensile and compressive stresses may occur in a repair material

in the field, creep properties of a repair material can be related to the results without concern for the stress history of the repair material.

Creep tests in both compression and tension were also carried out by Brooks and Neville [47]. A single type of concrete (proportions by weight 1:2:4) was used throughout the tests. The water:cement ratio was 0.5. From the age of one day to 28 days, the specimens were stored in water at 22°C, and thereafter either stored continuously in water or in air at a relative humidity of 60%. Creep was determined from the ages of 28 days for periods up to 84 days. The applied stresses were 14.0 N/mm^2 in compression and 0.93 N/mm^2 in tension (the stress/strength ratios were not given). Also, at 56 days, the specimens were unloaded and allowed to recover. Results show [47] that at 28 days, the initial rates of basic creep in tension and in compression are similar but at a later age (approximately 30 days after loading), the rate of compressive creep diminishes whereas the rate of tensile creep does not diminish with time. However, the initial rate of total creep (basic + drying) in tension is greater than the rate of total creep in compression, although later in the test, the rates are similar.

8.2.2.3.1 *Compressive and tensile creep recovery*

Creep recovery of concrete specimens loaded in tension and compression was also studied by Brooks and Neville [47]. Specimens were unloaded after 28 days under load. The final values are given in Table 8.10 [47]. Table 8.10 indicates that creep recovery differs for both tensile and compression states of stress. Concentrating on the specimens which were cured in water (Table 8.10), 40% of the basic creep in

Table 8.10 Creep recovery [47]

Storage	*Creep recovery (% of final creep)*	
	After compression	*After tension*
In water	40.0	-8.7
In water then air	16.3	22.4

compression was recovered whereas the tensile creep recovery showed a negative recovery (this is possibly associated with additional swelling over and above that given by the average of the control specimen). Nevertheless, a small recovery is still indicated if the negative recovery is ignored, which implies that tensile basic creep is mainly irrecoverable for specimens stored in water [47]. For specimens stored in air from 28 days onwards, the compression recovery is 16.3% of the final creep as opposed to the higher 22.4% recorded for tensile creep recovery. Illston [46] reported that there is no rapid delayed elastic strain in tension and that concrete in tension shows slow delayed elastic strain

To summarise, the experimental difficulties of testing concrete in tension, as reported by Illston [46], are such that it is perhaps too much to hope that full agreement can be reached between the results of different researchers. Therefore, based on this and on the contradicting results of the literature review, unless tensile and compressive creep properties of a specific repair material are fully investigated for use in the design of a repair patch, the tensile creep properties can be assumed to be similar to the compressive creep properties.

8.2.3 Elastic modulus of repair materials

8.2.3.1 Influence of material constituents

All repair materials under observation in this research are based on a cementitious binder, with or without polymer modification. Polymers are normally added to the mixture to give superior mechanical properties, but this is not always the case. Kuhlman [63] states that one of the many properties of hardened concrete which changes due to the addition of latex is the elastic modulus. This may result in an increase in the elastic modulus if a hard film is added, conversely, the elastic modulus may be reduced by approximately 15% to that of normal concrete if a soft film is used. Repair materials with polymer modifications (and coarse aggregates) in the current project generally exhibited higher elastic modulii than those without modification.

Figure 8.9 [43] shows the development of tensile elastic modulus versus time for the three repair materials as described in Section 8.2.2.2.2. All data points in Figure 8.9 [43] are at least the average of three specimens. The tensile elastic modulus of the vinyl acetate modified mortar was approximately 69% of the tensile elastic modulus of the unmodified mortar at 100 days, whereas the tensile elastic modulus of the acrylic modified mortar was only 34% of the 100 day value of the unmodified mortar.

The development of tensile elastic modulus is very important in the early stages of a repair material after application. Tensile stress will be evident in the repair patch due to the restraint to shrinkage provided by the substrate concrete. The magnitude of this stress will be directly related to the virtual tensile strain due to the restraint to shrinkage and the tensile elastic modulus of the repair material. Most of the shrinkage in the

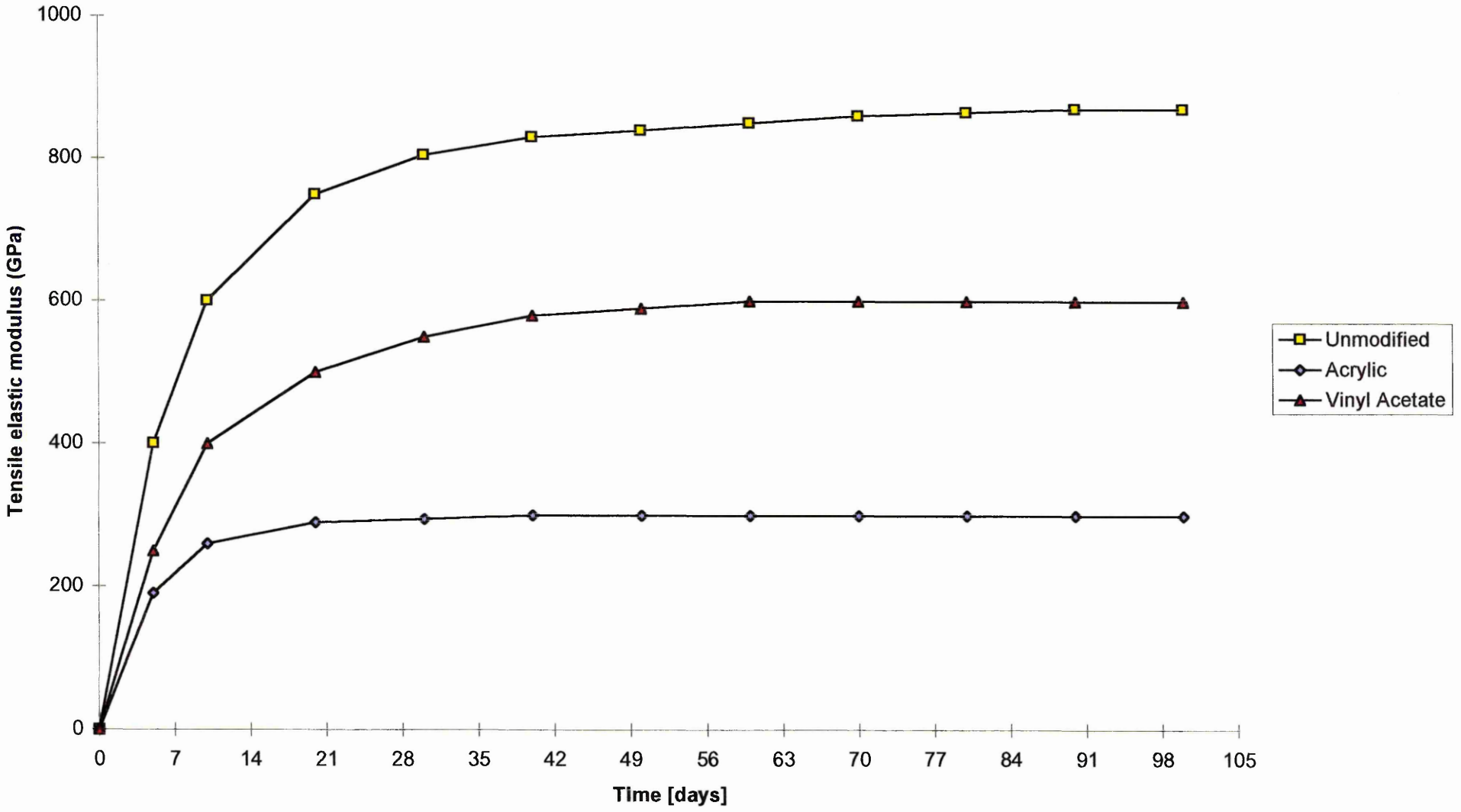

Figure 8.9 Development of tensile elastic modulus versus time for three repair materials [43]

repair material occurs within the first 28 days after application, the same period it takes the tensile elastic modulus to develop (see Figure 8.9). A summary of Figure 8.9 is given in Table 8.11. Referring to Table 8.11, the average 7 day tensile elastic modulus is approximately 65% of the 28 day value. This average increases to 85% and 96% at 14 and 21 days respectively. Therefore, in order to calculate a more accurate tensile stress in a repair material in the early ages, the tensile modulus of elasticity should be appropriately reduced as shown in Table 8.11.

8.2.3.2 Relationship between compression and tension elastic modulus

The relationship between compression and tension elastic modulus of concrete (both static and secant) is given by Brooks and Neville [47]. The mix proportions by weight (cement:sand:coarse aggregate) of the concrete used in the tests was 1:2:4. The water:cement ratio was 0.50. Referring to Table 8.12 [47], the static modulus of elasticity in tension, obtained under low stress, is slightly lower than the static elastic modulus of elasticity in compression obtained under high stress. This applies to

Table 8.11 Development of tensile elastic modulus (from Figure 8.9 [43])

	Percentage of 28 day tensile elastic modulus at:		
Material	*7 days* (%)	*14 days* (%)	*21 days* (%)
Unmodified	60	83	95
Vinyl Acetate	59	81	94
Acrylic	75	92	98
Average:	*65*	*85*	*96*

Table 8.12 Static modulus of elasticity at the age of 84 days [47]

Storage	*Static modulus of elasticity (GN/m^2)*			
	*Compression (high stress)**	*Compression (low stress)**	*Tension (low stress)*	*% difference [tens v comp (high)]*
In water	36.8	33.5	33.6	10
In air from the age of 28 days	35.7	32.4	33.2	8
				Average: 9

Note: ** High stress refers to a maximum stress equal to 0.3 x 28 day compressive strength*
Low stress refers to a maximum stress equal to 0.3 x 28 day tensile strength

specimens cured in water and in air from the age of 28 days (Table 8.12). This difference is attributed to the standard method for obtaining the elastic modulus of cylindrical specimens (BS 1881, Part 121 [3]). The static elastic modulus is measured by means of a test in which a cylinder is loaded to just above one-third of a corresponding cube stress and then cycled back to zero stress [64]. This preloading cycle is repeated at least three times [3]. This removes the effect of initial "bedding in" and minor stress redistribution in the concrete under load. Load is then reapplied and the stress-strain curve exhibits negligible curvature at high stresses. On the other hand, when low stresses are applied, the curve is concave to the stress axis due to microcracks which are capable of opening and closing with load. As a result, when low stresses are applied to both compression and tension tests, the static modulus in compression is similar to that in tension (see Table 8.12) [47].

Table 8.13 [47] shows that the secant modulus in tension is greater than the secant modulus in compression for concrete (the secant modulus, obtained from BS 1881 [3],

Table 8.13 Secant modulus of elasticity in compression and in tension [47]

Storage	*Secant modulus at loading (GN/m^2)*	
	Compression	*Tension*
Stored in water throughout, loaded at 28 days, unloaded at 56 days	29.0	34.3
Stored in air from 28 days onwards, loaded at 28 days, unloaded at 56 days	-	-
Stored in water throughout, loaded at 28 days, unloaded at 84 days	29.0	34.3
Stored in air from 28 days onwards, loaded at 28 days, unloaded at 84 days	-	-
Stored in water throughout, loaded at 56 days, unloaded at 84 days	35.4	36.7
Stored in air from 28 days onwards, loaded at 56 days, unloaded at 84 days	32.9	35.4
% increase in elastic modulus when stored in water	*8%*	*4%*

is the stress divided by strain obtained from a basic loading level of 0.5 N/mm^2 and an upper loading level of one-third of the compressive strength of the concrete). The reason for this is again attributed to the shape of the stress-strain curve. The secant modulus decreases with an increase in stress [65] because, at low stresses, the stress-strain curve, as before, is concave to the stress axis owing to the closing of microcracks. At high stresses, the stress-strain curve is convex owing to the opening of microcracks and creep. Hence, since secant modulus in tension is determined at low stress, a higher value is recorded [47]. Table 8.13 [47] also shows that the secant modulus of elasticity, for both compression and tension, increases with age [47]. The increase is greater for specimens stored in water. Brooks and Neville [47] attribute this increase in elastic modulus to adsorbed water in the saturated specimens. Applying this conclusion to repair materials in the field, enhanced curing techniques will not only reduce the shrinkage strain in the repair material, but also increase the elastic modulus of the repair material by approximately 8% in compression and 4% in tension.

Since the modulus of elasticity for repair materials will be obtained in accordance with BS 1881 [3], the static modulus of elasticity is more important than the secant modulus of elasticity. Although Brooks and Neville [47] differentiates between high stress (0.3 x 28 day compressive strength) and low stress (0.3 x 28 day tensile strength) to account for the difference in compressive and tensile elastic modulus, nevertheless, stresses equal to $\frac{1}{3}$ of the compressive and tensile strength would be used to determine the elastic modulus as specified in BS 1881 [3]. These are similar to the stresses used previously [47] (i.e. "high" stress for compressive testing and "low" stress for tensile testing). Therefore, based on previous investigations into the modulus of elasticity for concrete [47], the tensile modulus of elasticity is approximately 9% lower than the compressive modulus of elasticity (see Table 8.12).

8.2.3.3 Selection of repair material

The Hong Kong Housing Authority requirements for acceptable repair mortars is set out in Table 8.14 [66]. The mortar is classified into one of three groups based on its compressive strength. The correct material is then selected for repair based on the relationship between the mortar strength and elastic modulus, and the compressive strength of the concrete substrate (see Table 8.14 [66]). For example, a repair mortar in *Mortar Class 40* would exhibit a 28 day compressive strength of between 30-60 N/mm^2 and a 28 day elastic modulus of between 15-25 kN/mm^2. This repair material would then be suitable for repairing a deteriorated member with a substrate concrete compressive strength of between 12-31 N/mm^2. Based on this criteria, mortar selection is based on a knowledge of the repair material and concrete substrate strengths rather than the elastic modulus of the two materials. Since the HKHA requirements do not

Table 8.14 Relationship between mortar and concrete properties [66]

Mortar Class	*40*	*25*	*15*
Range of (28 days) compressive strength of mortar (MPa)	30-60	20-40	10-30
Range of (28 days) modulus of elasticity of mortar (GPa)	15-25	9-15	5-9
Applicable range of concrete substrate strengths (MPa)*	12-31	7-19	4-12
Modulus of elasticity of substrate concrete [23]	*<24-26*	-	-

** based on actual strengths for whole blocks, derived from random core tests [67]*

require the elastic modulus of the substrate concrete to be known, Table 8.14, nevertheless, shows the equivalent modulus of elasticity of the substrate concrete based on the relationship between compressive strength and modulus of elasticity [23]. The lowest substrate concrete strength in Table 8.14 is 12 N/mm^2, but the minimum strength specified in the compressive strength/elastic modulus relationship is 20 N/mm^2 [23]. A substrate concrete with a strength of 20 N/mm^2 will exhibit a mean elastic modulus of approximately 24 kN/mm^2. Similarly, the modulus of elasticity of a concrete with a strength of 31 N/mm^2 will exhibit a mean elastic modulus of approximately 26 kN/mm^2. These values are shown in Table 8.14. Comparing the elastic modulus of the substrate concrete (<24-26 kN/mm^2) with the elastic modulus of the repair material (<15-25 kN/mm^2), the elastic modulus of the substrate concrete is greater than the elastic modulus of the repair material. Results from the current research show that this would have an adverse influence on the performance of the repair, since the elastic modulus of the repair material should be greater than the elastic modulus of the substrate concrete [52]. This would enable a portion of the shrinkage strain to be distributed to the substrate concrete, hence reducing the tension induced in the repair material due to restraint. It will also allow external load to be transferred into the repair patch in the long term.

8.2.4 Tensile strength of materials

To determine the direct tensile strength of a repair material, a uniaxial test is needed which is simple, economic and truly uniaxial [68]. The most successful methods have been those in which the tensile loads have been applied to the concrete through friction-grip systems [69-72], through bars embedded in the concrete [68, 73-75] or through plates stuck onto the end of the specimens [76].

Due to the problems associated with direct tensile testing, Domone [77] reports that several indirect methods of tensile testing have been developed over a period of years, notably the modulus of rupture and cylinder-splitting tests [78]. In order to determine the relationship between direct tension, cylinder splitting and modulus of rupture, a series of uniaxial tensile tests were carried out on concrete [77] using an uniaxial test method developed by Elvery and Haroun [79]. The results of the uniaxial tests were compared to the results of cylinder splitting and modulus of rupture tests. The ratio of direct tension:cyclinder-splitting:modulus of rupture was found to be 1:1.5:2.2.

Brooks and Neville [47] investigated the relationship between direct tension and cube strength, cylinder splitting and modulus of rupture and found these properties to be related. The relationship between modulus of rupture and direct tension for concrete is given in Figure 8.10 [47]. Two relationships are given; one for dry stored specimens and the other for wet stored specimens. The equations for the regression lines are also given. Figure 8.10 also shows the relationship between direct tension and modulus of rupture for concrete as presented by Neville [65]. This relationship is linear and results in a ratio of direct tension to modulus of rupture of approximately 1:1.7.

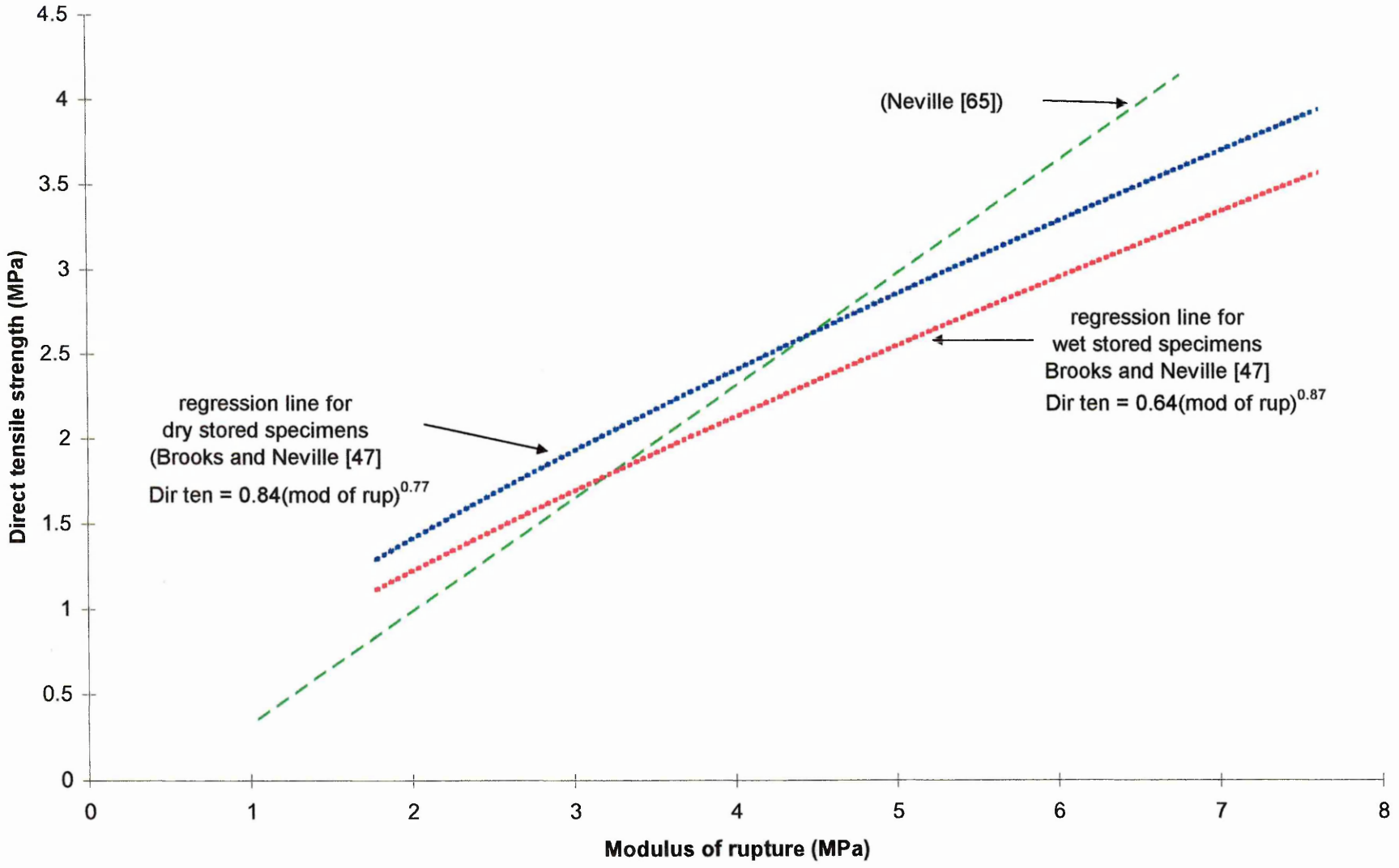

Figure 8.10 Relationship between direct tensile strength and modulus of rupture [47, 65]

This ratio will give different tensile strengths compared with the estimation given by Brooks and Neville (see Figure 8.10 [47]), but relationships involving modulus of rupture are dependent upon storage conditions [47] and properties of the mix [65]. Neville's relationship also gives a higher direct tension strength compared with the findings of Domone [77].

Figure 8.11 combines the findings of two researchers [28, 37] into the tensile strength of repair materials. Referring to Figure 8.11 [37], the development of tensile strength for three repair concretes which were modified with styrene acrylic, SBR and acrylic are given (details of these concretes are given in Section 8.2.1.2). The strengths were determined using a direct tensile test [76]. The tensile strengths ranged between approximately 1.87 N/mm^2 for the acrylic modified concrete and 4.7 N/mm^2 for the styrene acrylic modified concrete at 28 days. The strength of the SBR modified concrete was approximately 4 N/mm^2 at 28 days. High tensile strengths in the early ages (0 to 28 days) are also important so that cracking due to the restraint to shrinkage is avoided. Referring to Table 8.15, the acrylic modified concrete achieved the highest proportion of the 28 day strength at 7 days (86%) while this value for the SBR and styrene acrylic modified concretes was 67% and 70% respectively [37]. The results of direct tensile strength tests on SBR modified Portland cement mortars are also shown in Figure 8.11 [28]. The mortar was cured at 23°C and 50% RH - this information about curing conditions was not available for the previous tensile tests [37]. The 28 day tensile strength is 5.62 N/mm^2, higher than the value presented by Yuan and Marosszeky [37] of 4.7 N/mm^2 for SBR modified concrete (see Figure 8.11 and Table 8.15). The 7 day value of 5.69 N/mm^2 was in fact marginally higher than the 28 day

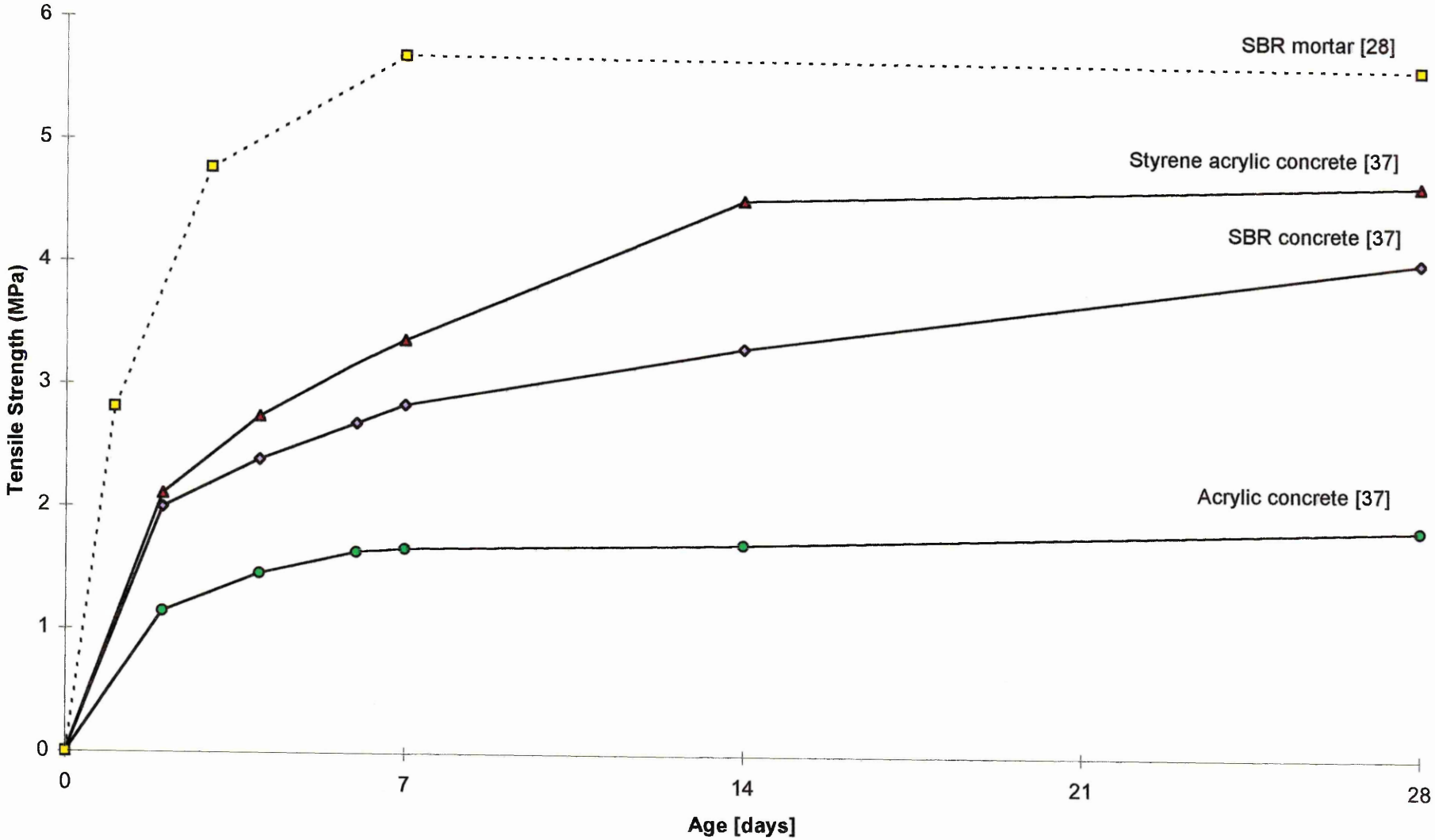

Figure 8.11 Development of tensile strength with age [28, 37]

Table 8.15 Direct tensile strengths of polymer modified repair materials [28, 37]

Repair material	*Exposure conditions*	*Direct tensile strength at: (MPa)*		$\frac{7day}{28day}$
		7 days	*28 days*	*(%)*
Acrylic concrete [37]	NA	1.61	1.87	86
SBR concrete [37]	NA	2.71	4.05	67
Styrene acrylic concrete [37]	NA	3.28	4.68	70
SBR mortar [28]	23°C, 50% RH	5.69	5.62	~100

value (see Table 8.15), indicating rapid tensile strength gain in the early stages for this repair material (see Figure 8.11 and Table 8.15).

8.3 EXPERIMENTAL PROGRAMME

An experimental study was carried out to establish the free shrinkage, creep and modulus of rupture properties of all the repair materials used in the project, along with the elastic modulus of both the repair materials and substrate concretes. This will allow the structural interaction between the repair patch and the substrate concrete to be related to the basic material properties.

8.3.1 Details of repair materials

Details of the repair materials used in the experimental programme are given in Table 8.16. These include fifteen repair materials which were used on site, four of which were

TABLE 8.16 Details of repair materials

Material	*Density of fresh material (kg/m^3)*	*Method of repair application*	*Water content*
G1	2250	spray	3.1 litres per 25kg bag
G2	2250	spray	water:cement ratio = 0.38
G3	2200	spray	water:cement ratio = 0.39
G4	2100	hand	3.5 litres polymer per 30kg pack
G5	1725	hand	3.5 litres per 30kg bag
G6	1250	hand	5.0 litres per 25kg bag
L1	2210	spray	2.9 litres per 25kg bag
L2	2100	spray	2.8 litres per 25kg bag
L3	1850	spray	4.5 litres per 25kg bag
L4	2270	spray	2.91 litres per 25kg bag
L5	2270	spray	2.91 litres per 25kg bag
S1	2250	flow	2.8 litres per 25kg bag
S2	2270	flow	3.8 litres per 30kg bag
S3	2270	flow	4.0 litres per 30kg bag
S4	2290	flow	water/cement ratio = 0.48
L3(L)	1850	hand	4.5 litres per 25kg bag
G4(L)	2100	hand	3.5 litres polymer per 30kg pack
G5(L)	1725	hand	3.5 litres per 30kg bag
G6(L)	1250	hand	5.0 litres per 25kg bag

also used in the laboratory investigation of repaired concrete beams. The range covers all materials used for hand applied, sprayed and flowing repairs. Detailed descriptions of these repair materials are given in sections 4.3.1 and 4.3.2 (Gunthorpe Bridge), 5.3.1 (Lawns Lane Bridge) and 6.3.1 (Sutherland Street Bridge).

8.3.2 Casting and curing

100 x 100 x 500mm prism specimens of repair materials were used for shrinkage, creep and modulus of rupture tests. 100mm diameter x 200mm high cylinders were used for elastic modulus tests. These are standard specimen sizes for testing concrete [80] rather than the smaller sizes allowable for testing repair materials [81]. The larger specimens which are standard for testing concrete were used so that the properties of repair materials determined in the tests could be meaningfully used with those of the substrate concrete when analysing theoretically the structural interaction between the repair patch and concrete substrate. It is important that in any such analysis all material properties are derived from common specimen sizes in order to exclude the influence of size effect on the results.

Mixing was carried out in accordance with the manufacturers' instructions. A forced action pan mixer was used for the purpose. A total of six prisms and two cylinders were cast for each material according to standard procedures [82]. Two prisms were used for free shrinkage and four for creep tests (two for creep measurements and two for corresponding shrinkage strains). The two prisms for free shrinkage were later tested for modulus of rupture data of the repair materials.

Repair materials were cast in three layers and each layer was compacted in a manner similar to that used on site. Hand applied repair materials were compacted by hand without the use of a tamping bar. Compaction of the flowing materials was provided by firmly tapping the moulds with a hammer at regular frequency. Materials which were spray applied on site were cast by hand in the laboratory. They were cast in three layers

and compacted by applying 25 strokes of a tamping bar on each layer. The top surface (as cast) of the specimens of all the materials was trowelled using a steel float and covered with polythene sheeting before being transferred to a mist curing room (RH = 95%) for 24 hours.

After 24 hours, the prisms and cylinders were transferred from the mist curing room to the laboratory and demoulded. After demoulding, demec points were attached with an adhesive (Chemical Metal) to the specimens. A warm air drier was used to dry the surface of the specimen to ensure good bond between the adhesive and the specimen. This operation took approximately 30 minutes. Demec points were attached in accordance with BS 1881 Part 121 [3] at a gauge length of either 50mm (cylinders) or 200mm (prisms). Prisms for shrinkage tests were transferred to a controlled environment room at 20°C and 55% RH for the duration of the tests [83]. Prisms for creep tests were cured in a water tank at 20°C prior to loading - the total curing period was 28 days (including one day in the mist curing room). Creep specimens were accompanied by identical shrinkage specimens so that net creep strain could be obtained by subtracting the free shrinkage strain from the gross strain measured under load. The two prisms that were initially used for the shrinkage measurements up to 100 days age, were subsequently tested at ages between 14 and 36 months for modulus of rupture data. These prisms were stored in a controlled environment throughout (20°C and 55% RH).

8.4 TESTING

8.4.1 Shrinkage deformation

8.4.1.1 Air cured specimens

Datum readings were taken at 24 hours after casting (immediately after the application of demec points). Specimens were stored in a controlled environment (20°C and 55% RH). Subsequent readings were taken every day for the first three days, every three days for the next sixty days and once a week thereafter to a total of 100 days (see Figure 8.12). The shrinkage presented is the average of eight readings from all the longitudinal faces of two prisms.

8.4.1.2 Water cured specimens

Specimens were initially mist cured for 24 hours and cured in water at 20°C for a further 27 days. Datum strain readings across a gauge length of 200mm (demec gauges) were taken at 28 days. Subsequently, specimens were transferred to a controlled environment (20°C and 55% RH) for the remainder of the test period for shrinkage and creep tests. Subsequent readings were taken every day for the first three days, every three days for the next sixty days and once a week thereafter to a total of 100 days. The shrinkage presented is the average of eight readings from all the longitudinal faces of two prisms. The shrinkage obtained from these prisms was also used to obtain the net creep of the repair materials under load.

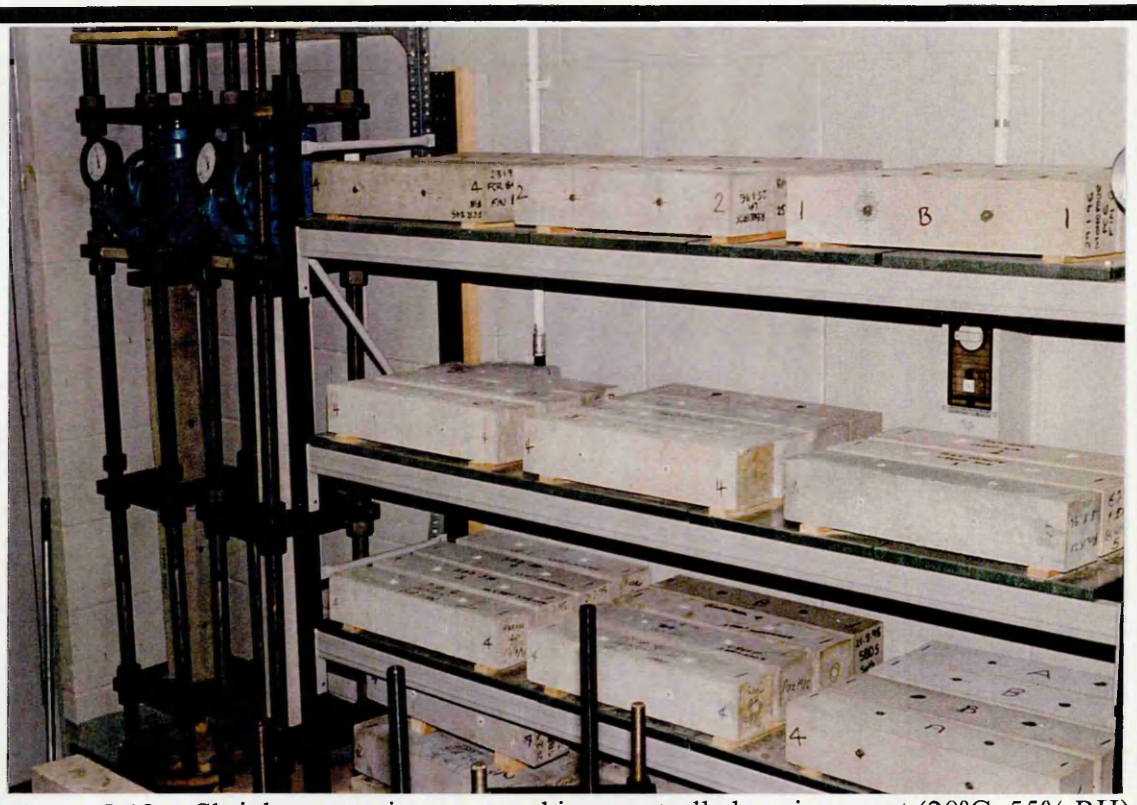

Figure 8.12 Shrinkage specimens stored in a controlled environment (20°C, 55% RH)

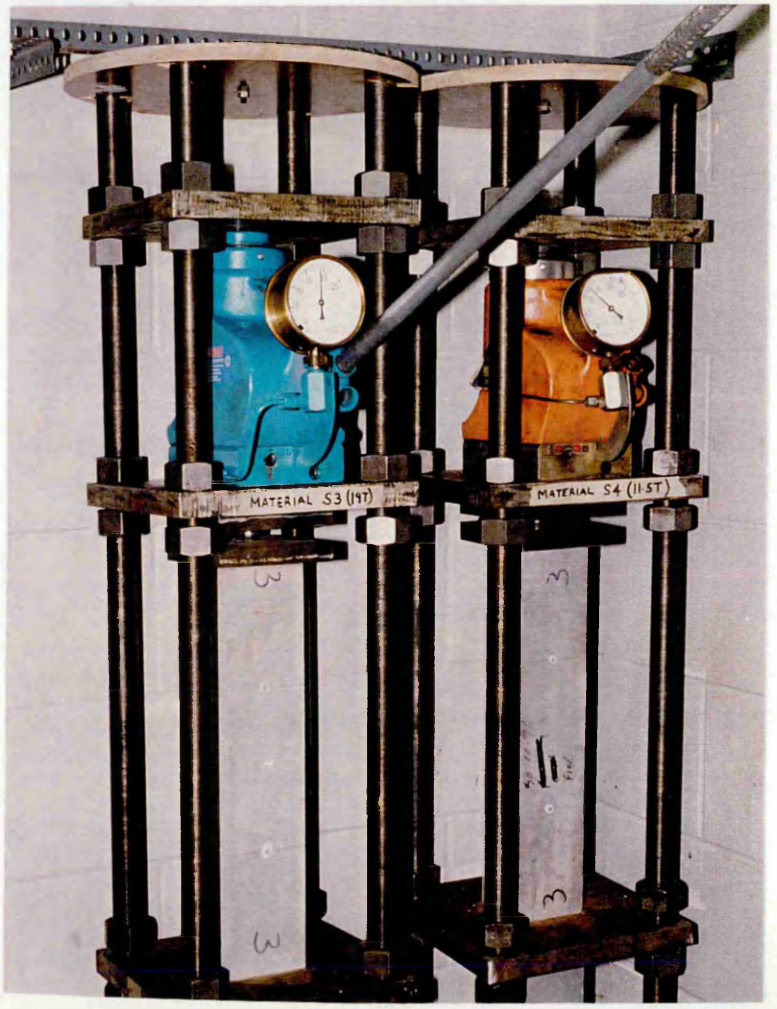

Figure 8.13 Creep specimens loaded in series in a standard creep rig (20°C, 55% RH)

8.4.2 Creep deformation

Two prisms of each material were loaded together (in series) in a standard creep rig (see Figure 8.13). Creep tests were carried out in accordance with standard procedures [83]. Each rig consisted of four steel end platens supported by nuts on four 36mm diameter high yield steel rods. The load was applied by means of a 25 ton capacity hydraulic jack (manufactured by Tangye) via the top platens. A ball-joint was incorporated in the rig to ensure concentric loading. The jack remained in place throughout the duration of each test (Figure 8.13). The sustained axial load on the specimens was achieved by regular loading and tightening the nuts against the end platens. To ensure that the specimens were loaded concentrically, a datum load (about 20% of the applied load) was first applied to ensure similar strains on all four faces of both prisms before the total load was applied. Throughout the duration of the creep study, the specimens were stored at 20°C and 55% RH. Each creep deformation recorded was the average of readings of eight faces of two prisms. The net creep strain was obtained by subtracting the shrinkage strain, measured on identical specimens, from the gross strain measured on the specimens under load in the rig.

8.4.3 Elastic modulus

200mm long x 100mm diameter capped specimens of each repair material were tested in an Avery Dennison Compression Testing Machine (model 7226-3000kN) in accordance with BS 1881:Part 121 [3]. An extensometer of gauge length 50mm was used to measure the strain. A minimum of two and a maximum of three cylinders were tested to determine the elastic modulus of each repair material. The elastic modulus of the

substrate concrete in the bridges, Gunthorpe Bridge, Lawns Lane Bridge and Sutherland Street Bridge, was obtained from cylindrical cores taken from these bridges. 180mm (approx) x 100mm diameter cores from Gunthorpe, Lawns Lane and Sutherland Street Bridges were capped in the laboratory and tested in an Avery Dennison Compression Testing Machine (model 7226-3000kN) in accordance with BS 1881:Part 121 [3]. A minimum of two cylinders and a maximum of three were tested to determine the elastic modulus of each substrate concrete.

No correction factor was applied to the measured elastic modulus values of the substrate cores since the *l/d* (length/diameter) ratio of the cylindrical specimens cast in the laboratory and cores obtained from site was within the range 2 to 5. This complied with the requirements of Clause 4 in BS 1881:Part 121 [3].

8.4.4 Modulus of rupture

100 x 100 x 500mm long specimens of each repair material were tested in an Avery Dennison Transverse Testing Machine (model 7123-100 kN) in accordance with BS 1881: Part 118. Two specimens of each repair material were also tested to determine the long term modulus of rupture of each repair material.

8.5 RESULTS AND DISCUSSION

8.5.1 Free shrinkage of repair materials

8.5.1.1 Air cured specimens

The free shrinkage of repair materials used at Gunthorpe Bridge, Lawns Lane Bridge and Sutherland Street Bridge are given in Figures 8.14 to 8.16 respectively. A summary of the results is also given in Table 8.17.

The free shrinkage of the repair materials used at Gunthorpe Bridge is shown in Figure 8.14 and Table 8.17. Materials G1-G3 are spray applied materials, whereas G4-G6 are hand applied materials. Material G3 is a conventional cement and sand mortar, without polymer modifications (mix proportions 1:3), and as a result, it can be used as a reference for all other commercially available repair materials under test. The water:cement ratio was 0.45. Material G3 has a 100 day shrinkage of 717 microstrain, which is greater than the shrinkage recorded for material G4 but less than the shrinkage recorded for all the other materials (G1, G2, G5 and G6).

Materials G2, G5 and G6 show rapid shrinkage for the first 15-20 days, followed by a negligible increase thereafter to reach a 100 day value of 1311, 1087 and 1100 microstrain respectively (Figure 8.14). Materials G1 and G4 show a lower rate of free shrinkage in the early stages which ultimately leads to a lower overall shrinkage deformation of 751 and 401 microstrain respectively at 100 days (Figure 8.14).

Figure 8.15 and Table 8.17 show the free shrinkage in the laboratory of the repair materials which were spray applied at Lawns Lane Bridge. Material L3 shows initial

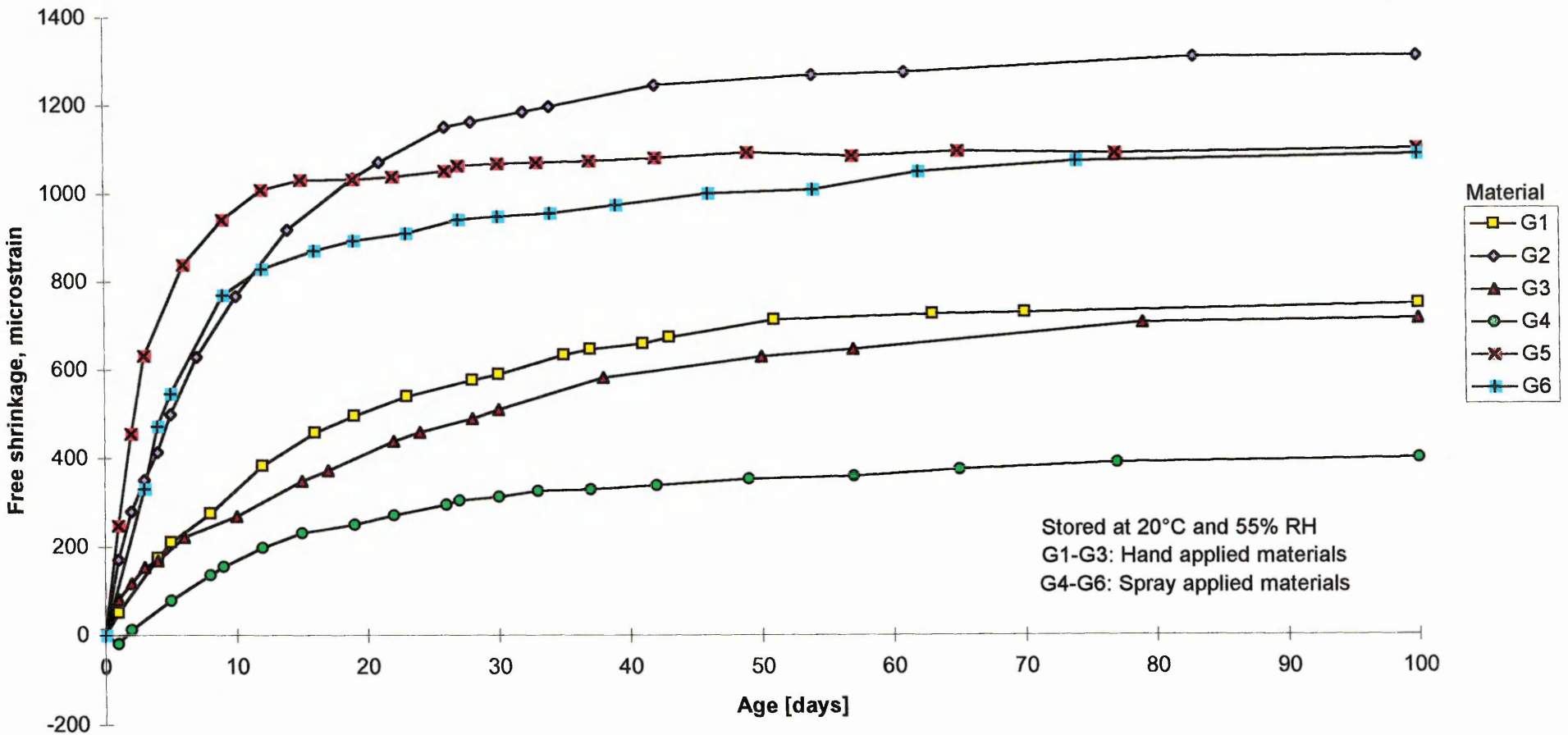

Figure 8.14 Free shrinkage of repair materials used at Gunthorpe Bridge (G1-G6)

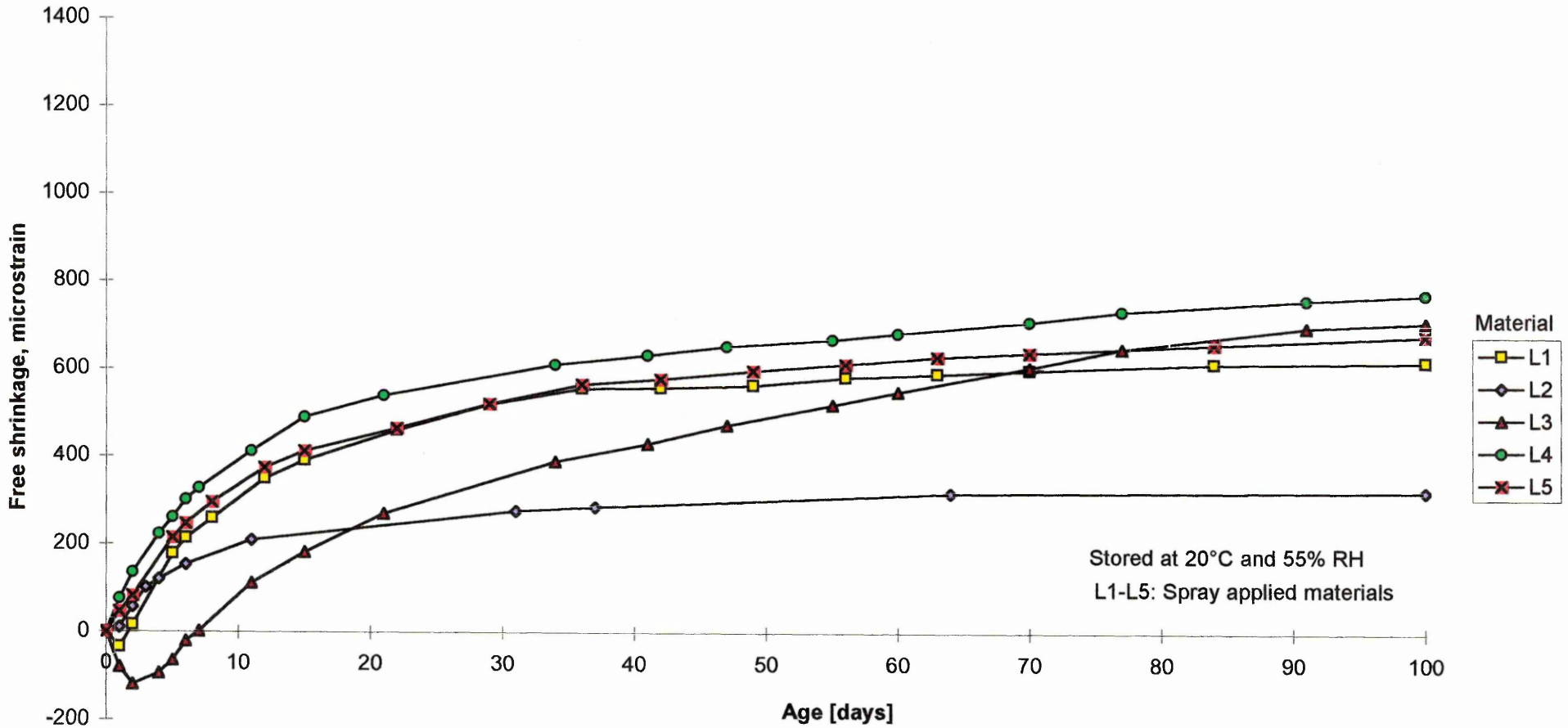

Figure 8.15 Free shrinkage of repair materials used at Lawns Lane Bridge (L1-L5)

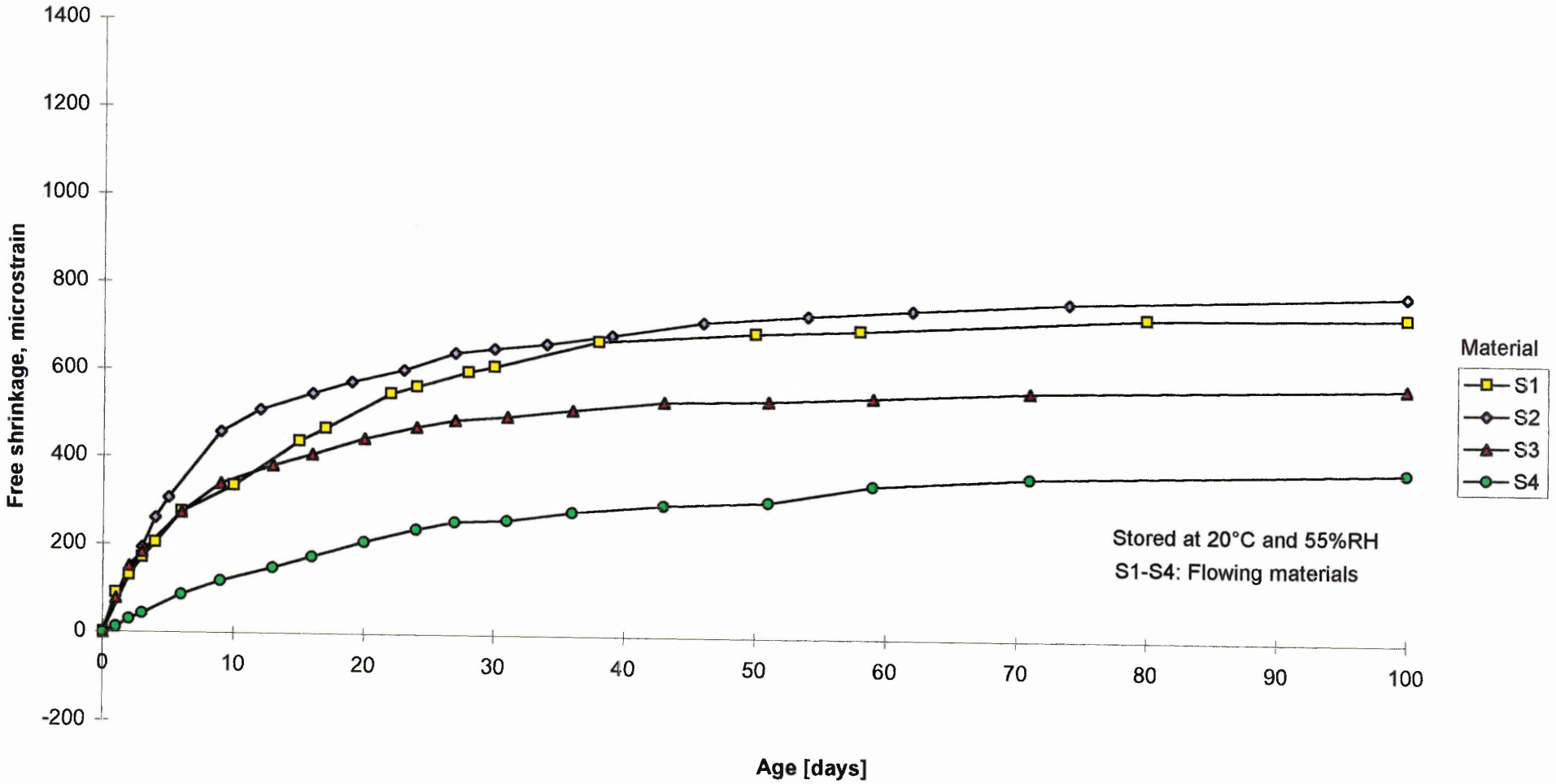

Figure 8.16 Free shrinkage of repair materials used at Sutherland Street Bridge (S1-S4)

TABLE 8.17 Shrinkage deformation at 100 days (dry cured specimens)

Material	*Shrinkage at 100 days (microstrain)*	*Aggregate*	*Main admixtures (from supplier's literature)*
G1	751	5mm graded	Copolymers
G2	1311	Grade M sand	Styrene acrylic + fibres
G3	717	Grade M sand	None
G4	401	10mm graded	Styrene acrylic + fibres
G5	1087	Fine*	Styrene acrylic + fibres
G6	1100	Fine*	Styrene acrylic
L1	620	3mm graded	Admixtures
L2	325	graded*	Copolymers
L3	710	graded*	Shrinkage compensating agents
L4	782	5mm graded	Admixtures
L5	680	5mm graded	Admixtures + fibres
S1	740	5mm graded	Shrinkage compensating agents
S2	791	graded*	Shrinkage compensating agents
S3	580	6mm graded	Copolymers
S4	388	10mm rounded	Fibres

*Note: * indicates that no specific information was supplied on aggregate size*

expansion for the first 7-8 days, possibly due to the fact that it is shrinkage compensated and may contain expansive cements (see Table 8.17) followed by a gradual contraction over the remaining monitoring period resulting in a shrinkage of 710 microstrain. Materials L1, L4 and L5 all show lower rates of free shrinkage in the early stages to reach a shrinkage strain of 620, 782 and 680 microstrain respectively at 100 days. All these values are similar to the shrinkage strain of 717 microstrain for the sand and cement mortar (material G3) used at Gunthorpe Bridge. Material L2 exhibits the lowest free shrinkage strain of 325 microstrain at 100 days.

Free shrinkage deformation of the pourable materials used at Sutherland Street Bridge is given in Figure 8.16 and Table 8.17. All the materials exhibit relatively slow rates of shrinkage in the early stages to reach 100 days shrinkage values of between 388 and 791 microstrain. Materials S1 and S2 exhibit shrinkage strains of 740 and 791 microstrain respectively, which are similar to the shrinkage strains in the sand and cement mortar (material G3, Figure 8.14). The shrinkage of material S3 is slightly lower (580 microstrain). Material S4, a flowing concrete which was designed in the laboratory with conventional concrete constituents and admixtures to give a high flow material with relatively large aggregate and low cement content, displays the lowest shrinkage (388 microstrain) of the four materials. This material also contains the largest aggregate particles (10mm rounded).

8.5.1.1.1 *Discussion*

Free shrinkage in normal concrete can be restricted by keeping the water:cement ratio and cement contents low [84]. The same practice applies to repair materials. Unfortunately, cement contents of repair materials are rarely given in manufacturers' literature and determination of cement contents by analysis was outside the scope of this project. Consequently, it is not possible to comment on the free shrinkage of the materials with respect to the water:cement ratio or cement content. Repair materials which comply with the current Highways Agency standard (clause 1702 of DoT Specifications for Highway Works, Part 5) [1] must have a minimum cement content of 400 kg/m^3. Therefore, assuming the cement contents are similar for all repair materials conforming to the standard, the variation in shrinkage of repair materials represented in

Figures 8.14 to 8.16 must be due to other material constituents. The inclusion of different aggregate sizes and/or admixtures may affect the shrinkage of the material. Referring to Table 8.17, materials G4 and G5 (hand applied materials from the same manufacturer which both comply with BD 27/86 [1]) includes a styrene acrylic copolymer along with polypropylene fibres within the mix constituents. Figure 8.14 and Table 8.17 shows that there is a massive difference in the free shrinkage of materials G4 and G5 at 100 days (401 versus 1087 microstrain respectively). Both materials contain the same polymers and fibres. The reason for this difference is the fact that material G5 contains a fine aggregate only whereas material G4 has a 10mm graded coarse aggregate which provide restraint to shrinkage. The same conclusions are given by Mangat and Limbachiya [29, 30], Schrader [40] and Lea [41] who conclude that the type and quantity of coarse aggregate have an enormous effect on the free shrinkage of repair materials.

When high volume repairs are required, the most economical method of application is either by spraying or by pouring. Materials which belong to these categories of application methods normally contain coarse aggregates (up to 10mm size) to make the material more economical. Materials used in high volume repairs are therefore expected to show less shrinkage than materials used in low volume repairs due to the fact that larger aggregates (quantity and size) are contained within the mix. This is evident in the results shown in Figures 8.14 to 8.16, where the spray applied and poured materials in Figures 8.14 to 8.16 generally have lower shrinkage than the hand applied materials in Figure 8.14. Exceptions to this rule are the spray applied material G2 and hand applied material G4 (see Figure 8.14). The explanation for this reversal in trend is that the spray

applied material G2 uses a medium grade sand as aggregate whereas the hand applied material G4 contains 10mm nominal size graded aggregate. Hence, the shrinkage is lower in material G4 due to the inclusion of the coarser aggregate in the mixture.

Finally, regardless of the manufacturers' literature stating that their material is shrinkage free or shrinkage compensated (materials G4, G5, G6, L1, L3, L5, S1, S2 and S3 are described as such in manufacturers' literature), all the materials tested in this investigation showed considerable free shrinkage (see Figures 8.14 to 8.16 and Table 8.17). The same conclusion was also reported by Morgan [28].

8.5.1.2 Water cured specimens

Deformation of repair materials used at Gunthorpe Bridge, Lawns Lane Bridge and Sutherland Street Bridge, which were initially mist cured for 24 hours and cured in water for a further 27 days at 20°C, is given in Figures 8.17 to 8.19. A summary of the results and comparisons with the air cured specimens is also given in Table 8.18.

The free shrinkage of the water cured repair materials used at Gunthorpe Bridge is shown in Figure 8.17 and Table 8.18. Repair materials G1-G3 are spray applied materials whereas materials G4-G6 are hand applied materials. All the repair materials in Figure 8.17 exhibit relatively low shrinkage in the early stages under test which ultimately results in lower free shrinkage at 100 days (between 184 and 649 microstrain). Referring to Table 8.18, the 100 day shrinkage of these specimens is

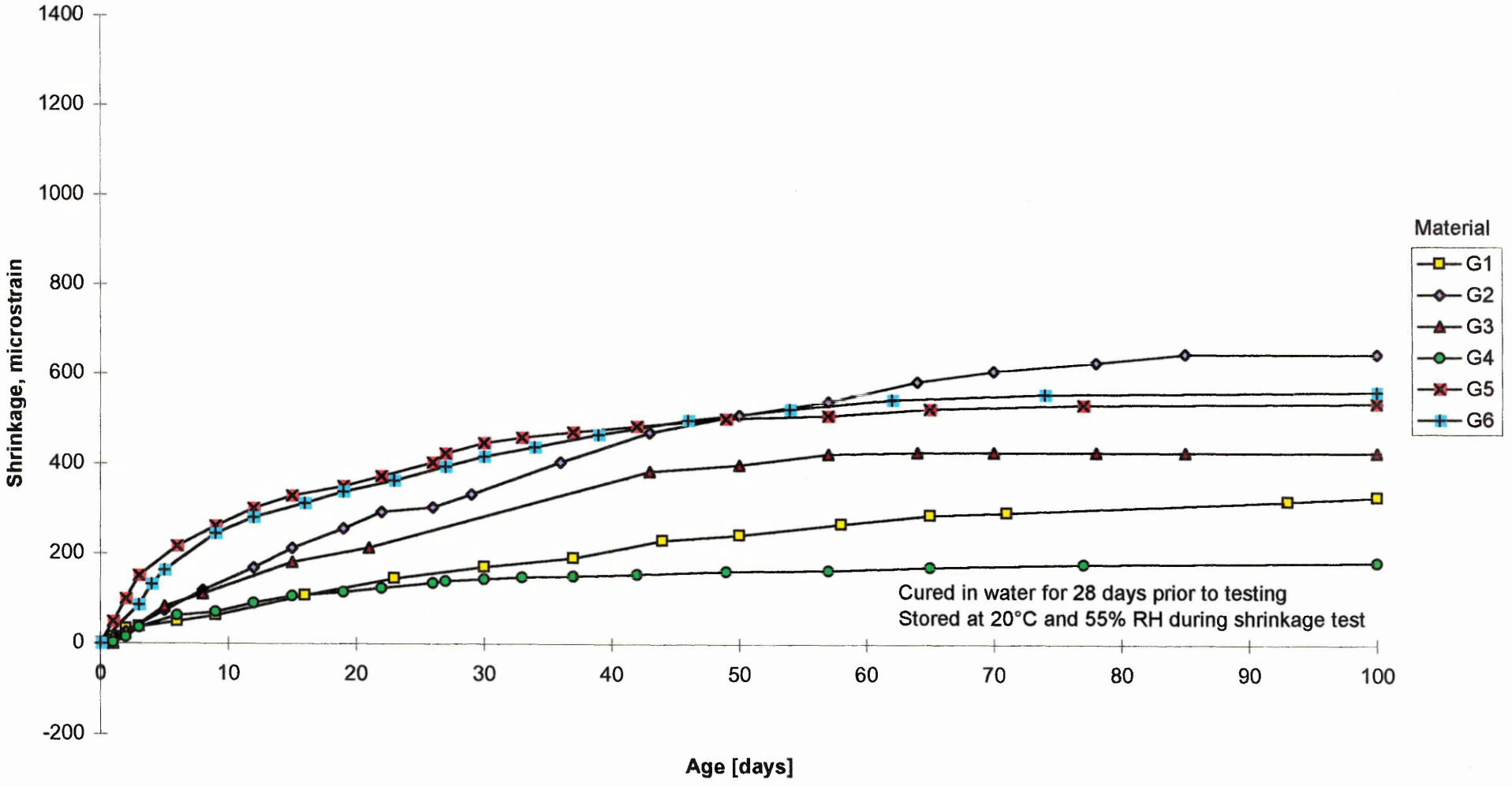

Figure 8.17 Free shrinkage (initial curing: 28 days in water, exposure during subsequent shrinkage testing 20°C and 55% RH) of repair materials used at Gunthorpe Bridge (G1-G6)

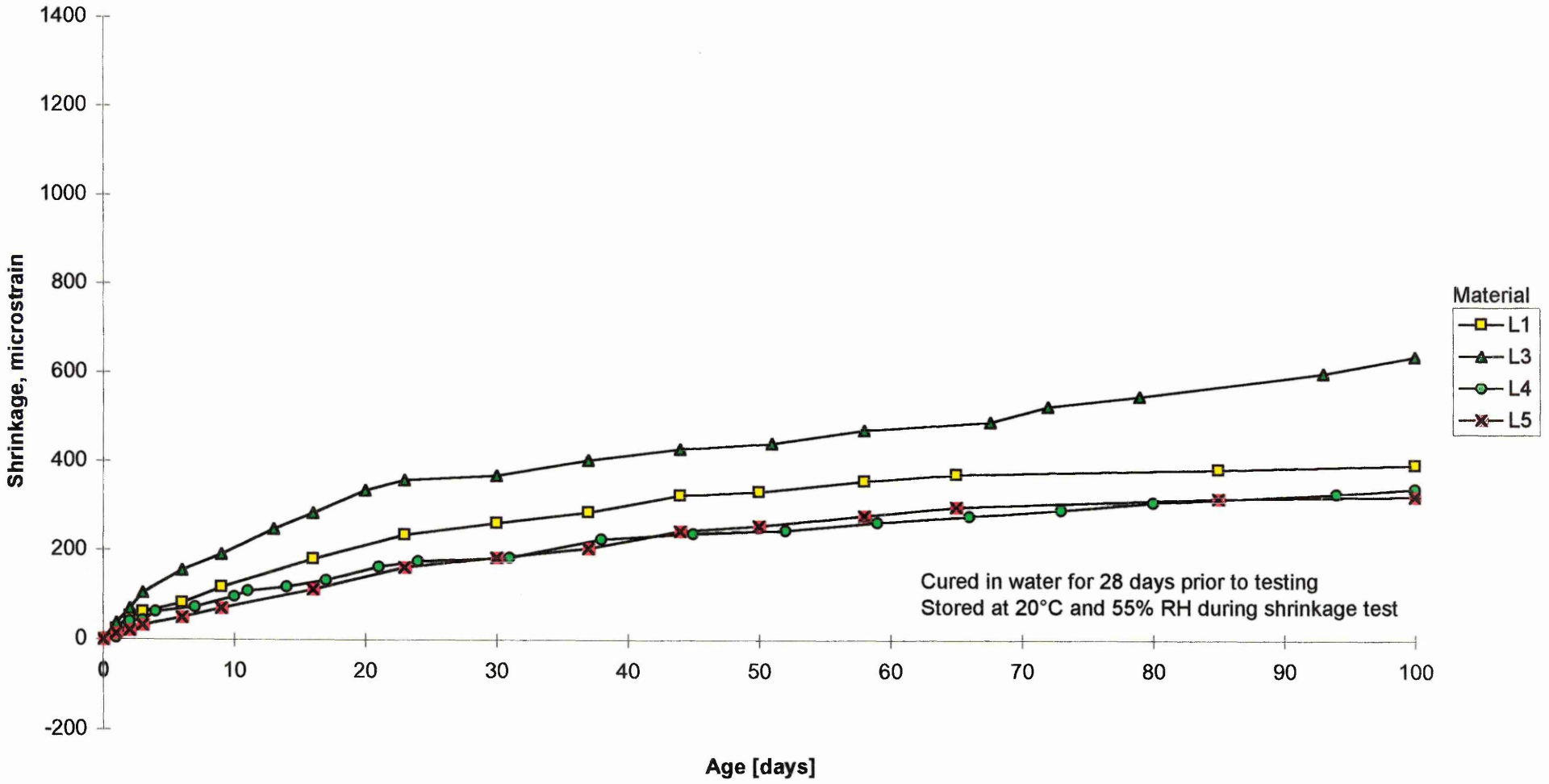

Figure 8.18 Free shrinkage (initial curing: 28 days in water, exposure during subsequent shrinkage testing 20°C, 55% RH) of repair materials used at Lawns Lane Bridge (L1, L3-L5)

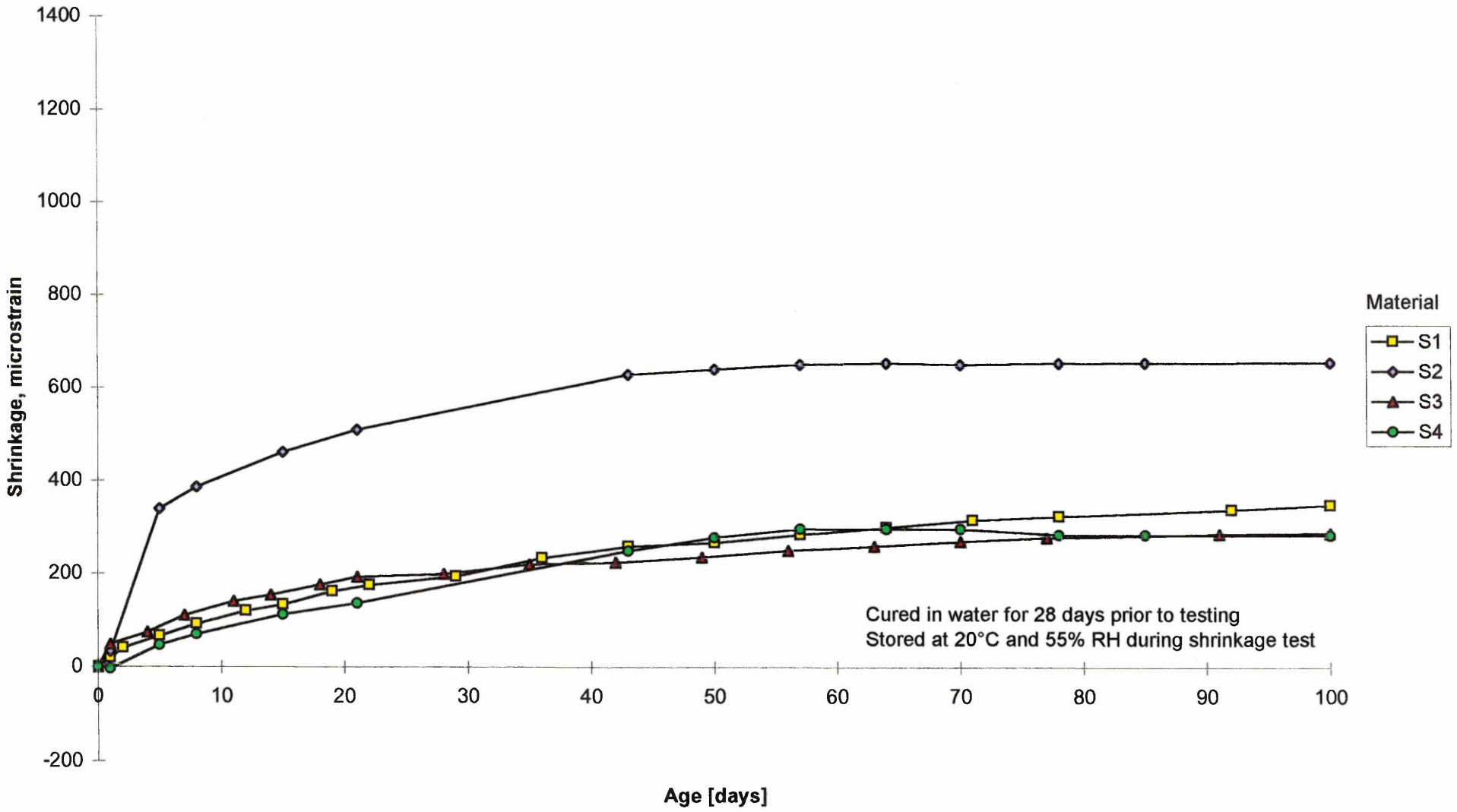

Figure 8.19 Free shrinkage (initial curing; 28 days in water, exposure during subsequent shrinkage testing 20°C, 55% RH) of repair materials used at Sutherland Street Bridge (S1-S4)

Table 8.18 Deformation from 28 to 100 days (water cured specimens)

Material	*Shrinkage at 100 days, microstrain (Dry cured)*	*Deformation at 100 days, microstrain (Wet cured)*	*Wet/Dry cured %*
G1	751	330	44
G2	1311	649	50
G3	717	429	60
G4	401	184	46
G5	1087	539	50
G6	1100	565	51
L1	620	395	64
L2	325	NA	NA
L3	710	640	90
L4	782	342	44
L5	680	325	48
S1	740	350	47
S2	791	657	83
S3	580	286	49
S4	388	285	73
		Average:	*57*

approximately between 44% and 60% of the 100 day shrinkage of specimens air cured in a controlled environment (20°C and 55% RH).

Figure 8.18 and Table 8.18 show the 100 day free shrinkage of the water cured materials used at Lawns Lane Bridge. Materials L1 and L3-L5 are spray applied materials. Referring to Table 8.18, the 100 day shrinkage of these specimens is between 325 and 640 microstrain. This is approximately between 44% and 90% of the 100 day shrinkage of air cured specimens.

Figure 8.19 and Table 8.18 show the 100 day shrinkage of the water cured repair materials used at Sutherland Street Bridge (between 285 and 657 microstrain). Referring to Table 8.18, the 100 day shrinkage of these specimens is approximately between 47% and 83% of the 100 day shrinkage of specimens cured in a controlled environment (20°C and 55% RH).

8.5.1.2.1 Discussion

Material G3, a cement and sand spray applied mortar (ratio 1:3) can be used as a reference for all other materials under test since the mortar is not polymer modified and consists of basic constituents. The ratio of wet cured shrinkage to dry cured shrinkage for this material is 60%. Four of the repair materials have ratios greater than this value (materials L1, L3, S2 and S4). Repair materials L3, a spray applied material, and S2, a flowing material, exhibit the highest ratios of 90% and 83% respectively. Both materials are supplied by the same manufacturer. The high shrinkage ratios of these repair materials indicate that significant shrinkage will occur regardless of the curing techniques adopted.

The overall ratio of the shrinkage of specimens cured in water to the shrinkage of specimens cured in air is 57%, as shown in Table 8.18. Therefore, curing the repair materials in water for the first 28 days substantially reduces the free shrinkage. Consequently, if proper curing techniques are implemented after the new repair materials are applied in the field, such as applying curing membranes and/or covering the repair patch with polythene to restrict the moisture loss from the repair patch, the

free shrinkage can be drastically reduced for most repair materials. Application of curing membranes and/or polythene may not reduce shrinkage to the same level as curing in water, but nevertheless, shrinkage will be lowered. This will reduce the risk of cracking in the repair material, since the tension induced in the repair material due to the restraint to shrinkage provided by the substrate concrete will be less.

8.5.2 Creep deformation of repair materials

Creep of repair materials was determined by subjecting prism specimens to a sustained compressive stress of 30% of their cube strength. Two specimens were loaded in series in a creep rig for 70 days. The gross strain was measured at regular intervals on the eight longitudinal faces of two prisms. Creep recovery was monitored for 30 days once the load was removed from the specimens. Net creep strains were calculated by subtracting the shrinkage strain measured on identical specimens from the gross strain

The creep curves of the materials are given in Figures 8.20 to 8.22, which includes the instantaneous elastic strain upon loading, the creep of the material whilst under sustained stress and the creep recovery upon unloading. Table 8.19 gives the repair material abbreviation and 28 day cube strength (columns 1 and 2), plus a summary of the instantaneous elastic strains upon loading (column 3), the 70 day creep strains (column 4) and the value of ϕ, the creep coefficient (column 5). The delayed elastic strain and flow creep for each repair material is given in column 6 and 7 respectively. The delayed elastic strain is also given as a percentage of the 70 day creep strain in

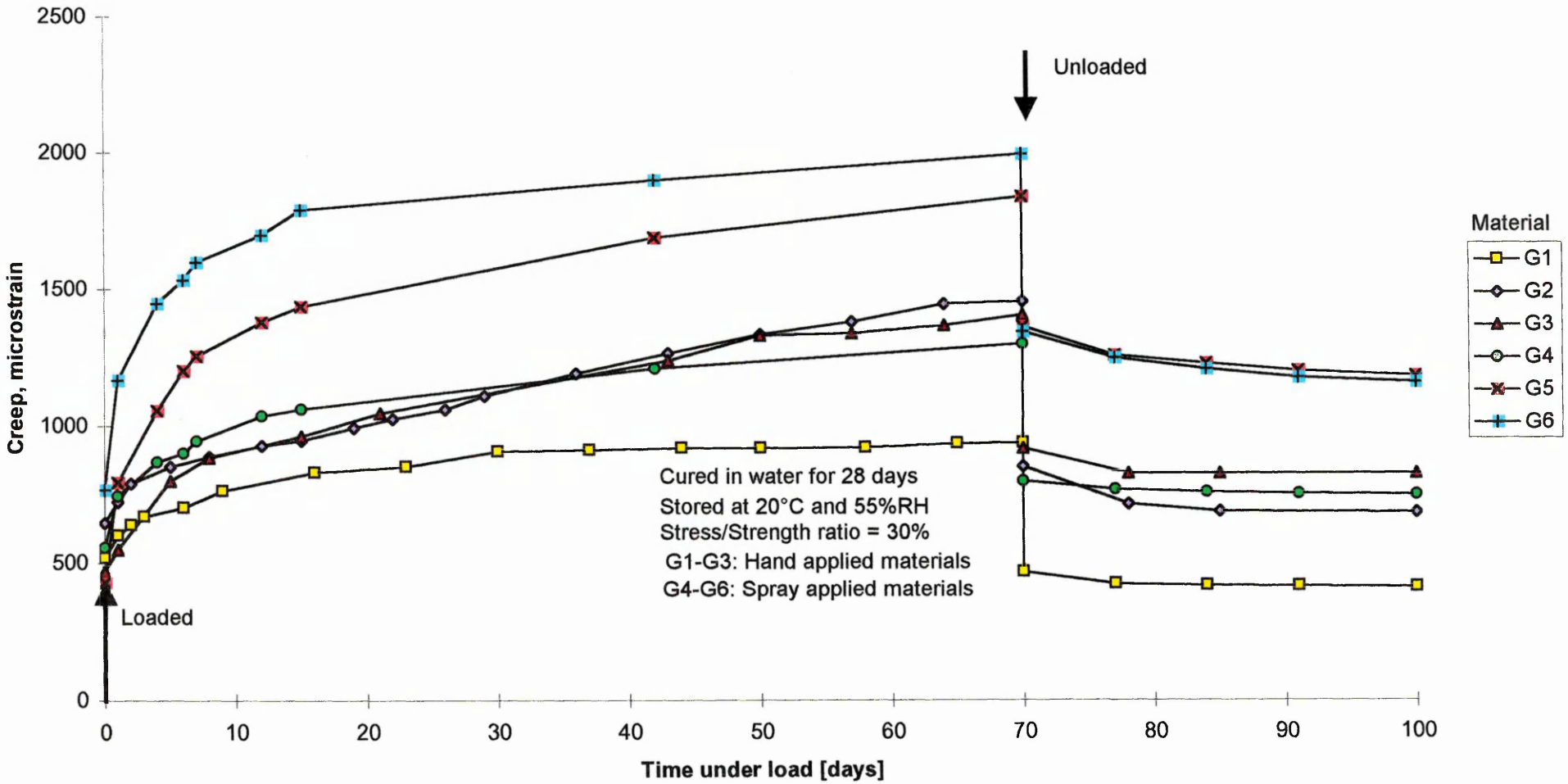

Figure 8.20 Creep of repair materials used at Gunthorpe Bridge (G1-G6)

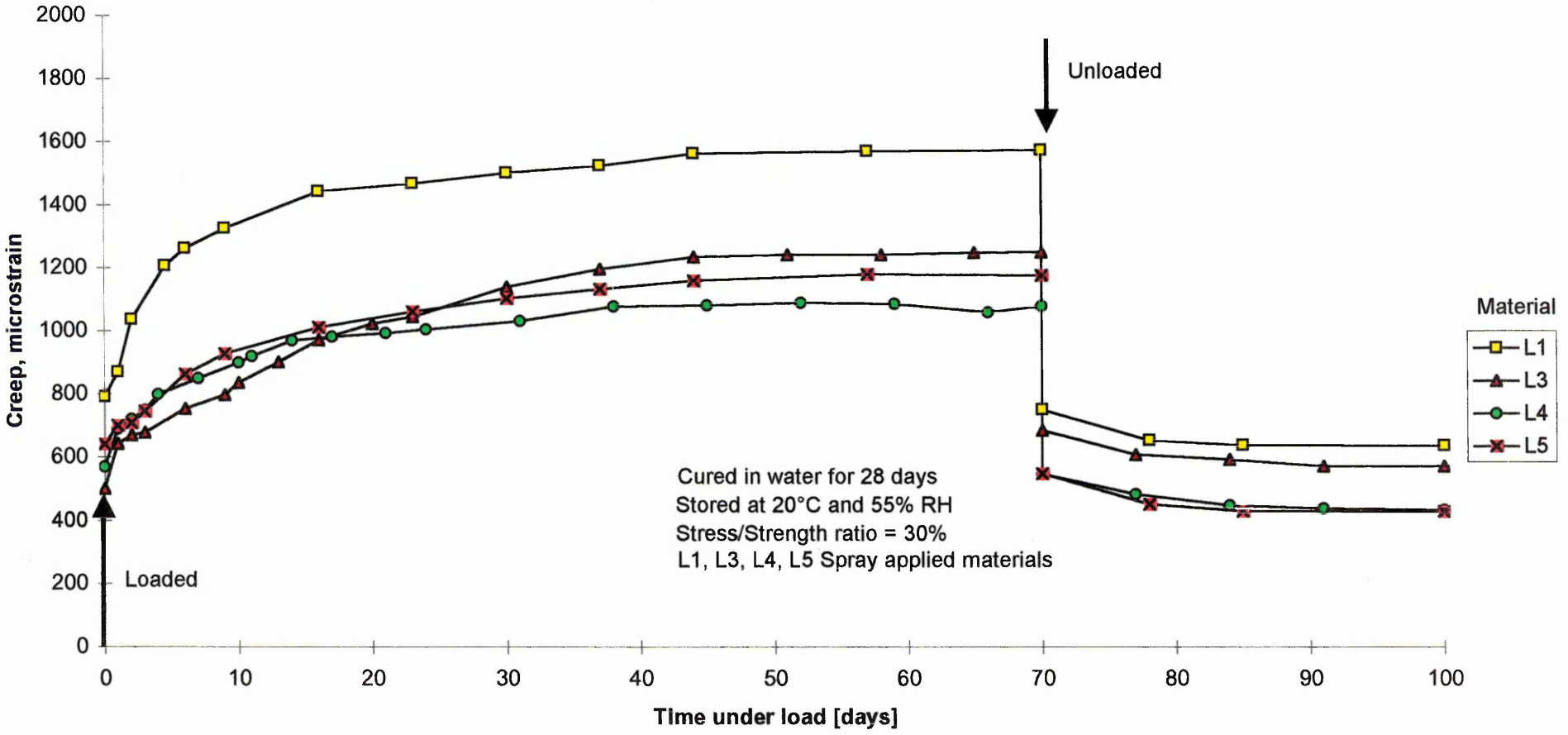

Figure 8.21 Creep of repair materials used at Lawns Lane Bridge (L1, L3, L4, L5)

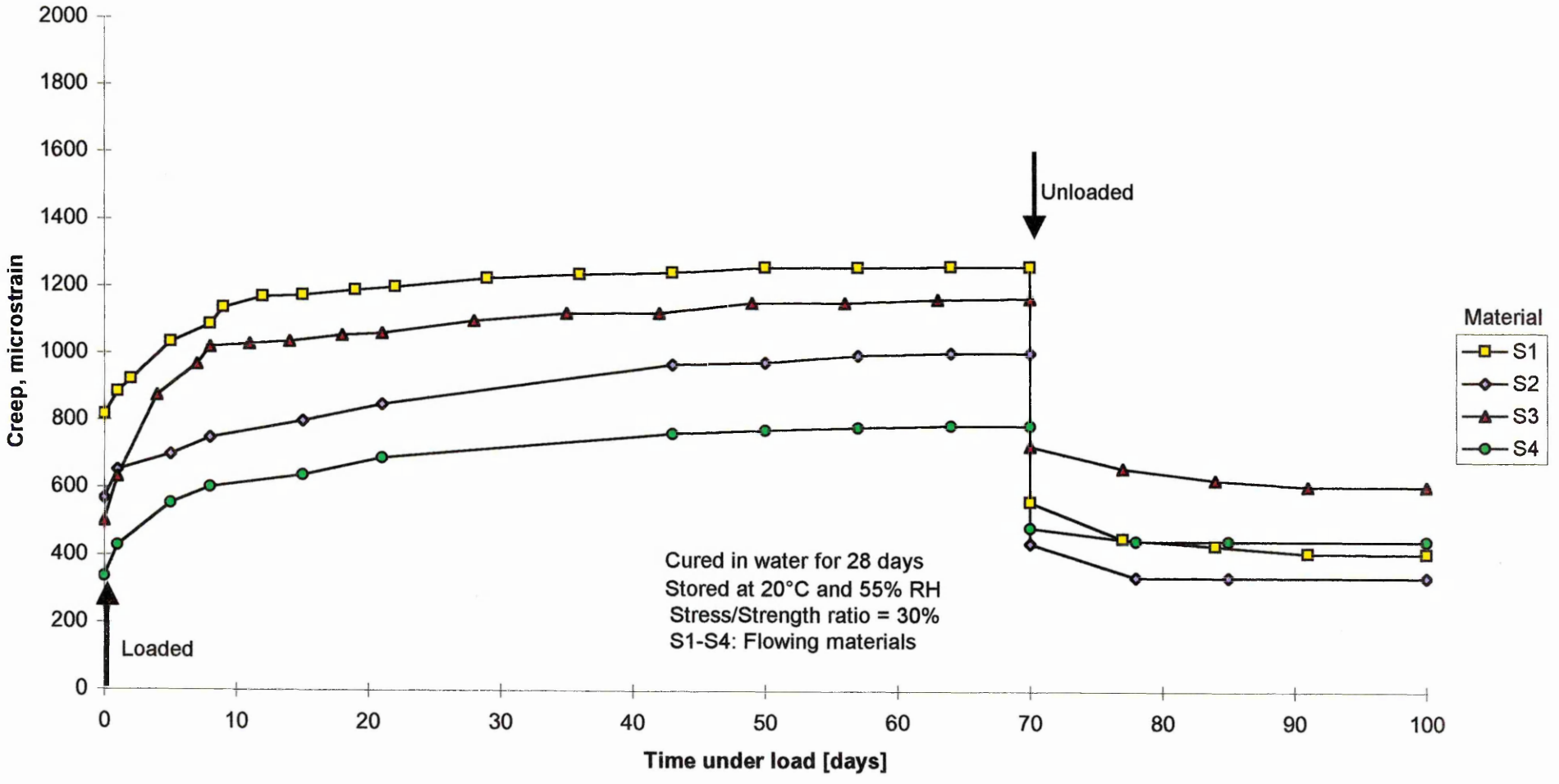

Figure 8.22 Creep of repair materials used at Sutherland Street Bridge (S1-S4)

TABLE 8.19 Creep properties and 28 day cube strength

Column							
1	*2*	*3*	*4*	*5*	*6*	*7*	*8*
Repair Mat.	*28 day cube strength (N/mm^2)*	*Inst. elast strain (μstrain)*	*70 day creep strain (μstrain)*	*ϕ $\frac{elastic}{creep}$*	*Del. elast strain (μstrain)*	*Flow creep (μstrain)*	*$\frac{Del+flow}{Total}$ (factor)*
G1	50	519	421	0.81	56 (13)	411	1.11
G2	44	647	809	1.25	169 (21)	685	1.06
G3	46	469	938	2.00	92 (10)	829	0.98
G4	46	557	745	1.34	49 (7)	751	1.07
G5	40	429	1411	3.29	180 (13)	1185	0.97
G6	31	767	1188	1.55	184 (15)	1162	1.13
L1	69	791	783	0.99	113 (14)	639	0.96
L2§	60	NA	NA	NA	NA (-)	NA	NA
L3	35	502	748	1.49	113 (15)	574	0.92
L4	73	570	510	0.89	114 (22)	435	1.08
L5	80	643	534	0.83	121 (23)	430	1.03
S1	79	818	445	0.54	154 (35)	410	1.27
S2	65	569	438	0.77	100 (23)	340	1.00
S3	68	502	667	1.33	120 (18)	611	1.10
S4	39	337	454	1.35	38 (8)	448	1.07

Note: § indicates that a creep test was not conducted on this material

brackets in column 6. The ratio of the sum of the delayed elastic and flow creep strains to the total (70 day) creep strains is given in column 8.

8.5.2.1 70 day creep strains

Referring to Figure 8.20 and Table 8.19, the total creep strains of the materials used at Gunthorpe Bridge (materials G1-G6) range from 421 to 1411 microstrain. Materials

G1, G2 and G4 exhibit creep strains of 421, 809 and 745 microstrain respectively, which are less than the creep strain of the conventional repair mortar G3 (938 microstrain). Materials G5 and G6 have creep strains (1411 and 1188 microstrain respectively) which are greater than the reference material, G3.

All materials used at Lawns Lane Bridge which were tested for creep (Figure 8.21) exhibited creep strains which were less than those of the reference material G3 (510 to 783 microstrain compared with 938 microstrain for G3, Figure 8.20 and Table 8.19). Material L2 was not tested for creep due to difficulty in obtaining material samples from the manufacturer.

The total creep of the materials used at Sutherland Street Bridge ranged between 438 to 667 microstrain, as shown in Figure 8.22 and Table 8.19. These values are less than the creep of the reference material (938 microstrain). Material S1, S2 and S4 exhibited similar creep strains (438 to 454 microstrain) whereas material S3 had a slightly higher creep strain of 667 microstrain.

Referring to Table 8.17, materials G2, G4 and G5 are all polymer modified materials with fibres included in the mix. The 70 day creep strains of these three materials (from Table 8.20) are 809, 745 and 1188 microstrain respectively. Materials G2 and G5 both contain fine aggregates whereas G4 contains 10mm graded coarse aggregate (see Table 8.17). It is therefore evident that the aggregate size influences the magnitude of creep in the repair materials, as the material with the larger aggregate, G4, exhibits lower creep than materials with finer aggregates. The same can be said for material S4 which

includes 10mm single sized aggregate. The 70 day creep in this instance was 388 microstrain. Other researchers have also found lower compressive creep in repair materials which contain coarse aggregate [29] An explanation to this is given by Neville *et al* [85], who state that the quantity and modulus of aggregate contributes to resisting the creep of cement paste.

Repair materials used in high volume repairs (sprayed and flowable materials) exhibited lower creep since such materials generally contain larger aggregates to make their use in large volume repair more economical (materials G1, L1-L5, S1-S4, Tables 8.17 and 8.19).

Other researchers [25, 29, 30] report high creep strains of polymer modified repair materials. Some of the materials tested in the current study have polymer modifications (G1, G2, G4-G6, L2, S3, see Table 8.17). The creep values for these materials cover a wide range, from 421 to 1036 microstrain. Therefore, it is difficult to isolate the influence that polymers have on the creep of these materials.

8.5.2.1.1 Creep coefficient

The values of ϕ, the creep coefficient, which is the ratio of creep strain to the instantaneous elastic strain upon loading are also given in Table 8.19, column 5. This coefficient is used to allow for the effect that creep will have on the elastic modulus of the material by calculating an effective elastic modulus, $E_{rm(eff)}$, as follows [64]:

$$E_{rm(eff)} = E_r / (1+\phi)$$

Equation 8. 4

where E_r is the instantaneous elastic modulus of the repair material. According to Equation 8. 4, a high creep coefficient will result in a low effective modulus (for example, material G5, Table 8.19). Creep will have a significant effect on the redistribution of stresses within a repair. For example, a material with an elastic modulus that was initially greater than that of the substrate concrete may in time have an effective elastic modulus less than that of the substrate concrete. As a result, the repair material may be ineffective in sharing load with the substrate concrete.

8.5.2.2 Creep recovery

The creep recovery, or delayed elastic strain of the repair materials used at Gunthorpe Bridge, Lawns Lane Bridge and Sutherland Street Bridge is given in Table 8.19 (column 6). The creep recovery is also presented as a percentage of the 70 day creep strain (shown in brackets in column 6, Table 8.19). The flow creep of the repair materials is also listed in Table 8.19, column 7.

Referring to Table 8.19, repair materials G4 and S4 exhibit the lowest creep recovery strains of 49 and 38 microstrain respectively. This corresponds to 7% and 8% respectively of the 70 day creep strain. These repair materials (G4 and S4) both contain 10mm sized coarse aggregate as shown in Table 8.17. Neville *et al* [85] state that creep recovery has been shown to be proportional to the cement paste content of the mix

(or inversely proportional to the aggregate content) [86]. Therefore, applying the conclusions found previously to repair materials [86], a repair material which contains coarse aggregate will tend to show less creep recovery as opposed to a repair material which contains fine aggregate. The results of this experiment did not prove that repair materials with fine aggregate exhibited higher creep recovery than repair materials with coarse aggregate (materials G5 and G6, Table 8.19). The creep recovery of the reference material, G3, also exhibited a low creep recovery (10%) despite the fact that a medium grade sand was used as aggregate (see Table 8.17). Material S1 showed the highest creep recovery of 35%, but it is thought that experimental error may be to blame, as the sum of the delayed elastic strain and the flow creep strain totalled 564 microstrain, which was far greater than the 70 day creep strain of 445 microstrain, see Table 8.19, (the relationship between creep, delayed elastic and flow creep strain is studied in the next section). The remainder of the repair materials exhibited creep recovery in the range of 13 to 23% of the 70 day creep.

8.5.2.3 Relationship between creep, delayed elastic and flow creep strain

Creep of concrete is normally the sum of the flow and delayed elastic components [46], therefore, for the repair materials under observation, Table 8.19 also lists the ratio of delayed elastic strain and flow creep strain to the 70 day total creep strain (column 8). Referring to Table 8.19, column 8, the ratio of the sum of delayed elastic strain and flow creep strain to the 70 day creep strain ranges between 0.92 and 1.27 (although experimental error may be at fault for the high ratio of 1.27 for material S1, as stated in

the previous section). Neglecting the 1.27 ratio, the range is between 0.96 and 1.13, giving an average of 1.04. This ratio can be considered similar to the ratio expected when testing concrete for creep (i.e. 1.00).

Both repair materials which contain large aggregates (G4 and S4) exhibit a ratio of 1.07. The ratios of repair materials with fine aggregates (G5 and G6) exhibit ratios of 0.97 and 1.13 respectively. Styrene acrylic, fibres and fine aggregate are included in the mix of materials G2 and G5, but the ratios of these materials are 1.06 and 0.97 respectively. Based on these observations, it is concluded that these small variations are due to experimental factors and that repair material constituents do not have an influence.

8.5.3 Elastic modulus of repair materials

Elastic modulus results obtained form 100mm diameter x 180mm deep cores of substrate concrete and 100mm diameter x 200mm long cylinders of repair material are given in Table 8.20.

The results in Table 8.20 show that material G1 is the only material used at Gunthorpe Bridge which is stiffer than the substrate concrete. Four of the five materials (L2-L5) used at Lawns Lane Bridge have elastic modulii greater than the elastic modulus of the substrate. All the materials used at Sutherland Street Bridge are stiffer than the concrete substrate. In laboratory concrete repairs, two of the materials, G4(L) and L3(L) are stiffer than the concrete substrate at 28 days whereas the other two materials [G5(L) and G6(L)] are less stiff than the substrate concrete at 28 days.

Table 8.20 Elastic modulus of repair materials and substrate concrete

Location	*Material*	*Elastic modulus* (kN/mm^2)
Gunthorpe Bridge	G1	31.1
	G2	17.6
	G3	23.8
	G4	24.0
	G5	19.6
	G6	11.5
	substrate	28.1
Lawns Lane Bridge	L1	22.7
	L2	30.3
	L3	27.4
	L4	29.1
	L5	29.1
	substrate	23.8
Sutherland Street Bridge	S1	24.2
	S2	32.2
	S3	31.9
	S4	27.4
	substrate	23.2
Laboratory Repairs	L3 (L)	27.4
	G4 (L)	24.0
	G5 (L)	19.6
	G6 (L)	11.5
	substrate	20.5

Referring to Tables 8.17 and 8.20, materials with contain both coarse aggregate and polymer additions generally exhibit higher elastic modulus values (see materials G1, L2, L4 and S3 in Tables 8.17 and 8.20). Kuhlman [63] found that the elastic modulus of a

repair material increased with the addition of a hard film latex. Mangat and Limbachiya [30] observed higher elastic modulus in repair materials that contained aggregate particles. Materials which contain fine aggregates with or without polymer additions generally have lower elastic modulii (materials G2, G5 and G6 in Tables 8.17 and 8.20).

8.5.4 Modulus of rupture

Figure 8.23 and Table 8.21 gives the 28 day modulus of rupture for some of the repair materials (obtained from the manufacturers' literature) along with the long term modulus of rupture of all the repair materials used in the project. The long term modulus of rupture was obtained by testing specimens in the laboratory approximately 14-36 months after casting (figure in brackets, Table 8.21). These specimens were tested in accordance with BS 1881, Part 118 [87]. This standard was also used to obtain the 28 day modulus of rupture of materials G1 and G2 (Table 8.21). Repair materials G4, G5 and G6 were tested at 28 days in accordance with BS 4551 [88], whereas material L3 was tested at 28 days in accordance with BS 6319 Part 3 [89]. No information was given on the test method used to obtain the modulus of rupture of material L5 at 28 days. The tensile strength of the repair materials at 28 days is also given in Table 8.21. This was obtained using the relationship between modulus of rupture and direct tensile strength for concrete found by Brooks and Neville [47] for dry stored specimens.

Referring to Table 8.21 and Figure 8.23, the modulus of rupture of the repair materials at 28 days varies from 4.1 N/mm^2 to 13.5 N/mm^2. The spray applied repair materials (G1 and G2) at Gunthorpe Bridge exhibit a modulus of rupture of 8.0 and 4.1 N/mm^2 at

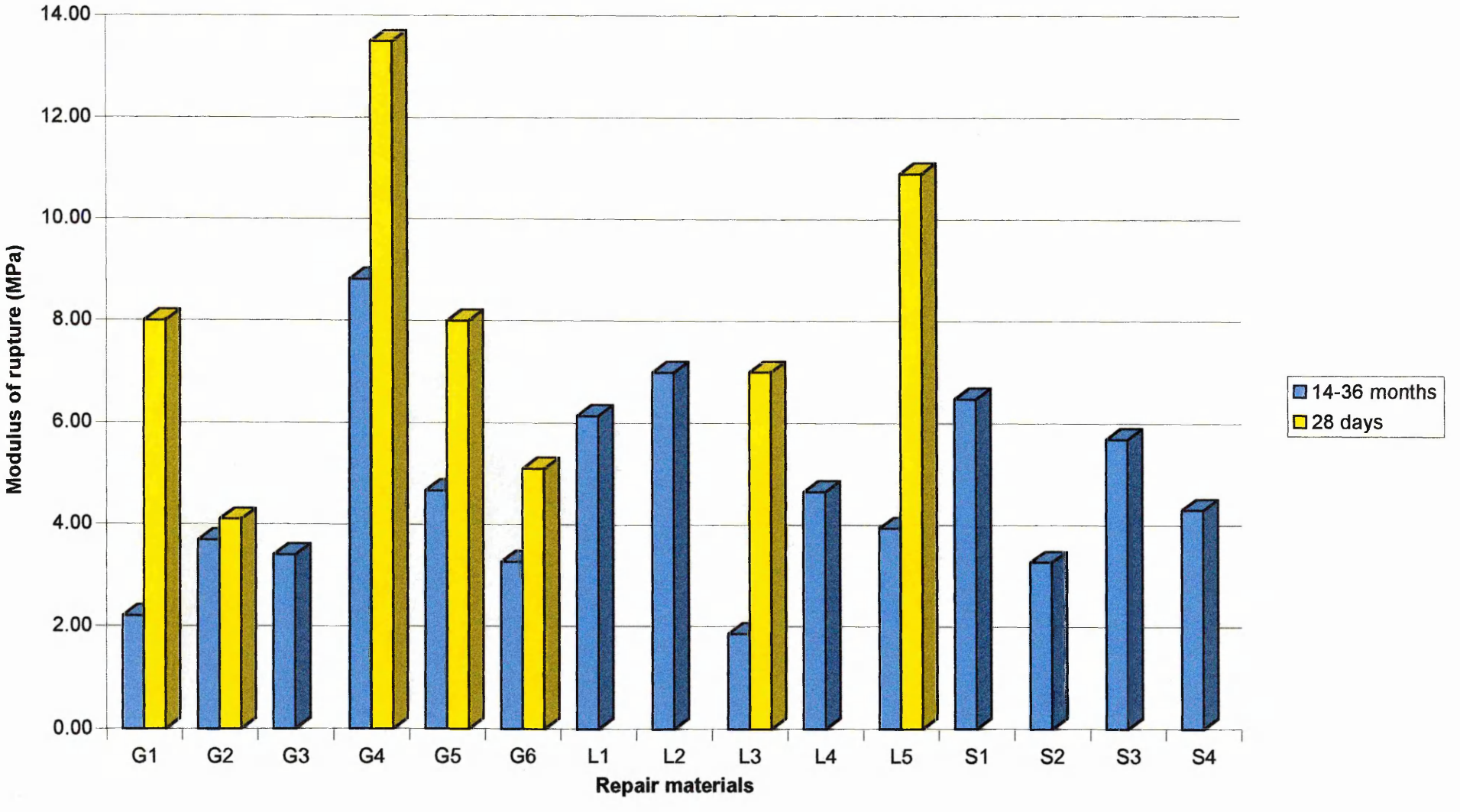

Figure 8.23 Modulus of rupture of repair materials tested at 28 days and 14-36 months

Table 8.21 Modulus of rupture of repair materials

Location	*Material*	*Modulus of rupture (N/mm²)*		*Tensile Strength [47] (N/mm²)*
		Literature	*Laboratory*	
		28 days	*(age in months)*	*28 days*
Gunthorpe Bridge	G1	8.0*	2.2 (20)	4.2
	G2	4.1*	3.7 (20)	2.5
	G3	NA	3.4 (20)	NA
	G4	13.5**	8.8 (21)	6.2
	G5	8.0**	4.7 (21)	4.2
	G6	5.1**	3.3 (21)	2.9
Lawns Lane Bridge	L1	NA	6.1 (16)	NA
	L2	NA	7.0 (36)	NA
	L3	7.0#	1.9 (18)	3.9
	L4	NA	4.7 (18)	NA
	L5	10.9^{NA}	4.0 (16)	5.3
Sutherland Street Bridge	S1	NA	6.5 (14)	NA
	S2	NA	3.3 (21)	NA
	S3	NA	5.7 (21)	NA
	S4	NA	4.3 (21)	NA

**Tested to BS 1881, Part 118 **Tested to BS 4551 #Tested to BS 6319, Part 3*

28 days respectively. The three hand applied materials at Gunthorpe Bridge show a modulus of rupture of 13.5, 8.0 and 5.1 N/mm^2 respectively at 28 days. Spray applied materials L3 and L5 at Lawns Lane Bridge exhibit a 28 day modulus of rupture of 7.0 and 10.9 N/mm^2 respectively. The long term modulus of rupture of all the repair materials used in the project is also given in Table 8.21 and Figure 8.23. The spray applied repair materials at Gunthorpe Bridge (G1-G3) show a modulus of rupture of between 2.2 and 3.7 N/mm^2. The spray applied materials at Gunthorpe Bridge exhibit a

long term modulus of rupture of between 3.3 and 13.5 N/mm^2. The long term modulus of rupture of the spray applied materials at Lawns Lane Bridge varies between 1.9 and 7.0 N/mm^2. Finally, the long term modulus of rupture of the flow applied repair materials at Sutherland Street Bridge varies between 3.3 and 6.5 N/mm^2.

Referring to Figure 8.23 and Table 8.17, the materials that generally exhibit the largest modulus of rupture at 28 days are the repair materials that contain coarse or graded aggregate in the mixture (materials G1, G4, G5, L3 and L5). Material G5 also exhibits quite a high modulus of rupture (8.0 N/mm^2 at 28 days, Figure 8.23) even though the repair material contains fine aggregate. This repair material also contains styrene acrylic and fibres which may be responsible for the high modulus of rupture. On the other hand, material G2 also contains fine aggregate with styrene acrylic and fibres added to the mixture, but the modulus of rupture of this repair material is relatively low (4.1 N/mm^2 at 28 days, Figure 8.23). Therefore, based on these two results, it is not possible to comment on the influence that styrene acrylic and fibres have on the modulus of rupture of the repair materials.

Comparing the 28 day modulus of rupture results to the long term modulus of rupture results, it is clear that the modulus of rupture decreases with time (see repair materials G1, G2, G5, G6, L3 and L5, Figure 8.23). The curing regimes adopted by the different manufacturers' may have differed to the curing regime adopted in the laboratory (20°C and 55% RH). For example, BS 1881 Part 118 [87] states that the specimens should be cured and stored in either the wet or dry condition prior to testing. BS 6319 Part 3 states

that specimens should be prepared in accordance with BS 6319 Part 1 [90]. This allows either wet or dry specimens to be tested. Finally BS 4551 [89] allows for either hydraulic or moist air curing prior to testing. Assuming that all specimens were cured under similar conditions, the difference between the 28 day modulus of rupture is significantly greater than the modulus of rupture of specimens tested in the long term. This will cause the repair material to become more brittle with time. Therefore, a repair material which carries a constant tensile stress may in fact crack in the long term since the modulus of rupture, and consequently, the direct tensile strength, may become less than the applied tensile stress. This, in fact, occurred with material L4 at Lawns Lane Bridge, where cracks appeared approximately 15 months after application of the repair material (full details are given in Chapter 9).

8.6 CONCLUSIONS

The following conclusions are based on the results of the materials tests carried out in the laboratory to determine the basic properties of the repair materials:

- Repair materials which contain coarse aggregate exhibit lower free shrinkage and creep compared with repair materials which contain fine aggregate only.
- Spray applied and flowable repair materials shrink and creep less than repair materials which are hand applied due to the inclusion of coarse aggregates in the spray applied and flowing repair materials.

- All the cementitious repair materials tested in this project exhibited significant free shrinkage regardless of some manufacturers' claims that their materials were shrinkage compensated or non-shrinking repair materials
- The free shrinkage of repair materials is reduced when the specimens are initially cured in water for 28 days after casting as opposed to curing in air from the age of 24 hours onwards.
- Repair materials which contain coarse aggregates exhibit lower creep recovery than repair materials with fine aggregates
- The addition of polymers and coarse aggregates generally increases the elastic modulus of a repair material.
- Repair materials with fine aggregates, with or without polymer additives, generally have lower elastic modulus.
- Repair materials which contain coarse aggregates generally exhibit higher modulus of rupture than repair materials with fine aggregate.
- The modulus of rupture of repair materials decreases with time

CHAPTER 9

IN-SERVICE PERFORMANCE OF REINFORCED CONCRETE REPAIR

9.1 INTRODUCTION

Reinforced concrete is used widely in construction due to its versatility and durability when properly designed and placed. However, deterioration occurs due to exposure to aggressive environments such as those containing chlorides and carbon dioxide. The deterioration can be arrested by removing the damaged concrete and replacing it with a new material. The assumption is made that the new repair material will restore the structural integrity of the member, but despite the extensive amount of research done in the general area of concrete repair, very little information exists on the in-service performance of repair materials. As a result, deteriorated structures are currently being repaired with inadequate knowledge of the structural interaction which occurs between the substrate concrete and repair material under in-service conditions.

This chapter presents the long term performance of different repair materials under service conditions from both field and laboratory studies. Recommendations for enhanced long term performance are given at the end of the chapter. A brief literature review is given on the subject at the beginning of the chapter.

9.2 LITERATURE REVIEW

9.2.1 Requirements of repair materials

Morgan [28] states that there is no such thing as the ideal repair material. Different types of repair materials will be required for different repair applications. In other words, the repair materials must be selected so that a durable and load sharing repair is provided. Selection of the correct material for a repair project is of utmost importance. Rizzo and Sobelman [91] report that repair to a structure should fulfil three basic requirements. First, the repair must arrest the deterioration of the structure, particularly by preventing further corrosion of reinforcement steel. This can be done by preventing access of oxygen, water and aggressive ions to the steel [92] or providing an environment that chemically passivates the steel reinforcement. This highlights the need for a material to be impermeable, but this property is meaningless if cracks occur in the material due to the restraint to shrinkage provided by the substrate concrete. A few cracks in the repair material drastically offset the benefit of having a low permeability repair material [49]. Therefore, it is vital that repair materials used to repair deteriorated concrete have low shrinkage deformation and/or a high tensile strain capacity.

The second requirement is restoration of structural integrity. It is reported [91] that there is some controversy as to how much load a patch repair carries. It is generally accepted that for all but purely cosmetic repairs the material used should have strength properties similar to those of the substrate concrete. Results from the current research show that strength is a relatively unimportant parameter. The elastic modulus of the repair material has a major influence on the distribution of strain between the repair

material and substrate concrete. A repair material that has an elastic modulus greater than that of the substrate concrete is able to distribute a proportion of the shrinkage strain to the substrate, thus reducing the magnitude of shrinkage that is restrained by the substrate concrete. It is also shown that a stiffer repair material will attract external load into the repair patch. A repair material with a high strain capacity will also show more resistance to cracking.

The final requirement of a successful repair is that it provides an aesthetically acceptable finish. It is stated that [91] a coating should be applied over the whole of the structure to give a uniform appearance which will also provide additional protection to both the repair and to areas not yet showing signs of distress. More importantly, the appearance of the material should not be affected by the presence of cracks. This would reduce the ability of the repair to carry load, aid the onset of further corrosion as well as being unsightly. It has been observed in the present research that a cracked repair material is unable to attract load into the repair patch.

Plum [93] states that the function performed by a repair will vary from one situation to another and may be required to satisfy several functions at once. The two principal functions may be defined as:

(a) structural, in which a stress carrying function is intended,

(b) cosmetic, in which restoration of structural appearance is a priority.

Furthermore, the properties required of a material to fulfil the requirements of a structural or cosmetic repair are clearly quite different [93] and may in some instances be completely opposite. The problem of choice of suitable properties is not solved by

seeking those closest to the values for the base concrete. This was evident in the current research, as a repair material with an elastic modulus which was similar to the substrate concrete performed as a cosmetic repair, whereas a repair material which was stiffer than the substrate concrete acted as a structural (load-sharing) repair.

9.2.2 Properties of repair materials which influence performance

Traditionally, specification of concrete repair mortars has been based on compressive strength, bond and shrinkage characteristics. While these properties form a useful guide, there are a number of other properties, such as elastic modulus, tensile strength and cracking characteristics, which are of greater importance for successful concrete repair [31]. The results from this research project show that material properties such as the elastic modulus, shrinkage and creep are primarily responsible for the structural interaction between the repair material and substrate concrete. Also, a repair material with a very high tensile strain capacity is less likely to crack when tensile stress is induced due to the restraint to shrinkage provided by the substrate concrete.

Compatibility between the repair material and substrate concrete is affected by volumetric deformation (i.e. dimensional), along with physical, chemical and electrochemical properties, see Figure 9.1 [95]. All these factors are responsible for ensuring that a repair will withstand all stresses induced by volume changes, and chemical and electrochemical effects without distress and deterioration [95]. Dimensional compatibility is responsible for the structural interaction between the

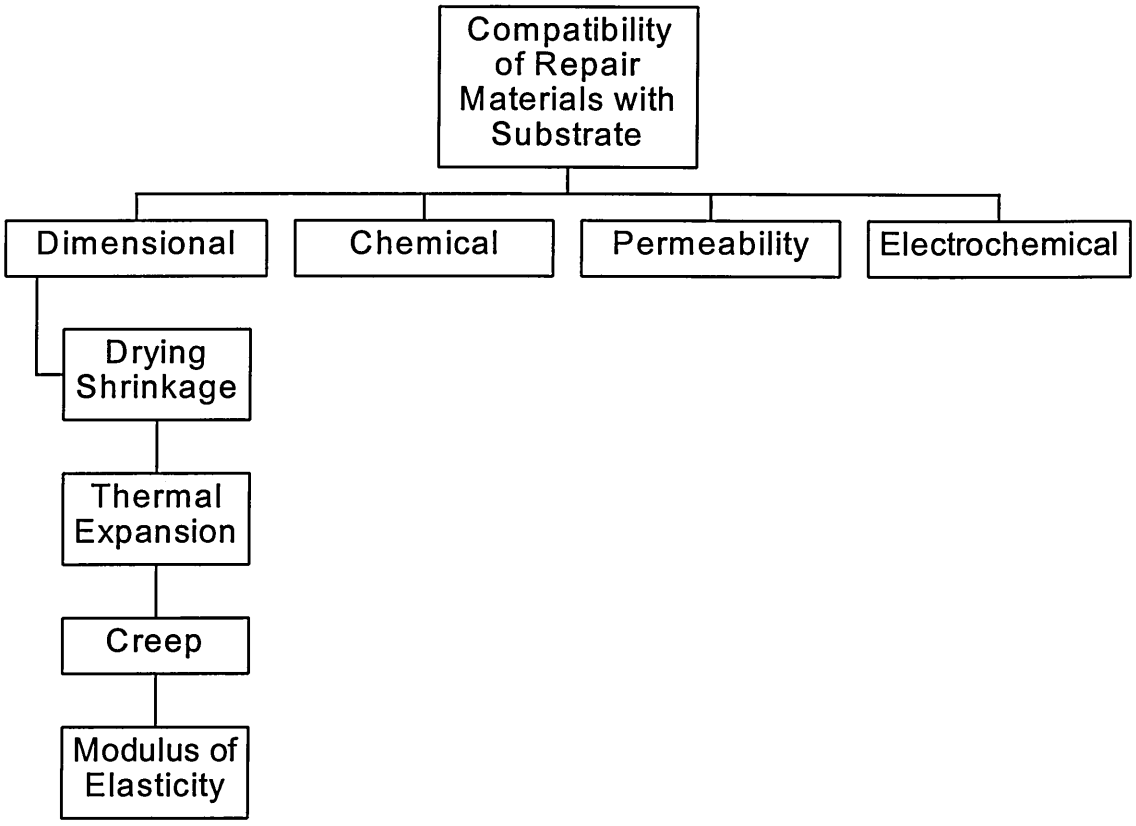

Figure 9.1 Factors affecting compatibility of repair materials [95]

repair material and substrate concrete. The material properties which are responsible for dimensional compatibility are given in Figure 9.1. Among these properties are drying shrinkage, creep and elastic modulus. Current research agrees that these properties have a significant contribution to the design of a durable repair. If high shrinkage occurs in a repair material, significant levels of tensile stress will be evident in the repair patch due to the restraint provided to shrinkage by the substrate concrete. However, if the repair material exhibits an elastic modulus which is greater than that of the substrate concrete, then the stiffer repair material will transfer a portion of the shrinkage strain to the substrate concrete. Nevertheless, a tensile stress will still be evident in the repair material, but this stress will be reduced by stress relaxation caused by creep in the repair material.

An important point to make is that the properties of a repair system change with time [49] (e.g. creep will lower the elastic modulus of the repair material which will render the load sharing ability of the repair patch less effective). Therefore, to successfully perform in a particular service environment, the specification of a repair patch needs careful considerations rather than simplistic approaches currently being used.

Investigations into the performance of concrete repair carried out elsewhere [95] highlights the modulus of elasticity, tensile strength coefficient of thermal expansion, early curing shrinkage strain and creep strain as important properties of a repair material. Materials with a low elastic modulus may generate relatively high stresses in the substrate concrete compared with those in the repair material. On the other hand, materials with a high elastic modulus tend to attract load away from the concrete and hence may place higher demands on interfacial adhesion. It was recommended that the modulus of elasticity of the repair material should lie within the range +/- 10 kN/mm^2 of that of the substrate concrete. A recommendation of this nature will not ensure a durable and load sharing repair, as the findings of this project show that the elastic modulus of the repair material must be higher than the elastic modulus of the substrate concrete to enable an efficient composite action to be developed.

9.2.2.1 Cracking in repair patches

Specification of a durable concrete repair includes the consideration of compatibility of properties. Studies show [94] that compatibility between the repair material and substrate concrete with respect to volume changes (dimensional compatibility) is

fundamentally important for ensuring freedom from cracking [49]. Volume changes must be controlled in concrete repairs to minimise cracking. When repair materials undergoing volume changes are restrained, tensile strains are induced. If these strains are greater than the tensile strain capacity of the material, cracking will occur. It is well known that cement based materials are weak in tension but strong in compression. The inherent weakness in tension and low strain capacity results in rapid propagation of cracks under tensile stress. If appropriate measures are to be taken to control cracking in repair materials, then an indication of the magnitude of tensile strains in the repair material due to the restraint to shrinkage, plus a knowledge of the tensile strain capacity of the repair material are essential.

The ability of cement based materials to resist cracking is dependent upon several factors [49]:

- the degree of restraint
- the magnitude of shrinkage
- the stress state
- the amount of stress relief due to creep
- the tensile strength of the material

Finally, to have good resistance to cracking [49], the material should have drying shrinkage, coefficient of thermal expansion and sustained modulus of elasticity as low as possible and a tensile strength and creep as high as possible. The results from the current research indicate that the modulus of elasticity of the repair material should be high to allow distribution of shrinkage strain to the substrate concrete, as will be

shown later in the chapter. This will help reduce the tensile stress induced in the repair material due to the restraint to shrinkage provided by the substrate concrete. On the other hand, since creep will lower the elastic modulus of the repair material, this property will be disadvantageous. Besides, high creep will not be required for tensile stress relaxation if the shrinkage of the repair material is low to begin with.

9.3 RESULTS AND DISCUSSION

9.3.1 Repairs to unpropped compression members

9.3.1.1 Spray applied repair patches

9.3.1.1.1 Repair material stiffer than substrate concrete

A number of spray applied repairs to Lawns Lane Bridge and Gunthorpe Bridge without propping the structure before the application of repair is considered. Figures 9.2 to 9.4 show the strains from the gauges in the repair materials at Lawns Lane Bridge for materials L4, L2 and L3 respectively. These repair materials do not comply with the current standard for material specification, BD 27/86, of the Highways Agency. Figure 9.5 shows the strains at Gunthorpe Bridge (material G1) which does conform with the current standard. The data are plotted at weekly intervals. Datum readings were taken 24 hours after the application of repair (week 0 on the graph). On occasions where the automatic logging device was not installed within the first few weeks, strains were linearly interpolated from the time of application of repair (origin on the graph) to the installation of the data logger (approximately week 3).

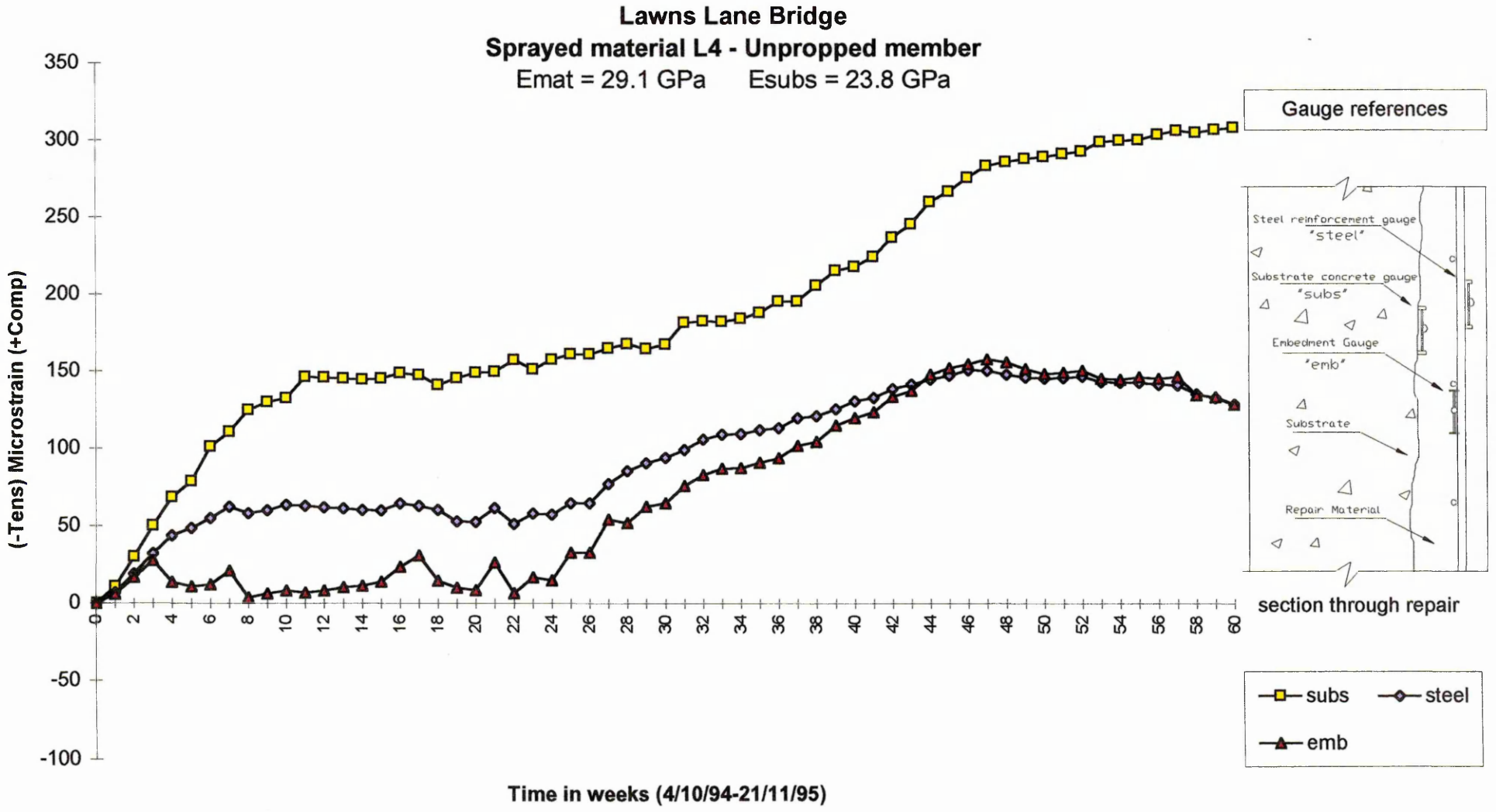

Figure 9.2 Strain distribution in repair patch of material L4 at Lawns Lane Bridge (Unpropped compression member)

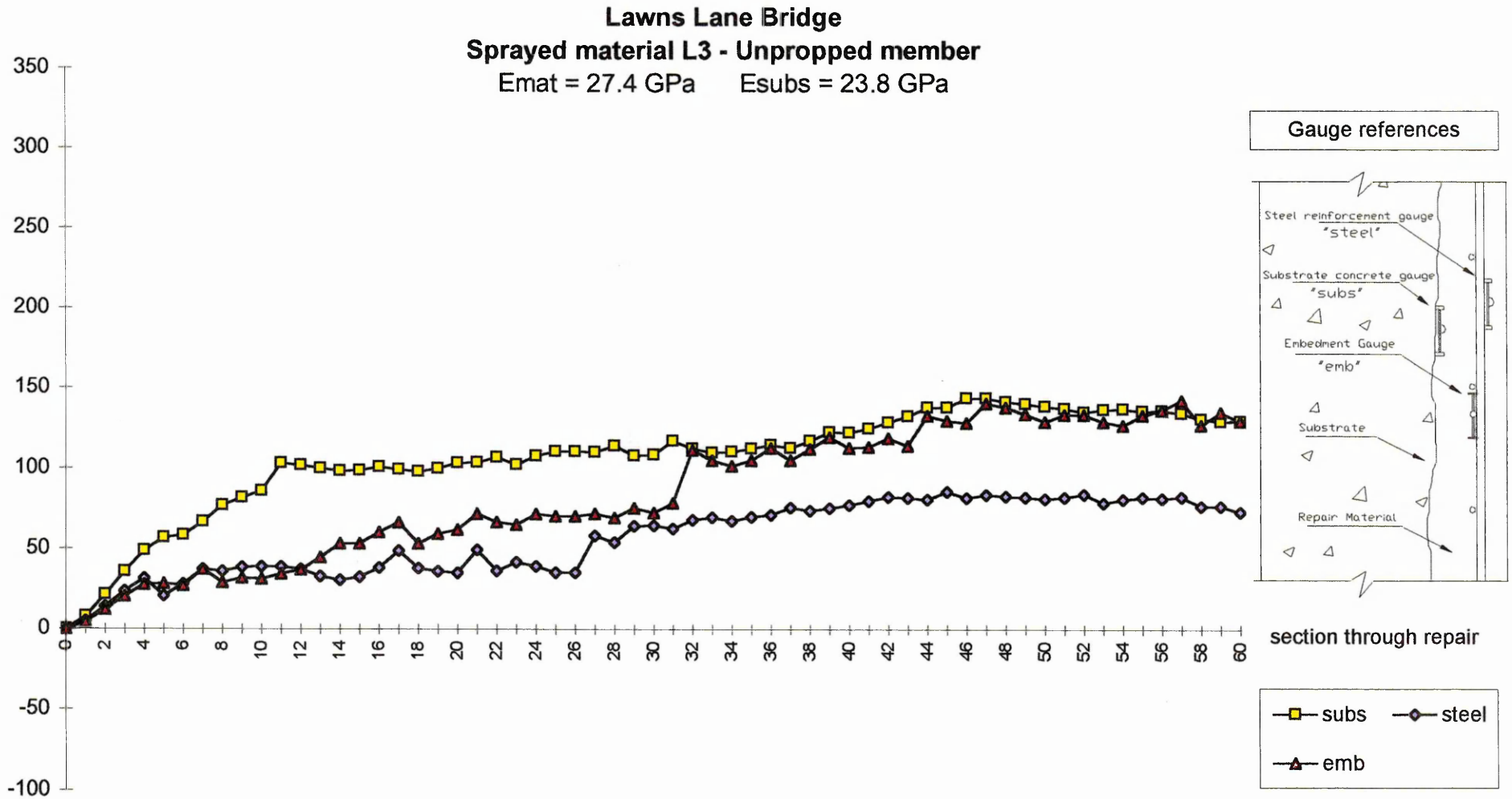

Figure 9.3 Strain distribution in repair patch of material L3 at Lawns Lane Bridge (Unpropped compression member)

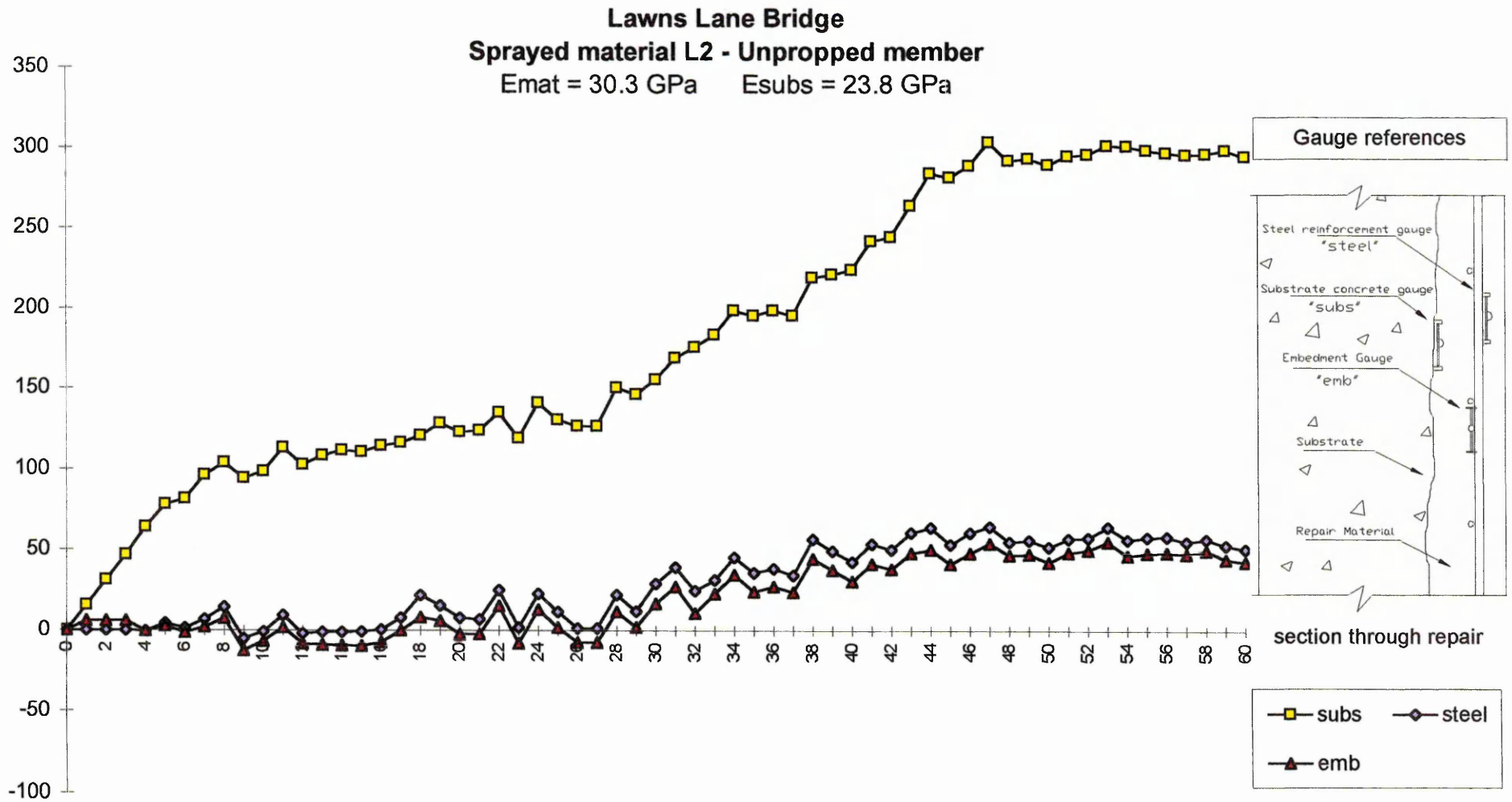

Figure 9.4 Strain distribution in repair patch of material L2 at Lawns Lane Bridge (Unpropped compression member)

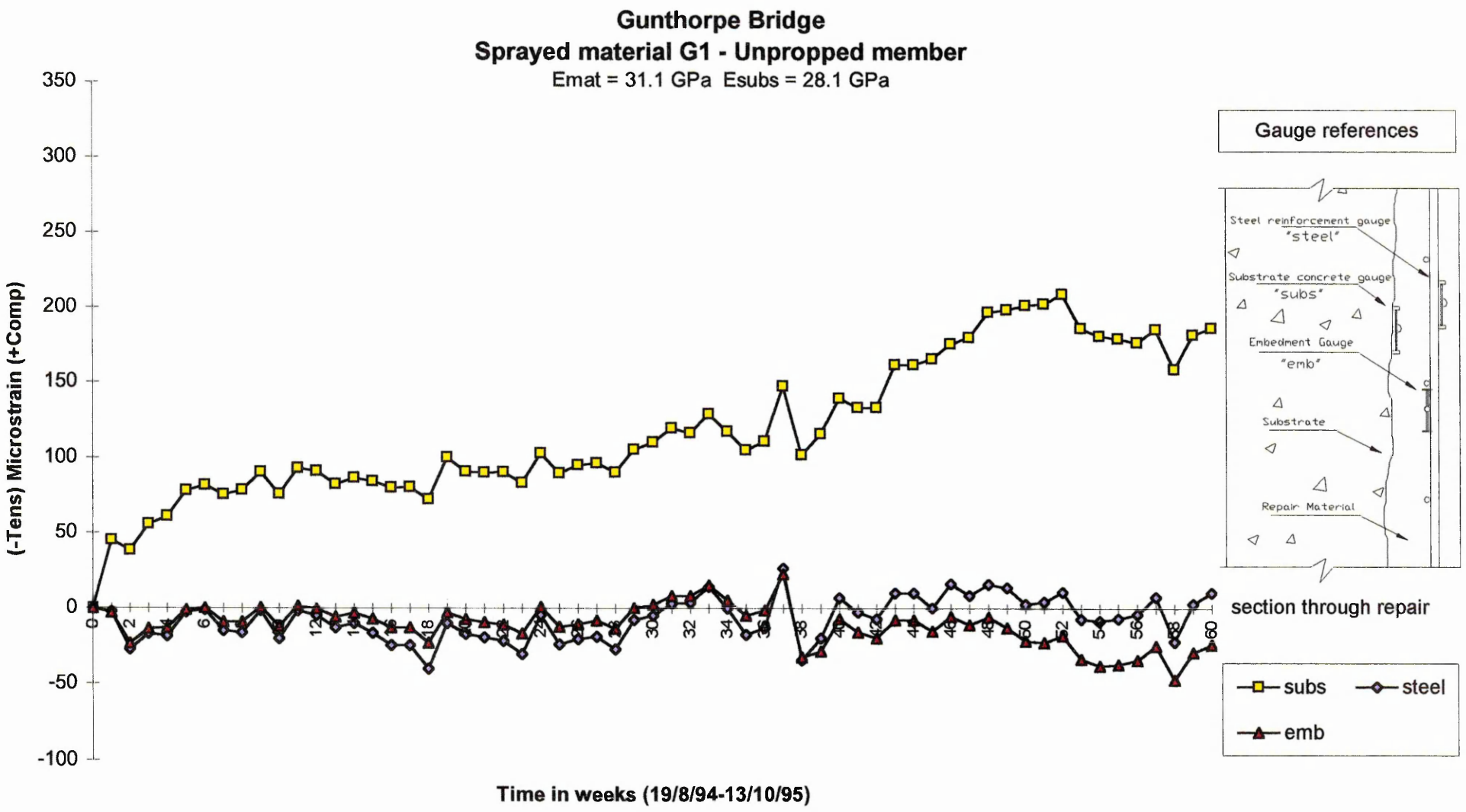

Figure 9.5 Strain distribution in repair patch of material G1 at Gunthorpe Bridge (Unpropped compression member)

The strains presented in Figures 9.2 to 9.5 are obtained from the vibrating wire strain gauges installed in the repairs, as described in Chapter 4 (Gunthorpe Bridge) and Chapter 5 (Lawns Lane Bridge). Vibrating wire strain gauges were attached to the cut-back substrate concrete surface, abbreviated to "subs" in Figures 9.2 to 9.5, steel reinforcement, abbreviated to "steel" and embedded in the repair material, abbreviated to "emb" (the embedment gauges are at the same level as the steel reinforcement but positioned centrally between two reinforcing bars). Locating the strain gauges in these positions allowed the distribution of shrinkage and external load transfer strains at prime locations within the repair patch to be determined.

Referring to Figures 9.2 to 9.5, the strain in the substrate concrete increases rapidly during approximately the first 11 weeks after application of the repair material. The substrate concrete strain then remains relatively constant between approximately week 11 and week 25 (Figures 9.2 to 9.5). After 25 weeks, an increase in strain is again observed in the substrate concrete until approximately week 47 (see Figures 9.2 to 9.5). From approximately week 47 onwards, the strain in the substrate concrete remains relatively constant until the end of the monitoring period (week 60, Figures 9.2 to 9.5). The strain in the steel reinforcement and repair material (gauge "emb") within this period (week 0 to week 60, Figures 9.2 to 9.4) show a fairly similar pattern to the strain in the substrate concrete (Figure 9.2 to 9.4), but the magnitude of strain is lower in the steel reinforcement and repair material. In Figure 9.5, however, the strains in the steel reinforcement and repair material remain relatively constant throughout.

9.3.1.1.1.1 *Discussion*

The spray applied materials represented in Figure 9.2 to 9.5 have elastic modulii which are greater than the elastic modulii of the substrate concrete (see Table 9.1). The compressive strengths of the repair materials and substrate concretes from both Lawns Lane Bridge and Gunthorpe Bridge are also listed in Table 9.1. As the stiffer repair materials exhibit shortening due to shrinkage (see Table 9.2), compressive strain is transferred into the less stiff substrate, which results in the high compressive strain in the substrate concrete, see Figures 9.2 to 9.5, week 0 to week 11. This occurs after the repair material has hardened and attained its full elastic modulus (i.e. the repair material becomes stiffer than the substrate concrete). It was reported in Chapter 8 (Figure 8.9 and Table 8.11) that on average, 96% of the 28 day elastic modulus of a repair material is achieved at 21 days. Therefore, it can be stated that the repair material reaches almost its full elastic modulus after three weeks. Since the automatic logging device was not installed until approximately 2-3 weeks after application of the repair patch, the measured strains within the first three weeks are unavailable, and as a result, the strains

Table 9.1 Elastic modulus and strength of substrate concrete and repair materials represented in Figures 9.2 to 9.5

Material	*Elastic Modulus* (kN/mm^2)		*Strength* (N/mm^2)	
	Lawns Lane	*Gunthorpe*	*Lawns Lane*	*Gunthorpe*
L4	29.1		73.0	
L2	30.3		60.0	
L3	27.4		35.0	
G1		31.1		50.0
substrate	23.8	28.1	34.1	36.2

Table 9.2 Free shrinkage* and creep strains of materials represented in Figures 9.2 to 9.5

Material	*100 day free shrinkage (μstrain) (stored at 20°C, 55%RH)*	*70 day compressive creep (μstrain) (30% stress/strength)*
L4	782	510
L2	325	Not available
L3	710	748
G1	751	421
G3 (Reference)	717	938

*Note: * indicates that a correction for volume/surface ratio has not been applied*

in Figures 9.2 to 9.5 are linearly interpolated within the first three weeks (except for the datum readings which were taken manually 24 hours after application of the repair patch). Compressive strain is also transferred to the steel reinforcement during this period, but is less than the strain transferred to the concrete substrate since the steel reinforcement is much stiffer than the substrate concrete. There will be a virtual tensile strain in the repair material which is caused by the restraint to shrinkage provided by the substrate concrete and the steel reinforcement. This tension will be equivalent to the free shrinkage strain of the repair material minus the compressive strain measured by the substrate concrete gauge. The virtual tensile strain will be greater at the steel reinforcement/repair material interface due to the greater shrinkage restraint provided by the relatively much stiffer reinforcement. In the case of the substrate concrete/repair material interface, the elastic modulus of the substrate concrete is marginally lower than that of the repair material (Table 9.1). The large surface area of contact, however, assists with the strain transfer from repair material to substrate concrete. The rate of the substrate strain increase in the first 11 weeks (see Figures 9.2 to 9.5) is steep after which it reaches a stable state when shrinkage in the repair material has reached negligible

levels (refer to Figures 8.14 to 8.16 for shrinkage data). This stable period lasts from approximately week 11 to week 25 (see Figures 9.2 to 9.5). This is the period when shrinkage reached negligible levels in the repair material but before external load is transferred into the repair patch.

A diagrammatic representation of the long term strain distribution in repair and substrate materials is made in Figure 9.6 (a) to (e), which is based on the observations from Figures 9.2 to 9.5. The effect of the steel reinforcement on the distribution of shrinkage strain is omitted for simplicity and to aid clarity. Figure 9.6 (a) shows a cross-section through an unpropped substrate concrete before the deteriorated concrete was removed. The same cross-section is shown in Figure 9.6 (b) after the deteriorated concrete was removed. Figure 9.6 (c) shows the cross-section upon application of the repair material. Figure 9.6 (c) considers a repair material stiffer than the substrate concrete and represents the shrinkage period from weeks 0 to 11 as identified in Figures 9.2 to 9.5 (the repair material is assumed to be stiffer than the substrate concrete throughout the first 11 weeks; this is of course untrue since the repair material will not attain its full elastic modulus until approximately 2-3 weeks after application). As the stiffer repair material shrinks, it transfers the equivalent of its restrained shrinkage strain to the less stiff substrate. The resulting idealised distribution of the shrinkage strain between the repair material and substrate concrete is shown in Figure 9.6 (d). The strains plotted in Figure 9.6 (c) onwards are exaggerated for clarity. The free shrinkage of the repair material is restrained by the substrate resulting in a net restrained shrinkage at the interface. The effect of the substrate restraint will be less at the free face of the repair, thereby resulting in slightly higher restrained shrinkage strains. Since $E_{rm} > E_{sub}$, the shrinking repair material will deform a zone (referred to as zone of influence)

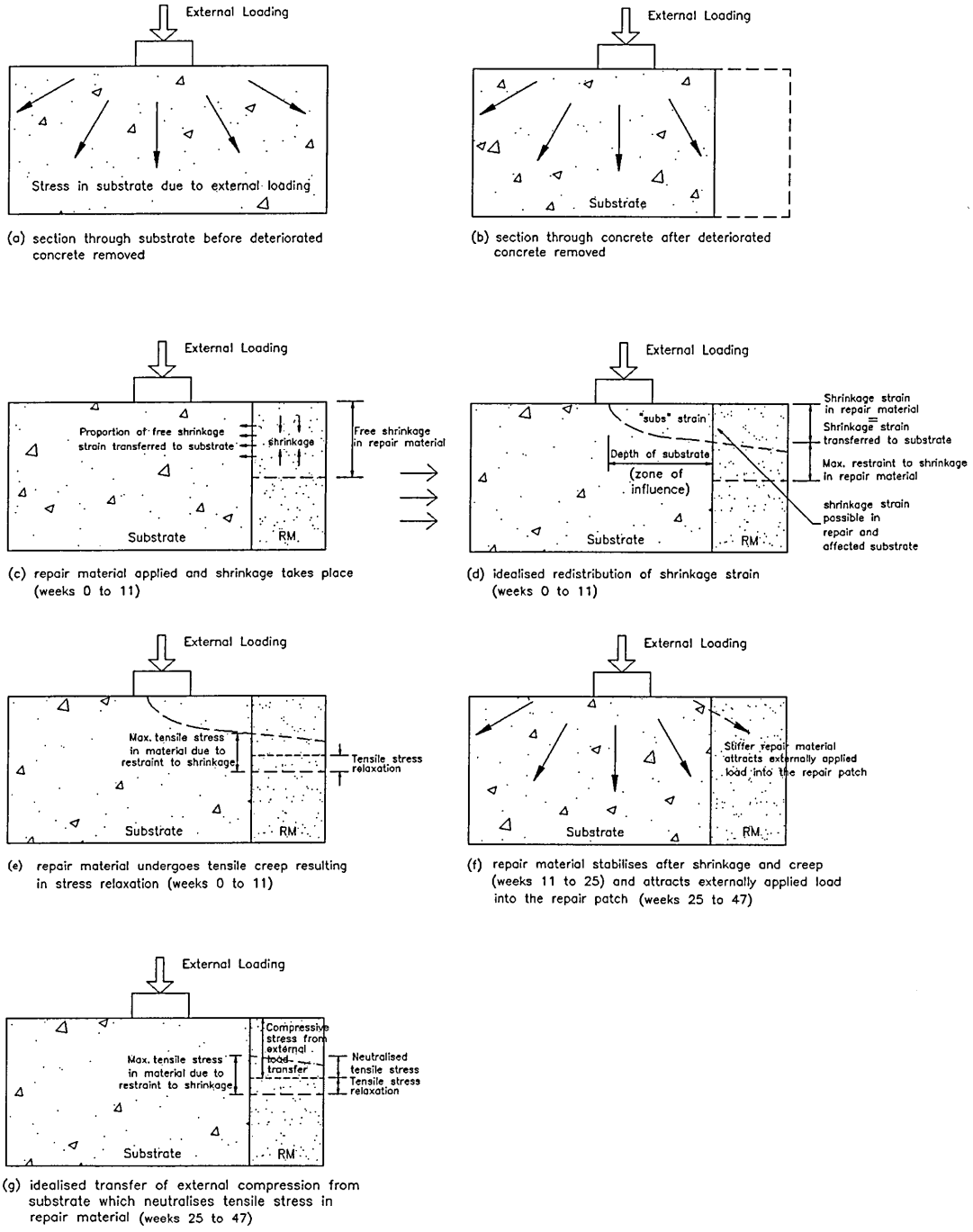

Figure 9.6 Simplified schematic distribution of shrinkage and creep strains in the repair patch of a compression member
Method of repair: spray application
Support during repair: unpropped
Properties: repair material stiffer than substrate concrete
(Steel reinforcement omitted for clarity)
(RM = repair material)

of the substrate concrete in the proximity of the interface as shown in Figure 9.6 (d). Therefore, the compressive strain transferred to the substrate by restrained shrinkage of the repair material will be maximum at the interface, gradually reducing to zero at the end of the affected zone of the substrate concrete.

The restraint to the free shrinkage of the repair provided by the substrate will result in tensile stress in the repair material. The stress will be maximum at the interface, reducing gradually towards the free face of the repair patch. The shrinkage strains transferred to the substrate concrete will result in compressive stress which will be of much lower magnitude relative to the compressive strength of the substrate concrete. For example, an increase in strain of 150 microstrain in the substrate concrete at Lawns Lane Bridge (E_{subs}=23.8 kN/mm^2) would result in a maximum stress of 3.57 N/mm^2 at the interface between the repair material and substrate concrete. It is shown in Chapter 11 that the core strength of the substrate concrete at Lawns Lane Bridge is 34.1 N/mm^2. The profile of restrained shrinkage in the repair patch and resulting tensile stress is shown in Figure 9.6 (d). The tensile stress in the repair material leads to tensile creep in the long term and a consequent relaxation of the tensile stress [see Figure 9.6 (e)]. The degree of relaxation will depend on the creep properties of the repair materials (Table 9.2) and the magnitude of tensile stress/strength ratio. Material L3 has particularly high creep characteristics (refer to Figure 8.21) and will show maximum stress relaxation due to creep. Sufficiently high levels of creep can ultimately reduce the effective modulus of elasticity of the repair material to less than that of the substrate concrete. This will result in less transfer of compressive strain to the substrate concrete due to shrinkage of the repair material. Refer to Figure 9.3 for material L3 which shows lower transfer of

strain to the substrate after 11 weeks compared with the other repairs represented in Figures 9.2 to 9.5. The advantage of having a higher elastic modulus is lost in this case due to the effects of high creep (Table 9.2) in the repair material.

The restraint to shrinkage provided by the substrate concrete causes a virtual tensile strain in the repair material. This virtual tensile strain will be the difference between the free shrinkage strain of the repair material and the restrained shrinkage in it [which equals the strain measured in the substrate concrete, Figures 9.2 to 9.5 and Figure 9.6 (d)]. This is also discussed in more detail in Chapter 10. Obviously, the repair material will crack if the virtual tensile strain due to restraint to shrinkage is greater than the tensile strain capacity of the material.

The next stage of redistribution of strain occurs from approximately week 25 to week 47 (see Figures 9.2 to 9.4). The increase in strain in the steel reinforcement ("steel") and repair material ("emb") which occurs in this period for the spray applied materials L4, L2, L3 (see Figures 9.2 to 9.4) is more pronounced than in spray applied material G1 (Figure 9.5). The compressive strain increases in the repair material ("emb" gauge) and consequently, due to strain compatibility, in the steel reinforcement ("steel" gauge) as externally applied load is attracted into the relatively stiffer repair material from the substrate concrete. The transfer of external load from the substrate concrete to the repair patch does not decrease the strain in the substrate concrete but in fact increases the compressive strain, see Figures 9.2 to 9.5, weeks 25 to 47. This is due to the restraint provided by the interfacial bond between the substrate concrete and stiffer repair material which helps to maintain strain compatibility. The fully bonded, stiffer repair

material prevents the substrate concrete from recovering. The transfer of the external compression from the substrate concrete may ultimately neutralise the tensile stress in the repair material caused by differential shrinkage (which is reduced to some extent by stress relaxation due to tensile creep). Figure 9.6 (f) and (g) shows schematically the strain distribution in Figures 9.2 to 9.4 between weeks 25 to 47. Figure 9.6 (f) shows that externally applied load is attracted into the repair patch at the end of the steady state period (week 25). This transfer of compressive force to the repair material may neutralise the residual tensile stress caused by the restraint to shrinkage, as shown in Figure 9.6 (g). The net compressive stress transfer to the repair patch from the external loading would cause creep of the repair patch. However, the compressive stress is found to be small and compressive creep strains are expected to be minimal. For example, the increase in compressive strain between weeks 25 and 47 (22 weeks) at the substrate concrete of material L4 repair patch (Figure 9.2) is 143 microstrain. Assuming strain compatibility at the interface between repair and substrate materials, the compressive stress in the repair is 143 microstrain multiplied by the elastic modulus of repair material L4 (29.1 kN/mm^2), which gives 4.2 N/mm^2. The compressive strength of the repair material is 73 N/mm^2 and therefore, the maximum stress-strength ratio applied on the repair patch at the interface is 5.8%. The average value across the repair patch cross-section would be even less due to the strain gradient up to the free surface of the repair. Consequently, the compression creep in the repair patch is expected to be negligible.

9.3.1.1.1.2 *Further discussion*

9.3.1.1.1.2.1 *Serviceability performance of repair*

The repair materials represented in Figures 9.2 to 9.5 performed well under service conditions in the 60 week monitoring period despite the fact that some of them (L2, L3 and L4) do not comply with the current repair standard of the Highways Agency, BD 27/86. In order to comply with the current standard, the criteria include, for example, limitations to the maximum aggregate size and type of fibre to be included in the mixture. The characteristic strength of the repair material is also specified (e.g. 40 N/mm^2 for sprayed concrete). In the current project, these properties did not influence repair material selection; the primary properties considered were the elastic modulus, shrinkage and creep. Referring to Table 9.1, the elastic modulus and compressive strength is given for repair materials L2, L3, L4 and G1. It is clear from Table 9.1 that the elastic modulus of each repair material is greater than the elastic modulus of the corresponding substrates, and as a result, these repair materials performed well in service. For example, in the 60 week monitoring period shown in Figures 9.2 to 9.5, repair materials L2, L3, L4 and G1 were able to transfer a portion of the shrinkage to the substrate concrete which reduced the risk of cracking, and also attracted external stress into the repair patch to reduce/neutralise the residual tensile stress in the repair patch. On the other hand, the compressive strength of material L3 is 35 N/mm^2, which is less than the requirement of 40 N/mm^2 as specified in BD 27/86. Nevertheless, this material performed well under service conditions. The fact that three non-standard materials (L2, L3 and L4) performed satisfactorily within the monitoring period indicates that the key properties required for satisfactory long term performance are the elastic modulus, shrinkage and creep of the repair material. These properties should, therefore, be the

most important criteria for material specification, but these are not considered by the standard, BD 27/86, of the Highways Agency.

Material L4 performed well within the monitoring period (60 weeks) but cracked soon afterwards (see Figure 9.7). A possible explanation for this is that the material became weaker in tension with time. There is evidence based on experimental data given in Chapter 8 (Section 8.5.4) which shows that some repair materials suffer serious reductions in flexural strength with time. For example, material L5, a repair mortar which consists of the same mixture constituents as material L4, except that fibres were added to the mixture of material L5, exhibited a 28 day modulus of rupture of 10.9 N/mm^2. The long term modulus of rupture of this repair material was only 4.0 N/mm^2. The long term modulus of rupture of material L4 was 4.7 N/mm^2. A 28 day modulus of rupture of this repair material was not available. The tensile stress in the repair material due to the restraint to shrinkage [Figure 9.6 (d)], may not have been fully neutralised during the external load transfer. Therefore, in the long term, the tensile strength of the repair material became less than the residual tensile stress in the repair material, and as a result, cracking occurred in the repair patch. This phenomena is further discussed in Chapter 10.

9.3.1.1.1.2.2 Schematic strain distribution-time relationship

Figure 9.8 shows a simplified schematic distribution with time of strain in the substrate concrete and the repair patch for a combination of repair and substrate materials where $E_{rm} > E_{sub}$. It is valid for spray applied materials to an unpropped compression

(a)

(b)

Figure 9.7 Cracking in the repair patch of material L4 at Lawns Lane Bridge:
(a) cracks in material L4 approximately 60 weeks after application
(b) close-up of cracking in material L4

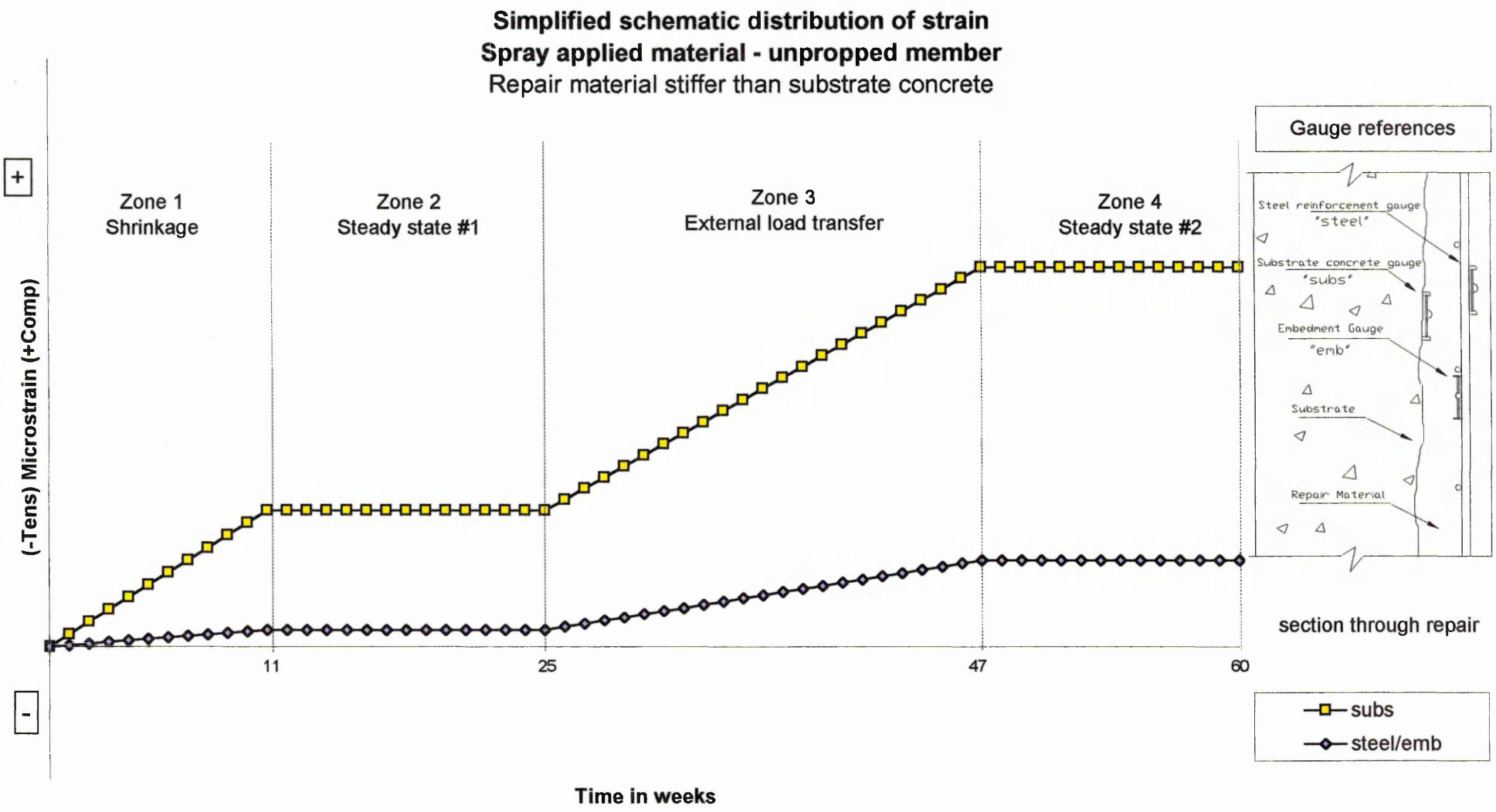

Figure 9.8 Simplified distribution of strain in a repair patch when the material is stiffer than the substrate concrete (Unpropped compression member)

member. Figure 9.8 is based on Figures 9.2 to 9.4 which provide repetitive experimental data of strain distribution with time of a similar profile as Figure 9.8. The strains in the steel reinforcement and repair material at a common level in the cross-section are assumed to be equal due to strain compatibility (Figure 9.8). This is an approximation of the experimental strains plotted in Figures 9.2 to 9.4 for steel and repair material ("emb" gauge). Four stages of distribution of strain can be identified in Figure 9.8, namely:

(i) shrinkage stage, where compressive strain is transferred into the substrate (and steel reinforcement) due to shrinkage in the repair material

(ii) steady state #1, caused by relaxation of the repair material due to tensile creep

(iii) external load transfer, where the repair material attracts externally applied load into the repair patch. Compressive strains are simultaneously transferred to the substrate concrete in the contact zone via interfacial bond.

(iv) steady state #2, when the transfer of the external load into the repair patch has ceased.

9.3.1.1.2 Substrate concrete stiffer than repair material

Two repairs to Gunthorpe Bridge carried out without propping the structure before the application of spray applied materials are considered. Two repair materials labelled G2 and G3 were used and their strains with time are presented in Figures 9.9 and 9.10. Material G2 conforms with the current repair specification, BD 27/86, whereas material G3 is a conventional sand/cement mortar which does not meet the requirements of the

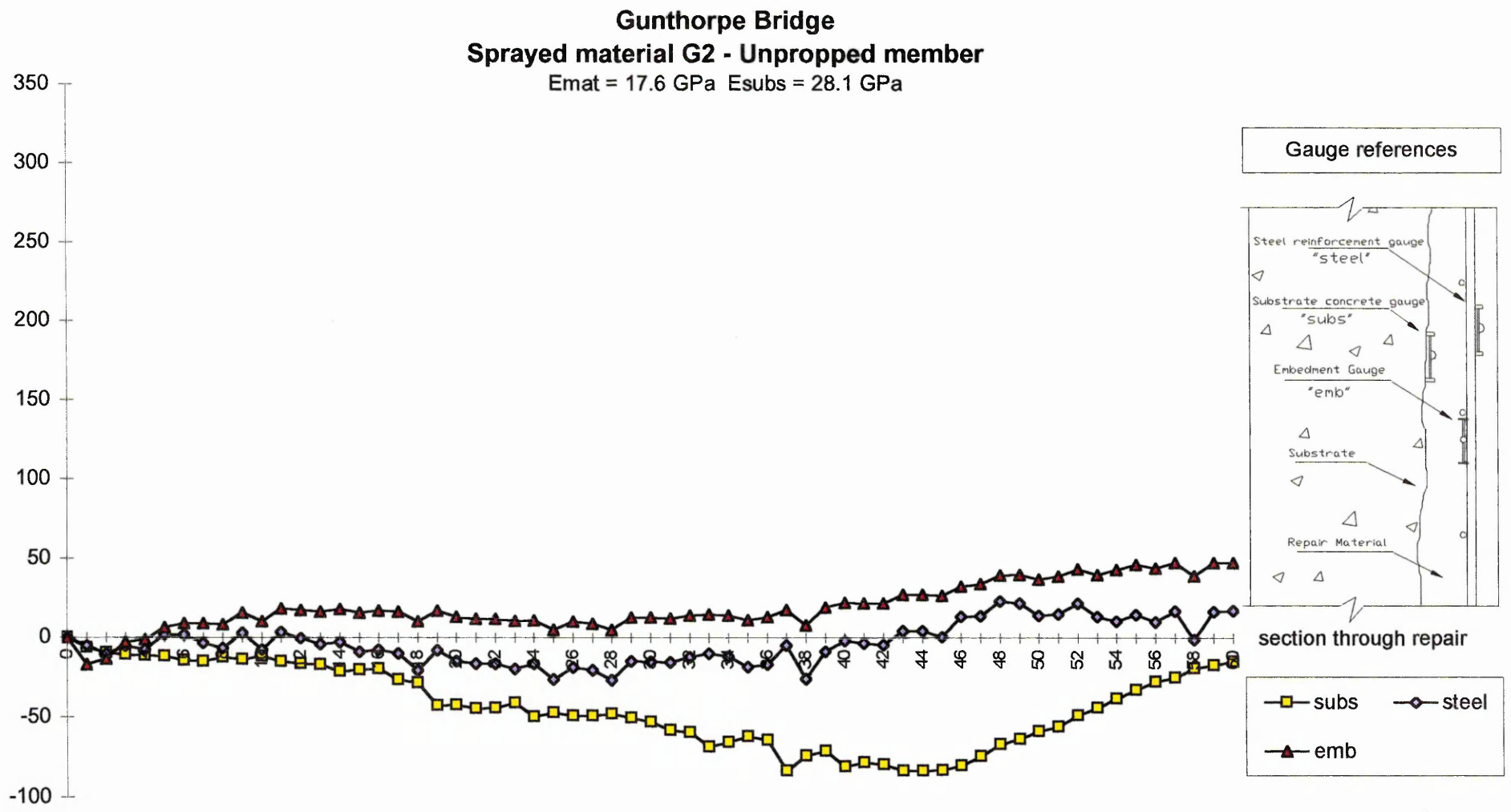

Figure 9.9 Strain distribution in repair patch of material G2 at Gunthorpe Bridge (Unpropped compression member)

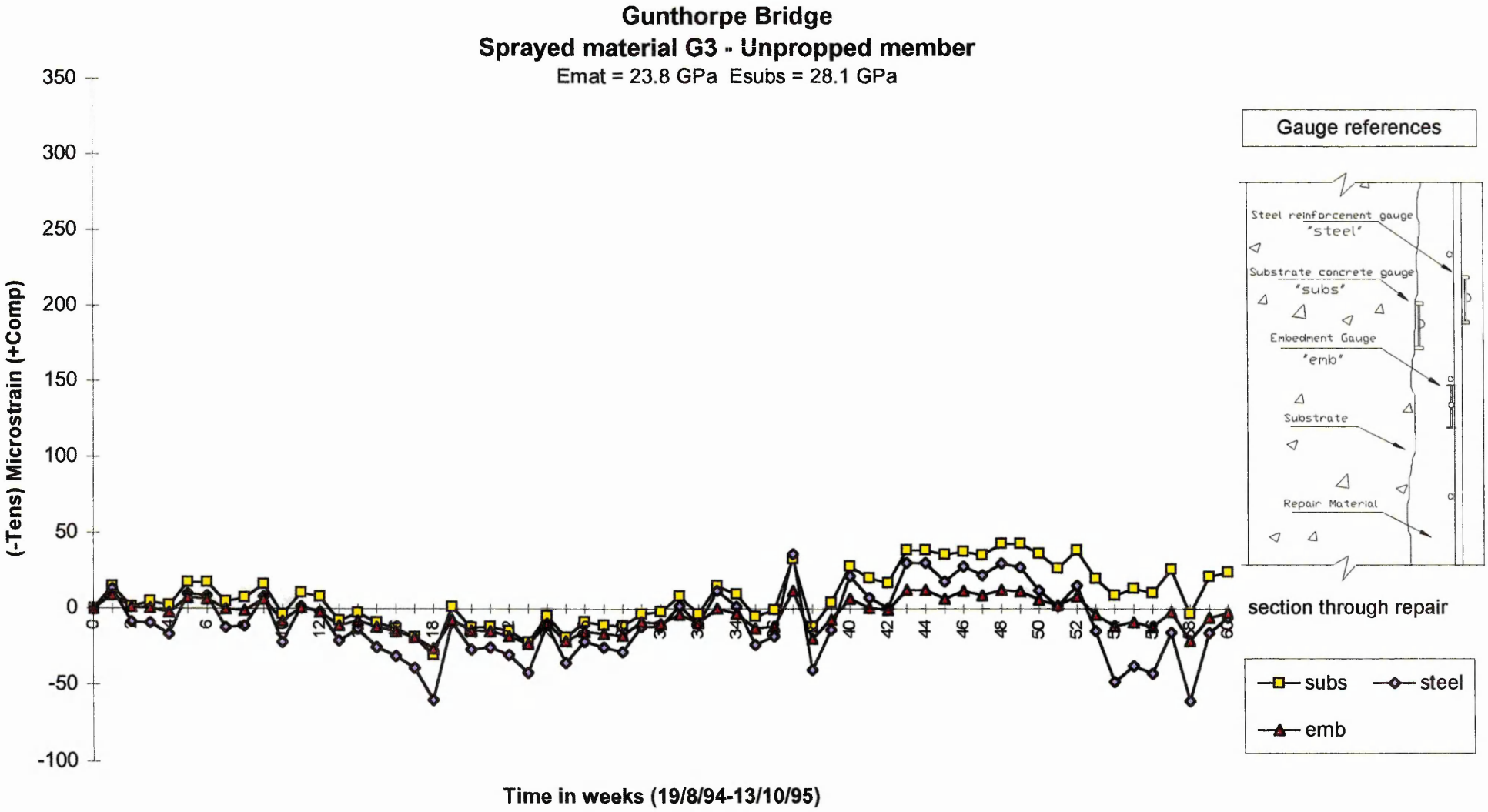

Figure 9.10 Strain distribution in repair patch of material G3 at Gunthorpe Bridge (Unpropped compression member)

specification The data are plotted at weekly intervals. Datum readings (origin on the graphs) were taken 24 hours after the application of repair. The elastic modulus and compressive strength of the repair materials are given in Table 9.3. Both materials have elastic modulii which are less than the elastic modulus of the substrate concrete (Table 9.3). The compressive strength of these repair materials (Table 9.3) are greater than the minimum specified (40 N/mm^2) in BD 27/86 [1].

The strains presented in Figures 9.9 and 9.10 are obtained from the vibrating wire strain gauges installed in the repairs, as described in Chapter 4. Vibrating wire strain gauges were attached to the cut-back substrate concrete surface, abbreviated to "subs" in Figures 9.9 and 9.10, steel reinforcement, abbreviated to "steel" and embedded in the repair material, abbreviated to "emb". The embedment gauges were at the same level as the steel reinforcement but positioned centrally between two reinforcing bars. Locating the strain gauges in these positions allowed the distribution of shrinkage and external load transfer strains within the repair patch to be determined.

Table 9.3 Elastic modulus and strength of substrate concrete and repair materials represented in Figures 9.9, 9.10 and 9.12

Material	*Elastic Modulus (kN/mm^2)*		*Strength (N/mm^2)*	
	Gunthorpe	*Lawns Lane*	*Gunthorpe*	*Lawns Lane*
G2	17.6		44.0	
G3	23.8		46.0	
L1		22.7		69.0
Substrate	28.1	23.8	39.0	45.0

9.3.1.1.2.1 *Discussion*

The data presented in Figures 9.9 and 9.10 show the strains from the gauges in two repair materials (G2 and G3) at Gunthorpe Bridge. Materials G2 and G3, having elastic modulii which are less than the elastic modulus of the substrate concrete (see Table 9.3), performed differently to materials which are stiffer than the concrete substrate (compare Figures 9.9 and 9.10 with Figure 9.8). In this instance, the less stiff repair materials are unable to transfer shrinkage strain into the stiffer substrate, as indicated by the negligible strains in the substrate concrete and steel reinforcement during the "shrinkage" period (approximately week 0 to week 11), in Figures 9.9 and 9.10. Further, negligible strains are observed in the repair materials (gauge "emb") in Figures 9.9 and 9.10 despite the high free shrinkage property of repair materials G2 and G3 - 1311 and 717 microstrain respectively (Table 9.4). This is due to the stiffer substrate concrete effectively restraining the repair material from shrinking and not undergoing any significant compressive deformation itself due to the force exerted at the interface by the shrinking repair material. The firm restraint to shrinkage will induce a tensile stress in the repair material and if this tensile stress is greater than the tensile strength of

Table 9.4 Free shrinkage* and creep strains of materials represented in Figures 9.9, 9.10 and 9.12

Material	*100 day free shrinkage (μstrain) (stored at 20°C, 55%RH)*	*70 day compressive creep (μstrain) (30% stress/strength)*
G2	1311	809
G3 (reference)	717	938
L1	620	783

*Note: * indicates that a correction for volume/surface ratio has not been applied*

the repair material, then the repair material will crack. Nevertheless, cracking was absent in materials G2 and G3. The tensile stress in the repair material at early ages after application will be reduced due to low elastic modulus of the repair material. On average, the tensile elastic modulus of the repair material at 7 days will be approximately 65% of the 28 day tensile elastic modulus (an indication of the development of elastic modulus with time is give in Figure 8.9 and Table 8.11). This will serve to reduce the tensile stress in the repair material. Furthermore, the repair material will not attain a sufficient bond strength until the repair material hardens (possibly 1-2 weeks after application) and as a result, some slip at the interface between the repair material and substrate concrete and the repair material and steel reinforcement will accommodate some shrinkage without causing tension in the repair. Once full bond and full elastic modulus had been achieved (approximately 2 weeks after application - see Table 8.11), tensile stress relaxation will occur as a result of tensile creep. Stress relaxation in the repair material is taken into account in more detail in the next chapter. Since the tensile stress in the repair material may be close to the tensile strength of the repair material (which will be shown in Chapter 10), then a very high tensile stress/strength ratio will result. Referring to Table 9.4, both materials exhibit relatively high creep (809 and 938 microstrain respectively), therefore, because of the high stress/strength ratio, high creep will occur. It is also evident in Figures 9.9 and 9.10 that the less stiff repair material is unable to attract any significant external load into the repair patch in the long term (weeks 25 to 47). This is shown by the negligible strains in the substrate concrete, steel reinforcement and repair material in the "external load transfer" period (week 25 to week 47, Figure 9.10). In material G2 (Figure 9.9), the substrate concrete does show an inexplicable decrease in compression (negative strain)

within this period. The steel reinforcement and repair material, on the other hand, both exhibit a slight increase in compression in the latter stages of the monitoring period (Figure 9.9).

Figure 9.11 diagrammatically illustrates the effect of a spray applied repair material to a stiffer substrate concrete of a compression member. A section through the unpropped substrate concrete member both before and after the deteriorated concrete is removed is shown in Figures 9.11 (a) and (b). The repair patch is applied in Figure 9.11 (c). As the repair material tries to shrink (shrinkage period assumed as week 0 to week 11, see Figure 9.8), the stiffer substrate concrete fully restrains the repair material [Figure 9.11 (c)]. Hence, the free shrinkage strain in the repair material [see Figure 9.11 (c)] translates into a tensile stress, shown idealised in Figure 9.11 (d). The strains plotted from Figure 9.11 (c) onwards are shown exaggerated for clarity. At early ages after application when the repair material is in a soft state, the tensile stress will be low in the repair material for two reasons. Firstly, the bond between the repair material and the substrate concrete/steel reinforcement will not have developed, hence, interfacial slip will allow deformation in the repair material to occur freely. Secondly, the elastic modulus of the repair material will be low, therefore, the tensile stress will be low. On the other hand, the tensile strength of the repair material will also be very low at early ages after repair application Hence, cracking may, nevertheless, occur as a result of the restraint to shrinkage as shown in Figure 9.11 (e). If repair material characteristics are suitable to prevent such early cracking, it will reach maturity and develop full tensile stress due to restrained shrinkage. Therefore, if the repair material exhibits high creep

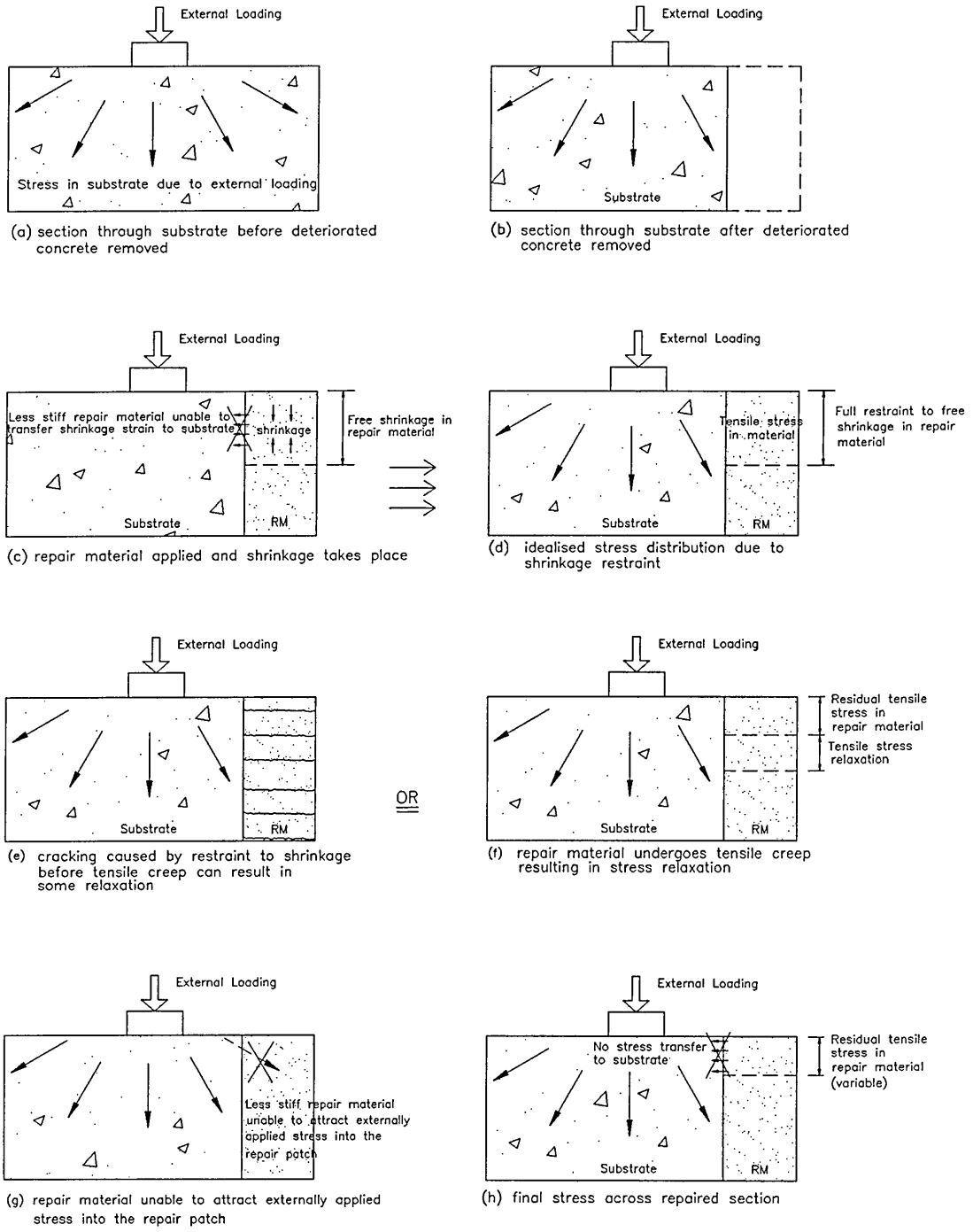

Figure 9.11 Simplified schematic distribution of strains in the repair patch of a compression member
Method of repair: spray application
Properties: substrate concrete stiffer than repair material
Support during repair: unpropped
(Steel reinforcement omitted for clarity)

characteristics, then tensile stress relaxation will help alleviate the tensile stress [Figure 9.11 (f)] and cracking may be avoided (this is further studied in Chapter 10, albeit for repair materials that are stiffer than the substrate concrete). The less stiff repair material was unable to attract externally applied stress into the repair patch as shown by the data in Figures 9.9 and 9.10. This fact is represented in Figure 9.11 (g). As a consequence, a residual tensile stress may remain in the repair material. The final distribution of stress across the repaired section is given in Figure 9.11 (h).

9.3.1.1.2.2 *Further discussion*

If the tensile strain induced is greater than the tensile strain capacity of the repair material, then the material will crack [see Figure 9.11 (e)]. This phenomenon occurred with material L1 at Lawns Lane Bridge. Material L1 complies with the current standard BD 27/86 [1] and its compressive strength exceeds the minimum requirement of 40 N/mm^2 in BD 27/86 (see Table 9.3). The fact that this material suffered extensive cracking confirms that compressive strength of a repair material is a relatively unimportant parameter for its specification. The data from the strain gauges in material L1 is shown in Figure 9.12. The strain in the substrate concrete ("subs") remains approximately between -50 microstrain and +50 throughout the monitoring period (weeks 0 to 60). The strain in the steel reinforcement and repair material increase rapidly in tension to approximately 275 microstrain and 375 microstrain at week 9, Figure 9.12. These strain subsequently remain relatively constant until the end of the monitoring period (week 60). The 100 day shrinkage strain of material L1 was 620 microstrain, as shown in Table 9.4 [which is less than the free shrinkage of repair materials G2 and G3 (1311 and 717 microstrain respectively)].

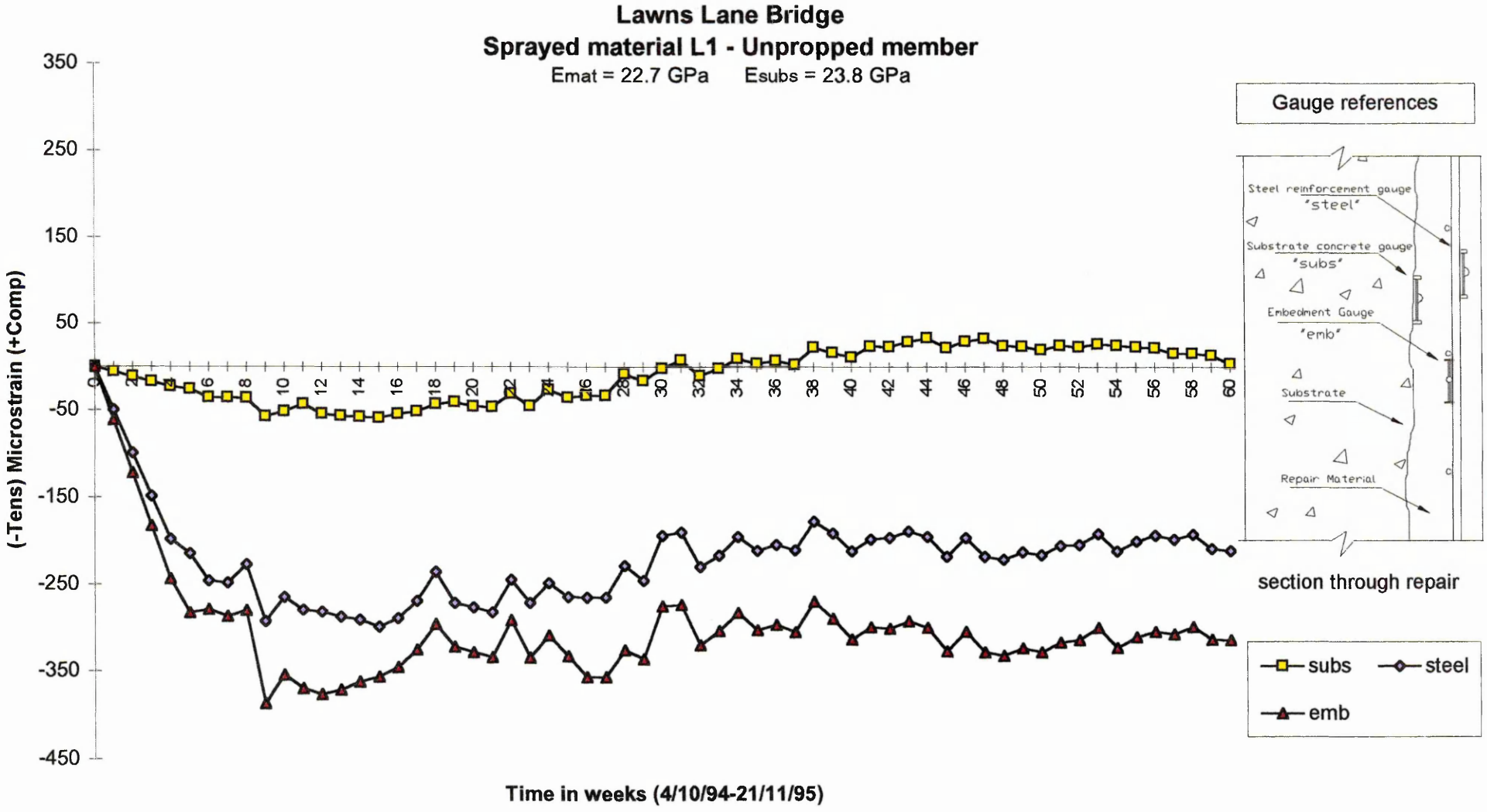

Figure 9.12 Strain distribution in repair patch of material L1 at Lawns Lane Bridge (Unpropped compression member)

The marginally stiffer substrate concrete (E_{sub}=23.8 kN/mm^2, E_{rm}=22.7 kN/mm^2, see Table 9.3) remains unaffected by shrinkage in the less stiff repair material, and as a result, there is little strain in it. This results in a strain in the substrate concrete of between +/- 50 microstrain (Figure 9.12). The restraint provided by the stiffer substrate concrete to the shrinking repair material led to a high tensile strain in the repair material (see emb gauge, Figure 9.12) which caused catastrophic cracking to occur in the repair material. The tensile strain in the repair material is 375 microstrain at week 9, but this would also include the crack width. Nevertheless, the tensile strain capacity of the repair material was exceeded and cracking occurred. A high tensile strain is also evident in the steel reinforcement as shown in Figure 9.12. This is approximately 275 microstrain at week 9. This could be as a result of a faulty gauge, since it is inconceivable that a cracked repair material could transfer such a high tensile strain to the steel reinforcement. Nevertheless, if this was the case, it would reduce the compressive stress in the steel reinforcement by approximately 57 N/mm^2.

Figure 9.13 shows the cracking in two of the repair patches of material L1 on the north abutment at Lawns Lane Bridge. Figure 9.14 diagrammatically shows the development of the cracks in the repair patch of the same repair material. Figure 9.14 (a) shows an elevation of the north abutment at Lawns Lane Bridge and the position of the repair patches (including material L1, L3, L4, and L5). Figures 9.14 (b) through (e) shows the cracks at approximately 1, 2, 8 and 16 months after application of repair. It is clear from Figure 9.14 that the repair material exhibited new cracks up to 16 months after repair application. The cracks in the early stages after application of repair were due to the high tensile stress in the repair material caused by restraint to shrinkage provided by

(a)

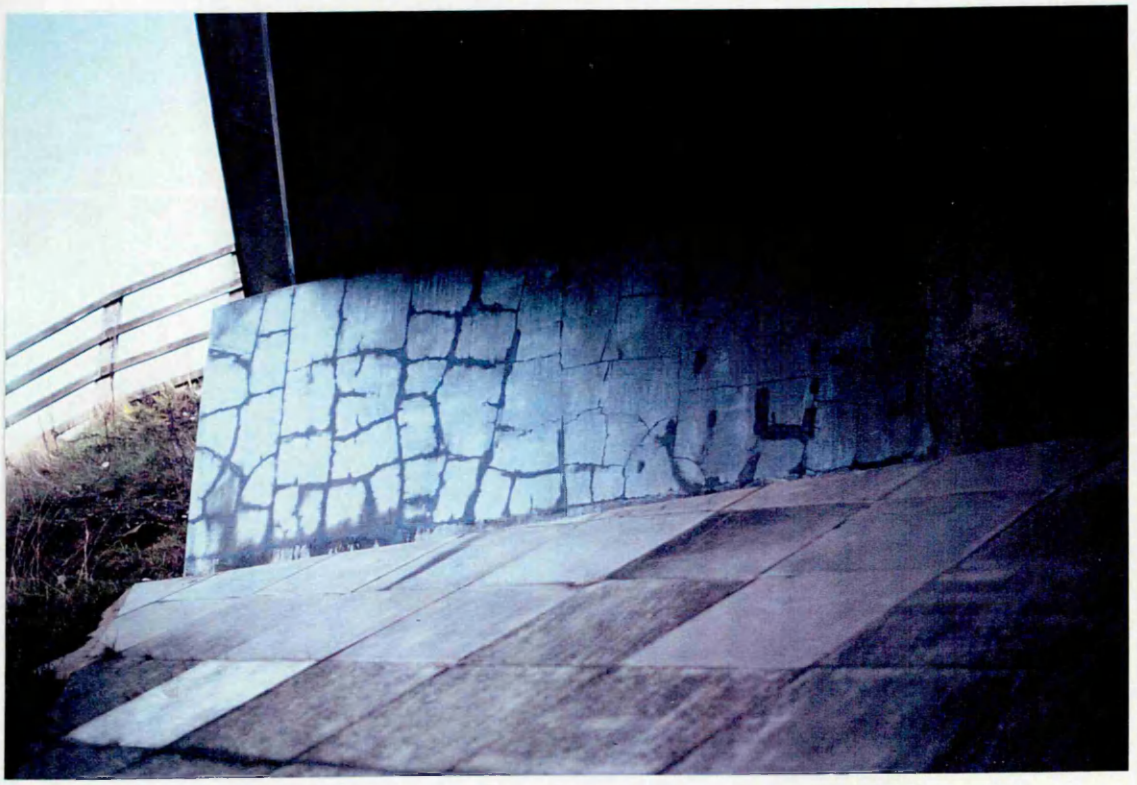

(b)

Figure 9.13 Cracking in repair patch of material L1 at Lawns Lane Bridge:
(a) and (b) repair patches on north abutment

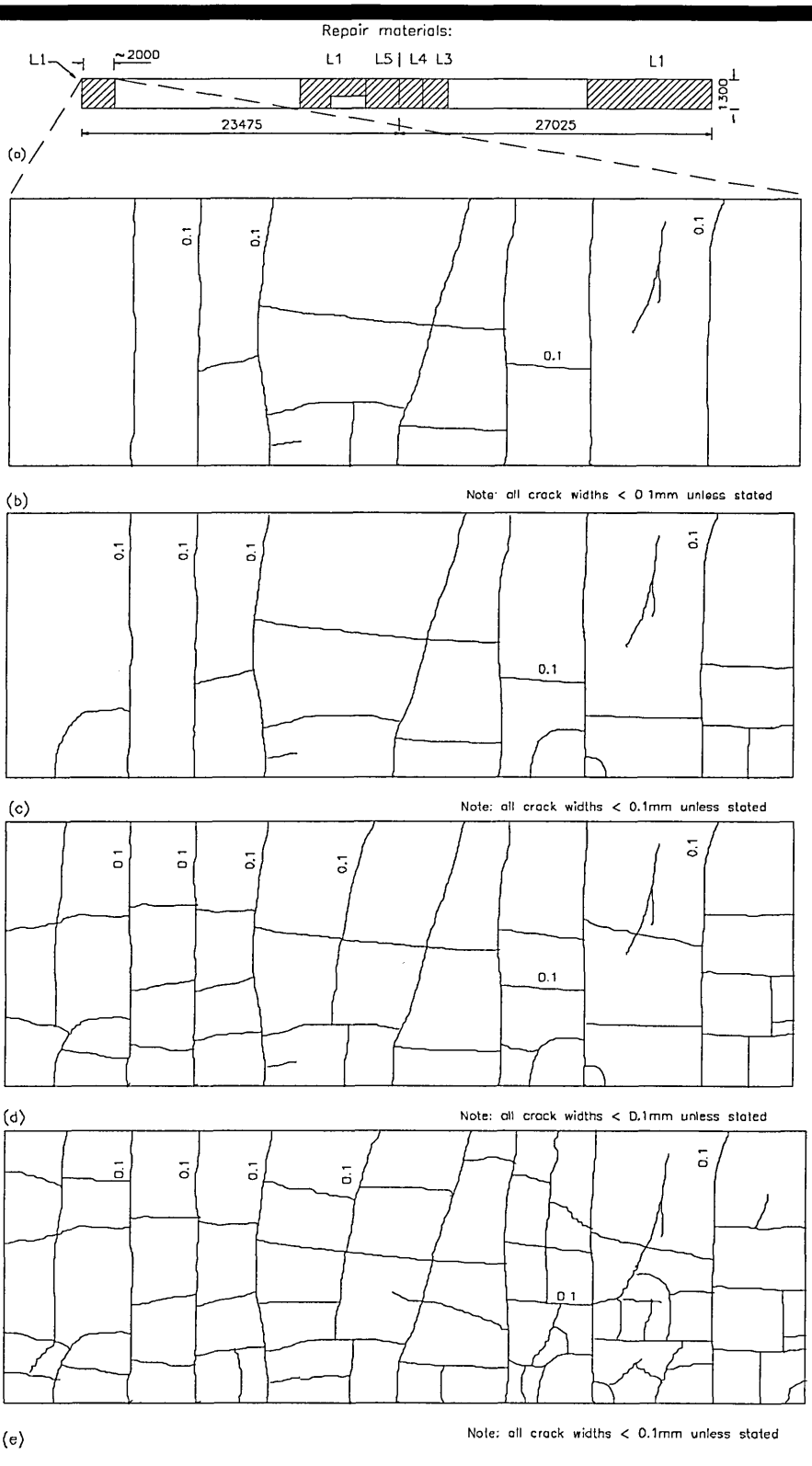

Figure 9.14 Cracking in material L1 at Lawns Lane Bridge:
(a) elevation of north abutment (b) 1 month after application
(c) 2 months after application (d) 8 months after application
(e) 16 months after application
Method of repair: spray applied Support during repair: unpropped
Properties: substrate concrete stiffer than repair material

the marginally stiffer substrate concrete. Cracking occurred before tensile creep could relieve the stress in the repair material. The long term modulus of rupture of this repair material was 6.1 N/mm^2, the 28 day modulus of rupture was not available. Material L1 exhibits lower creep than repair materials G2 and G3 (Table 9.4), indicating that stress relaxation due to creep will be lower and possibly explaining why material L1 cracked but repair materials G2 and G3 remained uncracked, despite the fact that the modulus of rupture of material L1 was greater than the modulus of rupture for both materials G2 and G3 (Table 8.23). Cracking in the long term in material L1 at Lawns Lane Bridge is possibly due to a decrease in tensile strength with time in the repair material. This was discussed in detail in Section 8.5.4, where the modulus of rupture of the repair materials, obtained from the manufacturers' literature, was greater than the modulus of rupture of repair materials obtained from laboratory tests approximately 14-36 months after casting. Therefore, since the tensile strength of the repair material changes with time, this may decrease to a value that is less than the residual tensile strength in the repair material and cracking could still occur in the long term. Referring to Figure 9.14, the cracking pattern in the repair patches of material L1 is fairly regular (predominantly vertical and horizontal cracks). Therefore, when the tensile stress exceeds the tensile strength of the repair material, the material is no longer able to resist the tensile stress and cracking occurs. This process is repeated until the repair material cracks into smaller sections that can accommodate the tensile stress (i.e. cracking in the repair material relieves tensile stress). Such a regular pattern, it has been observed, is synonymous with cracking caused by unsuitable repair material properties (compare Figure 9.13 with Figure 9.7). For instance, the majority of the cracking in material L1 at Lawns Lane Bridge is due to the fact that the elastic modulus of the repair material

was less than the elastic modulus of the substrate concrete at application of repair. High tensile stress was evident in the repair patch as a result of the restraint to shrinkage provided by the stiffer substrate concrete and steel reinforcement. Consequently, cracks occurred in the repair material which were predominately horizontal and vertical, as shown in Figure 9.13. On the other hand, the properties of material L4 were suitable for concrete to begin with, i.e. high elastic modulus, medium shrinkage and creep. Over a long period of time (+60 weeks), the tensile strength of the repair material decreased. Consequently, the residual tensile stress in the repair material due to the restraint to shrinkage provided by the substrate concrete and steel reinforcement became greater than the tensile strength of the repair material. As a result, a cracking pattern which resembles the predominantly horizontal and vertical cracks, as shown in Figure 9.13 for material L1, was also evident in material L4 (Figure 9.7).

9.3.1.2 Flow applied repair patches

9.3.1.2.1 Repair material stiffer than substrate concrete

Two repairs to Sutherland Street Bridge without propping the structure before the application of (flowing) repair are considered (see Figure 6.4). Figures 9.15 and 9.16 show the strains monitored over time from the gauges in the repair for materials S2 and S1 respectively. Both these repair materials complied with the current standard, BD 27/86 [1]. The data are plotted at weekly intervals. Datum readings were taken 24 hours after the application of repair. The strains presented in Figures 9.15 and 9.16 are obtained from the vibrating wire strain gauges installed in the repairs, as described in Chapter 6. Vibrating wire strain gauges were attached to the cut-back substrate

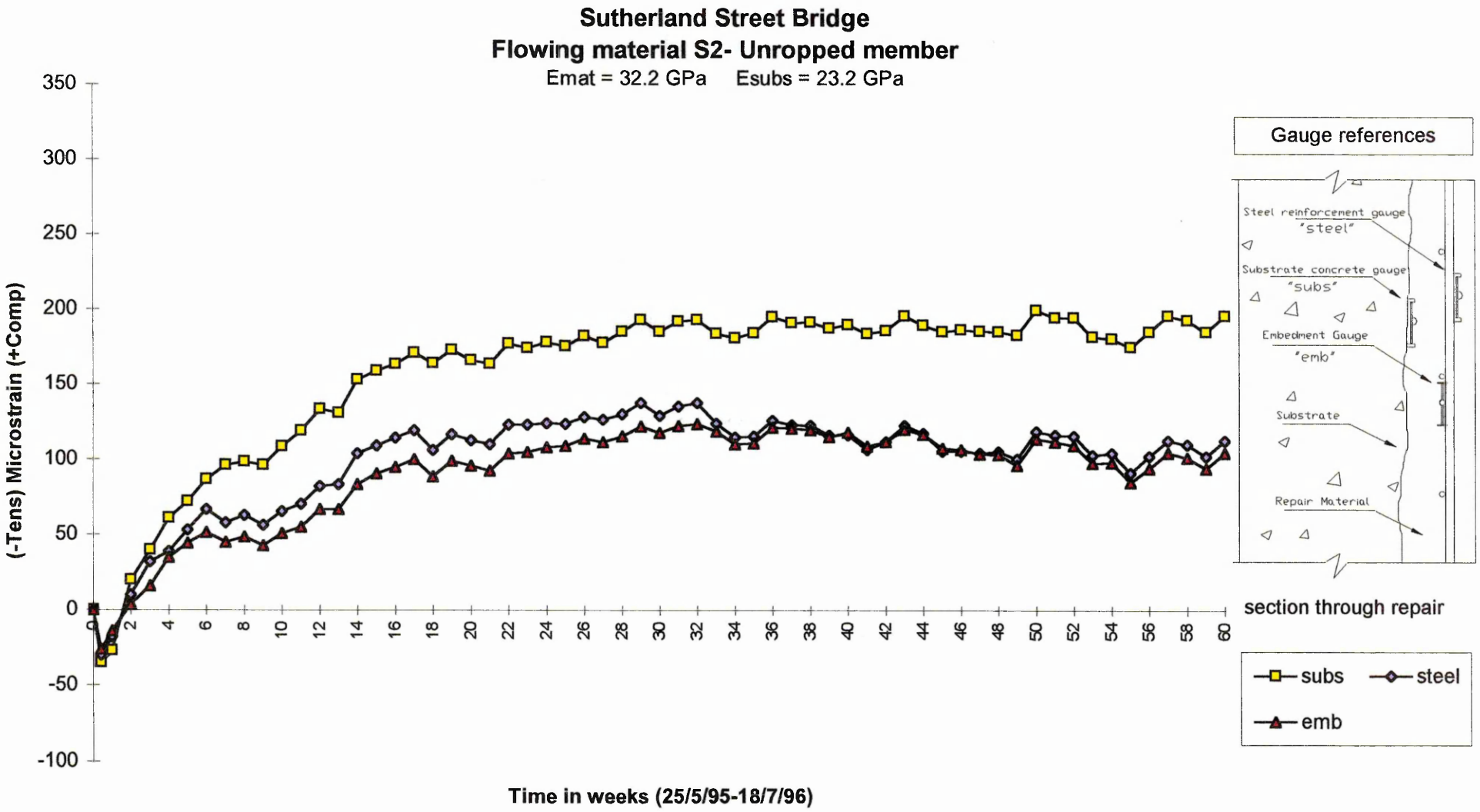

Figure 9.15 Strain distribution in repair patch of material S2 at Sutherland Street Bridge (Unropped compression member)

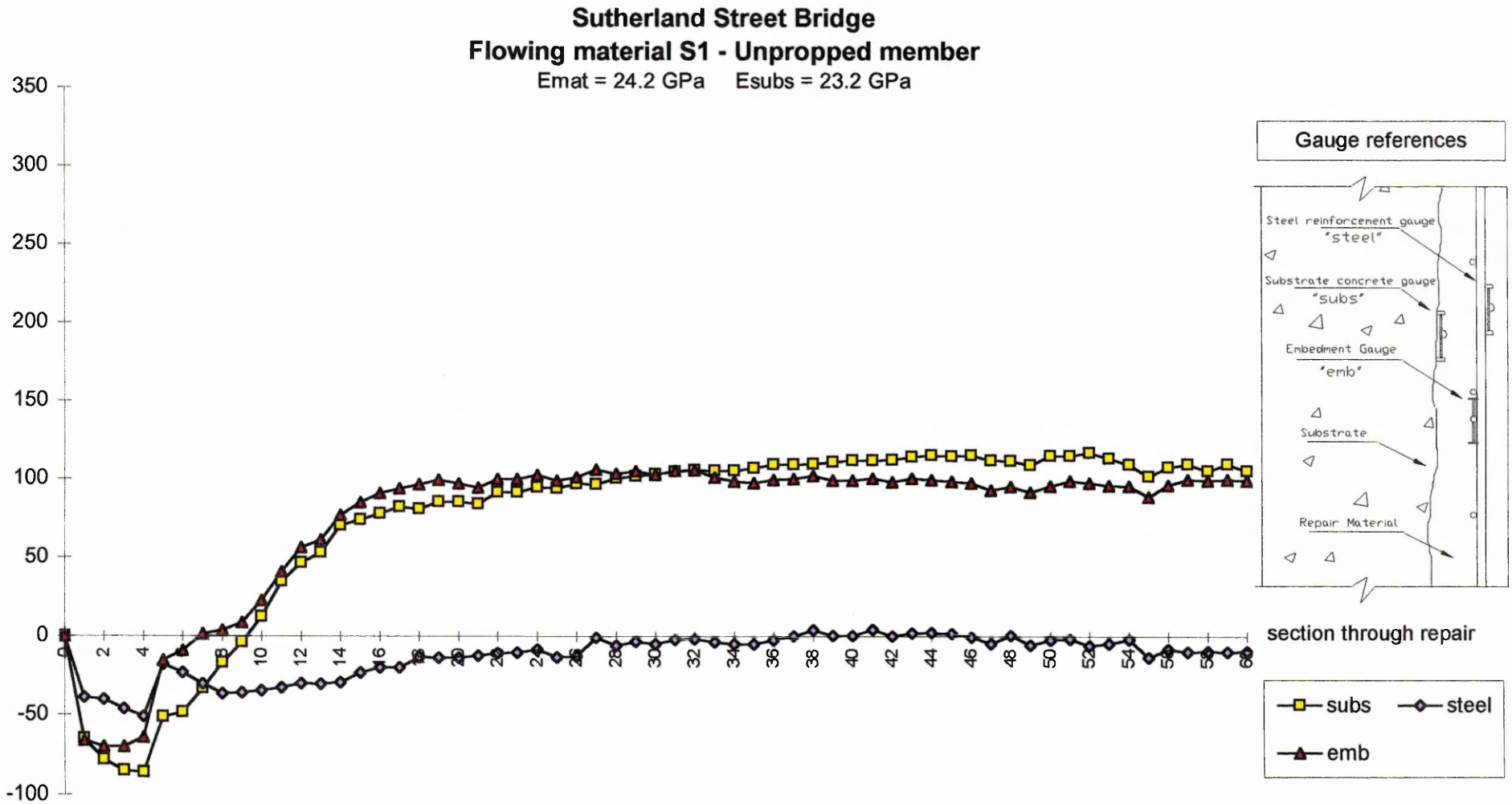

Figure 9.16 Strain distribution in repair patch of material S1 at Sutherland Street Bridge (Unpropped compression member)

concrete surface, abbreviated to "subs" in Figures 9.15 and 9.16, steel reinforcement, abbreviated to "steel" and embedded in the repair material, abbreviated to "emb". The embedment gauges are at the same level as the steel reinforcement, but positioned centrally between two reinforcing bars.

The strains in the substrate concrete, repair material and steel reinforcement in Figure 9.15 (material S2), all show increasing values (in tension) with time soon after application of the repair (within the first two weeks). Thereafter, the strains in the substrate concrete, repair material and steel reinforcement increase in compression (between weeks 2 and 16) to reach approximately 175, 120 and 100 microstrain respectively. These strains remain relatively constant thereafter to the end of the monitoring period at week 60. The gauges in the same locations (substrate concrete, repair material and steel reinforcement) in Figure 9.16 (material S1) all show increasing tensile strains within the first 4 weeks of monitoring (-80, -60 and -50 microstrain respectively). The strains in the substrate concrete and repair material start increasing from week 4 to reach about 100 microstrain (compression) at week 18 (Figure 9.16). These strains remain relatively constant for the remainder of the monitoring period. The strain in the steel reinforcement starts to increase from -50 microstrain at week 4 to reach 0 microstrain at week 27. The steel reinforcement strain remains relatively constant from week 27 until the end of the monitoring period (week 60).

9.3.1.2.1.1 <u>*Discussion*</u>

The tensile strains in the repair patch of material S2 within the first week after application are due to the fact that the shuttering was removed after approximately three

days which tended to induce tension in the repair patch. From this age onwards, the repair patch would have to fully support its own weight. The repair materials were applied to unpropped compression members, but nevertheless, the shuttering formed a partial support in the early stages after repair application (see Figures 6.4 and 6.7). The shuttering was left in place for approximately three days after application to assist with curing. When the shuttering was removed, the repair patch had a tendency to pull away from the substrate concrete, thereby inducing slight tensile strains in the substrate concrete, steel reinforcement and repair material. These early age tensile strains were evident in nearly all the repair materials under test at Sutherland Street Bridge [see Figures 9.15 (S2), 9.16 (S1), 9.18 (S1), 9.20 (S3), and 9.21 (S4)]. Shortly after striking the shuttering (from week 1 onwards), the strains in the substrate concrete [Figure 9.15 (material S2)] start changing to compressive strains as the stiffer repair material begins to develop its stiffness (Table 8.11) and transfers shrinkage strain to the less stiff substrate concrete (see Tables 9.5 and 9.6). Compressive strain is also transferred to the steel reinforcement during this period, but is less than the strain transferred to the substrate concrete since the steel is much stiffer than the substrate concrete. There will be a virtual tensile strain in the repair material which is caused by the partial restraint to

Table 9.5 Comparison of elastic modulus between substrate concrete and repair materials represented in Figures 9.15 and 9.16

Material	*Elastic Modulus (kN/mm^2)* *Sutherland Street Bridge*
S1	24.2
S2	32.2
substrate	23.2

Table 9.6 Free shrinkage* and creep strains of materials represented in Figures 9.15 and 9.16

Material	*100 day free shrinkage (μstrain) (stored at 20°C, 55%RH)*	*70 day compressive creep (μstrain) (30% stress/strength)*
S1	740	445
S2	791	438
G3 (Reference)	717	938

*Note: * indicates that a correction for volume/surface ratio has not been applied*

shrinkage provided by the substrate concrete and steel reinforcement (equivalent to the free shrinkage of the repair material minus the compressive strain measured by the substrate concrete gauge). The shrinkage restraint will be greatest at the steel reinforcement/repair material interface as the steel reinforcement has a much larger stiffness. The slope of the strain versus time graph in Figure 9.15 is steep between weeks 1 and 16 after which it reaches a stable state when shrinkage in the repair material has reached negligible levels. The strains in the substrate concrete, steel reinforcement and repair material remain constant thereafter. Material S2 does not attract externally applied stress into the repair patch, as indicated by the constant strains in the substrate concrete, steel reinforcement and repair material strains from week 27 (Figure 9.15). This may be due to minor cracking which is visible in the repair material, as shown in Figure 9.17. It has been observed in many other instances in this project that a cracked material is unable to attract externally applied load into the repair patch. Figure 9.17 (a) shows an elevation of the north face of the north frame at Sutherland Street Bridge, including the positions of the repair patches of repair materials (S1-S4)

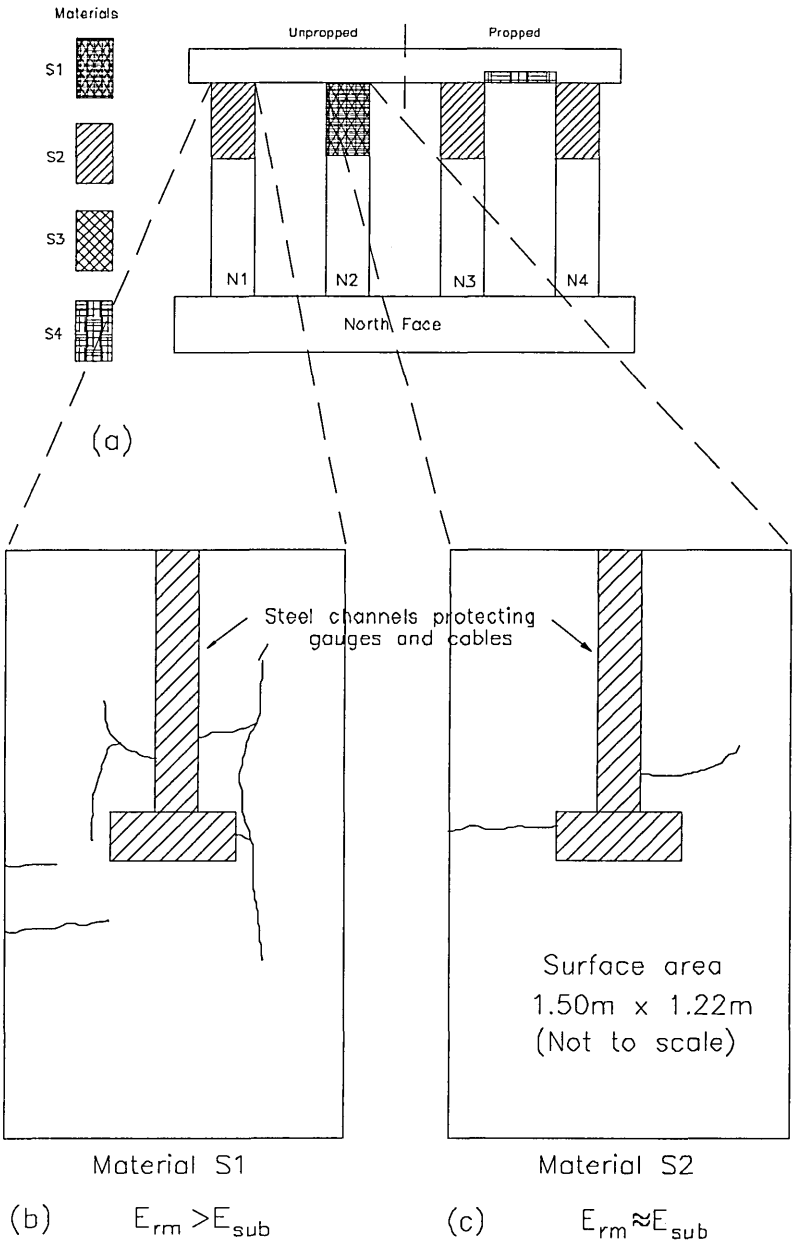

Crack widths < 0.1mm unless otherwise stated

Figure 9.17 Crack patterns in repair patches at Sutherland Street Bridge

(a) North face of north frame at Sutherland Street Bridge

(b & c) Cracking in repair patches of materials S1 and S2 at Sutherland Street Bridge

Method of repair: flowing repair materials

Support during repair: unpropped

Properties: repair material stiffer than substrate concrete

on the frame. Figure 9.17 (b) shows the cracks in the repair patch of material S2. In this instance, a mismatch in repair material properties is not responsible for cracking in the repair material, since the repair material exhibits properties that are deemed acceptable for concrete repair (i.e. relatively higher elastic modulus compared to the substrate concrete elastic modulus, and medium shrinkage, see Tables 9.5 and 9.6). Referring to Figure 9.17 (b), mild steel covers were placed over the strain gauges and gauge cables to protect them from the threat of vandalism (views of these steel covers are also shown in Figure 6.8). These steel covers were intermittently bolted to the surface of the repair material. It is, therefore, evident that the bolted steel covers provided a restraint which induces localised tensile stress in the repair material. This results in localised cracking in the area around the steel covers, as shown in Figure 9.17 (b).

Material S1, as shown in Figure 9.16, performs differently to material S2 (Figure 9.15). The strains in the steel reinforcement, substrate concrete and repair material show tensile strains in the first 4 weeks. Removal of the shuttering after three days again induces tension in the repair patch, since from this age onwards the repair patch would have to fully support its own weight. There is a marginal difference in elastic modulus between the repair material and substrate concrete (Table 9.5), hence the degree of restraint will be high. The material also exhibits relatively high shrinkage (740 microstrain, Table 9.6). From week 4 onwards, the substrate concrete and repair material (Figure 9.16) starts deforming compressively and after about 15 weeks exhibit compressive strain of approximately 100 microstrain. This compression in the substrate concrete is due to net shrinkage in the repair material. The strains in the substrate concrete and repair material remain relatively constant thereafter. The strain in the steel

reinforcement, however, returns to approximately zero at week 29 and remains there until week 54, as shrinkage strain is slowly transferred to the steel reinforcement to neutralise the initial tensile strain in the steel reinforcement caused by the removal of shuttering. It is clear that from approximately week 29 onwards no external load is attracted into the repair material [indicated by the almost constant strains in the substrate concrete, steel reinforcement and repair material ("emb" gauge)]. Again, this is due to the cracking which occurred in the repair patch. Referring to Figure 9.17 (c), cracking is evident in the vicinity of the steel protective covers due to the restraint provided by the holding bolts.

Comparing Figure 9.17 (b) and (c) with the cracking observed in Figure 9.7 (material L4 at Lawns Lane Bridge) and Figure 9.13 (material L1 at Lawns Lane Bridge), the cracking pattern in materials S1 and S2 is much more irregular than the cracking pattern in material L4 and L1 (Figures 9.7 and 9.13). The majority of the cracks in materials S2 and S1 [Figure 9.17 (b) and (c) respectively] originate in the area around the holding bolts of the steel covers. Therefore, it is evident that the restraint provided by the bolted steel covers is responsible for the cracking in materials S2 and S1 at Sutherland Street Bridge, as opposed to the cracking due to inadequate properties of materials L4 and L1 at Lawns Lane Bridge.

9.3.1.2.1.2 *Further discussion*

It is clear from Figures 9.15 and 9.16 that both flowing repair materials performed differently to each other. Material S2 [Figure 9.17 (b)] exhibited more cracking than

material S1 [Figure 9.17 (c)], but this is mainly due to the restraint to shrinkage provided by the connections of the steel covers. Nevertheless, there is only a marginal difference in elastic modulus between the repair material S1 and the substrate concrete (Table 9.5). This will result in higher shrinkage restraint in the material since repair material S1 will not be able to transfer as much shrinkage strain to the substrate concrete and steel reinforcement as material S2. This is shown with reference to Figures 9.15 and 9.16. The initial tension in the repair patches of materials S2 and S1 in Figures 9.15 and 9.16 respectively, is due to the removal of the shuttering. From this point onwards, the initial tensile strain in the substrate concrete, steel reinforcement and repair material in material S2 (Figure 9.15) is neutralised at approximately week 2. This is because the stiffer repair material is shrinking and transferring shrinkage strain to the substrate concrete and steel reinforcement. This is also the case for material S1 (Figure 9.16), but the transfer of shrinkage strain is slower since there is only a marginal difference in stiffness between the repair material and substrate concrete. Therefore, this repair material will have to attain its full elastic modulus before distribution of shrinkage strain can take place. The initial tensile strains in the substrate concrete, steel reinforcement and repair material are neutralised at approximately weeks 9, 7 and 27 respectively due to shrinkage in the repair material. The much stiffer repair material (S2, Figure 9.15) transfers approximately 230 microstrain of shrinkage strain to the substrate concrete (-30 microstrain to +200 microstrain). This value is approximately 160 microstrain in material S1 (-80 microstrain to +80 microstrain, Figure 9.16). Similarly, the stiffer repair material S2 (Figure 9.15) transfers approximately 150 microstrain of shrinkage to the steel reinforcement (-25 microstrain to +125 microstrain), as opposed to approximately 40 microstrain to the steel reinforcement in repair patch of material S1 (-

50 microstrain to -10 microstrain, Figure 9.16). The free shrinkage of both repair materials S1 and S2 are similar (Table 9.6).

It is also possible that the flowing technique of repair may have an influence on the performance of the material. The distribution of strain in the repair patch of a spray applied materials could be categorised into four distinct stages i.e. Shrinkage, Steady state #1, External load transfer and Steady state #2 (see Figure 9.8). The distribution of strain in the repair patch of a flowing repair material was different to the distribution of strain in a spray applied material (compare Figures 9.15 and 9.16 with Figure 9.8), even though the relative properties of the flowing materials were similar to the relative properties of the spray applied materials (i.e. high elastic modulus, medium shrinkage, low creep). For example, the flowing repair materials did not attract externally applied stress into the repair patch (see Figures 9.15 and 9.16, weeks 25 to 47). It is therefore possibly that spray applied repair perform better than flowing repairs when applied to unpropped members in compression.

9.3.2 Repairs to propped compression members

9.3.2.1 Flow applied repair patches

9.3.2.1.1 Repair material stiffer than substrate concrete

Repairs to propped members were carried out at Sutherland Street Bridge in Sheffield. The load was removed from the bridge during the application of the repair patches. Details of the propping procedure are given in Chapter 6. A total of four different repair materials were monitored, which were applied using the flowing technique. Three of the

materials were commercially available (S1-S3), whereas S4 was a laboratory designed flowing concrete mix. Repair materials S1-S3 complied with the current standard, BD 27/86 [1], whereas material S4 did not.

Vibrating wire strain gauges were attached to the cut-back substrate ("subs"), steel reinforcement ("steel") and embedded in the repair material ("emb"). Data from these strain gauges in a number of the propped compression members (materials S1-S4) at Sutherland Street Bridge are presented in Figures 9.18 to 9.21. Datum readings were taken 24 hours after the application of the repair patch. Depropping occurred approximately three weeks after the application of the repair when the cube strength of the repair material reached the design strength of the substrate concrete. Strains are plotted at weekly intervals.

Referring to material S1 in Figure 9.18, tensile strains are evident in the substrate concrete, steel reinforcement and repair material in the first 3 weeks of monitoring. The load was removed from the member during this period by propping. These strains return to approximately zero before depropping occurs at approximately week 4 (Figure 9.18). After depropping, the strains in the embedment, steel and substrate gauges increase steadily to reach approximately 170, 50 and 40 microstrain respectively at 17 weeks. From week 17 onwards, the strains remain relatively constant (Figure 9.18).

The strains from the substrate concrete, steel reinforcement and repair material gauges in material S2 are shown in Figure 9.19. The substrate concrete strain increases rapidly to reach approximately 240 microstrain at week 29, but remains relatively constant

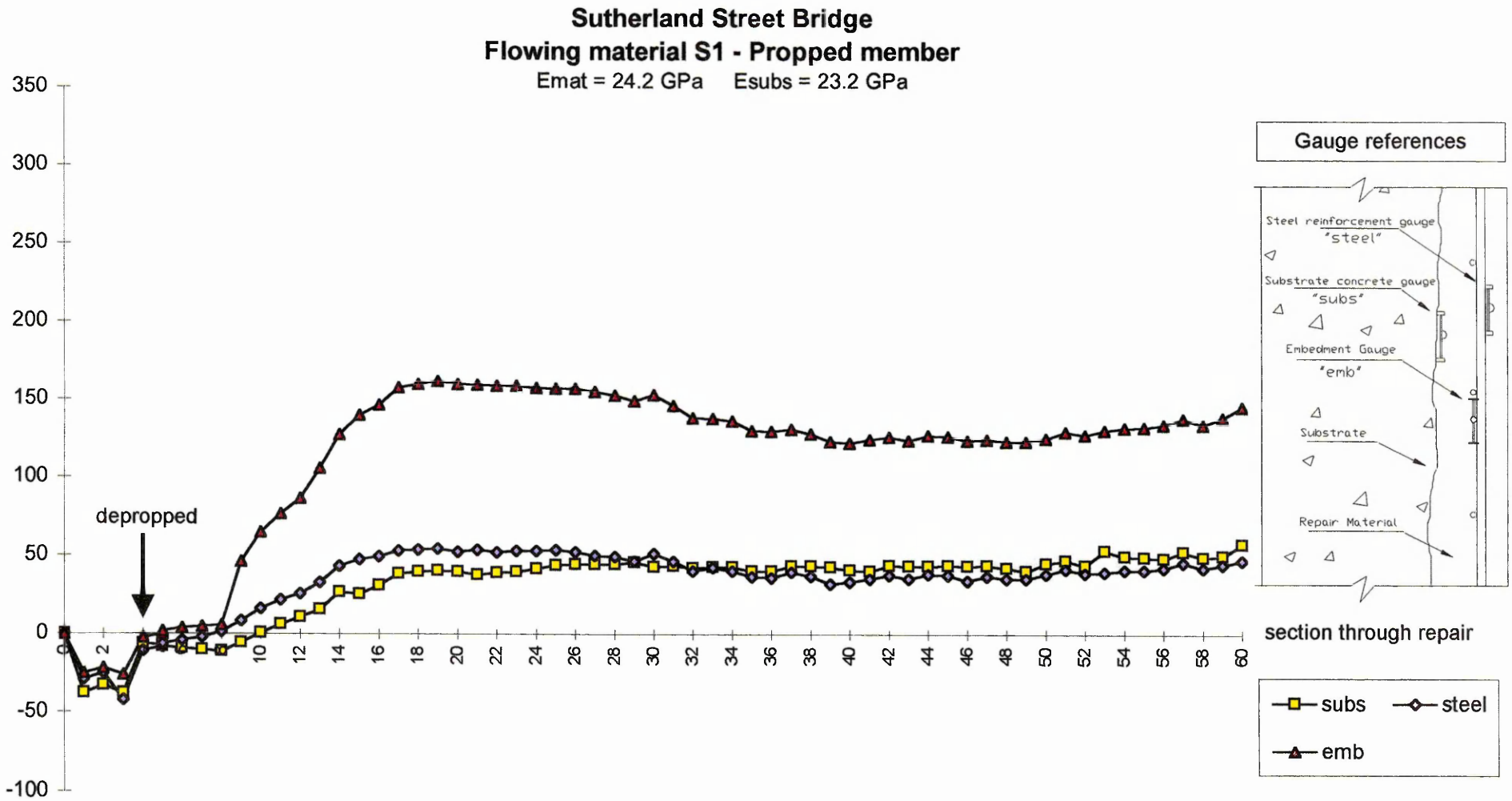

Figure 9.18 Strain distribution in repair patch of material S1 at Sutherland Street Bridge (Propped compression member)

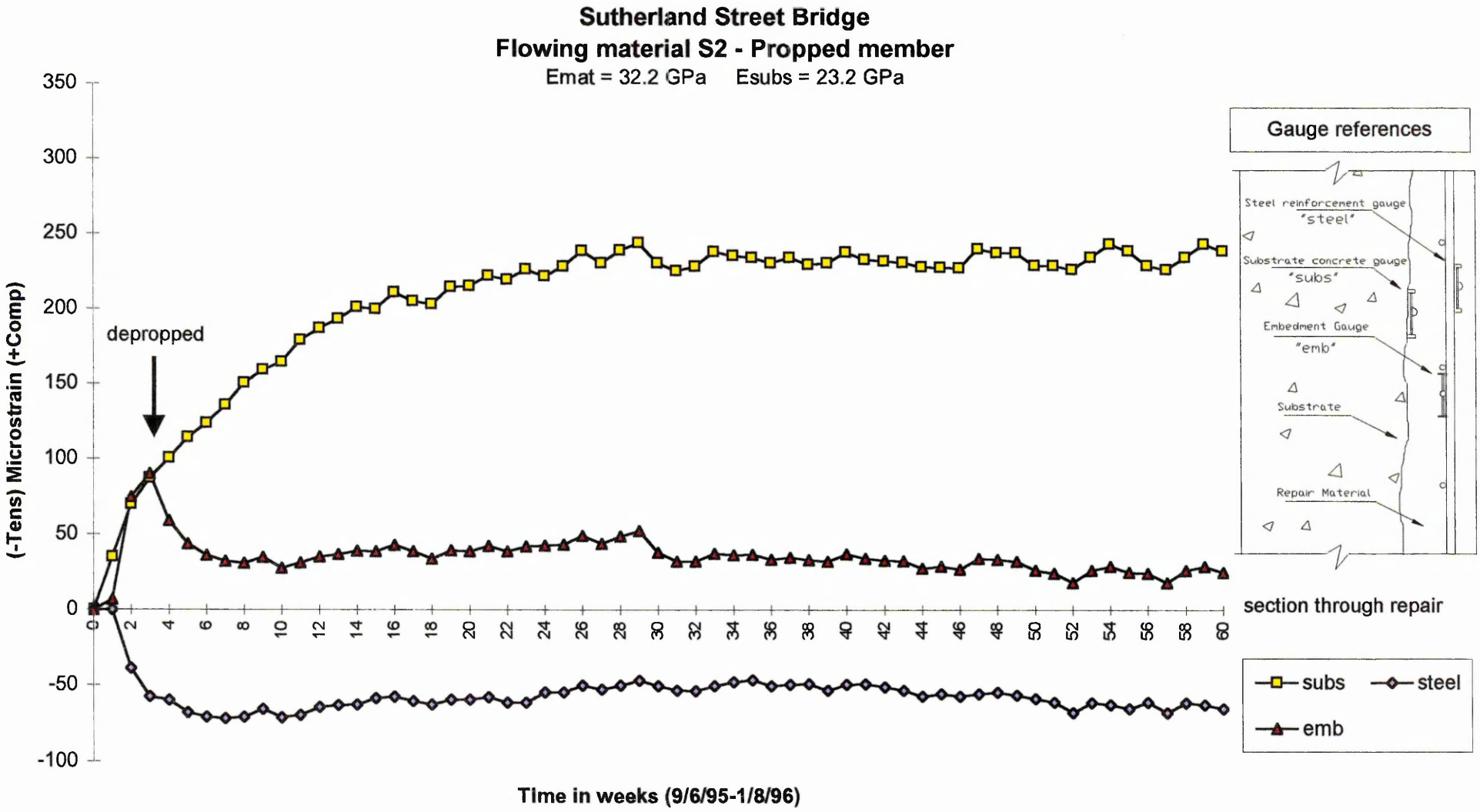

Figure 9.19 Strain distribution in repair patch of material S2 at Sutherland Street Bridge (Propped compression member)

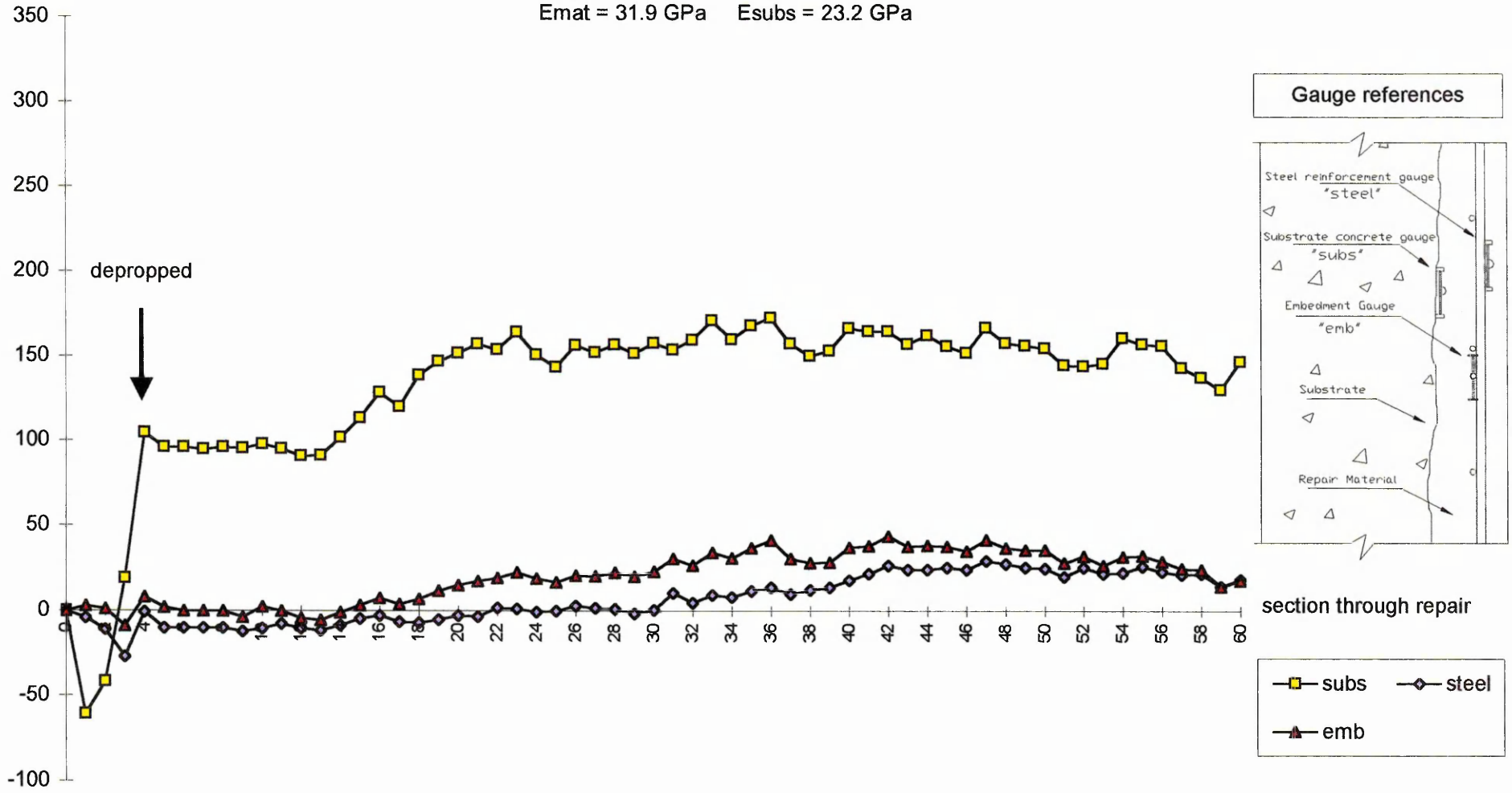

Figure 9.20 Strain distribution in repair patch of material S3 at Sutherland Street Bridge (Propped compression member)

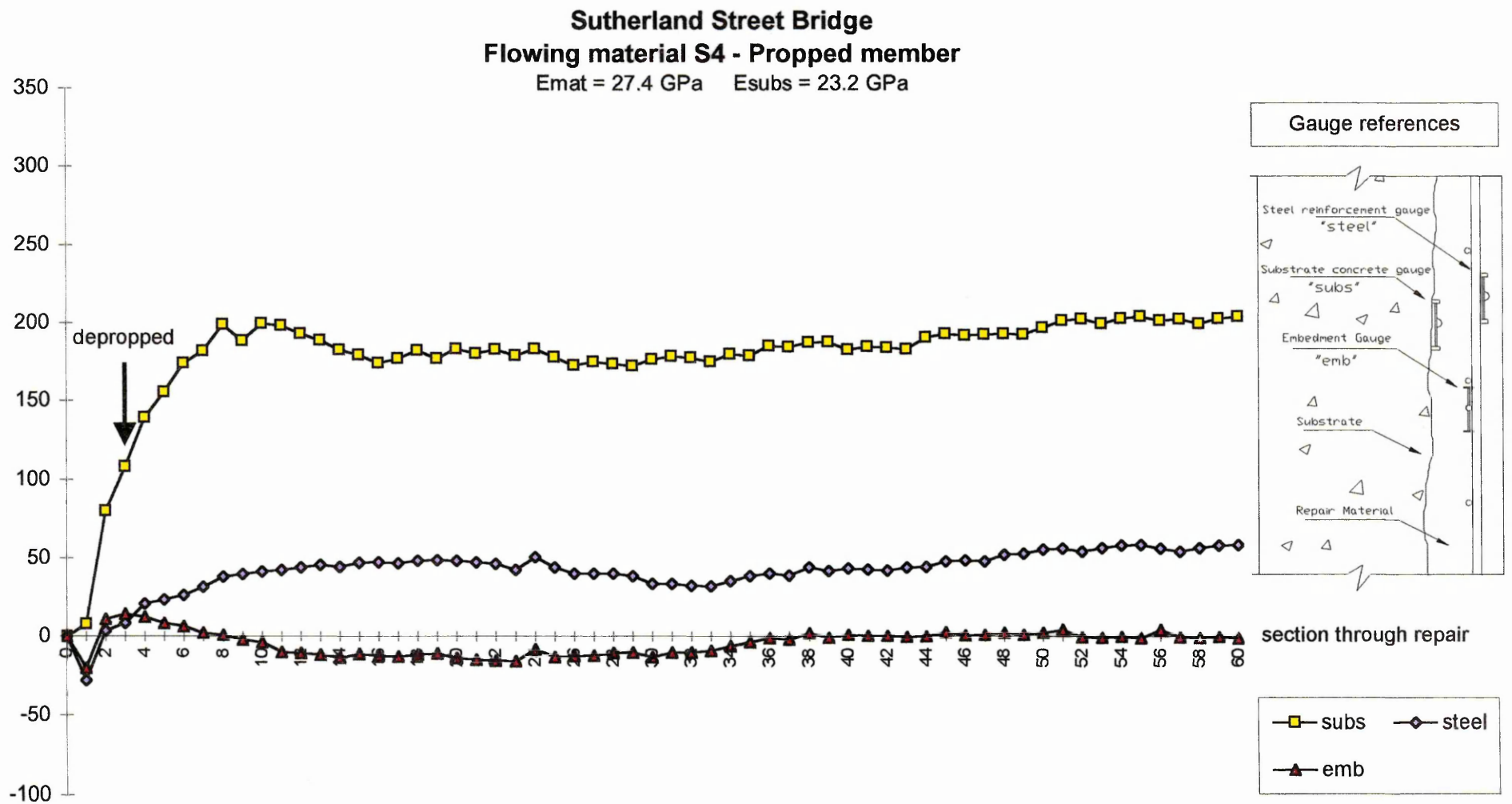

Figure 9.21 Strain distribution in repair patch of material S4 at Sutherland Street Bridge (Propped compression member)

thereafter. The substrate concrete strains undergo no sudden change due to depropping at week 3. The strain in the repair material (gauge: emb) reaches approximately 90 microstrain at week 3 but decreases sharply to approximately 30 microstrain soon after depropping (Figure 9.19). This strain remains relatively constant thereafter. The strain in the steel reinforcement decreases sharply to approximately 70 microstrain (tension) between weeks 2 and 5. There is no sudden change upon depropping at week 3. This strain remains relatively constant from week 5 to the end of the monitoring period (week 60, Figure 9.19)

The strains from material S3 are shown in Figure 9.20. The substrate concrete strain increases in tension to approximately 60 microstrain at week 1 before rapidly changing to approximately 100 microstrain before depropping at week 4. Thereafter, this strain remains relatively constant until week 12. A gradual increase then occurs until week 22, where the strain reaches approximately 175 microstrain (compression). From week 22 onwards, this strain remains relatively constant (Figure 9.20). The steel reinforcement and repair material show slight tensile strains (approximately -25 and -10 microstrain) until week 3 before returning to 0 microstrain at week 4. They then show negligible strains until week 14 when a slight increase in compression is observed. This increase in strain continues until week 41, after which a steady state is reached (Figure 9.20).

The distribution of strain in repair patch of material S4 is given in Figure 9.21. The substrate concrete strain increases to reach a maximum of approximately 210 microstrain (compressive) at week 8 and remains relatively constant thereafter. The substrate concrete strain remains unaffected by depropping at week 3. The steel

reinforcement shows an initial tensile strain (week 1) before gradually changes to a compressive strain reading 50 microstrain at week 10. This strain remains relatively constant throughout the remainder of the monitoring period (Figure 9.21). The repair material (gauge: emb) also exhibits an initial tensile strain (week 1, Figure 9.21) but returns to 0 microstrain at week 3. After depropping at week 3, the strain in the repair material gradually increases to approximately 30 microstrain (tensile) and remains relatively constant thereafter (Figure 9.21).

9.3.2.1.1.1 Discussion

The tensile strains in the steel reinforcement, substrate concrete and repair material in repair materials S1 and S3, and in the steel reinforcement and repair material of S4 (Figures 9.18, 9.20 and 9.21 respectively) is as a result of removing the shuttering within the first week after application of the repair material. A similar tensile strain is evident in the steel reinforcement within the repair patch of material S2 (Figure 9.19). Similar tensile strains were also observed in repairs to unpropped compression members within the early stages after application (Figures 9.15 and 9.16, materials S1 and S2). Since the shuttering provides a support to the repair material in the early stages, this support is lost when the shuttering is removed. Consequently, the repair material will then have to fully support its own weight resulting in a tendency to pull away from the substrate concrete and steel reinforcement. This induces tension in the steel reinforcement, substrate concrete and repair material due to the bond at the interface and steel reinforcement. The subsequent high compressive strains in the substrate concrete with materials S2, S3 and S4 (Figures 9.19 to 9.21) are due to the stiffer repair material

Table 9.7 Comparison of elastic modulus between substrate concrete and repair materials represented in Figures 9.18 to 9.21

Material	*Elastic Modulus (kN/mm^2)* *Sutherland Street Bridge*
S1	24.2
S2	32.2
S3	31.9
S4	27.4
substrate	23.2

transferring shrinkage strain to the substrate concrete during the shrinkage period, assumed as week 0 to week 11 from Figure 9.8 (see Tables 9.7 and 9.8). Conversely, the relatively low compressive strain developed in the substrate concrete of the repair patch of material S1 (Figure 9.18) is due to a lower transfer of shrinkage strain to the substrate concrete from material S1 since there is only a marginal difference in elastic modulus between material S1 and the substrate concrete (see Table 9.7). Hence, the restraint to shrinkage in this material will be higher and less shrinkage strain is transferred to the substrate concrete. Depropping the bridge slows the rate of shrinkage

Table 9.8 Free shrinkage* and creep strains of materials represented in Figures 9.18 to 9.21

Material	*100 day free shrinkage (μstrain) (stored at 20°C, 55%RH)*	*70 day compressive creep (μstrain) (30% stress/strength)*
S1	740	445
S2	791	438
S3	580	667
S4	388	454
G3 (Reference)	717	938

*Note: * indicates that a correction for volume/surface ratio has not been applied*

strain transfer to the steel reinforcement, substrate concrete and repair material in material S1 between weeks 4 and 8 (Figure 9.18), but from week 8 to week 17, shrinkage strain is distributed within the repair patch (Figure 9.18). A similar restraint is visible (Figure 9.20) in the substrate concrete, steel reinforcement and repair material strains of the repair patch of material S3; upon depropping at week 3 (Figure 9.20), the substrate concrete, steel reinforcement and repair material strains remain relatively constant until week 13. Thereafter, some increase in compression is observed, as shrinkage strain is distributed within the repair patch. Depropping the bridge did not significantly alter the rate of strain increase in the substrate concrete in materials S2 and S4 (Figures 9.19 and 9.21). On the other hand, depropping reduced the compressive strain in the repair material in the repair patch of material S2 (Figure 9.19), and to a lesser extent, the repair material strain in the repair patch of material S4 (Figure 9.21). Referring to Figure 9.18, external load is not attracted into the repair patch of material S1, indicated by the almost horizontal strains from week 17 onwards. This effect is also clearly evident in the other three flow applied repair materials (materials S2-S4, see Figures 9.19 to 9.21).

9.3.2.1.1.2 *Further discussion*

9.3.2.1.1.2.1 *Cracking in repair patches*

A visual survey was carried out on the repair patches whose strains are presented in Figures 9.18 to 9.21 a few months after the application of the repair materials. The results of the visual survey are given in Figure 9.22. An elevation of the south frame (south face) is given in Figure 9.22 (a), along with the position of the repair patches on this frame. The whole of the south frame was propped during application of the repair

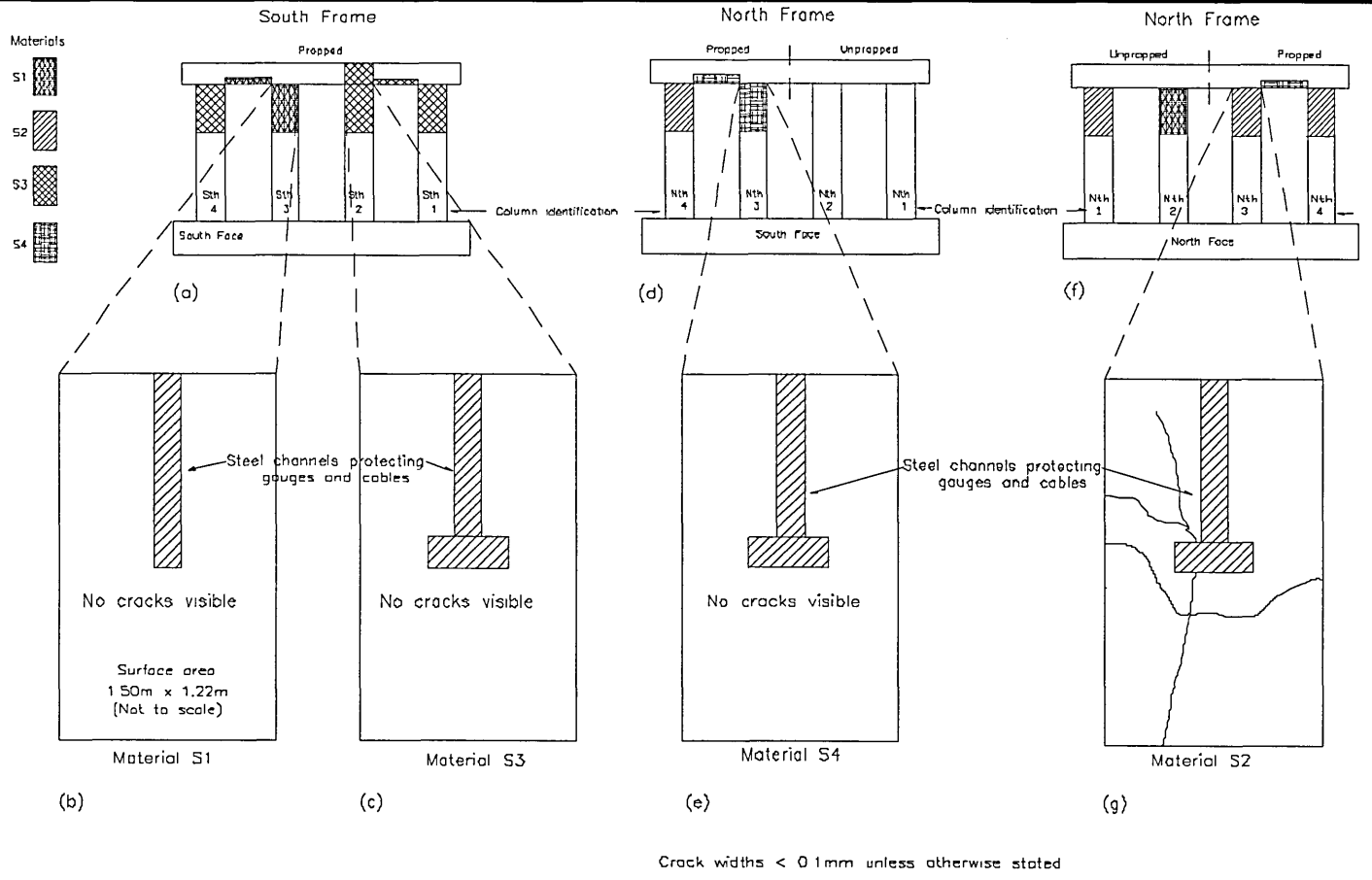

Figure 9.22 Cracking patterns in repair patches at Sutherland Street Bridge
(a) Elevation of south frame (south face) (b) Material S1 (c) Material S3
(d) Elevation of north frame (south face) (e) Material S2 (f) Elevation of north frame (north face) (g) Material S4
Method of repair: flowing Support during repair: unpropped or unpropped Properties: repair material stiffer than substrate concrete

patches. Figures 9.22 (b) and (c) show an enlarged elevation of the repair patches of materials S1 and S3. No cracking was visible in these repair materials. Figure 9.22 (d) shows an elevation of the north frame (south face) at Sutherland Street Bridge along with the position of the repair patches. Half of the north frame was propped during application of the repair materials. Figure 9.22 (e) shows an enlarged elevation of the repair patch of material S4, which was applied to the propped part of the frame. Again, no cracking was evident. Referring to Tables 9.7 and 9.8, the properties of the repair materials were considered appropriate for concrete repair (i.e. high elastic modulus, medium shrinkage, low creep). As a result, cracking was absent from these repair materials. Figure 9.22 (f) shows an elevation of the north frame (north face) at Sutherland Street Bridge and the position of the repair patch of material S2 (the bridge was propped during application of the repair patch). An enlarged elevation of the repair patch of material S2 is given in Figure 9.22 (g). Some cracking was evident in this material [Figure 9.22 (g)], even though the properties of the material (high elastic modulus, medium shrinkage and low creep, see Tables 9.7 and 9.8) are considered appropriate for concrete repair. Referring to Figure 9.22 (g), the cracks in the repair patch mostly originate around the steel covers which protect the gauges and gauge cables. Similar cracking was also observed in materials S1 and S2 when applied to an unpropped bridge [see Figure 9.17 (b) and (c)]. Therefore, it is thought that the steel bolts for connecting the steel covers to the repair materials act as a restraint which causes localised cracking in the repair patch. This restraint did not cause cracking in repair materials S1, S3 and S4, but the modulus of rupture of these repair materials (6.5 N/mm^2, 5.7 N/mm^2 and 4.3 N/mm^2 respectively, albeit in the long term) was greater

than the modulus of rupture of material S2 (3.3 N/mm^2 in the long term, see Figure 8.23).

9.3.2.1.1.2.2 Comparison between repairs to propped and unpropped members

Similarities exist in the performance of flowing repairs to propped compressive members (Figures 9.18 to 9.21) with the performance of flowing repairs to unpropped compressive members (Figures 9.16 and 9.15). In the early ages after application, tension is induced in the repair patch when the shuttering is removed after approximately 3 days (see Figures 9.15, 9.16, 9.18, 9.20 and 9.21). Shrinkage strain is transferred to the substrate concrete, and to a lesser extent, to the steel reinforcement in flowing repairs to both unpropped (Figures 9.15 and 9.16) and propped members (Figures 9.18 to 9.21). This is shown by the increase in strain in the substrate concrete and steel reinforcement in Figures 9.15 to 9.21. In both cases (flowing repairs to unpropped and propped members), external load is not transferred from the substrate concrete into the repair patch. This is evident in Figures 9.15 to 9.21 as the strain in the in the steel reinforcement, repair material and substrate concrete remain relatively constant during the external load transfer stage (assumed as week 25 to 47 from Figure 9.8). Cracking is evident in some of the flow applied repairs to both the propped and unpropped members (Figures 9.17 and 9.22), but this is due to the restraint to shrinkage that the protective steel covers provide.

9.3.2.1.1.2.3 Comparisons with spray applied repair materials

The distribution of strain to the substrate concrete, steel reinforcement and repair material in repair patches of flowing materials, applied to members in compression when the external load was removed (i.e. propped, represented in Figures 9.18 to 9.21), show some similarities with the distribution of strain in spray applied materials to members in compression when the external load remained in place (unpropped, represented in Figure 9.8). Comparing Figures 9.18 to 9.21 with Figure 9.8, the stiffer repair materials transfer some shrinkage strain to the less stiff substrate concrete, shown by the increase in strain in the substrate concrete in Figures 9.8, and Figures 9.18 to 9.21. On the other hand, differences exist since the flowing repair materials do not attract external load in the repair patch (compare Figures 9.18 to 9.21 with Figure 9.8, weeks 25 to 47). This is shown by the relatively constant strain in the steel reinforcement, substrate concrete and repair material. Flow applied repair materials have a disadvantage in this respect, since a tensile stress in the repair material due to the restraint to shrinkage provided by the substrate concrete will remain in the repair patch in the long term due to no transfer of external compressive load. It has been shown that the tensile stress in the repair patch of a spray applied repair material decreases when compressive stress is attracted into the repair patch during the "external load transfer" stage (Figure 9.8, Zone 3). Therefore, a tensile stress may remain in the repair patch of a flow applied repair material in the long term. This could cause durability problems, as it has been shown that the tensile strength of some repair materials decreases with time, hence, cracking could occur (see Section 9.3.1.1.1.2). Since the properties (elastic modulus, shrinkage and creep) of both sprayed and flowing material are similar for both the sprayed and flowing repairs under observation, it seems that spray applied repair

materials will attract external load into the repair patch (see Figure 9.8) whereas the flowing repair materials do not attract external load into the repair patch (see Figures 9.18 to 9.21). This was evident in the flowing repairs to both propped and unpropped members.

The basic properties of the flowing materials (high elastic modulus, low to medium shrinkage and creep - see Tables 9.7 and 9.8 respectively) are similar to the properties of the spray applied materials which performed satisfactorily at Lawns Lane Bridge (L4, L2 and L3) and Gunthorpe Bridges (G1), shown in Tables 9.1 and 9.2. Materials S1, S3 and S4 (Figures 9.15, 9.17 and 9.18) performed satisfactorily with respect to cracking at Sutherland Street Bridge. Material S2 (Figure 9.16), however, exhibited some cracking due to the restraint provided by the bolts used to connect the steel covers. Therefore, the recommendation of specifying repair materials with basic properties such as high elastic modulus (relative to the substrate concrete), medium shrinkage and low creep is valid for both sprayed and flowing repair materials. Low creep is desirable to ensure that the elastic modulus of the repair material does not decrease with time and become less than that of the substrate concrete. It should, however, be noted that higher creep is beneficial in causing tensile stress reduction due to the restraint to shrinkage provided by the substrate concrete and steel reinforcement. Therefore, a balance is desirable.

9.3.3 Repairs to unpropped flexural members

9.3.3.1 Hand applied repair patches extending 25mm behind steel reinforcement

9.3.3.1.1 Repair material stiffer than substrate concrete

Repairs were carried out to unpropped flexural members both in the field (Gunthorpe Bridge) and in the laboratory. The unpropped flexural repairs at Gunthorpe Bridge did not yield consistent results, and consequently, will not be presented at this stage. Deterioration due to corrosion was simulated in reinforced concrete beams manufactured in the laboratory and repair was subsequently applied using different generic repair materials. The beam size was 2740 x 100 x 200mm. Repair patches, measuring 640mm long x 100mm wide x 71mm deep (extending 25mm behind steel reinforcement) were applied symmetrically at mid-span. In order to simulate actual field conditions, each simply supported reinforced concrete beam was loaded for approximately 6 weeks prior to application of repair in order to eliminate the effects of creep in the substrate concrete. Custom built creep rigs, shown in Figure 7.3 (a) (Chapter 7), were used to apply a constant load on the repaired reinforced concrete beams. The rig consists of a 203 x 102 x 23 kg/m universal beam. Two-point bending loads (2 x 11 kN, approximately 40% of the maximum capacity) were applied to the beam in order to introduce a constant bending moment zone in the middle-third portion of the beam.

A combination of demec points and electrical resistance gauges was used to monitor the distribution of strain along the depth of the beam section. Strains were measured at mid-span on the beams in the constant bending moment zone (see Figures 7.2, 7.4 and

7.5). The strain in the substrate (denoted "Dem 1", "Dem 2", and "Dem 3") was obtained from a demec extensometer of 100mm gauge length. Each strain value is the average of readings on two faces, as shown in Figure 7.5). The strain in the steel reinforcement was monitored from an electrical resistance gauge attached to the steel reinforcement, shown as "Steel 1" in Figure 7.4. The strain in the repair material was obtained from embedded electrical resistance gauges denoted "RM 1", "RM 2" and "RM 3", as shown in Figure 7.4.

The strain-time relationship for beams repaired with materials G4(L) and L3(L) [the letter in brackets denotes Laboratory investigation] are plotted in Figures 9.23 and 9.24. E_{rm} of each repair material was significantly greater than E_{sub} (see Table 9.9). Datum readings of strain for repair materials G4(L) and L3(L) (Figures 9.23 and 9.24) were taken 24 hours after the application of the repair patch (represented by week 0 in Figures 9.23 and 9.24). Residual strains in the substrate concrete and steel reinforcement were present at week 0, since the beam had been loaded at approximately week -6 to eliminate the effects of creep in the substrate concrete (see Figures 9.23 and 9.24). After casting, beams were cured for 4 weeks prior to the creep loading. This curing period

Table 9.9 Elastic modulus of substrate concrete and repair materials represented in Figures 9.23, 9.24, 9.27 and 9.28

Beam	*Material*	*Elastic Modulus (kN/mm^2)*
2, 5	substrate	20.5†
2	G4(L)	24.0
5	L3(L)	27.4

† Does not take into account the effects of creep in the pre-loaded substrate concrete

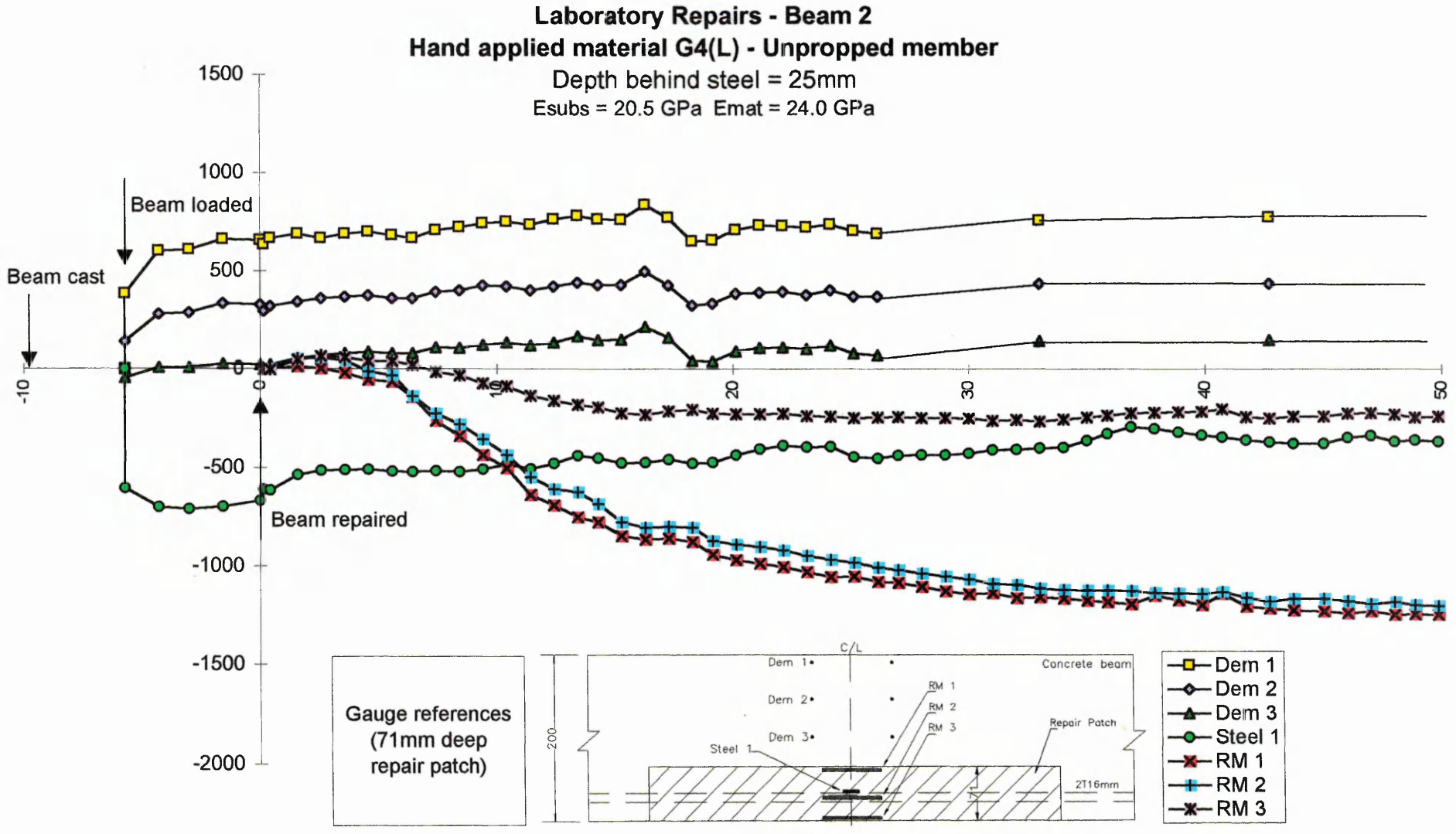

Figure 9.23 Strain distribution in beam 2 repaired with material G4(L) in the laboratory (Unpropped flexural member)

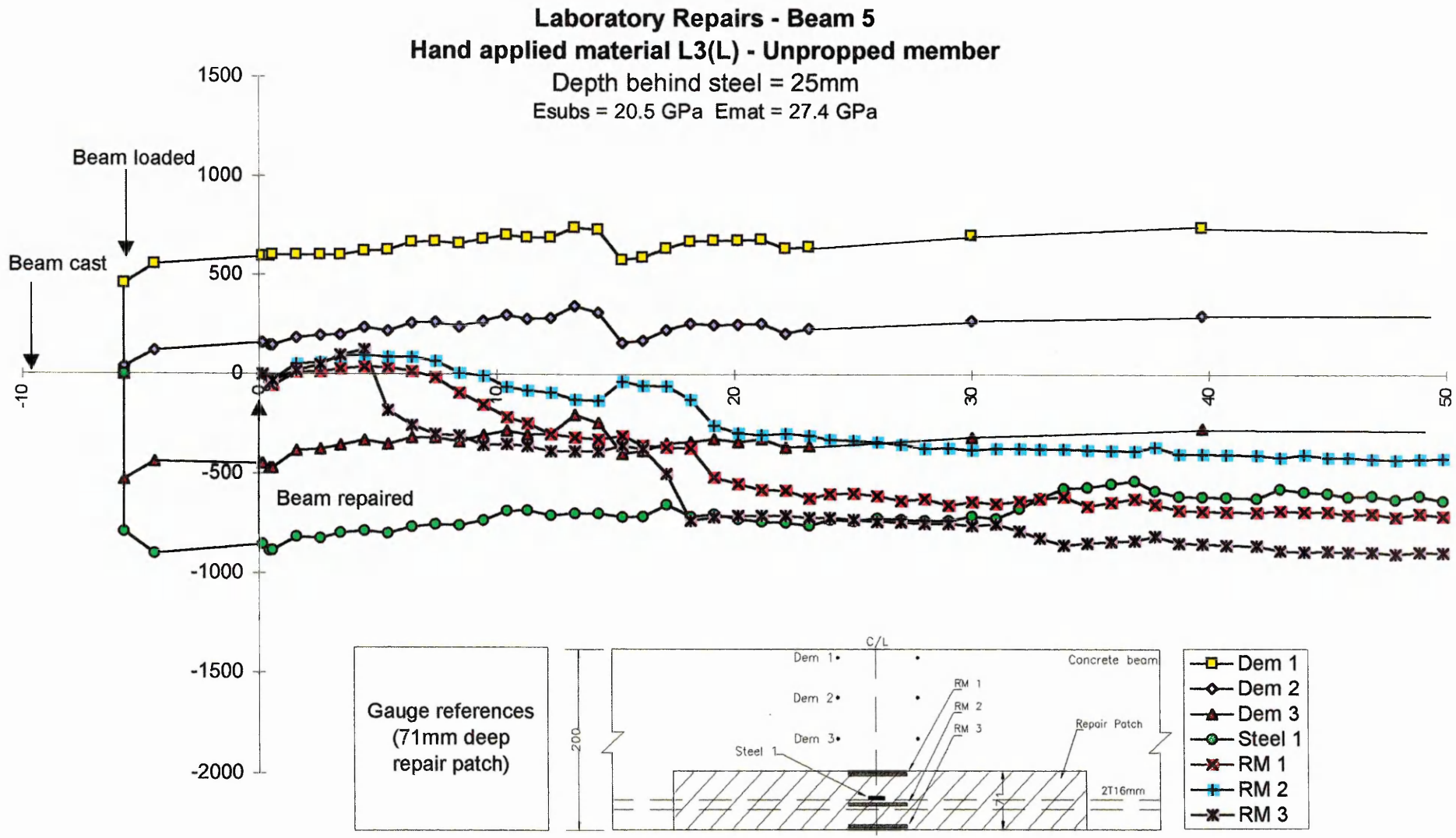

Figure 9.24 Strain distribution in beam 5 repaired with material L3(L) in the laboratory (Unpropped flexural member)

is shown as approximately weeks -10 to -6 in Figures 9.23 and 9.24. Strain readings after the application of the repair patch, in Figures 9.23 and 9.24, are plotted at weekly intervals, except for the demec gauge readings after approximately week 25 being plotted more intermittently .

Figure 9.23 shows the strain distribution in the beam (beam 2) which was patch repaired with material G4(L). The elastic modulus of repair material G4(L) is greater than the elastic modulus of the substrate concrete (see Table 9.9). The free shrinkage and creep of this material is presented in Table 9.10. This was the only beam repaired in the laboratory which did not exhibit any visible cracking during the monitoring period. Figure 9.25 (a) shows an elevation of a typical beam under load and the position of the repair patch on the beam. Figure 9.25 (b) shows an enlarged elevation of the repair patch of material G4(L). Cracking is not visible in this repair material. Cracking in the shrinkage period (assumed as week 0 to week 11 from the spray applied materials to unpropped members, Figure 9.8) was absent due a combination of high stiffness (Table 9.9) and low shrinkage (Table 9.10) in the material. This material also exhibited the highest modulus of rupture (13.5 N/mm^2 at 28 days from Table 8.21) of all the repair

Table 9.10 Free shrinkage* and creep strains of materials represented in Figures 9.23, 9.24, 9.27 and 9.28

Material	*100 day free shrinkage (μstrain) (stored at 20°C, 55%RH)*	*70 day compressive creep (μstrain) (30% stress/strength)*
G4(L)	401	745
L3(L)	710	748
G3 (Reference)	717	938

*Note: * indicates that a correction for volume/surface ratio has not been applied*

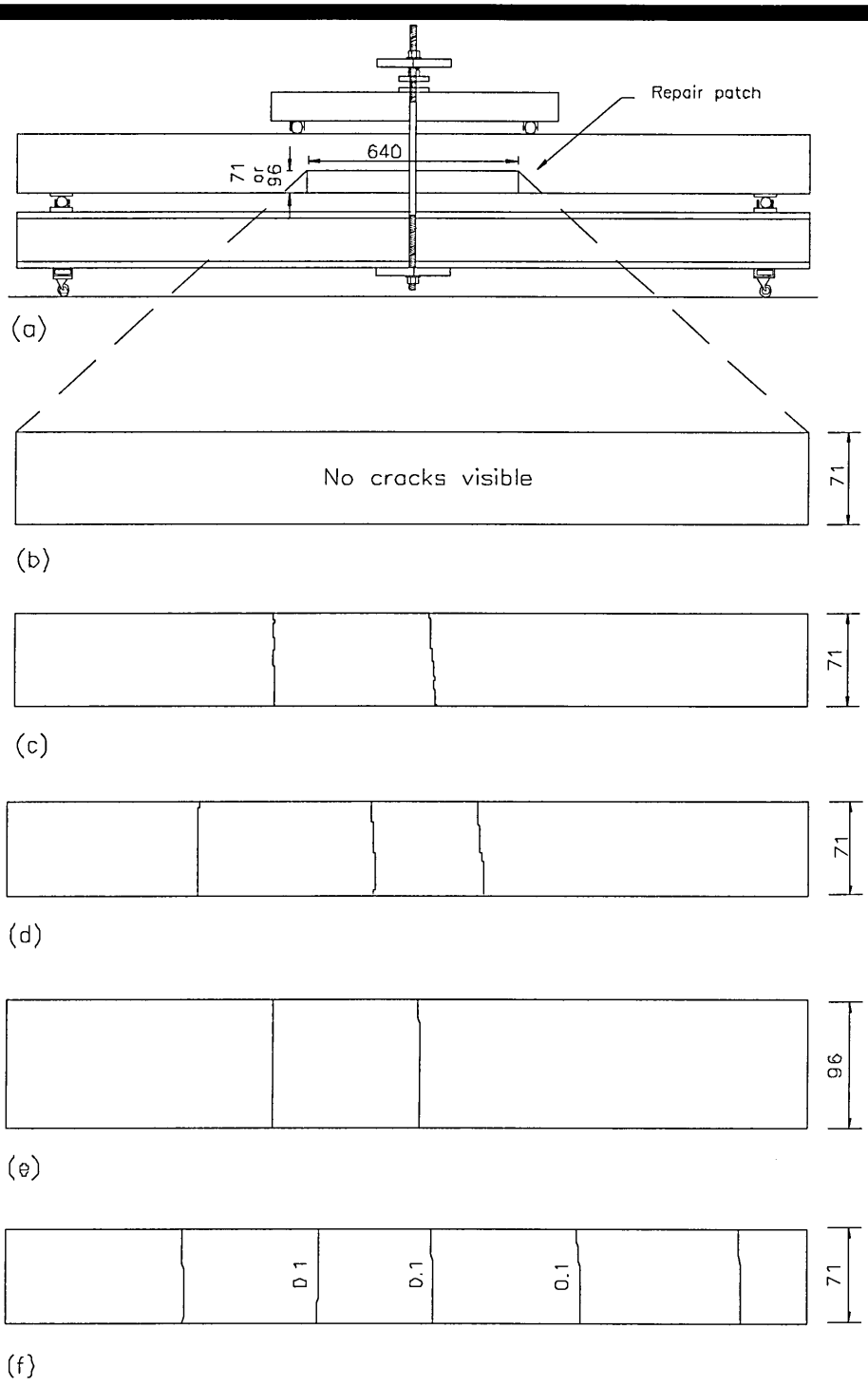

Figure 9.25 Cracking patterns in repair patches in the laboratory
(a) Elevation of repaired beam under load
(b) Material G4(L) (unpropped)
(c) Material L3(L) (unpropped)
(d) Material G6(L) (unpropped)
(e) Material L3(L) (unpropped)
(f) Material L3(L) (propped)

materials under test. The material shows slight contraction (positive strain) in the early stages from week 0 to week 5 (see "RM 1", "RM 2" and "RM 3", Figure 9.23). The contraction is less in "RM 1" compared with "RM 2" and "RM 3" due to the higher restraint provided at the repair material/substrate concrete interface (Figure 9.23). From week 5 onwards, it is noticeable that the tensile strain in the repair material gradually increases (see "RM 1", "RM 2" and "RM 3" in Figure 9.23). The tensile strain in the steel reinforcement simultaneously decreases during this period (see "Steel 1", Figure 9.23). The steel reinforcement is clearly shedding tensile load to the repair material. The tensile strains in "RM 2" and "RM 3" approach 1300 microstrain towards the end of the monitoring period with no visible sign of cracking. The high modulus of rupture of this repair material (see Table 8.21) combined with the fact that there is some creep relaxation is the reason for no visible cracking at the surface. Furthermore, the compressive strain in the substrate concrete ("Dem 1", "Dem 2" and "Dem 2", Figure 9.23) remains relatively constant throughout, except for some variation between weeks 16 to 20 due an operational fault in the controlled environment room which affected the surface strains "Dem 1", "Dem 2" and "Dem 3". As far as the effect of repair is concerned, redistribution of strain is therefore taking place within the repair patch only and does not have an appreciable effect on the strain in the substrate concrete. This repair material represents the ideal flexural repair situation, as the repair material is alleviating (tensile) load from the steel reinforcement but is not showing signs of cracking.

A similar situation occurs in the repair material L3(L) (beam 5) as shown in Figure 9.24, even though the material exhibits some cracking. The repair material is stiffer than the

substrate concrete, as shown in Table 9.9. The free shrinkage and creep of the material is given in Table 9.10 - shrinkage is much higher than material G4(L) but creep is similar. In this beam, cracking occurred at mid-span in the substrate concrete (within the gauge length of "Dem 3", see Figure 9.24) during the loading operation at week -6. This is indicated by "Dem 3" showing instantaneous "tension" of over 500 microstrain (Figure 9.24).

In the early weeks immediately after the application of the repair (weeks 0 to 5), the repair patch exhibits slight contraction due to shrinkage in material L3(L) (see "RM 1", "RM 2" and "RM 3", Figure 9.24). "RM 1" shows the lowest contraction in this period since it is adjacent to the substrate concrete which restrains its shrinkage through the interfacial bond with the substrate concrete. Subsequently, the strains increase in tension in "RM 1", "RM 2" and "RM 3", Figure 9.24. The transition from compression to tension of "RM 1", "RM 2" and "RM 3" in material L3(L) (week 5 to week 19) is more irregular than the same transition in G4(L) (Figure 9.23) because cracking occurred in the material L3(L) within this period. Referring to Table 9.10, the shrinkage of repair material L3(L) is much higher than the shrinkage of material G4(L). Therefore, a higher tensile stress will occur in material L3(L) due to the restraint to shrinkage provided by the substrate concrete. Furthermore, material L3(L) has a lower modulus of rupture than material G4(L) (7.0 N/mm^2 versus 13.5 N/mm^2 at 28 days, see Figure 8.23). Consequently, cracking in material L3(L) has effected the redistribution of strain (see "RM 1" and "RM 2" at week 19, "RM 3" at week 5 and 18, Figure 9.24).

There is a decrease in the strain in the steel reinforcement, as shown in "Steel 1", Figure 9.24, but due to cracking in the material, the effect of redistribution is not as pronounced as the redistribution in material G4(L) (Figure 9.23). Referring to Figure 9.23, the reduction in tensile strain in the steel reinforcement in the repair patch of material G4(L) was approximately 280 microstrain over the 50 week monitoring. The reduction in tensile strain in the steel reinforcement in the repair patch of material L3(L) was only approximately 200 microstrain. Figure 9.25 (c) shows the cracking pattern in the repair patch of material L3(L). Cracking was monitored approximately 2 months after application of the repair material. Two cracks were evident in the repair patch, which had a crack width of less than 0.1mm [Figure 9.25 (c)].

9.3.3.1.2 *Substrate concrete stiffer than repair material*

The elastic modulus of material G6(L) was approximately half that of the substrate concrete (Table 9.11). Data for the beam repaired with G6(L) are plotted in Figure 9.26. The free shrinkage and creep of this material are given in Table 9.12. Both properties are very high relative to other repair materials (see Table 9.10). In the early weeks immediately after the application of the repair patch (weeks 0 to 5), gauges "RM 2" and "RM 3" (Figure 9.26) show increasing compressive strains due to shrinkage in the repair material. The compressive strain is lowest in "RM 1" compared to "RM 2" and "RM 3" since it is adjacent to the substrate concrete which restrains the shrinkage through interfacial bond (see Figure 9.26). The restraint due to interfacial bond decreases as the distance from the interface increases. The shrinkage strains measured at "RM2" and "RM3" are much higher than the corresponding values recorded in

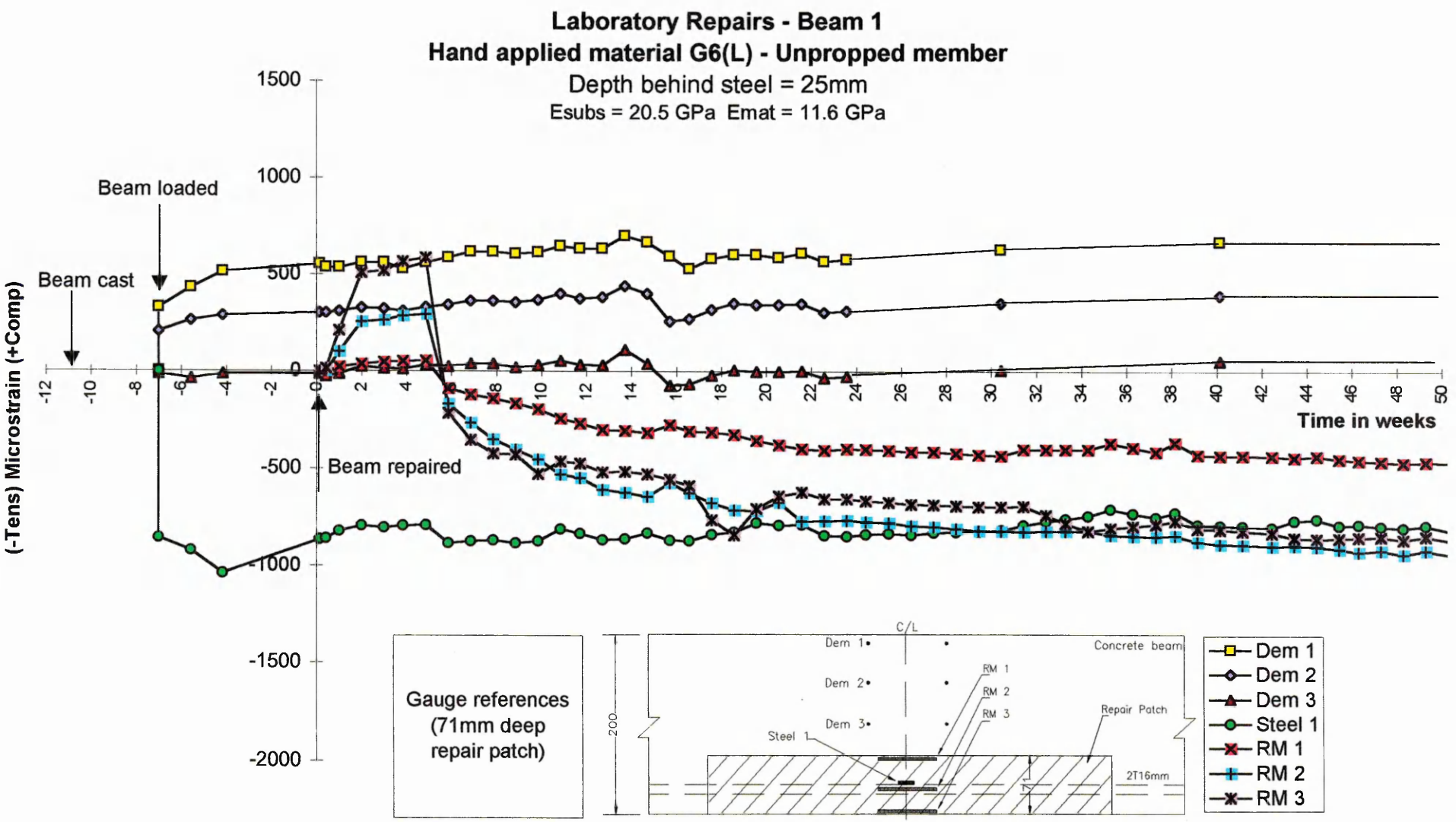

Figure 9.26 Strain distribution in beam 1 repaired with material G6(L) in the laboratory (Unpropped flexural member)

Table 9.11 Elastic modulus of substrate concrete and repair materials represented in Figure 9.26

Beam	*Material*	*Elastic Modulus (kN/mm^2)*
1	substrate	20.5†
1	G6(L)	11.5

† Does not take into account the effects of creep in the pre-loaded substrate concrete

materials G4(L) and L3(L) (Figures 9.23 and 9.24). This is due to the greater free shrinkage of material G6(L) (1100 microstrain) compared with 401 microstrain and 710 microstrain for materials G4(L) and L3(L) respectively. The virtual tensile strain in the repair material at this stage will be the free shrinkage of the repair material (1100 microstrain) minus the strain reading in the gauges ("RM 1", "RM 2" or "RM 3"). As material G6(L) has a relatively high creep (Table 9.12), tensile stress relaxation will occur due to tensile creep in the repair material. This contributed towards alleviating the tensile stress in the repair patch between week 0 to week 5. At week 5, the compressive strains abruptly change to tensile (see "RM 1", "RM 2" and "RM 3", Figure 9.26). This is due to cracking occurring in the material, as the virtual tensile strain due to shrinkage restraint has obviously exceeded the tensile strain capacity of the repair material. The cracking pattern in this repair material is shown in Figure 9.25 (d).

Table 9.12 Free shrinkage* and creep strains of materials represented in Figure 9.26

Material	*100 day free shrinkage (μstrain) (stored at 20°C, 55%RH)*	*70 day compressive creep (μstrain) (30% stress/strength)*
G6(L)	1100	1188
G3 (Reference)	717	938

*Note: * indicates that a correction for volume/surface ratio has not been applied*

Three cracks were evident in the repair patch due to a combination of low stiffness (which will increase the level of restraint by the substrate concrete) and high shrinkage. These cracks were less than 0.1mm in width.

The strain in the steel reinforcement (see "Steel 1", Figure 9.26) remains virtually constant from the time of repair, as the low stiffness and cracked repair material is unable to transfer stress from the steel reinforcement. The strain gauges on the substrate concrete ("Dem 1", "Dem 2" and "Dem 3") remain relatively constant throughout, except for some variation between weeks 14 to 18, again due to the operational fault in the controlled environment which affected the surface strains. This is similar to the distribution of strain in materials G4(L) and L3(L) (Figures 9.23 and 9.24), where distribution of strain in the tension zone had a negligible effect on the strain in the compression zone. It can be concluded that repair materials with low elastic modulus would be unsuitable for concrete repair, since the repair material is unable to attract load from the steel reinforcement in a similar manner to a stiffer repair material (compare "Steel 1" in Figure 9.26 with "Steel 1" in Figures 9.23 and 9.25). Furthermore, the restraint provided by the stiffer substrate concrete will inevitably cause cracking in the repair material. The very high shrinkage strains will aggravate the cracking. This will result in even more insignificant transfer of strain from the steel reinforcement to the repair patch, hence the repair patch would be non-load sharing.

9.3.3.2 Hand applied repair patches extending 50mm behind steel reinforcement

9.3.3.2.1 Repair material stiffer than substrate concrete

When the depth of repair material is increased to 50mm behind the steel reinforcement for material L3(L) (beam 8), as shown in Figure 9.27, the effect on performance is similar to that of 25mm behind the steel reinforcement, as shown in Figure 9.24. Material L3(L) properties are given in Tables 9.9 and 9.10. "RM 1" at the repair material/substrate concrete interface goes into tension immediately after the application of the repair material (Figure 9.27). "RM 2" and "RM 3" show slight expansion in the early stages (see Figure 9.27) as the effect of the interfacial restraint is less at these locations than at "RM 1". The strain in the repair material ("RM 2" and "RM 3", Figure 9.27) changes from compression to tension over a 6 week period (week 2 to 8, Figure 9.27). Although a gradual change takes place from compression to tension within weeks 2 to 8, Figure 9.27, as opposed to the sudden change which occurred in Figure 9.24, nevertheless, cracking occurred. The cracking pattern is shown in Figure 9.25 (e). Two cracks are evident in this repair material, similar to the cracking which was observed in the same material when the depth of repair material behind the steel reinforcement was 25mm [see Figure 9.25 (c)]. The crack widths were less than 0.1mm. The strain in the steel reinforcement decreases slightly over the monitoring period (week 0 to week 50, Figure 9.27), similar to the decrease in strain in when the depth behind the steel reinforcement is 25mm (see Figure 9.24). The strain in the substrate concrete ("Dem 1", "Dem 2" and "Dem 3") remain relatively constant throughout, again similar to the distribution of strain in the substrate concretes in Figures 9.23, 9.24 and 9.26). This again indicates that the distribution in the tension zone has a negligible effect on

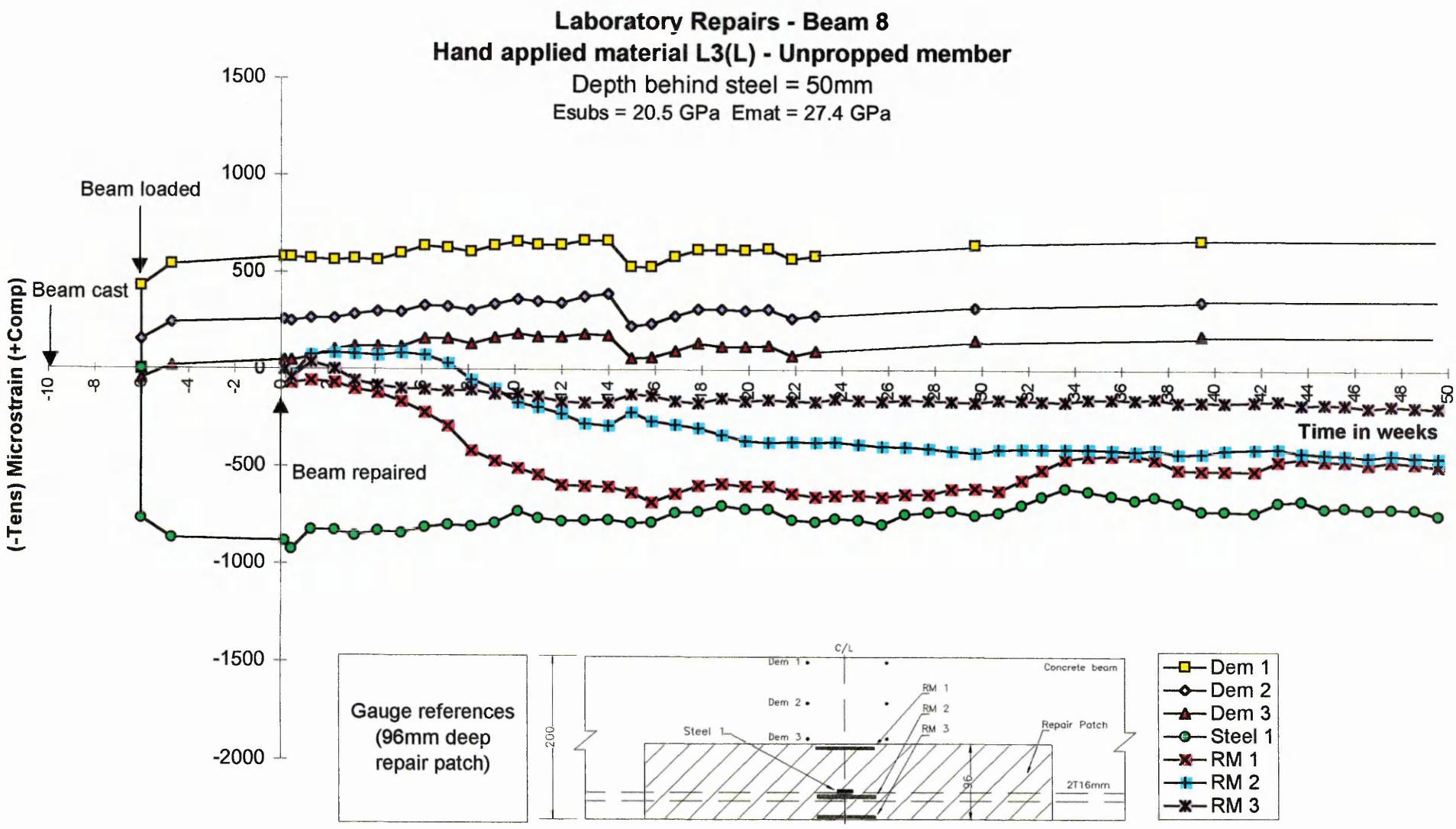

Figure 9.27 Strain distribution in beam 8 repaired with material L3(L) in the laboratory (Unpropped flexural member)

the strain in the compression zone. Overall, the long term performance of material L3(L), with a depth of 50mm behind the steel reinforcement, is similar to the performance when the depth is 25mm behind the steel (compare Figure 9.27 with Figure 9.24) Therefore, increasing the depth of repair does not influence the performance of the repair. In fact, a deeper repair will be uneconomical due to an increase in concrete removal time and an increase in the cost of the repair material.

9.3.4 Repairs to propped flexural members

9.3.4.1 Hand applied repair patches extending 25mm behind steel reinforcement

9.3.4.1.1 Repair material stiffer than substrate concrete

Repairs to propped flexural members were carried out both in the field (Sutherland Street Bridge) and in the laboratory. The laboratory repairs consisted of beam specimens as described in previous sections. Two generic repair materials L3(L) and G5(L) were applied to simulated deteriorated reinforced concrete beams in the laboratory. The reinforced concrete beams were loaded for approximately 9 weeks prior to application of repair in order to eliminate the effects of creep in the substrate concrete. The load was removed during application of the repair material. When the cube strength of the repair material reached the design strength of the beam, or the repair was cured for 28 days, whichever was sooner, the load was reapplied. The results of one of these repairs is given in Figure 9.28. The field repairs consisted of repairs to propped reinforced concrete beams. The results from two of the repairs are presented in

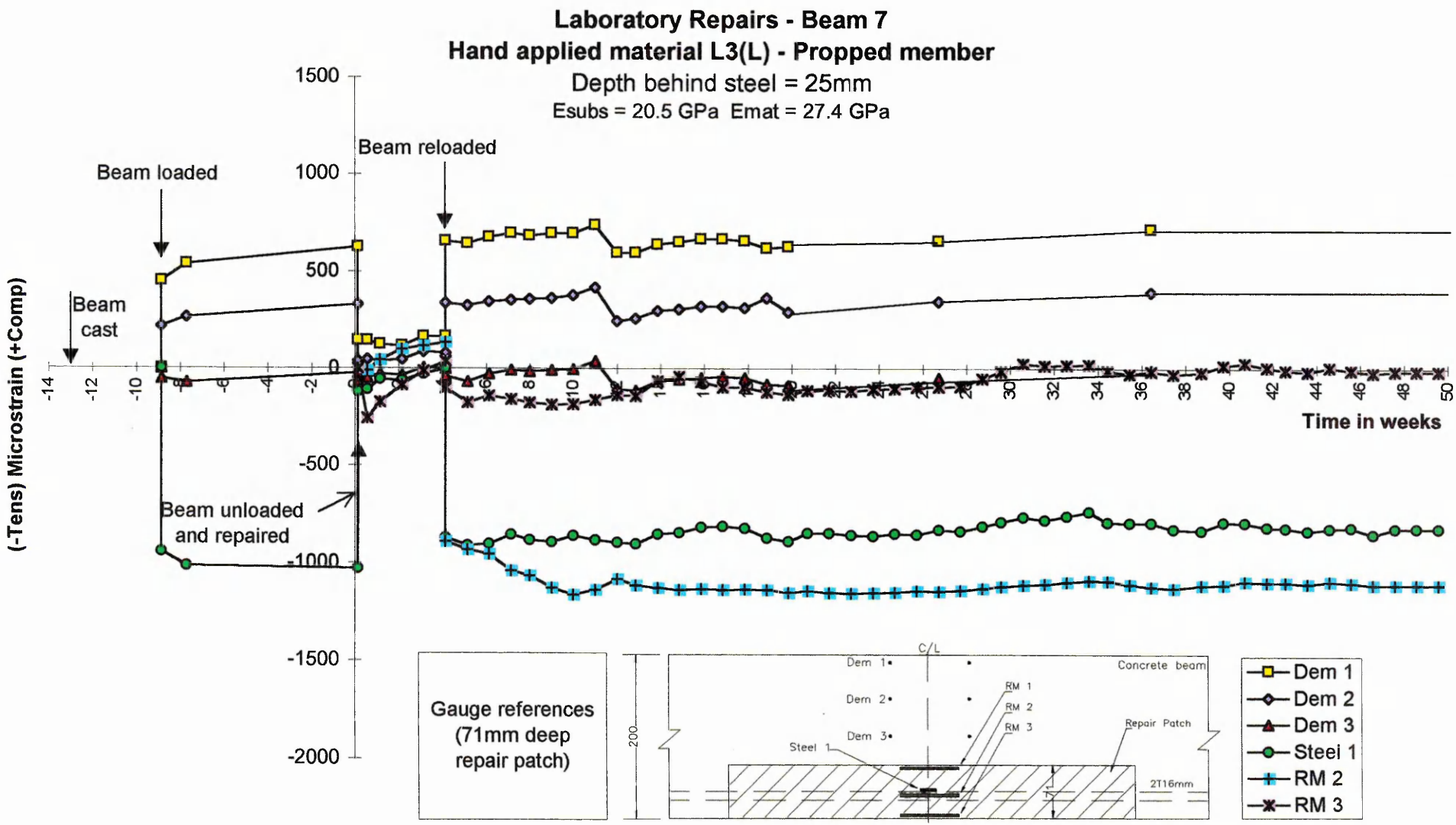

Figure 9.28 Strain distribution in beam 7 repaired with material L3(L) in the laboratory (Propped flexural member)

this section (materials S1 and S4, Figures 9.29 and 9.30). The load was removed from the members during application of the repair materials. When the cube strength of the repair materials reached the design strength of the bridge, the external load was reapplied to the member by removing the propping.

9.3.4.1.1.1 *Laboratory repairs*

The strain versus time graphs of the beam repaired with material L3(L) in the laboratory are plotted in Figure 9.28. Datum readings were taken 24 hours after the application of the repair patch (represented as week 0 in Figure 9.28). Residual strains in the substrate concrete and steel reinforcement were present at week 0, as the beam had been loaded at approximately week -9 to eliminate the effects of creep in the substrate concrete (see Figure 9.28). The beams were cured for 4 weeks prior to loading, shown as approximately weeks -9 to -13 in Figure 9.28. Strain readings after the application of the repair patch in Figure 9.28 are plotted at weekly intervals, except for the demec gauge readings after approximately week 20 being plotted more intermittently

The difference in elastic modulus between the stiffer repair material L3(L) and the substrate concrete is given in Table 9.9. The free shrinkage and creep of the material is given in Table 9.10. Referring to Figure 9.28, the beam is loaded at week -9 and remains under load for approximately 9 weeks. Upon propping at week 0, it can be seen that compressive strain remain in the substrate concrete ("Dem 1" and "Dem 2" in Figure 9.28, weeks 0 to 4) due to the effects of creep in the substrate concrete. A small tensile strain is also evident in the steel reinforcement at week 0, but this decreases towards 0 at week 4 as shrinkage strain is transferred to the steel reinforcement whilst

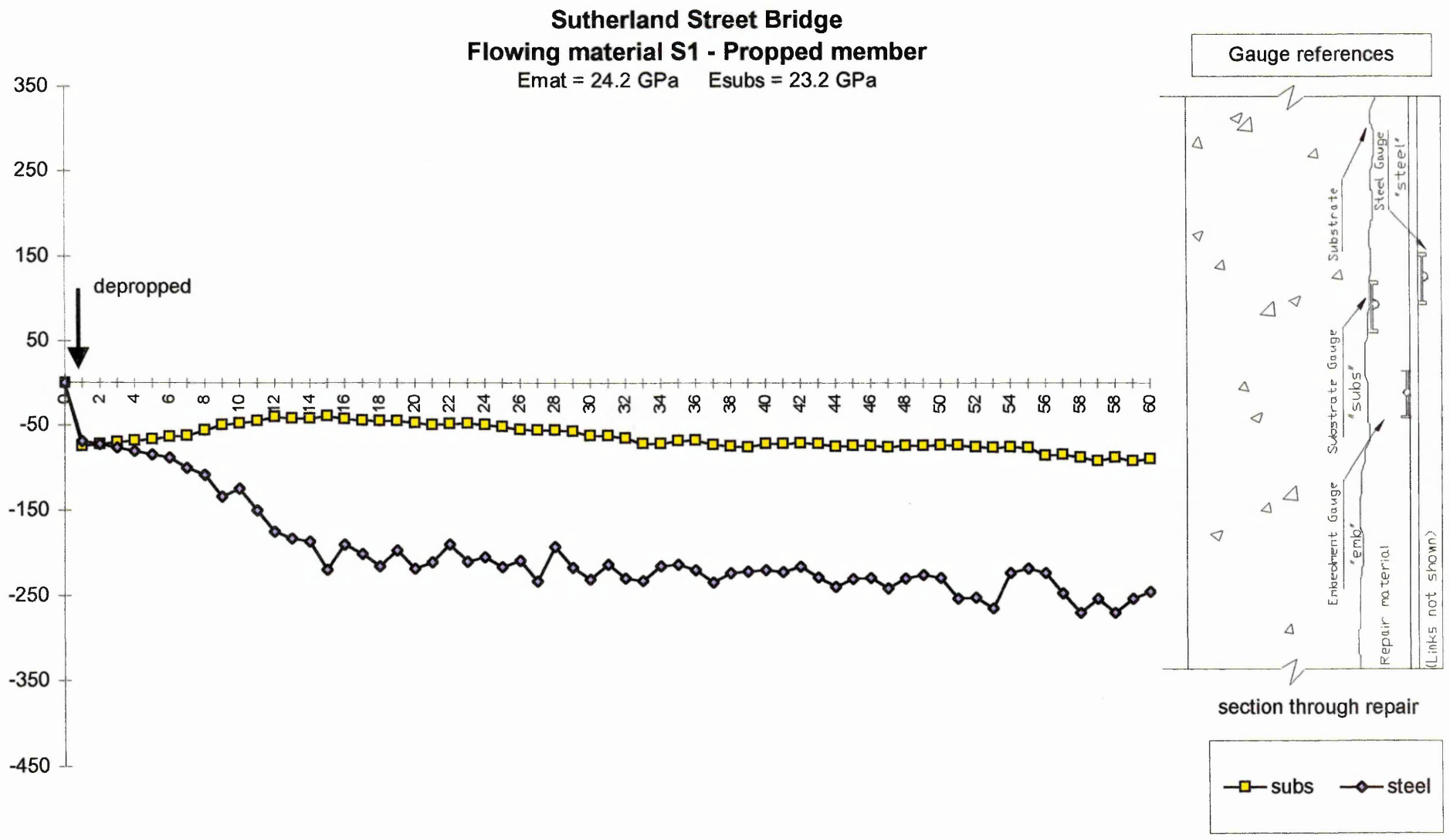

Figure 9.29 Strain distribution in repair patch of material S1 at Sutherland Street Bridge (Propped flexural member)

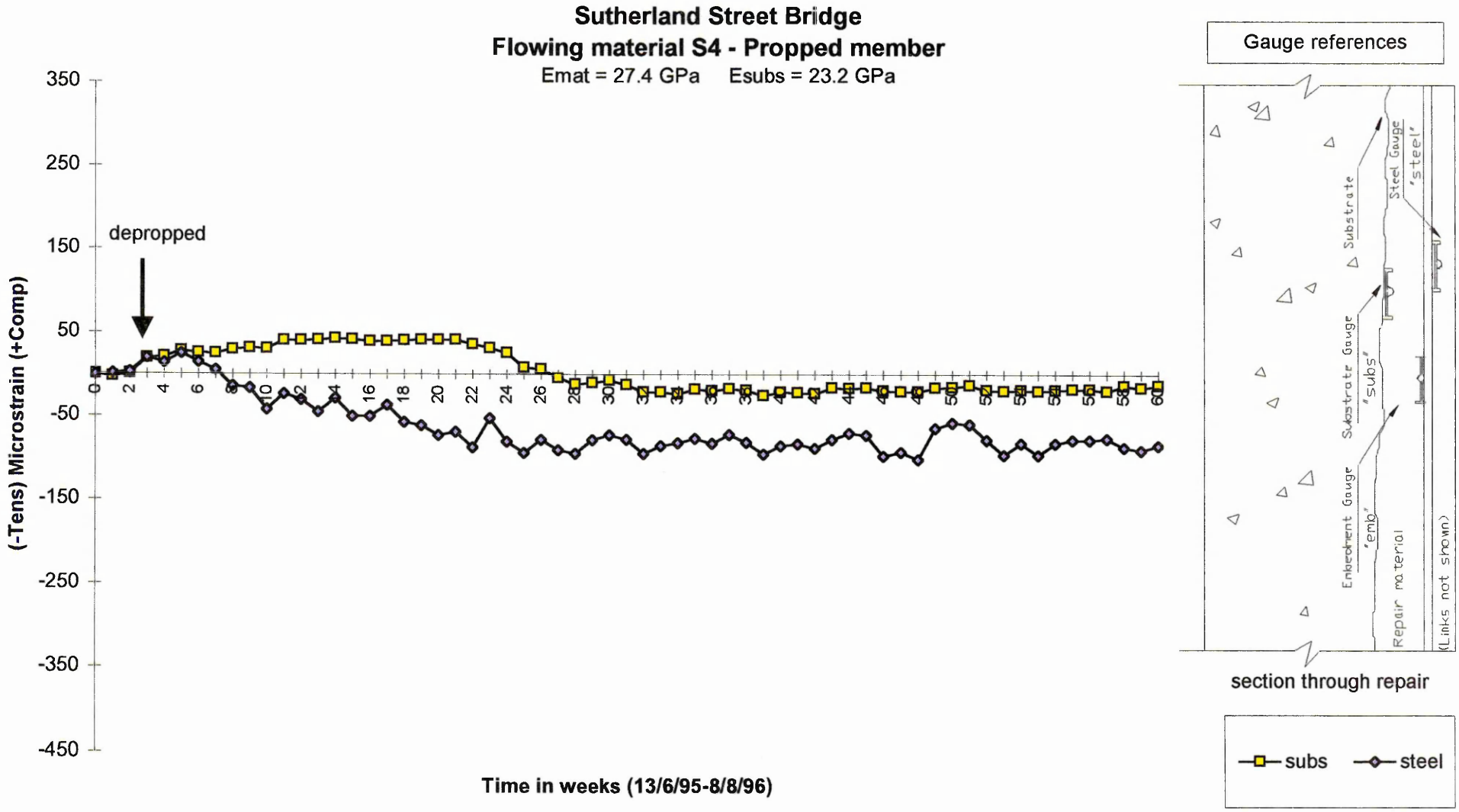

Figure 9.30 Strain distribution in repair patch of material S4 at Sutherland Street Bridge (Propped flexural member)

the beam remains in an unpropped state. In the first week after application of the repair material, a tensile strain is evident in "RM3", possibly due to removal of the shuttering at approximately 3 days after application. This strain decreases towards 0 at week 4 due to shrinkage in the repair material. Upon reapplication of the load at week 4, "Dem 1" and "Dem 2" show high compressive strains in the compressive zone. "Dem 3" is obviously near the neutral axis since a negligible strain is evident in this part of the beam. "Dem 1", "Dem 2" and "Dem 3" all remain relatively constant for the remainder of the monitoring period (Figure 9.28). Tensile strain is induced in the steel reinforcement ("Steel 1") and "RM2" and "RM3" upon reloading ("RM 1" is excluded from Figure 9.28 due to suspected damage in the gauge). These strains, again, remain relatively constant throughout the remainder of the monitoring period. Very little redistribution of strain took place in this repair patch as indicated by the almost constant strains in the steel reinforcement ("Steel 1") and repair material ("RM 2" and "RM 3") in Figures 9.28, weeks 4 to week 50. The reason for the limited redistribution of strain was due to the fact that severe cracking occurred in the repair material during the reloading operation at week 4 (sudden large tensile strain in "RM 3", Figure 9.28). The maximum bending stress was 15 N/mm^2, obtained from transforming the section to an equivalent concrete section and applying the theory of simple bending to obtain the stress. The applied stress was much greater than the flexural strength of the repair material of 7 N/mm^2 at 28 days, obtained from the manufacturers' literature. The cracking pattern in this repair patch is shown in Figure 9.25 (f). This repair patch exhibited the worst cracking of the repair materials under test, but the cracking was mainly due to reapplication of the load after repair. Some of the crack widths were greater than 0.1 mm. Comparing the performance of this repair patch with the

performance of a similar repair patch applied to an unpropped member (Figure 9.24), it is clear that removal of the load during application of the repair material and subsequent reloading greatly increases the tensile strains in the repair patch (compare "RM2" in Figure 9.24 with "RM2" in Figure 9.28). The cracking in material L3(L) applied to an unpropped member [Figure 9.25 (c)] is less than the cracking in material L3(L) applied to a propped member [Figure 9.25 (f)]. Therefore, in this instance, the poor performance of the repair material was attributed to the effects of propping during repair rather than mismatch of material properties.

9.3.4.1.1.2 Field repairs

The strain versus time graph for materials S1 and S4 are presented in Figures 9.29 and 9.30. Only two strain gauges were installed in the repair patch of these materials due to limitations on the data logger. One gauge was attached to the cut back substrate, labelled "subs" in Figures 9.29 and 9.30, and one gauge was attached to the steel reinforcement, labelled "steel" in Figures 9.29 and 9.30. Datum readings were taken 24 hours after the application of the repair patch (origin on the graphs).

Referring to Figure 9.29, material S1, the member was depropped at week 1. This induces instantaneous tensile strains in the substrate concrete and steel reinforcement (approximately 75 microstrain) at depropping. The strain in the substrate concrete decreases to approximately 40 microstrain in tension at week 12 (Figure 9.29). From week 12 onwards, the strain in the substrate concrete shows a negligible increase in tension (approximately 20 microstrain) to the end of the monitoring period (week 60).

After depropping, the strain in the steel reinforcement rapidly increases to approximately 220 microstrain in tension at week 18 (Figure 9.29). From week 18 onwards, the strain in the steel reinforcement remains relatively constant until the end of the monitoring period. The strain versus time graph material S4 is given in Figure 9.30. There are negligible strains in the substrate concrete and steel reinforcement in weeks 0 to 2, Figure 9.30. Upon depropping at week 3, the strains in the substrate concrete and steel reinforcement increase to approximately 25 microstrain in compression. The strain in the substrate concrete increases slowly to reach approximately 45 microstrain at week 21. Thereafter, the strain in the substrate concrete decreases over the next 7 weeks to reach a tensile strain of approximately 10 microstrain in tension at week 28. From week 28 onwards, the strain in the substrate concrete remain relatively constant. Meanwhile, the strain in the steel reinforcement shows a slight increase in compression until week 5 (Figure 9.30). From week 5 onwards, the strain rapidly decreases to reach a tensile strain of approximately 90 microstrain at week 28. Thereafter, the strain in the steel reinforcement remains relatively constant until the end of the monitoring period.

Referring to Figure 9.29, it is obvious that tension is induced into the steel reinforcement and substrate concrete due to a combination of removing the shuttering (day 3) and depropping the member. The strain then decreases in tension in the substrate concrete as the slightly stiffer repair material (see Table 9.7) transfers some shrinkage strain to the substrate concrete (the free shrinkage of the repair material is given in Table 9.8). Since the repair material is only marginally stiffer than the substrate concrete, the restraint provided by the substrate concrete will be high and therefore, virtual tensile strain will be evident in the repair material at the interface with the substrate concrete will also be high. On the other hand, the strain in the steel

reinforcement increases rapidly until week 18. This is because cracking occurs in the repair patch at the steel reinforcement level due to two reasons: (i) there is a high restraint to shrinkage provided by the much stiffer steel reinforcement. It has been observed in many instances in the project that the degree of restraint is much higher at the steel reinforcement level than at the substrate concrete interface and (ii), the externally applied load at depropping induces tension in the repair patch. Consequently, the steel reinforcement has to take more of the applied load as the repair material cracks in the tension zone. The cracking pattern in this repair patch is given in Figure 9.31 (a) and (b). Figure 9.31 (a) shows an elevation of the south frame (south face) and the position of the repair patches on the frame. An enlarged view of the soffit of the beam is shown in Figure 9.31 (b) showing the cracking patterns in the repair patch. The cracking pattern consists of predominantly equally spaced cracks except for minor irregularities around the protective steel covering. The cracks around the protective covers are due to the localised restraint to shrinkage provided by the bolts of the steel covers. Overall, the regular cracking in material S1 at Sutherland Street Bridge is similar to the fairly regular cracking patterns observed in material L4 (Figure 9.7) and material L1 (9.14). It has been observed that the cracking pattern will be regular when the properties of the repair material are insufficient to offset cracking. For example, the tensile strength of repair material S1 was obviously less than the tensile stress applied in the repair patch. The tensile stress will consist of stress due to the restraint due to shrinkage and stress due to the applied load. When material S1 was applied to a propped member in compression (Figure 9.18), cracking was absent in the repair patch [see Figure 9.22 (b)]. It is therefore evident that material S1 cracked when applied to a propped member in flexure due to a combination of tensile stress induced due to

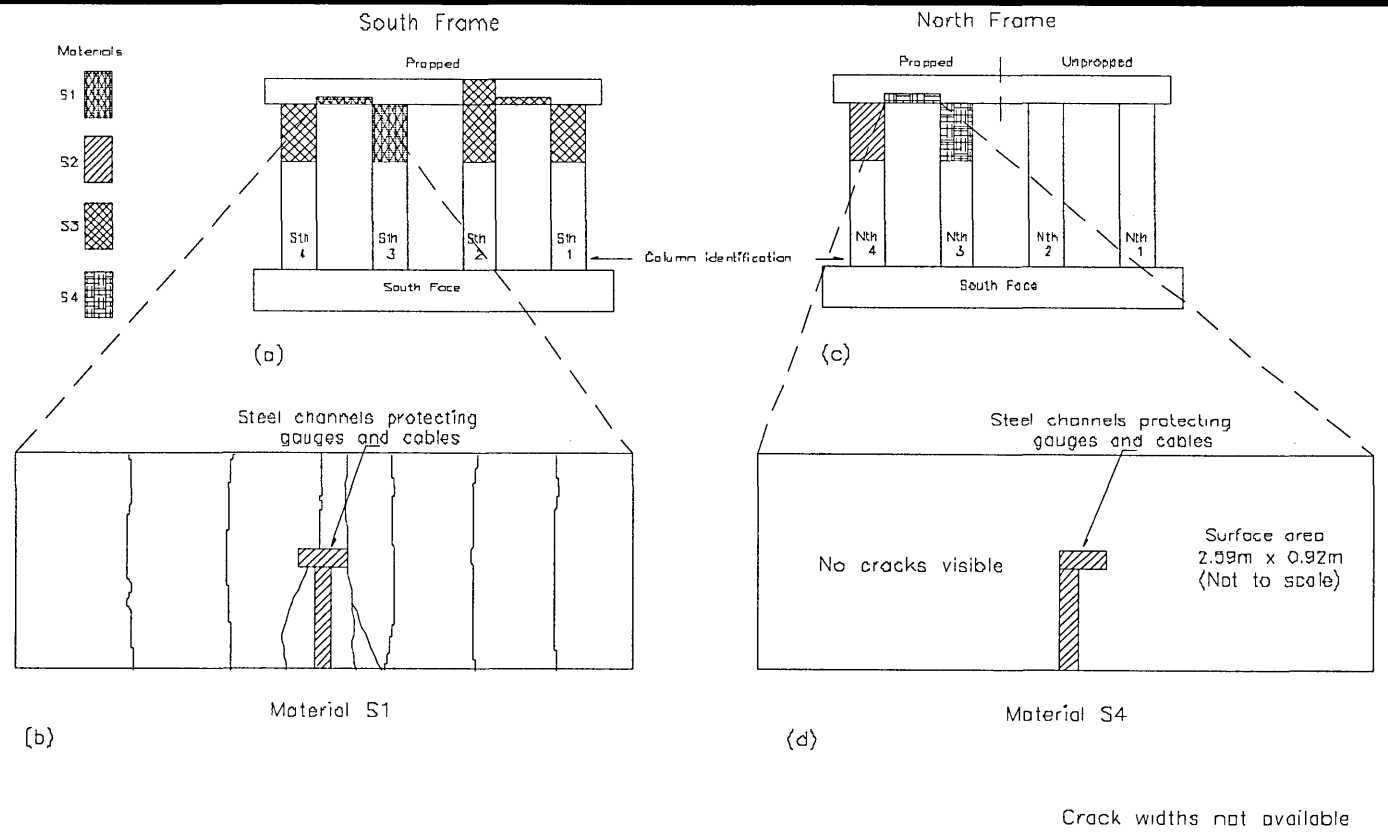

Figure 9.31 Cracking patterns in soffit repairs at Sutherland Street Bridge
(a) Elevation of south frame (south face) (b) Material S1
(c) Elevation of north frame (north face) (d) Material S4
Method of repair: flowing Support during repair unpropped
Properties: repair material stiffer than substrate concrete

external loading and tensile stress induced due to the restraint to shrinkage provided by the steel reinforcement. From week 18 onwards, there is very little redistribution of strain taking place since the load has already been applied to the repair patch and this contributed to cracks occurring in the repair material (Figure 9.29).

Referring to Figure 9.30, the strains in the substrate concrete and steel reinforcement remain relatively stable between weeks 0 and 2. Possible tensile strains that occurred due to removal of the shuttering could have been neutralised by the stiffer repair material (Table 9.7) transferring shrinkage strain (Table 9.8) to the substrate concrete. Depropping the member inexplicably increases the strain in both the substrate concrete and steel reinforcement at week 3. From week 3 until week 21, the strain in the substrate concrete increases due to transfer of shrinkage strain from the stiffer repair material. On the other hand, the strain in the steel reinforcement increases in tension over the same period as presumably more load is being taken by the steel reinforcement. The increase in strain in the steel reinforcement in material S4 is not as sudden as the increase in strain in material S1 as the repair material remains uncracked [as shown in Figure 9.31 (c) to (d)]. Figure 9.31 (c) shows the elevation of the north frame (south face) and the position of the repair patches on the frame. Figure 9.31 (d) shows an enlarged view of the soffit of the repair patch. No cracks are evident. When material S4 was applied to a propped member in compression (Figure 9.21), a similar crack-free repair patch was evident [Figure 9.22 (e)]. Therefore, since the elastic modulus of repair material S4 was greater than the elastic modulus of repair material S1 (Table 9.7), plus the fact that material S4 exhibited lower shrinkage than material S1 (Figure 9.8), the virtual tensile strain in material S4 due to the restraint to shrinkage provided by the

substrate concrete was less than that induced in material S1. Therefore, the tensile strain capacity of the repair material was not reached, and consequently, a further increase in tensile strain due to external loading was not sufficient to cause cracking in the repair material (even though the long term modulus of rupture of material S4 (4.3 N/mm^2, Figure 8.23) was less than the long term modulus of rupture of material S1 (6.5 N/mm^2, Figure 8.23). From approximately week 21 onwards, little redistribution of strain takes place, as was commonly observed in repair patches of flow applied materials, whether cracked or uncracked.

9.4 FURTHER DISCUSSION

9.4.1 Influence of material properties on long term performance

The results of the field and laboratory repairs presented in this chapter indicate that the basic material properties elastic modulus, shrinkage and creep of the repair materials have an enormous effect on the in-service performance of concrete repair. Compressive strength is relatively unimportant. Flexural strength in itself is of secondary importance but the relationship with the tensile strain capacity of a repair material will be of great significance.

General requirements for repair materials as given by Emberson and Mays [25] are listed in Table 9.13. It is stated that the elastic modulus of the repair materials should be similar to the elastic modulus of the substrate concrete. Other researchers have also

Table 9.13 General requirements of patch repair materials for structural compatibility [25]

Property	*Relationship of repair mortar (R) to concrete substrate (C)*
Strength in compression, tension and flexure	R >C
Modulus in compression, tension and flexure	R ~ C
Poisson's ratio	Dependent on modulus and type of repair
Coefficient of thermal expansion	R ~ C
Adhesion in tension and shear	R > C
Curing and long term shrinkage	R < C
Strain Capacity	R > C
Creep	Dependent on whether creep causes desirable or undesirable effects
Fatigue performance	R > C

stated this in the past [31, 96]. Findings of this research, however, show that if the elastic modulus of the repair material is similar to that of the substrate concrete, the repair material is unable to transfer shrinkage strains to the substrate concrete. This will induce relatively high tensile stress in the material since the substrate concrete will provide a fuller restraint to shrinkage. Cracking may occur in the repair material as a result. Therefore, the elastic modulus of the repair material should be greater than the elastic modulus of the substrate concrete to allow more distribution of shrinkage strain to the substrate concrete. However, the effect of applying a repair material with a relatively low elastic modulii becomes less pronounced if a repair material is specified with low shrinkage. Consequently, the possibility of cracking is decreased.

Table 9.13 [25] also states that the long term shrinkage of the repair material should be less than the long term shrinkage of the substrate concrete (i.e. R<C). Similarly, the creep of the repair material is also related to the creep of the substrate concrete. Based on the fact that the substrate concrete in the field will be much older than the repair material (the substrate concrete at Gunthorpe Bridge in the current project was 67 years in service at the time of repair), the substrate concrete will be dimensionally stable (i.e. shrinkage and creep will be insignificant). Therefore, it is impossible to have the shrinkage of the repair material less than the shrinkage of the substrate concrete. Likewise, since the substrate concrete is stressed for a long period of time due to external loading, creep in the substrate concrete will have reached negligible levels. On the other hand, the repair material will still have to undergo creep, especially in the shrinkage stage (Figure 9.8, Zone 1) as tensile stress is induced in the repair material due to the restraint to shrinkage provided by the substrate concrete.

9.4.1.1 Compression members

When repairs are carried out on deteriorated reinforced concrete members, the aim of the repair is to restore the structural integrity of the member and provide a durable repair which will protect the steel reinforcement from further corrosion. Selecting a repair material in conjunction with the recommendations given in this thesis will provide such a repair. Normally, the cross-sectional area of a repair patch is insignificant to the cross-sectional of the repaired member, especially in compression members. Therefore, regardless of whether or not the repair patch is load sharing, the reinforced concrete member will still continue to function in-service. This was obviously the case for

unpropped repairs in the current project. The bridges remained in service whilst the repairs were carried out, hence the cross-sectional area lost when the deteriorated concrete was removed did not substantially affect the in-service performance of the member during repair. Therefore, since the repair patch has insignificant load sharing responsibilities compared with the overall load carrying capacity of the original member, it could be argued that the most important criterion of a repair patch is to protect the steel reinforcement from further corrosion (i.e. become a durable repair). It is, therefore, important that the repair material remains crack free. In order to limit the tensile stress due to shrinkage restraint, it is obvious that the free shrinkage in the repair material should be as low as possible, as restraint provided by the substrate concrete will induce tensile stress in the repair patch. A very low tensile stress is unlikely to cause cracking in the repair patch. If cracking in the repair patch is absent, then it is likely that durability will be satisfied. The results of the current project found that the magnitude of shrinkage in repair materials is likely to induce enough tensile stress to cause cracking, irrespective of the manufacturers' claims that the repair materials had low shrinkage or were shrinkage compensated. Therefore, relying on the shrinkage characteristics of the repair material to be low is not enough to ensure good durability. It was observed in the current project that a portion of the shrinkage strain is transferred to the substrate concrete when the elastic modulus of the repair material was greater than the elastic modulus of the substrate concrete (spray applied materials L4, L2, L3 and G1, Figures 9.2 to 9.5 respectively; flow applied materials S1-S4, Figures 9.15, 9.16, 9.18 to 9.21). Consequently, this reduced the tensile stress in the repair material which attributed to crack free repair materials in many instances. Creep, on the other hand, proved to be beneficial when the tensile stress in the repair material was high,

since tensile creep reduced the tensile stress through stress relaxation (materials G2 and G3, Figures 9.9, 9.10). On the other hand, creep also lowered the elastic modulus of the repair material, therefore the advantage of having a repair material with a high elastic modulus was lost. Overall, if the shrinkage in the repair material is low and the elastic modulus of the repair material is high, then tensile stress in the repair material will be of an insignificant magnitude such that stress relaxation is not required. Therefore, in this instance, high creep characteristics are definitely a disadvantage since they would reduce the elastic modulus. It was also observed that the spray applied materials L4, L2 and L3 (Figures 9.2 to 9.4) which were stiffer than the substrate concrete attracted external applied stress into the repair patch. This not only made the repair patch load sharing, but also served to reduce or neutralise the tensile stress that remained in the repair patch due to the restraint to shrinkage provided by the substrate concrete. Hence, when specifying a durable and load sharing repair patch, the repair material should exhibit low shrinkage, high elastic modulus and low creep.

9.4.1.2 Flexural members

Repair of a flexural member with a repair material that has a high elastic modulus allows more redistribution of externally applied stress to the repair material. The stress due to external load in the steel reinforcement reduced with time whereas the stress in the repair patch increased over the same time period. Thus, assuming that the repair material remains uncracked, the steel reinforcement is able to redistribute load to the repair material. This is clearly evident in repair material G4(L) (Figure 9.23), where the stiffness of the repair material is substantially greater than the stiffness of the

substrate concrete. Tensile stress in the repair material due to shrinkage restraint was also low since the free shrinkage in the material was relatively low. This contributed enormously to the performance of the repair, as cracking due to restrained shrinkage stress was absent, so redistribution of strain was able to occur resulting in effective load sharing by the repair.

It was obvious in both the laboratory and field repairs that the repairs to propped flexural members have the highest risk of cracking due to the tensile stresses induced upon depropping. Material L3(L) cracked upon reapplication of the external load (depropped) in the laboratory. Material S1 at Sutherland Street Bridge cracked due to a combination of tensile stress induced by shrinkage restraint and tensile stress induced by reapplication of external load on depropping. Therefore, it is better for long term performance, that flexural repairs are carried out on unpropped members, assuming of course that the unpropped members can safely continue to perform in service whilst the repair materials are being applied.

9.5 CONCLUSIONS

The following conclusions are based on the results of the in-service monitoring carried out on repairs which were applied in the field and in the laboratory:

General

- Recommendations given in the current repair specification, BD 27/86, are not suitable for all concrete repairs. The specification does not adequately take into

account the potential mismatch in key properties which may occur between the repair material and substrate concrete. It also gives emphasis to some properties of repair materials which are of secondary importance.

- The long term performance of a repair is superior when the repair is applied to an unpropped member as opposed to a propped member.
- The risk of cracking in the repair patch is greatly increased when the repair material is applied to a propped flexural member.
- Spray applied repair materials to unpropped members perform better than flowing repair materials applied to unpropped members.
- Four stages of distribution of strain (and consequently stress) are evident in spray applied repairs to unpropped compression members:

  (i) shrinkage stage (weeks 0 to 11)

  (ii) steady state #1 (weeks 11 to 25)

  (iii) external load transfer (weeks 25 to 47)

  (iv) steady state #2 (weeks 47 to 60)

- Increasing the depth of repair behind the steel reinforcement in repairs to flexural members does not significantly influence the performance of the repair.

Properties of materials

- The elastic modulus is a vitally important property to be considered when selecting a repair material for concrete repairs. The elastic modulus of the repair material should be greater than the elastic modulus of the substrate concrete.
- The possibility of cracking in the repair patch is greatly increased when the repair material exhibits high shrinkage.

- High creep repair materials exhibit stress relaxation when subjected to a tensile stress caused by restraint to shrinkage by the substrate concrete.
- If the elastic modulus of the repair material is greater than the elastic modulus of the substrate in a compression member repaired in the unpropped state, the stiffer repair is able to transfer shrinkage strain to the concrete substrate.
- A spray applied material of $E_{rm} > E_{sub}$, when applied to an unpropped member in compression, will attract externally applied load into the repair patch in the long term.
- A spray applied material of $E_{rm} < E_{sub}$, when applied to an unpropped member in compression, will not attract externally applied load into the repair patch in the long term.
- A flowing repair material of $E_{rm} > E_{sub}$, when applied to a propped member in compression, will not attract externally applied load into the repair patch.
- Repair materials for both flexural and compression members should have low shrinkage and creep characteristics.
- Cracking will occur in a repair material when the virtual tensile strain due to restraint to shrinkage is greater than the tensile strain capacity of the repair material (including creep effects).
- Repairs to flexural members carried out with high modulus materials ($E_{rm} > E_{sub}$) attract tensile load from the steel reinforcement.

CHAPTER 10

LONG TERM STRUCTURAL INTERACTION IN REPAIRED REINFORCED CONCRETE MEMBERS

10.1 INTRODUCTION

Deterioration of reinforced concrete structures is a problem that is demanding increasing attention world-wide. As a result, concrete repair has recently become the growth sector of the construction industry. Within that sector, the issue of durability has replaced concerns about strength as the most pressing problem [26], since a repair material must not only restore the structural integrity of the member, it must also serve as a durable barrier against the ingress of chlorides and carbon dioxide to arrest the deterioration of the steel reinforcement. To ensure that the repair system will function properly, a basic understanding of the interaction between the repair material and the concrete substrate must be known. This will allow repairs to be specified on scientific evidence rather than on the *ad hoc* approaches currently being used.

In order to be able to design a durable repair that will last indefinitely, it is important that the mechanics of concrete repair is fully understood. This involves having an adequate understanding of the interaction between the repair material and the concrete substrate. The basic repair material properties, such as elastic modulus, shrinkage and creep are primarily responsible for this interaction. It was determined in the

previous chapter that spray applied repair materials that have an elastic modulus greater than the elastic modulus of the substrate concrete ($E_{rm} > E_{sub}$) will perform satisfactorily in the long term when applied to unpropped members in compression. The aim of this chapter, therefore, is to relate the basic material properties to the performance of the spray applied repair materials under service loading. This will enable a prediction of the stress distribution within a repair patch to be determined.

10.2 RESULTS AND DISCUSSION

10.2.1 Spray applied repairs to unpropped compression members, $E_{rm} \geq E_{sub}$

It was observed in Chapter 9 that spray applied repair materials that have an elastic modulus greater than that of the substrate concrete perform better than spray applied repair materials that exhibit an elastic modulus that is less than that of the substrate concrete. This is because the stiffer repair material is able to transfer a portion of the shrinkage strain to the substrate concrete which helps to reduce the tension induced in the repair due to the shrinkage restraint provided by the substrate concrete and steel reinforcement. Consequently, this chapter concentrates on repair materials that have an elastic modulus greater than the elastic modulus of the substrate concrete. These are materials L2, L3 and L4 from Lawns Lane Bridge and material G1 from Gunthorpe Bridge.

10.2.1.1 Actual distribution of strain

Figures 10.1 to 10.4 show the actual distribution of strain, as obtained in field trials, in the repair patches of materials L4, L3, and L2 at Lawns Lane Bridge and material G1 at Gunthorpe Bridge. The strains in the repair patch were measured from the age of 24 hours after application of repair to 60 weeks, by means of vibrating wire strain gauges. These gauges were attached to the cut back substrate concrete (labelled "subs" in Figures 10.1 to 10.4), welded to the steel reinforcement ("steel") and embedded in the repair material ("emb"). Strain readings are plotted at weekly intervals. A detailed explanation of the distribution of strain in these repair materials was given in Chapter 9, Section 9.3.1.1.1.

10.2.1.2 Simplified distribution of strain

Figures 10.5 to 10.8 show simplified schematic distribution of strain for materials L4, L3, L2 and G1 respectively based on the actual distribution of strain in Figures 10.1 to 10.4. The repair material and steel reinforcement strains are averaged (due to strain compatibility) and are presented as one in Figures 10.5 to 10.8. The distribution of strains in Figures 10.5 to 10.8 are represented as a series of straight lines within four zones, namely shrinkage (Zone 1), steady state #1 (Zone 2), external load transfer (Zone 3) and steady state #2 (Zone 4). The cumulative strains for each zone obtained from Figures 10.5 to 10.8 are given in Table 10.1. Table 10.1 is divided into four Zones (as in Figures 10.5 to 10.8) and presents the cumulative strains at the end of each zone.

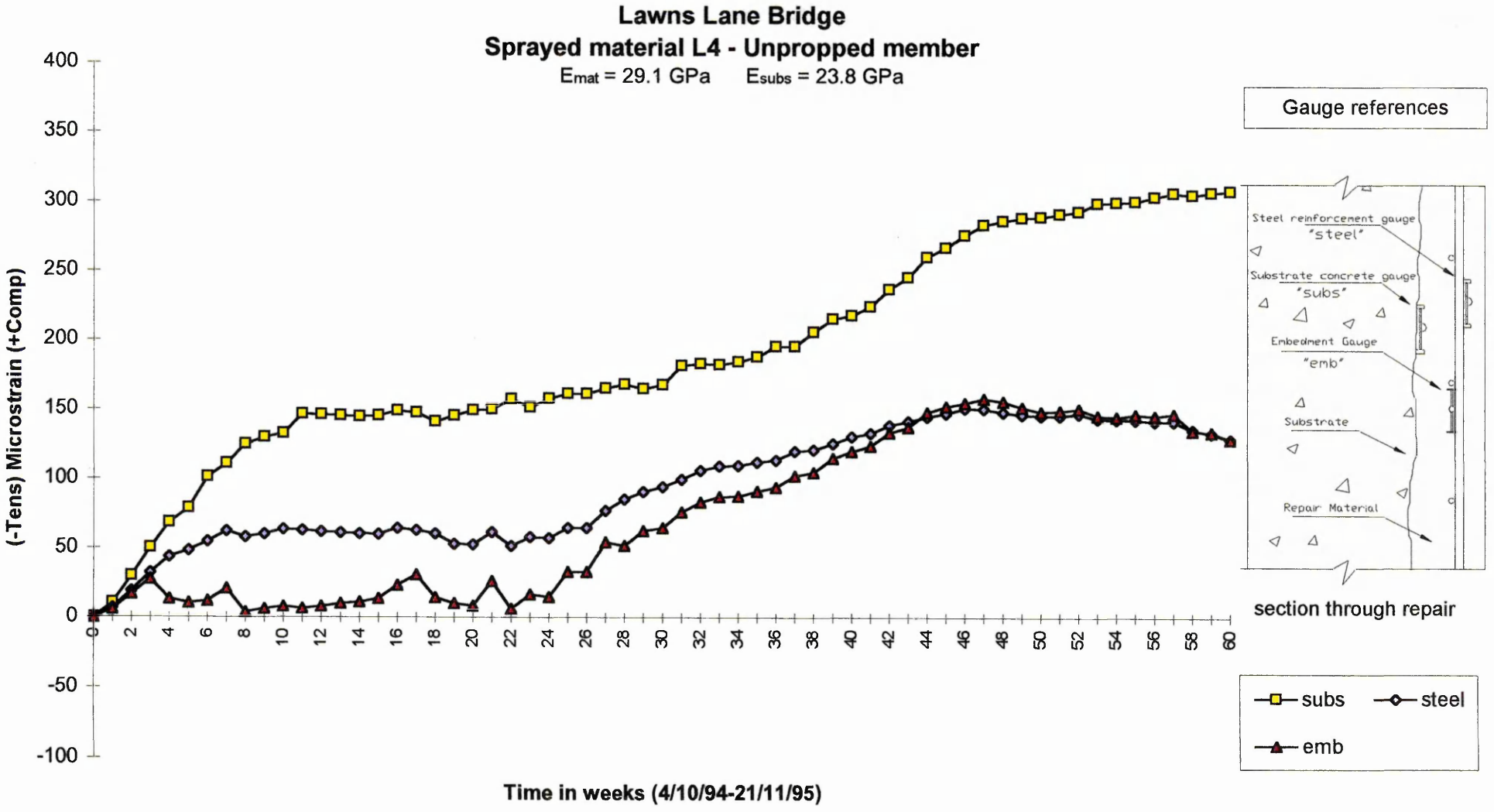

Figure 10.1 Strain distribution in repair patch of material L4 at Lawns Lane Bridge (Unpropped compression member)

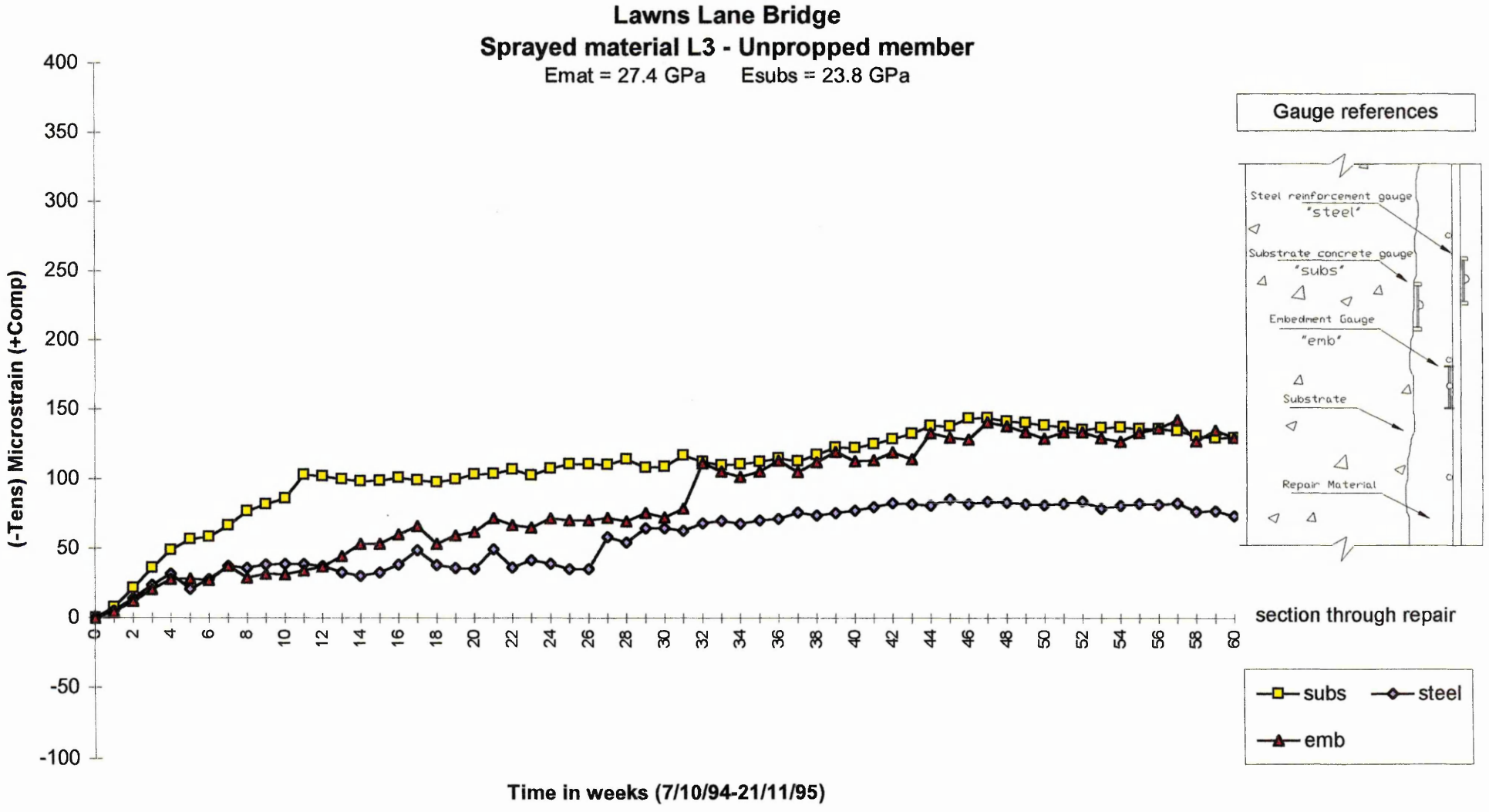

Figure 10.2 Strain distribution in repair patch of material L3 at Lawns Lane Bridge (Unpropped compression member)

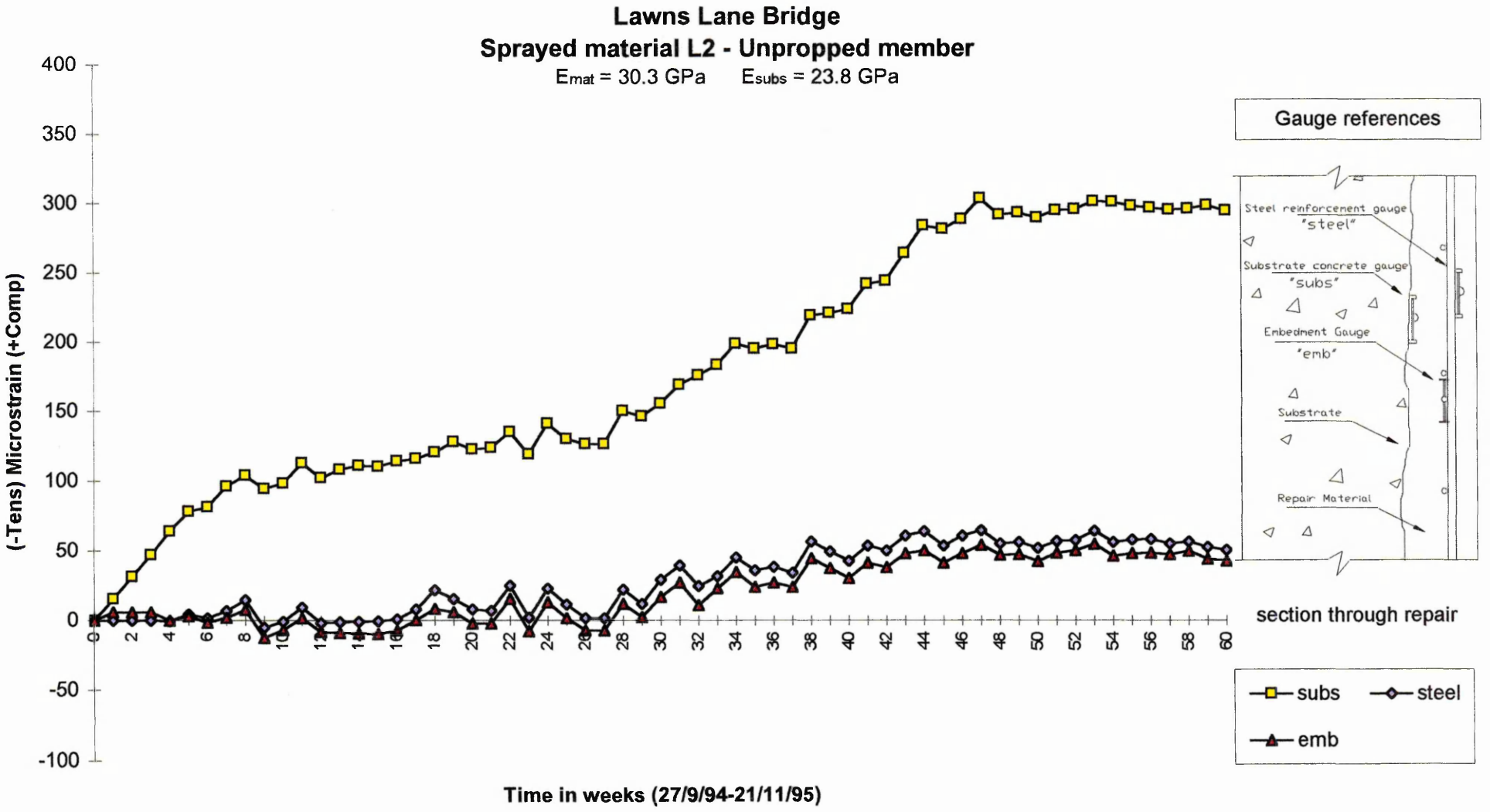

Figure 10.3 Strain distribution in repair patch of material L2 at Lawns Lane Bridge (Unpropped compression member)

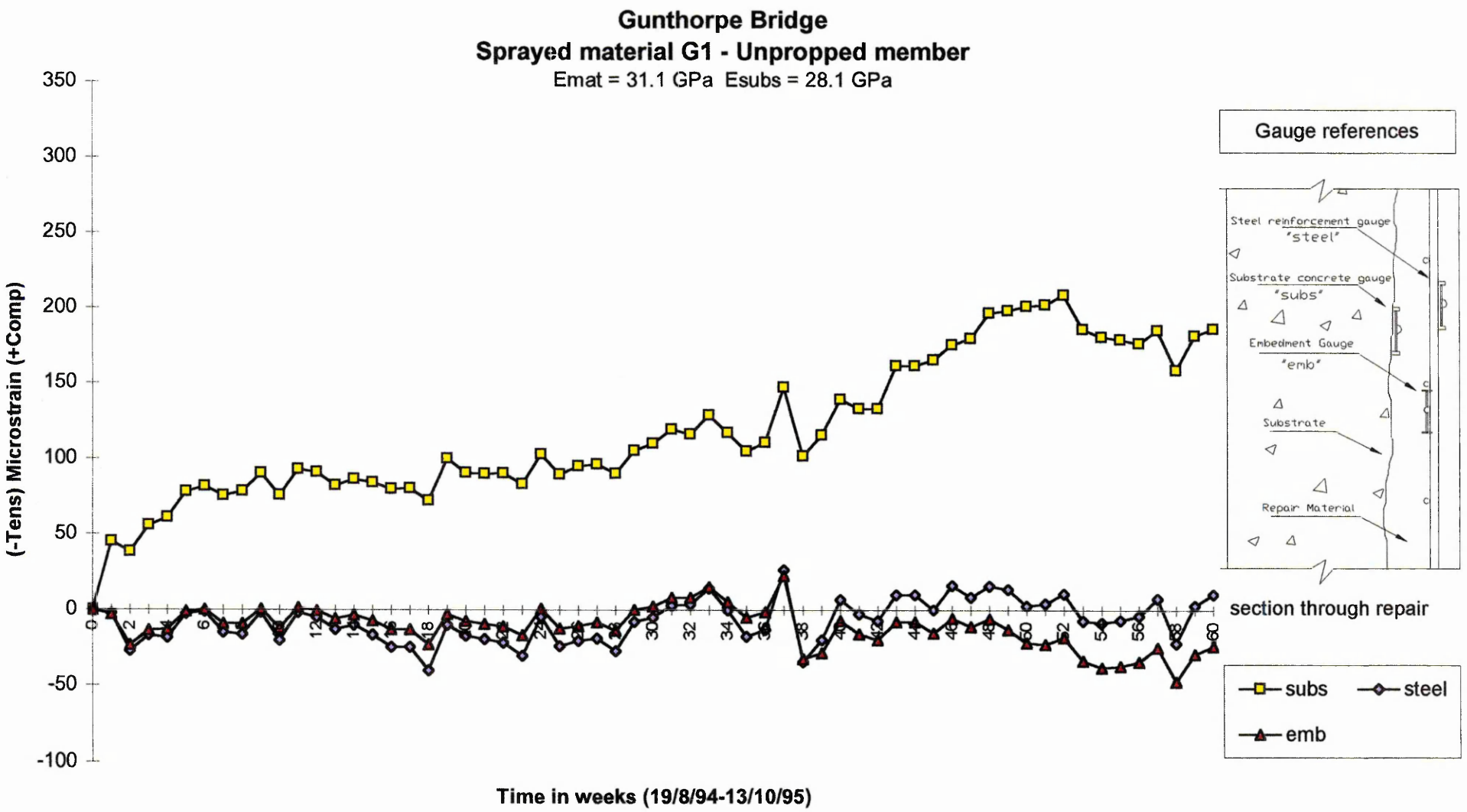

Figure 10.4 Strain distribution in repair patch of material G1 at Gunthorpe Bridge (Unpropped compression member)

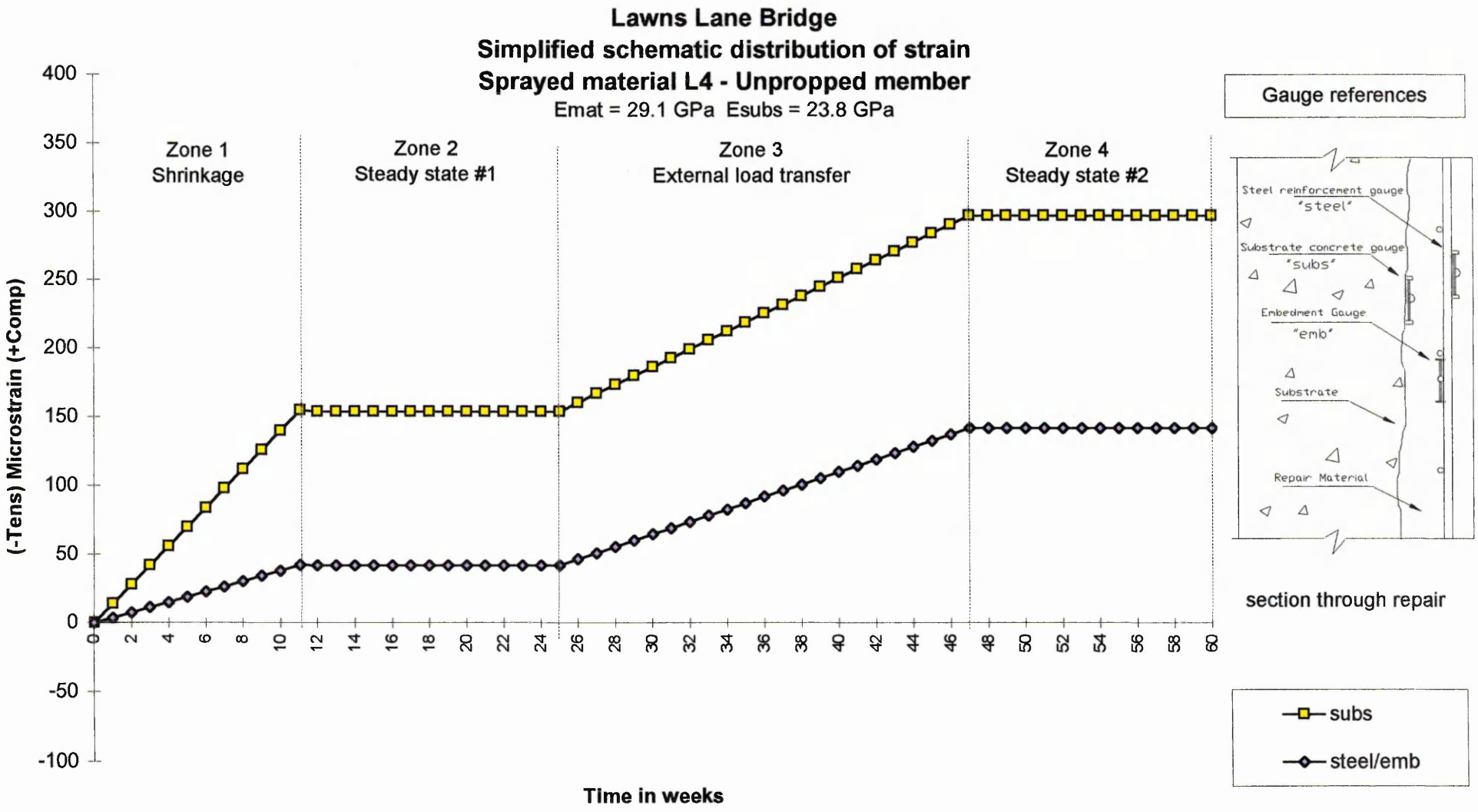

Figure 10.5 Simplified distribution of strain in repair patch of material L4 at Lawns Lane Bridge (Unpropped compression member)

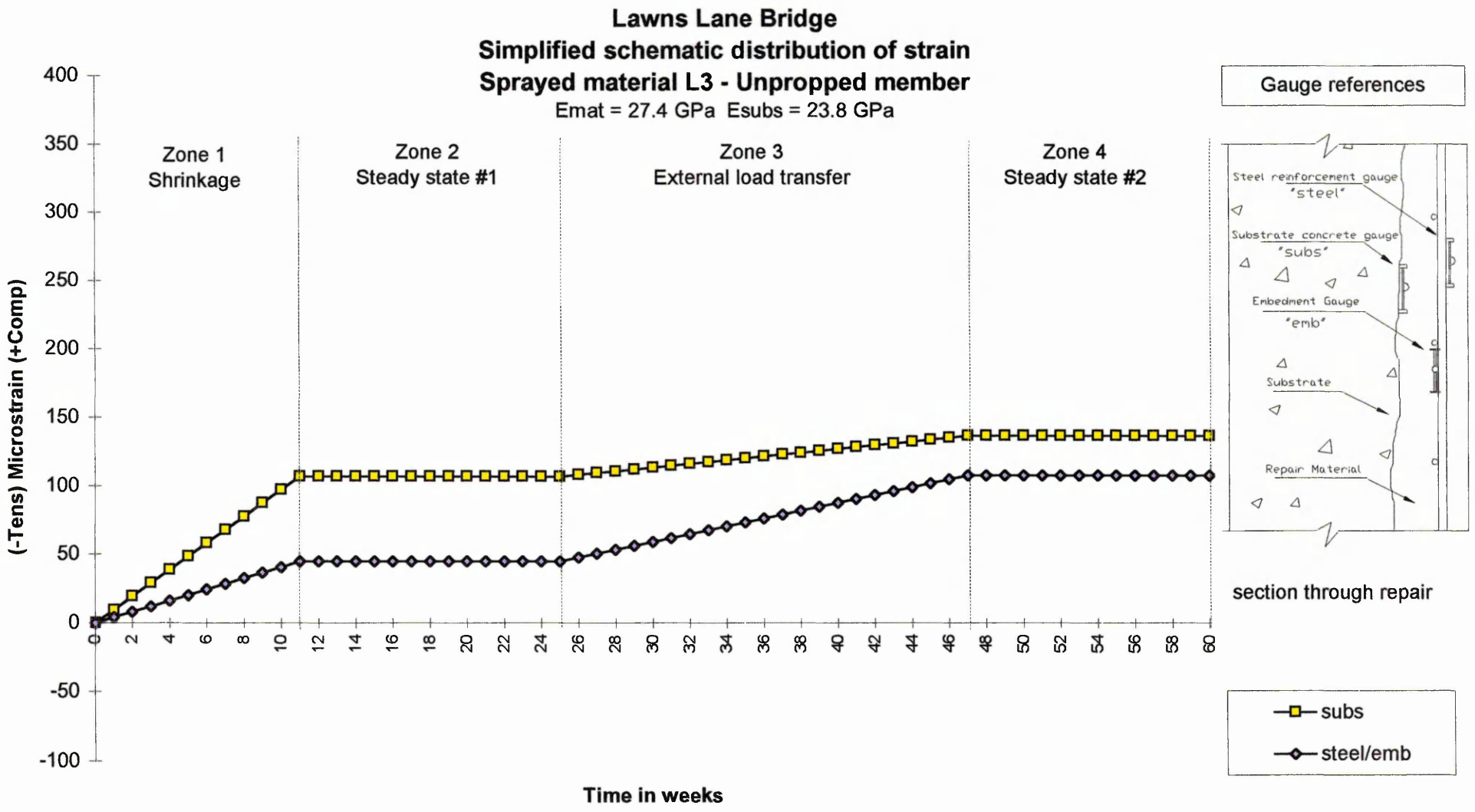

Figure 10.6 Simplified distribution of strain in repair patch of material L3 at Lawns Lane Bridge (Unpropped compression member)

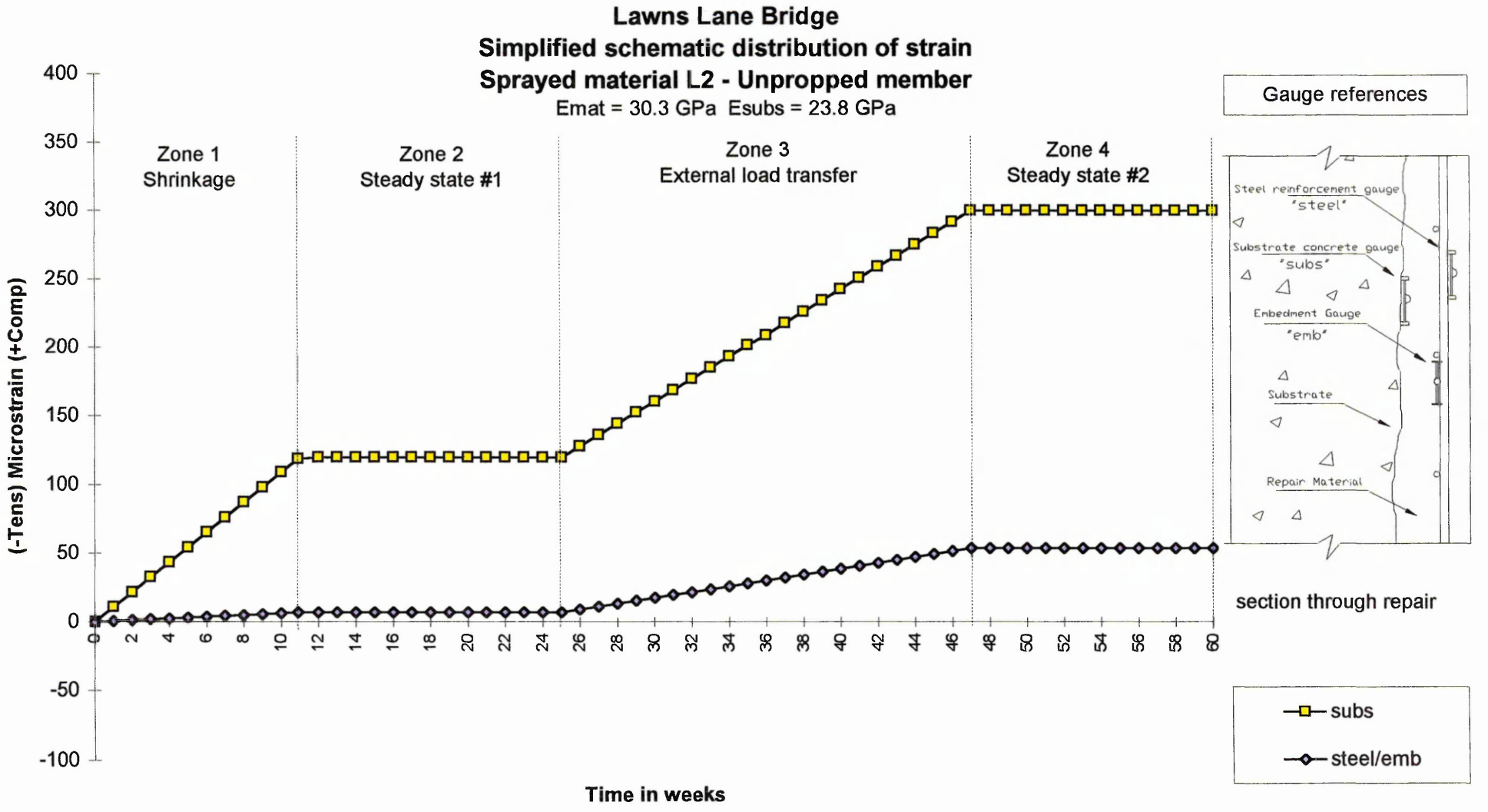

Figure 10.7 Simplified distribution of strain in repair patch of material L2 at Lawns Lane Bridge (Unpropped compression member)

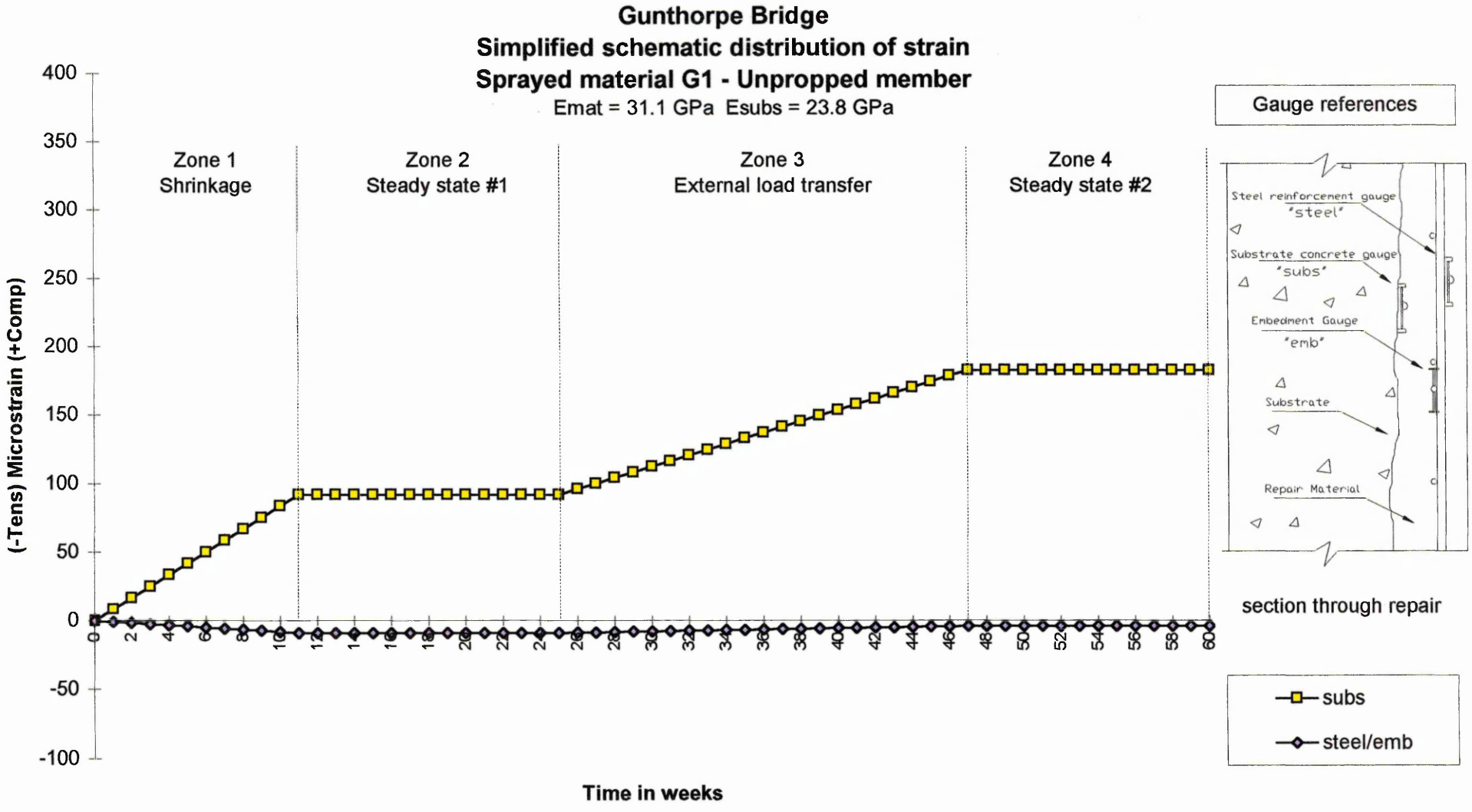

Figure 10.8 Simplified distribution of strain in repair patch of material G1 at Gunthorpe Bridge (Unpropped compression member)

Table 10.1 Cumulative shrinkage and external load transfer strains

Material	*Location*	*Strain at end of : (microstrain)*			
		Zone 1 (week 11)	*Zone 2 (week 25)*	*Zone 3 (week 47)*	*Zone 4 (week 60)*
L4	subs	+154	+154	+297	+297
	steel/emb	+ 42	+ 42	+142	+142
L3	subs	+107	+107	+137	+137
	steel/emb	+ 45	+ 45	+108	+108
L2	subs	+120	+120	+300	+300
	steel/emb	+ 7	+ 7	+ 54	+ 54
G1	subs	+ 92	+ 92	+183	+183
	steel/emb	- 9	- 9	- 4	- 4

Note: Negative values indicate tensile strains

Referring to Figure 10.5 and Table 10.1 (material L4), the strain in the substrate concrete after transfer of shrinkage strain from the repair material is 154 microstrain at the end of Zone 1. This strain is assumed to remain constant throughout Zone 2 (Figure 10.5 and Table 10.1). The strain in the substrate concrete then increases to 297 microstrain by the end of the external load transfer stage (Zone 3), and remains constant thereafter until the end of the monitoring period (Zone 4, week 60, Figure 10.5 and Table 10.1). The strain in the steel reinforcement/repair material at the end of the shrinkage stage for material L4 (Figure 10.5) is 42 microstrain. A similar strain is assumed at the end of Zone 2. The strain in the steel reinforcement/repair material increases to 142 microstrain by the end of Zone 3 after external load is attracted into the

repair patch. It is assumed to remain constant thereafter until the end of Zone 4 (week 60, Figure 10.5 and Table 10.1).

The simplified distribution of strain in the repair patch of material L3 is shown in Figure 10.6 and Table 10.1. The strain in the substrate concrete at the end of Zone 1 is 107 microstrain. A similar strain is assumed at the end of Zone 2, the steady state #1 stage (Figure 10.6 and Table 10.1). External load is attracted into the repair patch in Zone 3, and this increases the strain in the substrate concrete to 137 microstrain. This strain subsequently remains constant in Zone 4. The strain in the steel reinforcement/repair material in the shrinkage stage for material L3 is 45 microstrain. This strain is assumed to remain constant in Zone 2. The strain in the steel reinforcement/repair material increases to 108 microstrain after transfer of externally applied load into the repair patch. The strain in Zone 4 again remains constant (Figure 10.6 and Table 10.1).

Figure 10.7 and Table 10.1 shows the simplified strain in the substrate concrete in the repair patch of material L2 (120 microstrain at week 11). A constant strain of 120 microstrain remains in the substrate concrete at the end of Zone 2, the steady state #1 stage. After external load is attracted into the repair patch, the strain in the substrate concrete increases to 300 microstrain (Zone 3). This strain is assumed to remain constant throughout Zone 4 (Figure 10.7 and Table 10.1). The strain in the steel reinforcement/repair material at the end of the shrinkage stage (Zone 1) and during steady state #1 stage (Zone 2) for material L2 is 7 microstrain. This increases to 54 microstrain at the end of Zone 3 and is assumed to remain constant until the end of the monitoring period (week 60, Figure 10.7 and Table 10.1).

Referring to Figure 10.8 and Table 10.1, the simplified strain in the substrate concrete in the repair patch of material G1 at Gunthorpe Bridge is 92 microstrain at the end of Zone 1 and Zone 2. An increase to 183 microstrain is observed in the substrate concrete after transfer of external load into the repair patch at the end of Zone 3. This strain is assumed to remain constant until week 60 (Zone 4, Figure 10.8 and Table 10.1). The strain in the steel reinforcement/repair material show a loss in compression of -9 microstrain (tension) at the end of the shrinkage period for material G1 (Figure 10.8 and Table 10.1). This is assumed constant throughout Zone 2. A negligible increase in compression is observed at the end of Zone 3 for the steel reinforcement/repair material in the repair patch of material G1. This reduces the strain to -4 microstrain. This strain is assumed constant throughout Zone 4 (Figure 10.8 and Table 10.1)

10.2.1.2.1 Discussion

Zone 1 (Figures 10.5 to 10.8) represents the shrinkage stage (weeks 0 to 11), where the repair material shrinks and transfers a portion of the shrinkage strain to the substrate concrete and steel reinforcement. The strain in the substrate concrete and steel reinforcement is assumed to increase linearly within Zone 1 to reach a maximum at week 11, the end of the shrinkage period (Figures 10.5 to 10.8). The strain in the steel reinforcement is lower in magnitude due to the much higher elastic modulus of the steel reinforcement. Zone 2 represents the first of two steady states, as shrinkage in the repair material has virtually ceased and as a result, strains remain constant in the substrate concrete and the steel reinforcement (Figures 10.5 to 10.8, weeks 11 to 25). Zone 3 is referred to as the external load transfer stage, as the stiffer repair attracts external load

into the repair patch. The repair material deforms due to the increase in compressive stress and since the repair material is fully bonded to the steel reinforcement, the steel reinforcement also shows an increase in compression (Figures 10.5 to 10.8). The strain in the substrate concrete, at the interface with the repair, also increases within the external load transfer stage due to full bond between the repair material and the substrate concrete of lower elastic modulus (Figures 10.5 to 10.8, weeks 25 to 47). Zone 4 represents the second steady state period, since by this time the transfer of external load into the repair patch has ceased (Figures 10.5 to 10.8, weeks 47 to 60)

Table 10.2 gives the magnitude of the shrinkage strains developed in Zone 1 (from week 0 to 11) and external load transfer strains developed in Zone 3 (from weeks 25 to 47) for the same four repair materials L4, L2, L3 and G1 (Figures 10.5 to 10.8). The values given in Table 10.2 are the maximum shrinkage strains in the substrate concrete and steel reinforcement/repair material at the end of Zone 1 (week 11). The external load transfer strains in Table 10.2 are the maximum values transferred to the substrate concrete and steel reinforcement/repair material during Zone 3, from week 25 to 47.

Referring to Table 10.2, the strain in the substrate concrete in the repair patches of materials L4, L3, L2 and G1, after end of Zone 1 (after transfer of shrinkage from the repair material) are 154, 107, 120 and 92 microstrain respectively. The average strains in the repair material/steel reinforcement at the end of Zone 1 (Table 10.2) are considerably lower since the steel reinforcement has a much higher elastic modulus than the substrate concrete (42, 45, 7 and -9 respectively). At the end of Zone 3, the external load transfer stage, the strain in the substrate concrete is 143, 30, 180 and 91 microstrain

Table 10.2 Average distributed shrinkage and external load transfer strains

Material	*Location*	*Strain in: (microstrain)*	
		Zone 1 (weeks 0 to 11)	*Zone 3* (weeks 25 to 47)
L4	subs	+154	+143
	steel/emb	+ 42	+100
L3	subs	+107	+ 30
	steel/emb	+ 45	+ 63
L2	subs	+120	+180
	steel/emb	+ 7	+ 47
G1	subs	+ 92	+ 91
	steel/emb	- 9	+ 5

Note: Negative values indicate tensile strains

for repair materials L4, L3, L2 and G1 respectively. The strains in the steel reinforcement/repair material are 100, 63, 47 and 5 microstrain for materials L4, L3, L2 and G1 respectively.

10.2.1.3 Tension due to restraint to shrinkage

Figures 10.9 to 10.12 show the simplified distribution of strain in the substrate concrete and steel reinforcement/repair material for materials L4, L3, L2 and G1 along with the modified free shrinkage curve for the same repair materials between weeks 0 to 11 (i.e. shrinkage stage, Zone 1, see Figures 10.5 to 10.8). The free shrinkage curve is

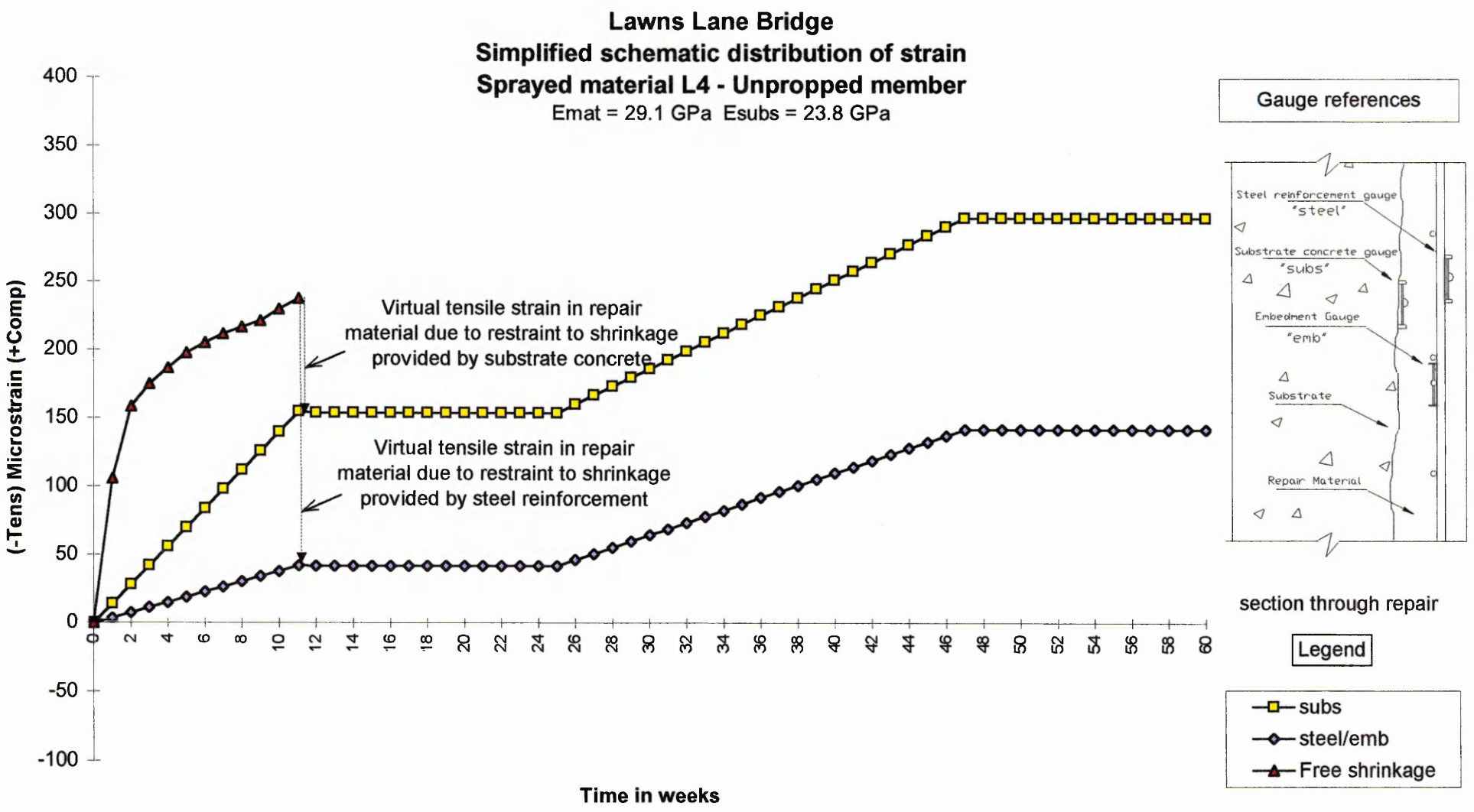

Figure 10.9 Virtual tensile strain in repair patch of material L4 at Lawns Lane Bridge (Unpropped compression member)

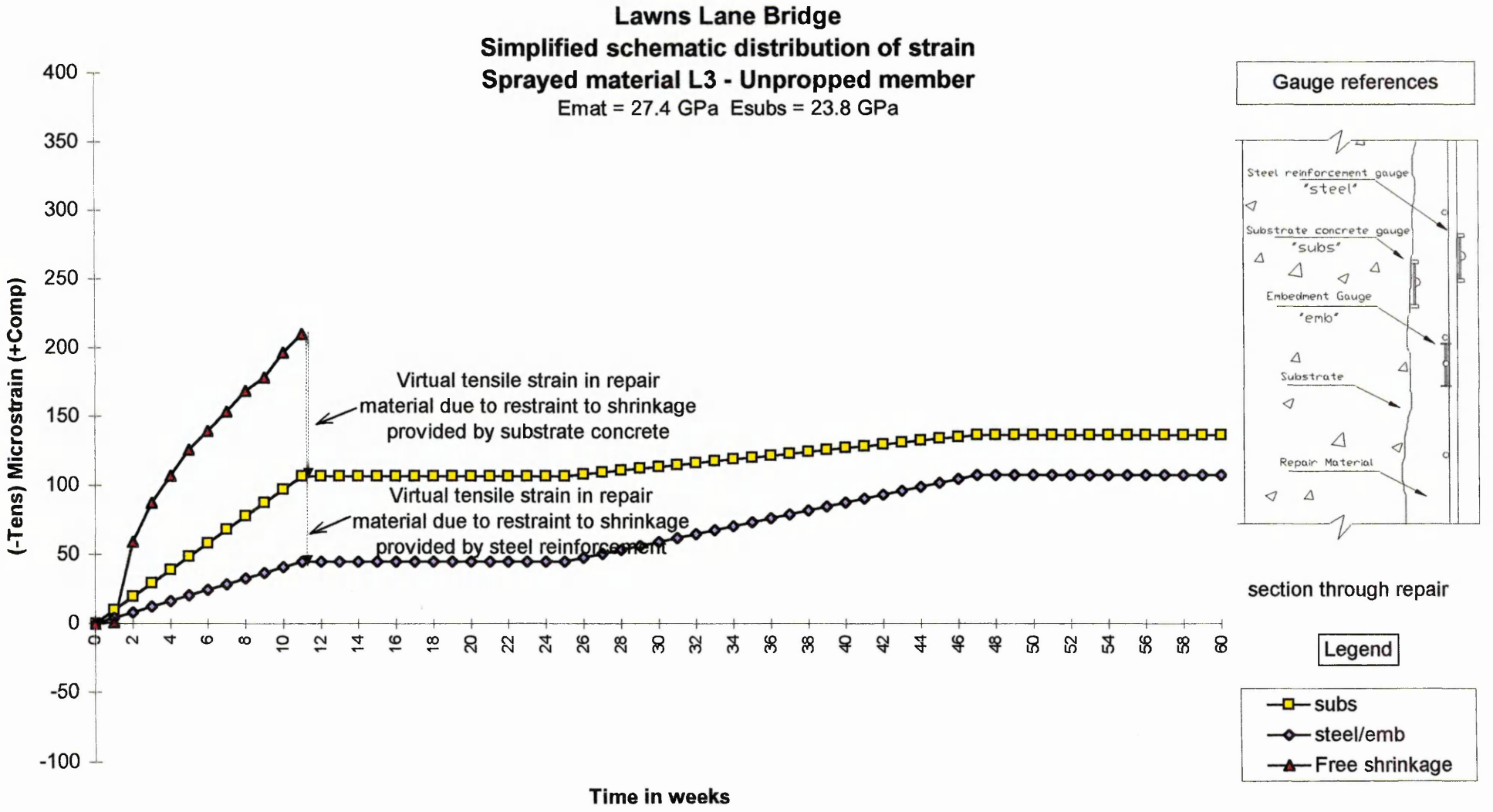

Figure 10.10 Virtual tensile strain in repair patch of material L3 at Lawns Lane Bridge (Unpropped compression member)

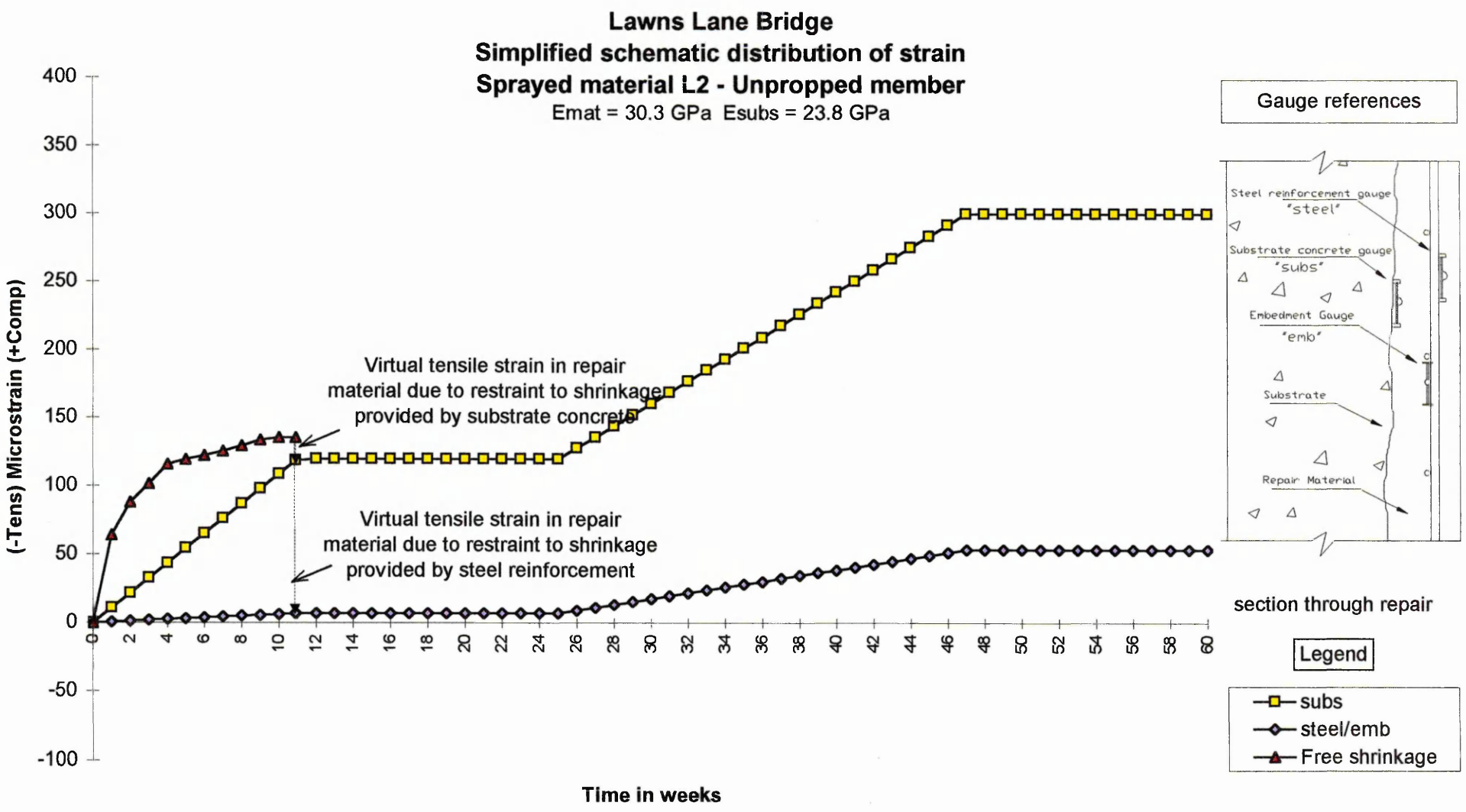

Figure 10.11 Virtual tensile strain in repair patch of material L2 at Lawns Lane Bridge (Unpropped compression member)

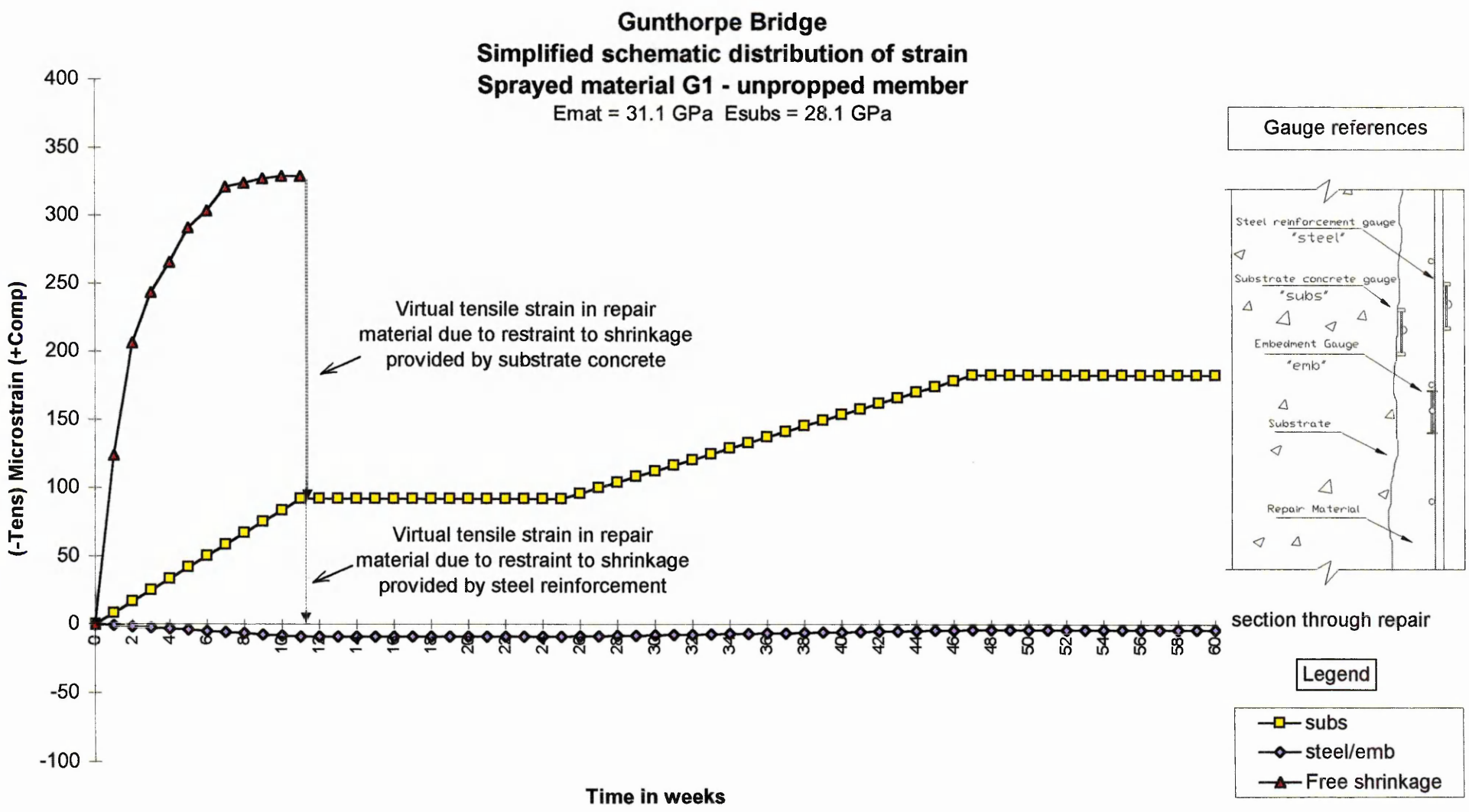

Figure 10.12 Virtual tensile strain in repair patch of material G1 at Gunthorpe Bridge (unpropped compression member)

modified to take into account differences that exist between laboratory and field measurements. For instance, prisms in the laboratory will have a different surface/volume ratio to the field repair patches (external surfaces only were used to calculate the surface area of the repair patches in the field). A higher surface/volume ratio will contribute towards higher shrinkage in the repair material [29-31]. Prisms stored under a higher laboratory temperature of 20°C will exhibit more shrinkage than the repair patches in the field which were exposed to a lower temperature (averaged at 10°C over the eleven week shrinkage period). Finally, a curing membrane was applied to the surfaces of the repair patches at Lawns Lane Bridge to assist with curing of the repair material (see Section 10.2.1.5.3). Therefore, depending on the efficiency of the membrane, a repair material treated with a curing membrane would shrink less than an untreated repair patch. A correction for relative humidity was not applied, since the relative humidity in the laboratory (55%) was similar to the field average over the eleven week shrinkage period.

The magnitude of virtual tensile strain due to the shrinkage restraint provided by the substrate concrete and steel reinforcement is also shown in Figures 10.9 to 10.12 and Table 10.3. The virtual tension is defined as the difference between the modified free shrinkage of the repair material, and the compressive strain in either the substrate concrete or steel reinforcement. Strain compatibility is assumed between the repair material and the substrate concrete at the interface, and between the repair material and steel reinforcement at the steel reinforcement level. The restraint to shrinkage strain is greater at the steel reinforcement level than at the interface between the repair material and substrate concrete (Figures 10.9 to 10.12). This is due to the higher stiffness of the

Table 10.3 Virtual tensile strain in the repair materials

Material	*Location*	*Modified free shrinkage (microstrain)*	*Elastic modulus repair (substrate) (kN/mm^2)*	*Strain at week 11 (microstrain)*	*Virtual tension (microstrain)*
L4		238	29.1 (23.8)		
	subs			154	- 84
	steel/emb			42	-196
L3		210	27.4 (23.8)		
	subs			107	-103
	steel/emb			45	-165
L2		136	30.3 (23.8)		
	subs			120	- 16
	steel/emb			7	-129
G1		329	31.1 (28.1)		
	subs			92	-237
	steel/emb			-9	-338

steel reinforcement which provides a higher restraint to shrinkage. Consequently, less shrinkage strain is transferred to the steel reinforcement resulting in a higher virtual tensile strain in the repair material (Figures 10.9 to 10.12).

Referring to Figure 10.9 and Table 10.3, the modified free shrinkage of material L4 is 238 microstrain at week 11. The maximum strain transferred to the substrate concrete and steel reinforcement at week 11 (Figure 10.9) is 154 and 42 microstrain respectively. This gives a virtual tensile strain in the repair material of 84 and 196 microstrain at the interface between the substrate concrete/repair material and steel reinforcement level

respectively. The modified free shrinkage for material L3 is given in Figure 10.10 and Table 10.3. Also shown is the compressive strain in the substrate concrete and steel reinforcement at week 11, the end of the shrinkage period. This gives a virtual tensile strain of 103 microstrain in the repair material at the substrate concrete/repair material interface and a virtual tensile strain of 165 microstrain in the repair material at the steel reinforcement level at week 11. Figure 10.11 and Table 10.3 show that the modified free shrinkage in material L2 at week 11 was 136 microstrain. The shrinkage strain transferred to the substrate concrete was 120 microstrain, whereas the shrinkage strain transferred to the steel reinforcement was 7 microstrain at the end of week 11. This gives a virtual tensile strain in the repair material of 16 microstrain at the interface and 129 microstrain at the steel reinforcement level. Referring to Figure 10.12 and Table 10.3, the modified free shrinkage of material G1 at Gunthorpe Bridge is 329 microstrain. This is higher than the modified free shrinkage of the materials used at Lawns Lane Bridge (see Table 10.3), mainly because a curing membrane was not applied to the repair materials at Gunthorpe Bridge. The shrinkage strain transferred to the substrate concrete in the repair patch of material G1 was 92 microstrain. The steel reinforcement showed tensile strain of 9 microstrain. This gave a virtual tensile strain of 237 microstrain in the repair material at the interface and a virtual tensile strain of 338 microstrain in the repair material at the steel reinforcement level.

10.2.1.3.1 Discussion

It has already been established in Chapter 9 that if the elastic modulus of the substrate concrete is greater than the elastic modulus of the repair material, then the substrate

concrete and steel reinforcement would provide a full restraint to shrinkage in the repair material. Thus, the (modified) free shrinkage strain in the repair material would in fact become a virtual tensile strain. This would increase the likelihood of cracking in the repair material. Referring to Table 10.3, materials L4, L3, L2 and G1 all have an elastic modulus that is greater than the elastic modulus of the substrate concrete. Consequently, the repair materials are able to transfer a portion of the shrinkage strain to the substrate concrete, and to a lesser extent, to the steel reinforcement. The steel reinforcement is much stiffer than the repair material, but since the cross-sectional area of the steel reinforcement is negligible compared with the cross-sectional area of the repair patch, the repair material is able to transfer some of the large virtual force due to shrinkage to the steel reinforcement. This reduces the virtual tensile strain in the repair material at the interface with the substrate concrete and at the level of the steel reinforcement. Furthermore, if the elastic modulus of the repair material is substantially greater than the elastic modulus of the substrate concrete, then more of the shrinkage strain will be transferred to the substrate concrete. This is clearly evident in material L2 (Figure 10.11 and Table 10.3). The modified free shrinkage strain in this material is 136 microstrain. The strain transferred to the substrate concrete in this instance is 120 microstrain. Therefore, the virtual tensile strain in the repair material at the substrate concrete/repair material interface is only 16 microstrain. It is highly unlikely that a tensile strain of this magnitude would cause cracking. Materials L4 and L3 also show considerable transfer of shrinkage strain to the substrate concrete and steel reinforcement (Table 10.3), thereby reducing the virtual tensile strains in the repair material. The highest virtual tensile strain occurs in material G1 at Gunthorpe Bridge. This repair material does not transfer any shrinkage strain to the steel reinforcement, and

as a result, a relatively high virtual tensile strain is evident in the repair material at week 11. Cracking, nevertheless, was absent in the repair patch since this repair material exhibited a relatively high modulus of rupture and consequently a high tensile strain capacity (see Chapter 8, Figure 8.23).

10.2.1.4 Stress in the repaired section

10.2.1.4.1 Substrate concrete and steel reinforcement

Figures 10.13 to 10.16 show the stress in the repair patch throughout the monitoring period (weeks 0 to 60) for repair materials L4, L3, L2 and G1 respectively. The stress locations within the repair patches are illustrated in Figures 10.13 to 10.16. The stress in the substrate concrete ("subs") is at the substrate concrete/repair material interface. Therefore, the strain measured on the surface of the substrate concrete by the vibrating wire strain gauge (see Figures 10.1 to 10.4) is converted to a stress by multiplying the strain by the elastic modulus of the substrate concrete. The elastic modulus was obtained by testing cores in the laboratory in accordance with BS 1881, Part 121 [3], to determine the elastic modulus of the substrate concrete. It is assumed that creep is negligible in the substrate concrete due to the age of the bridge and, therefore, the elastic modulus of the substrate concrete was taken as a constant throughout the monitoring period (weeks 0 to 60). The stress in the steel reinforcement (weeks 0 to 60, Figures 10.13 to 10.16) was obtained by multiplying the measured strain in the steel reinforcement by the elastic modulus of steel reinforcement (the strain in the steel reinforcement was taken as the average of the embedment and steel reinforcement gauge

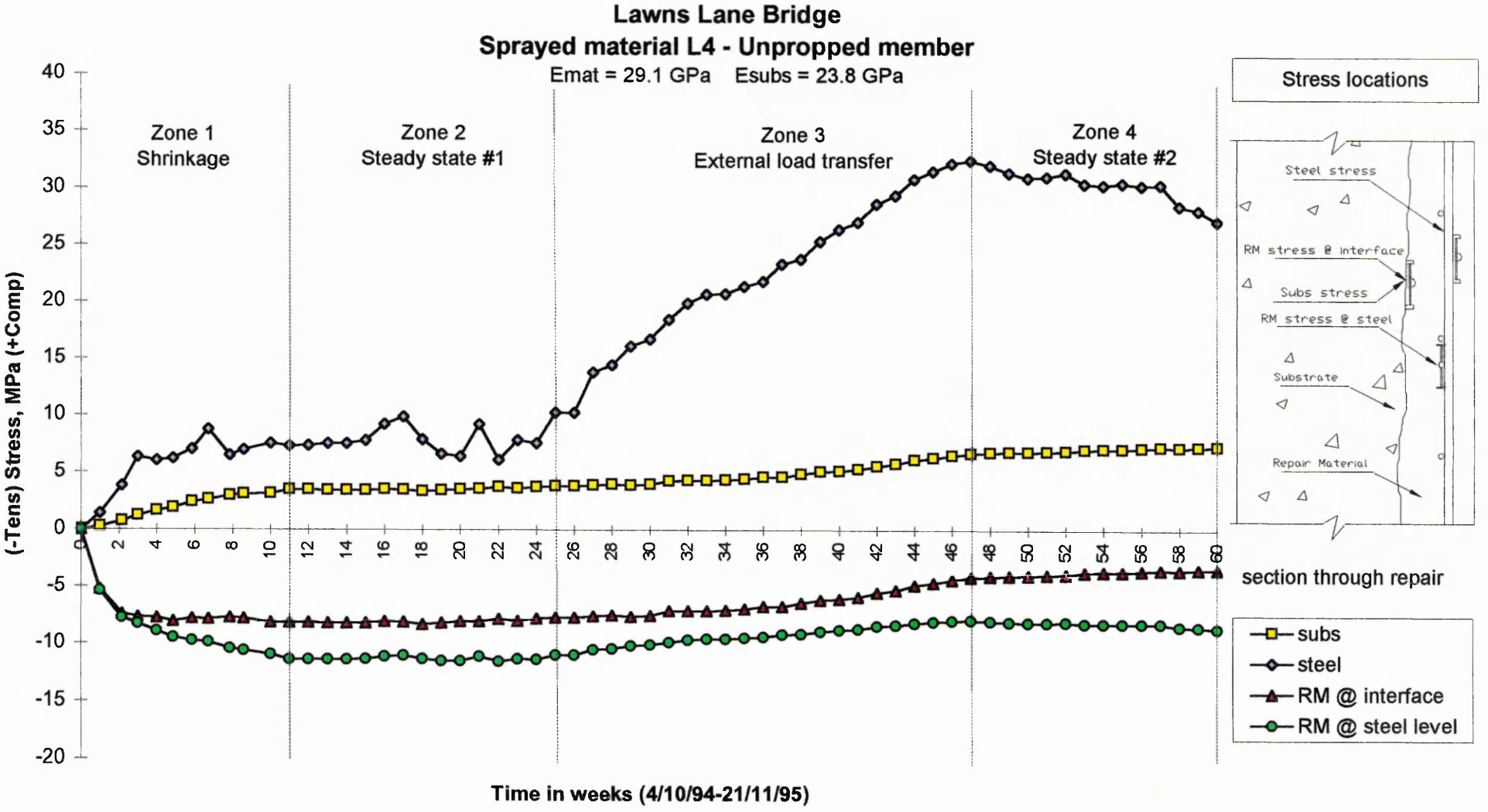

Figure 10.13 Stress distribution in repair patch of material L4 at Lawns Lane Bridge (Unpropped compression member)

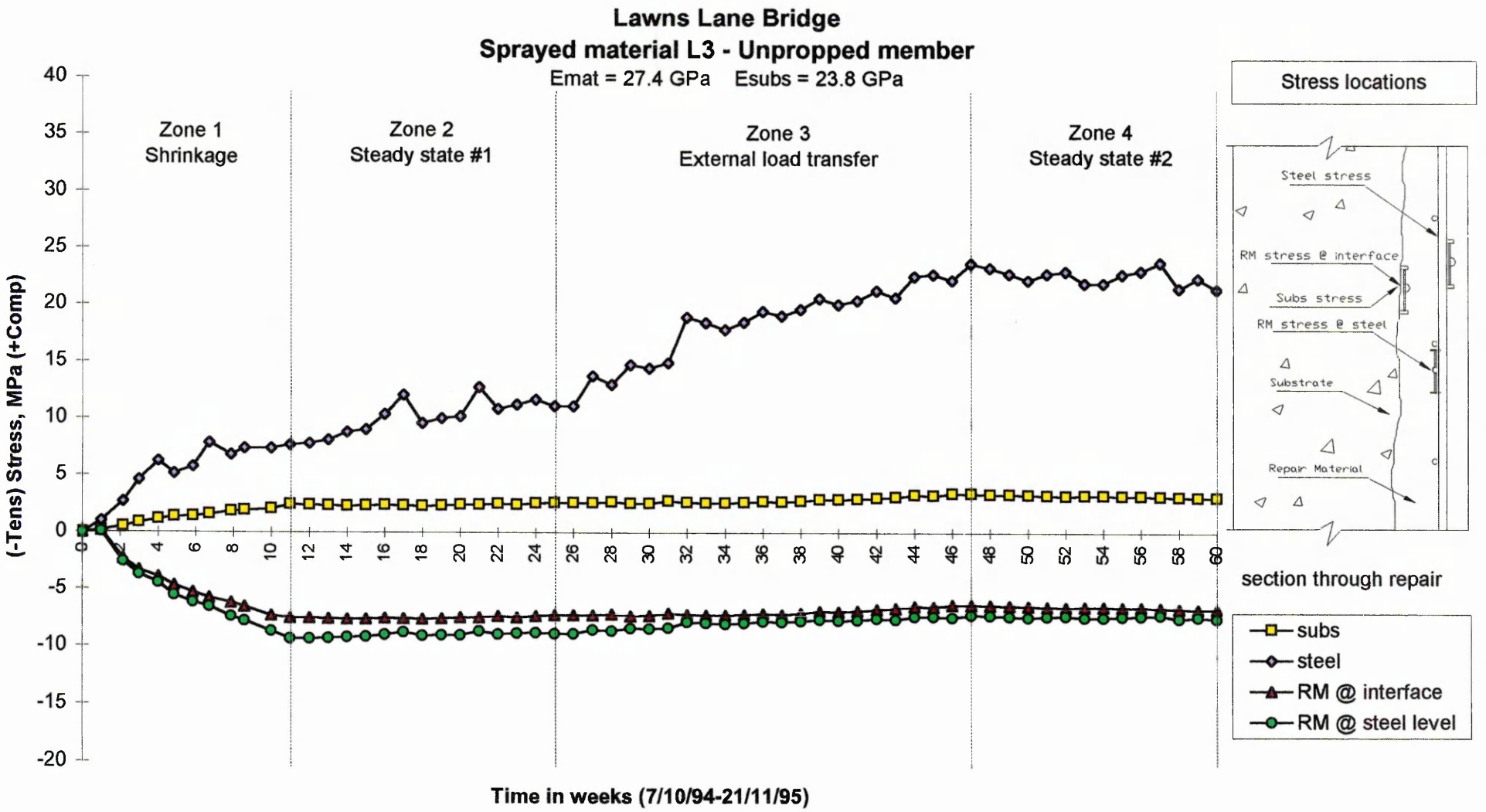

Figure 10.14 Stress distribution in repair patch of material L3 at Lawns Lane Bridge (Unpropped compression member)

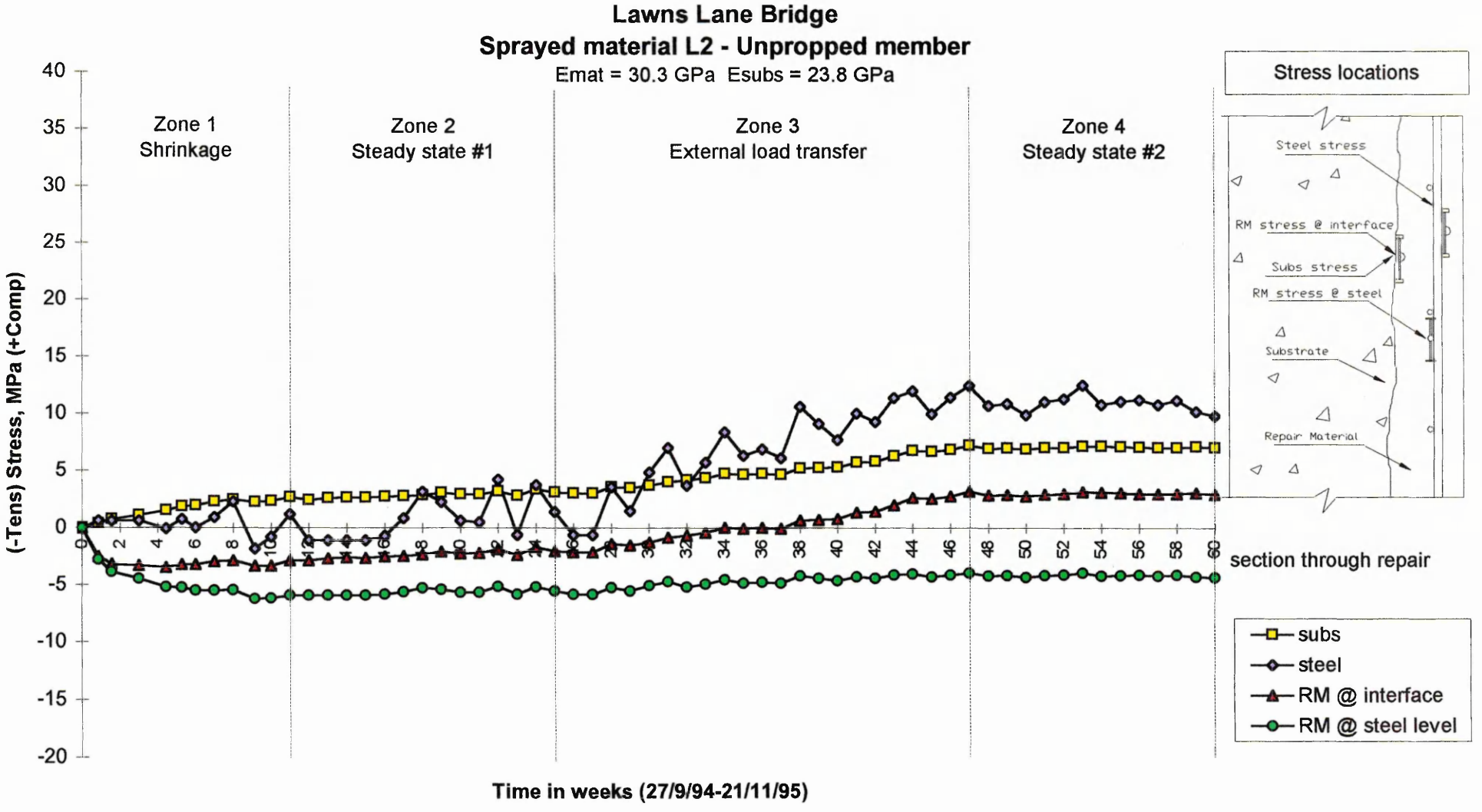

Figure 10.15 Stress distribution in repair patch of material L2 at Lawns Lane Bridge (Unpropped compression member)

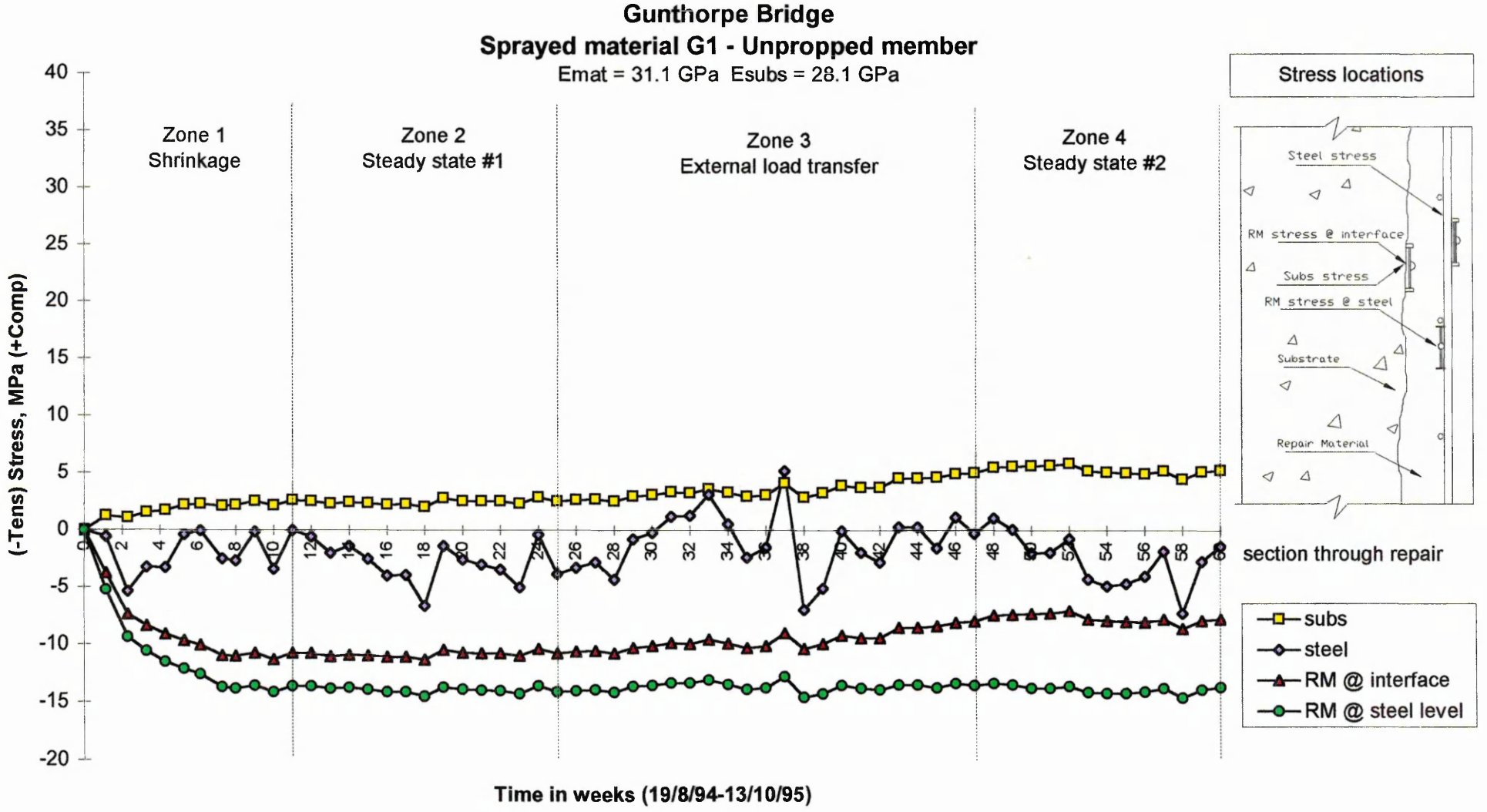

Figure 10.16 Stress distribution in repair patch of material G1 at Gunthorpe Bridge (Unpropped compression member)

due to strain compatibility - see Figures 10.1 to 10.4). The elastic modulus of the steel reinforcement was assumed as 210 kN/mm^2 throughout.

10.2.1.4.2 Repair material

With regards to the stress in the repair material, two locations are represented in Figures 10.13 to 10.16, namely at the interface between the substrate concrete and repair material, and at the steel reinforcement level. Strain compatibility at the interface between the substrate concrete and repair material was assumed, and consequently, the restrained shrinkage strain of the repair material was considered to be the same as the compressive strain transferred to the substrate concrete. Consequently, the virtual tensile strain in the repair material at the interface was obtained by subtracting the strain measured in the substrate concrete from the modified free shrinkage strain in the repair material (see Figures 10.9 to 10.12). This strain was then converted to an equivalent repair material stress by multiplying initially by the 28 day elastic modulus of the repair material (weeks 0 to 11, Figures 10.13 to 10.16). The elastic modulus of the repair material was obtained by casting cylinders in the laboratory and testing in accordance with BS 1881, Part 121 [3] (details are given in Sections 8.3.2 and 8.4.3). Similarly, the average strain recorded from the steel reinforcement and embedment gauges in the repair material at the steel reinforcement level (see Figures 10.1 to 10.4) was also subtracted from the modified free shrinkage strain in the repair material to give a virtual tensile strain in the repair material at the steel reinforcement level (Figures 10.1 to 10.4). Subsequently, a tensile stress in the repair material at this location was obtained by

multiplying by the elastic modulus of the repair material (weeks 0 to 11, Figures 10.13 to 10.16).

In order to represent the stress in the repair material from Zone 2 onwards (i.e. steady state #1, external load transfer and steady state #2), the strains in the repair material at the substrate concrete/repair material interface, and at the steel reinforcement level at the end of the shrinkage stage (week 11, Figures 10.13 to 10.16) were considered as a new datum at week 11 (i.e. no further increase in virtual tensile strain since the shrinkage is assumed to have ceased, see Figures 10.9 to 10.12). Therefore, the new datum strain at week 11 was subtracted from subsequent strains in Zones 2, 3 and 4 (weeks 11 to 60) and converted to a stress by multiplying by the 28 day elastic modulus of the repair material. This stress was then algebraically added to the tensile stress at week 11 which gave the stress in the repaired sections in Zones 2, 3 and 4 as shown in Figures 10.13 to 10.16.

10.2.1.4.3 Discussion

Figures 10.13 to 10.16 show that the compressive stress in the substrate concrete increases within Zone 1, the shrinkage period. This compressive stress in the substrate concrete remains relatively constant in Zone 2, Figures 10.13 to 10.16. In Zone 3 (weeks 25 to 47), the external load transfer stage, an increase in compressive stress in the substrate concrete is observed. Finally, the compressive stress in the substrate concrete again reaches a steady state (Figures 10.13 to 10.16, Zone 4) between weeks 47 and 60. The compressive stress in the steel reinforcement generally follows a similar pattern to the compressive stress in the substrate concrete (Figures 10.13 to 10.15,

Zones 1-4). An increase in compressive stress is observed in Zones 1 and 3 whereas the compressive stress remains relatively constant in Zones 2 and 4. On the other hand, the stress in the repair material at both the interface ("RM @ interface") and at the steel reinforcement level ("RM @ steel") is quite different to the stress in the substrate concrete and steel reinforcement. The stress in the repair material increases in tension in Zone 1 (weeks 0 to 11), for both "RM @ interface" and "RM @ steel". The tensile stress in the repair material remains relatively constant in Zone 2. A slight decrease in tension occurs in the repair material in Zone 3. In fact, the tensile strain in material L2 at the interface ("RM @ interface", Figure 10.15) changes from tension to compression. In Zone 4, the stress in the repair material exhibits a relatively constant behaviour.

10.2.1.4.4 Further discussion

Referring to Figures 10.13 to 10.16, the compressive stress in the substrate concrete increases steadily within the shrinkage stage, Zone 1. This is because the stiffer repair material is transferring shrinkage strain, and consequently compressive stress, to the less stiff repair material. The compressive stress reaches a maximum at approximately week 11, the end of the shrinkage period. The compressive stress in the substrate concrete remains relatively constant within Zone 2, (steady state #1), since shrinkage in the repair material will have reached negligible levels (Figures 10.13 to 10.16, Zone 2). An increase in compressive stress in the substrate concrete (at the interface) is again observed in Zone 3, the external load transfer stage. External stress is attracted into the repair patch, and due to strain compatibility at the interface, the interfacial zone of the substrate concrete is also affected (Figures 10.13 to 10.16) The compressive stress in

the substrate concrete remains relatively constant in Zone 4, Figures 10.13 to 10.16, since external load transfer in the repair material has virtually ceased and compression is no longer forced into the substrate concrete through strain compatibility at the interface. The compressive stress in the steel reinforcement broadly follows a similar pattern to the compressive stress in the substrate concrete (Figures 10.13 to 10.16, Zones 1-4), but the magnitude of stress is higher in the steel reinforcement in most cases. Referring to Figures 10.1 to 10.4, the shrinkage strain transferred to the steel reinforcement is lower than the strain transferred to the substrate concrete. This is because the steel reinforcement is much stiffer than the substrate concrete and therefore, provides more restraint to shrinkage. However, when the strains are converted to an equivalent stress, the stress in the steel reinforcement may in fact be higher than the stress in the substrate concrete due to the higher elastic modulus of steel. This was clearly evident in materials L4 and L3 (Figures 10.13 and 10.14).

The tensile stress in the repair material increases rapidly in Zone 1, the shrinkage stage (Figures 10.13 to 10.16), for both the repair material at the substrate concrete interface ("RM @ interface") and the repair material at the steel reinforcement level ("RM @ steel"). This is due to the rapid shrinkage of the repair materials during this stage, which is restrained by the substrate concrete and steel reinforcement. The tensile stress in the repair material reaches a maximum value at approximately week 11 (end of Zone 1), since the shrinkage in the repair materials will have stabilised at this stage. From week 12 until approximately week 25, the tensile stress in the repair material (both at the interface and at the steel reinforcement level) remains relatively constant since the free shrinkage curve of the repair material would generally exhibit asymptotic behaviour

at this stage (Figures 10.13 to 10.16). Compressive stress is subsequently attracted into the repair patch from the substrate concrete, and this is shown by the reduction in tensile stress in the repair material at both the interface and steel reinforcement level (Zone 3, Figures 10.13 to 10.15). The stress in Zone 4 remains relatively constant since the transfer of external load into the repair patch has ceased by this stage.

10.2.1.5 Modifications to repair material properties

Figures 10.13 to 10.16 assumes a steel reinforcement elastic modulus (stiffness) of 210 kN/mm^2 and a substrate concrete elastic modulus equivalent to that obtained from testing cores extracted from field structures. The assumption that creep will have ceased in the substrate concrete is made on the basis that the substrate concrete in the bridges was under load for over 30 years. Figures 10.13 to 10.16 also assume that the stiffness of the repair material remains constant at the value determined under compression at 28 days age. However, this does not truly represent the actual distribution of stress with time across the repair patch since, for example, tensile creep would reduce the elastic modulus and consequently the tensile stress in the repair material. Also, at early ages, the elastic modulus of the repair material will be less than the 28 day value since time is needed for the repair material to develop its properties. Consequently, adjustments should be made to the properties of the repair materials represented in Figures 10.13 to 10.16 to better represent the actual situation.

10.2.1.5.1 Elastic modulus

The assumption is made that for repair materials, the tensile modulus of elasticity is the same as the compressive modulus of elasticity. The literature review in Chapter 8 shows that the static modulus of elasticity of concrete in tension is approximately 9% less than that in compression. By applying this conclusion to the stiffness of the repair material, a lower elastic modulus, and consequently a lower tensile stress will be evident in the repair material. This will result in a tensile stress reduction of about 9% in the repair materials in Figures 10.13 to 10.16. Furthermore, the elastic modulus of the repair material was taken as the 28 day value throughout in calculating the stresses plotted in Figures 10.13 to 10.16. The elastic modulus of the repair material at earlier ages will invariably be less than the 28 day elastic modulus, since the repair material will need time to develop its full properties. Table 10.4 [43] shows the elastic modulus of three repair materials at 7, 14 and 21 days in relation to the 28 day value. The 7, 14, and 21 day elastic modulii are approximately 65%, 85% and 96% of the 28 day elastic modulus value.

Table 10.4 Development with age of tensile elastic modulus of repair materials (from Figure 8.9 [43])

	Percentage of 28 day tensile elastic modulus at:		
Material	*7 days* (%)	*14 days* (%)	*21 days* (%)
Unmodified	60	83	95
Vinyl Acetate	59	81	94
Acrylic	75	92	98
Average:	*65*	*85*	*96*

The 28 day elastic modulus should therefore be reduced to values similar to those listed in Table 10.4 to better represent the tensile stress in the repair patch at early ages after application of repair, since the strains and subsequently the stresses in the repair materials were plotted form the age of 24 hours in Figure 10.2 onwards. A lower elastic modulus will result in lower tensile stress in the repair material.

10.2.1.5.2 Creep

The allowance for stress relaxation in the repair material was also unaccounted for in Figures 10.13 to 10.16. A repair material that exhibits tensile stress due to the restraint to shrinkage provided by the substrate concrete will undergo tensile creep. This will reduce the elastic modulus of the repair material which will consequently reduce the tensile stress. Therefore, an effective elastic modulus should be employed to account for tensile creep in the repair material within the shrinkage period (weeks 0 to 11, Figures 10.13 to 10.16). The value of ϕ, the creep coefficient, which is the ratio of creep strain to the instantaneous elastic strain upon loading has been obtained for the repair materials under investigation (see Table 8.19). This coefficient is used to allow for the effect that creep will have on the elastic modulus of the repair material by calculating its effective elastic modulus, $E_{rm(eff)}$, as follows [62]:

$$E_{rm(eff)} = E_{rm} / (1+\phi)$$

Equation 10. 1

where E_{rm} is the 28 day elastic modulus of the repair material.

Although the creep coefficient has been obtained (Table 8.19) for the repair materials under a compressive stress, the same coefficient can equally be applied to repair materials in tension [46, 58, 59], based on the findings of the literature review in Chapter 8. The creep coefficient, however, was obtained for repair materials under investigation in this project (Table 8.19) that were loaded at 28 days age. It is well established that concrete (and similarly repair materials) loaded at later ages will show less creep than materials loaded at early ages. Table 10.5 shows the relationship between creep coefficients for a repair material loaded at 2, 4, 7 and 14 days after casting, to the creep coefficient of a repair material loaded 28 days after casting. The creep coefficient is higher for repair materials loaded at earlier ages. Hence, the creep coefficient obtained in the laboratory (Table 8.19) should be increased by ratios similar to those given in Table 10.5 to better represent the in situ creep of the repair materials at early ages. A lower effective elastic modulus, and consequently a lower tensile stress will result.

Table 10.5 Ratio of early age creep coefficient to 28 day creep coefficient for SBR modified concrete (From Figure 8.6 [37])

	Age (days)				
t =:	*2*	*4*	*7*	*14*	*28*
Creep coefficient	2.49	2.10	1.81	1.19	1.14
Ratio $\left[\frac{(t)day}{28day}\right]$	2.18	1.84	1.59	1.04	1.00

10.2.1.5.3 Shrinkage

The final correction to be made to the tensile stress in the repair material is the effect that the curing membrane will have on the shrinkage of the repair material. This is relevant to the repairs applied at Lawns Lane Bridge where a curing membrane was used. The literature review undertaken in this study was unable to determine accurately the effectiveness of curing membranes in reducing the shrinkage in concrete/repair materials. The only information that was obtained related to the efficiency of curing compounds, to BS 7542 [97], which determined the effectiveness of curing membranes in preventing moisture loss from a sample of concrete. Other researchers have also tested the efficiency of curing compounds with respect to moisture loss [98, 99, 100]. Russell [101] reports tests which show that a curing membrane applied at a rate of $5m^2$ per litre on a reasonably smooth concrete surface will provide the equivalent of continuous moist curing. In Chapter 8, it was reported that the 100 day shrinkage of the Lawns Lane Bridge repair materials stored in water for the first 28 days was between 44% and 90% of the shrinkage of the air cured specimens. The average was 62%. Although water curing will control shrinkage better than moist curing, nevertheless it will be assumed, for the purpose of better representing the tensile stress in the repair materials, that the curing membrane reduces the shrinkage of the repair materials to 62% of the free shrinkage of untreated repair materials.

10.2.1.6 Modified stress in the repaired section

Figures 10.17 to 10.19 show the stress in the repair patch of materials L4, L3 and G1 after modifying the properties of the repair materials as described in the previous section

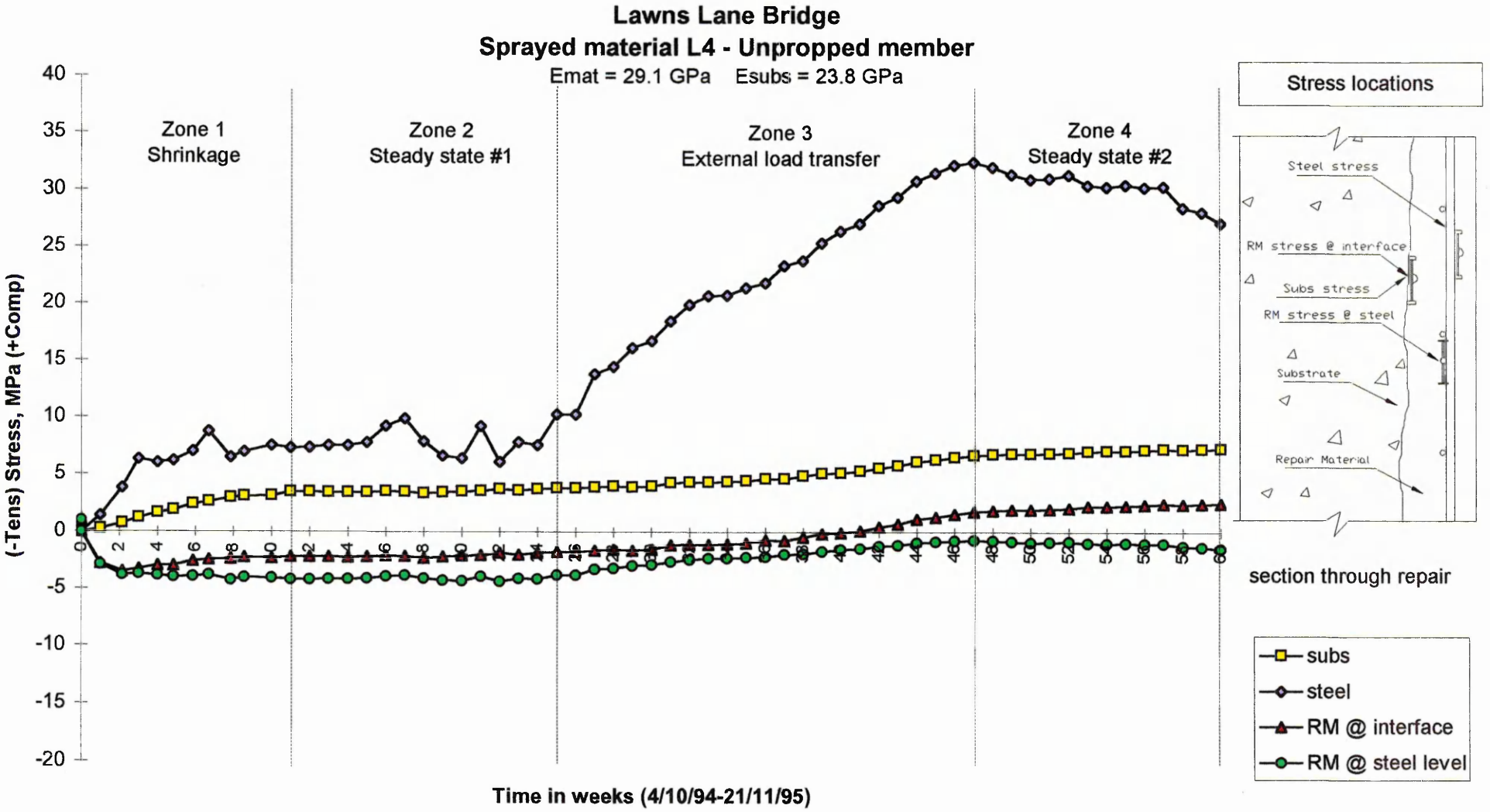

Figure 10.17 Modified stress distribution in repair patch of material L4 at Lawns Lane Bridge (Unpropped compression member)

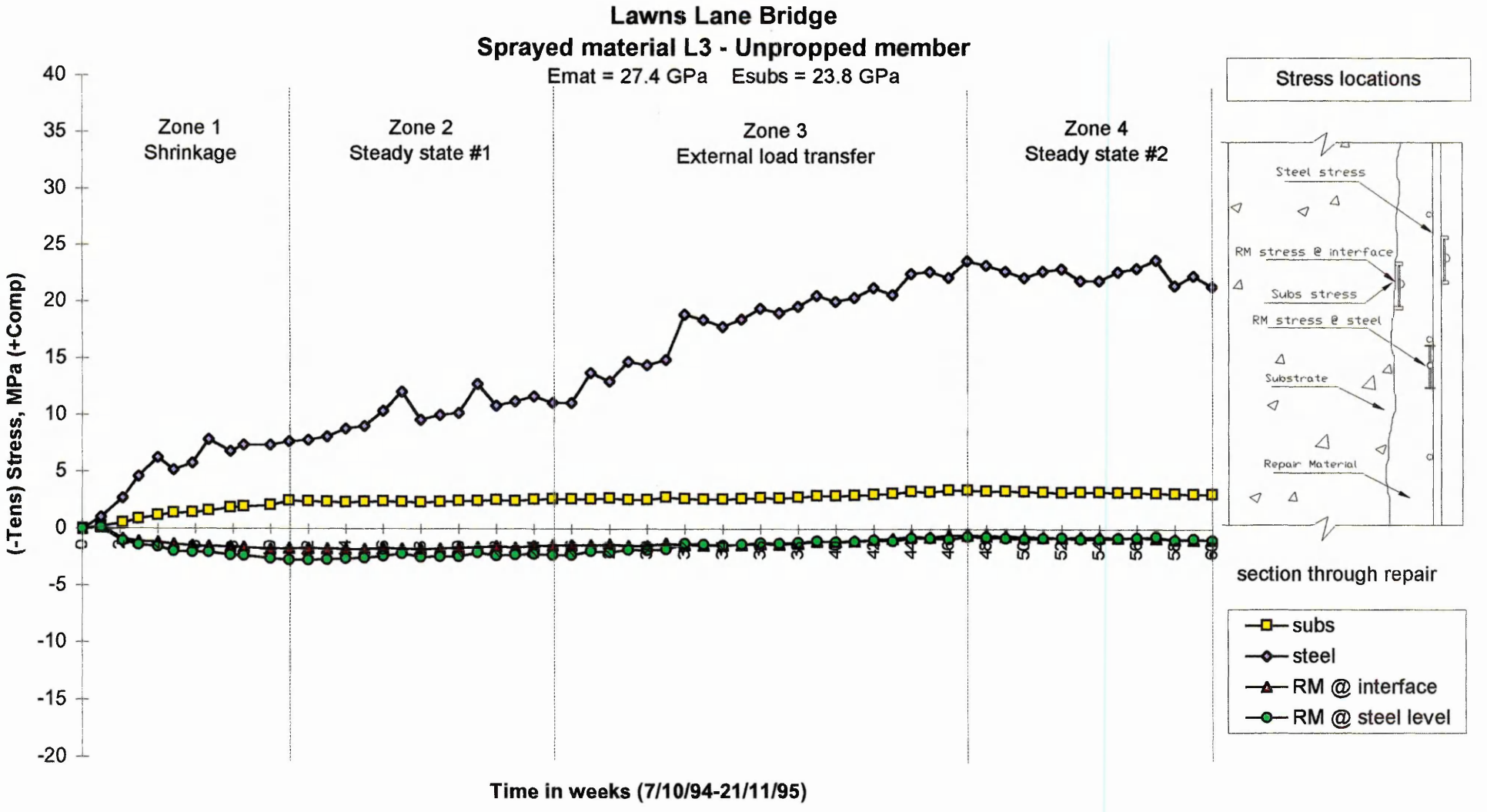

Figure 10.18 Modified stress distribution in repair patch of material L3 at Lawns Lane Bridge (Unpropped compression member)

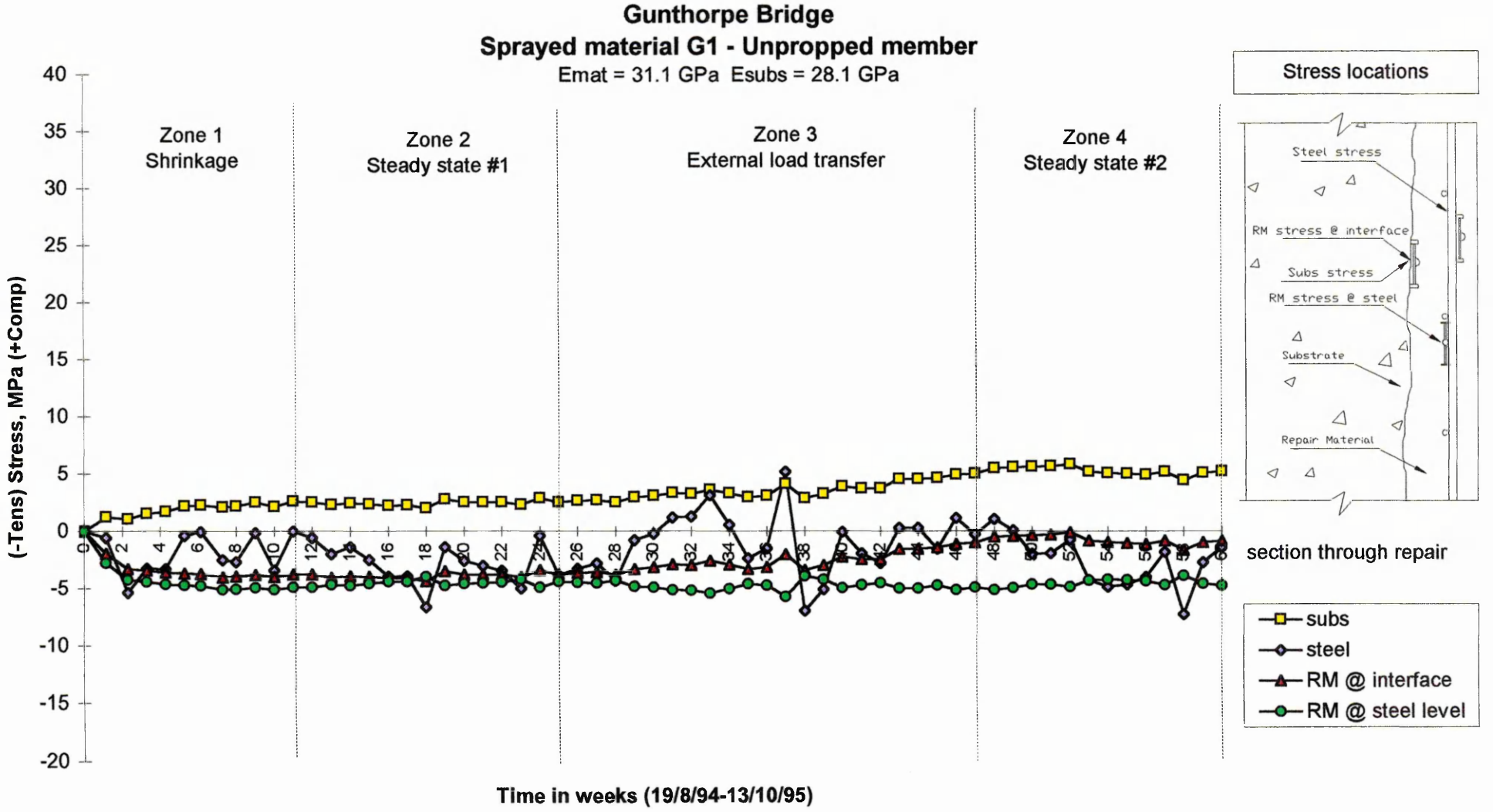

Figure 10.19 Modified stress distribution in repair patch of material G1 at Gunthorpe Bridge (Unpropped compression member)

i.e. the effect of tensile creep and lower elastic modulus in the early ages, the difference between compression and tension elastic modulus and correction to shrinkage data for curing membrane application. The stress in repair material L2 was not modified since creep data was not available for this repair material. The compressive stress in the substrate concrete and steel reinforcement did not alter form that presented in Figures 10.13 to 10.16. The results in Figures 10.17 to 10.19 show that the tensile stress in the repair material is lowered considerably as a result of applying the adjustments to the properties of the repair materials as outlined above (compare Figures 10.17 to 10.19 with Figures 10.13 to 10.16). The tensile stress in the repair material in both "RM @ interface" and "RM @ steel" (Figures 10.17 to 10.19) still increases within Zone 1, but the magnitude of stress is less than that of Figures 10.13 to 10.16. Furthermore, the tensile stresses in the repair material at the interface and steel reinforcement level ("RM @ interface" and "RM @ steel") show a negligible difference (compare "RM @ interface" and "RM @ steel" in Figures 10.17 to 10.19 with the equivalent in Figures 10.13, 10.14 and 10.16) In Zone 2, the stress again remains relatively constant since shrinkage had virtually ceased in the repair material (Figures 10.17 to 10.19). In the external load transfer stage (Zone 3, Figures 10.17 to 10.19), the tensile stress remaining in the repair material is reduced since external stress is attracted into the repair patch from the substrate concrete. The external compressive stress transfer neutralises the tensile stress at the interface ("RM @ interface") in material L4 at week 40 (Figure 10.17). In Zone 4 (Figures 10.17 to 10.19), the stress in the repair material remains relatively constant as before.

10.2.1.6.1 Further discussion

It is clear from the results presented in Figures 10.17 to 10.19 that the repair material exhibits a relatively high tensile stress in the shrinkage period (Zone 1), but this tensile stress in reduced or even completely neutralised through the transfer of external stress into the repair patch (Zone 3, Figures 10.17 to 10.19). It is vitally important that the stress in the repair material in Zone 1 (weeks 0 to 11) does not exceed the tensile strength of the repair material, otherwise cracking will occur and durability will become a problem. Obviously, the only way to ensure that the tensile stress in the repair material is low is to specify a repair material with low shrinkage characteristics. This is not a straight forward task, since virtually all of the repair materials tested in the current project exhibited considerable shrinkage, despite the claims from the manufacturers' that they were low shrinkage repair materials or were shrinkage compensated. Therefore, assuming that the material specified for a particular repair will undergo considerable shrinkage, is essential that the repair material exhibits an elastic modulus that is greater than the elastic modulus of the substrate concrete. In these instances, some of the shrinkage strain is transferred to the substrate concrete and steel reinforcement (see Figures 10.9 to 10.12). Hence, the virtual tensile strain in the repair material will be lower than its tensile strain capacity and consequently, the tensile stress could be reduced to acceptable levels. Clearly, cracking would be absent in the repair material. It has been observed in many instances in this project that a cracked repair material will not attract load into the repair patch. The benefit of a stiffer repair material attracting load into the repair patch is clear to see in the spray applied materials (Figures 10.17 to 10.19). The tensile stress in the repair material is reduced in the external load transfer stage (Zone 3, weeks 25 to 47). It was concluded in Chapter 8 that the modulus

of rupture of some repair materials decrease with time (see Section 8.5.4). Since the modulus of rupture is related to the direct tensile strength, the tensile strength of the repair material will also decrease with time. Consequently, if significant tensile stress is still evident in the repair patch even after a year of application, then cracking can occur due to a decrease of tensile strength in the repair material with time. This situation occurred with material L4 at Lawns Lane Bridge, where significant cracking occurred outside the monitoring period (see Figure 9.4). Referring to Figure 10.17, Zone 4, a small tensile stress is evident in the repair material in the repair patch of repair material L4 (see "RM @ steel", weeks 47 to 60). Obviously, the tensile strength of the repair material has decreased below this level and as a result, cracking occurred in the repair material.

10.2.1.7 Simplified stress distribution in the repaired section

Figures 10.20 to 10.23 show a simplified distribution of stress in the repair patch of materials L4, L3 and L2 at Lawns Lane Bridge and G1 at Gunthorpe Bridge. On occasions where the stresses plotted in Figures 10.17 to 10.19 exhibit irregular behaviour with time, an average stress is assumed in Figures 10.20 to 10.23. The stress distribution in the repair material in material L2 is omitted from Figure 10.22 since no data was available on the creep of this repair material, hence the modified stress could not be obtained. A summary of the stresses is also given in Table 10.6. Referring to Figures 10.20 to 10.23, the stress in the substrate concrete and steel reinforcement in Zone 1 increases linearly to reach a maximum at week 11. The stress in the substrate concrete and steel reinforcement is compressive, whereas the stress in the repair material

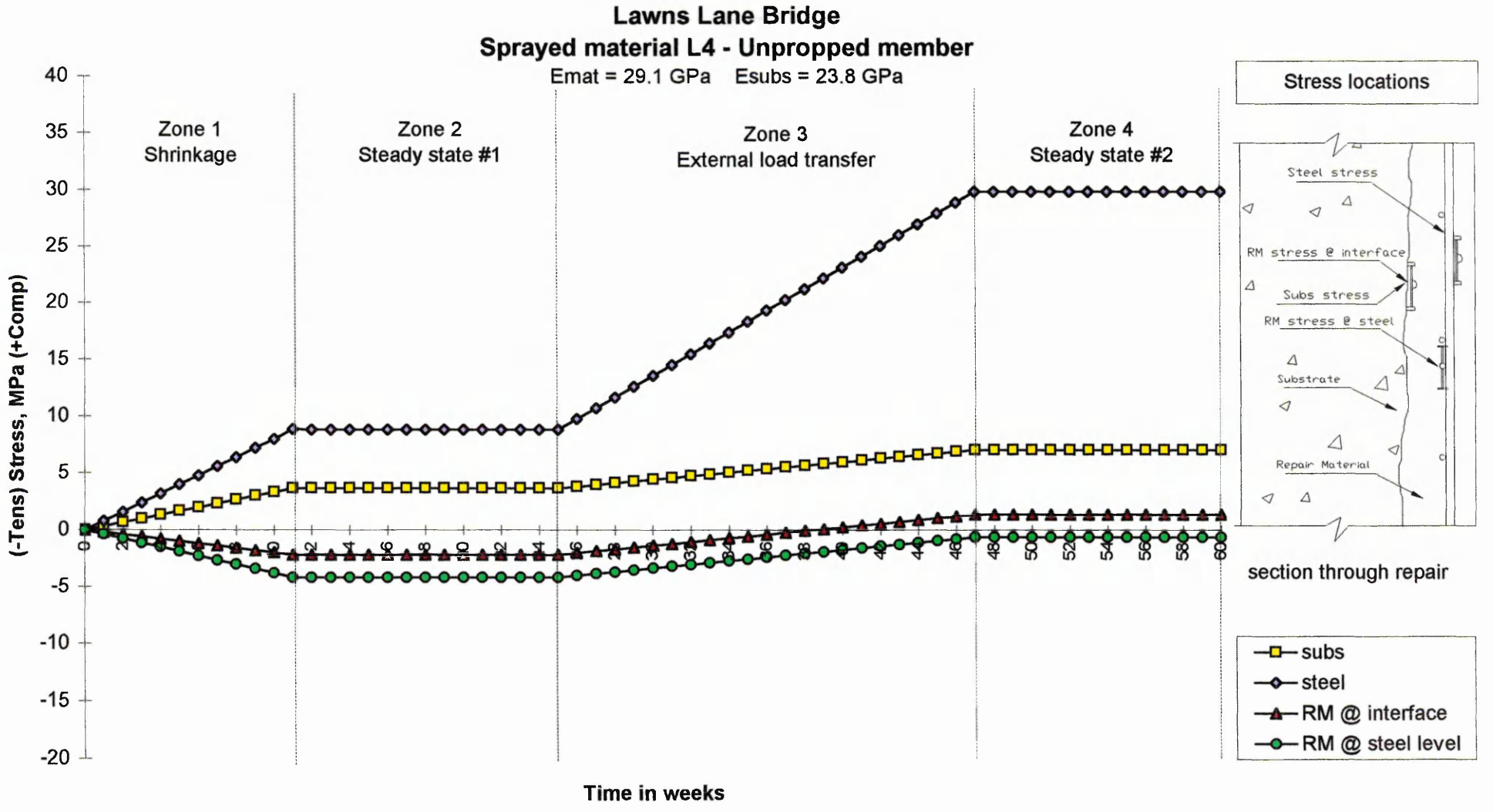

Figure 10.20 Simplified stress distribution in repair patch of material L4 at Lawns Lane Bridge (Unpropped compression member)

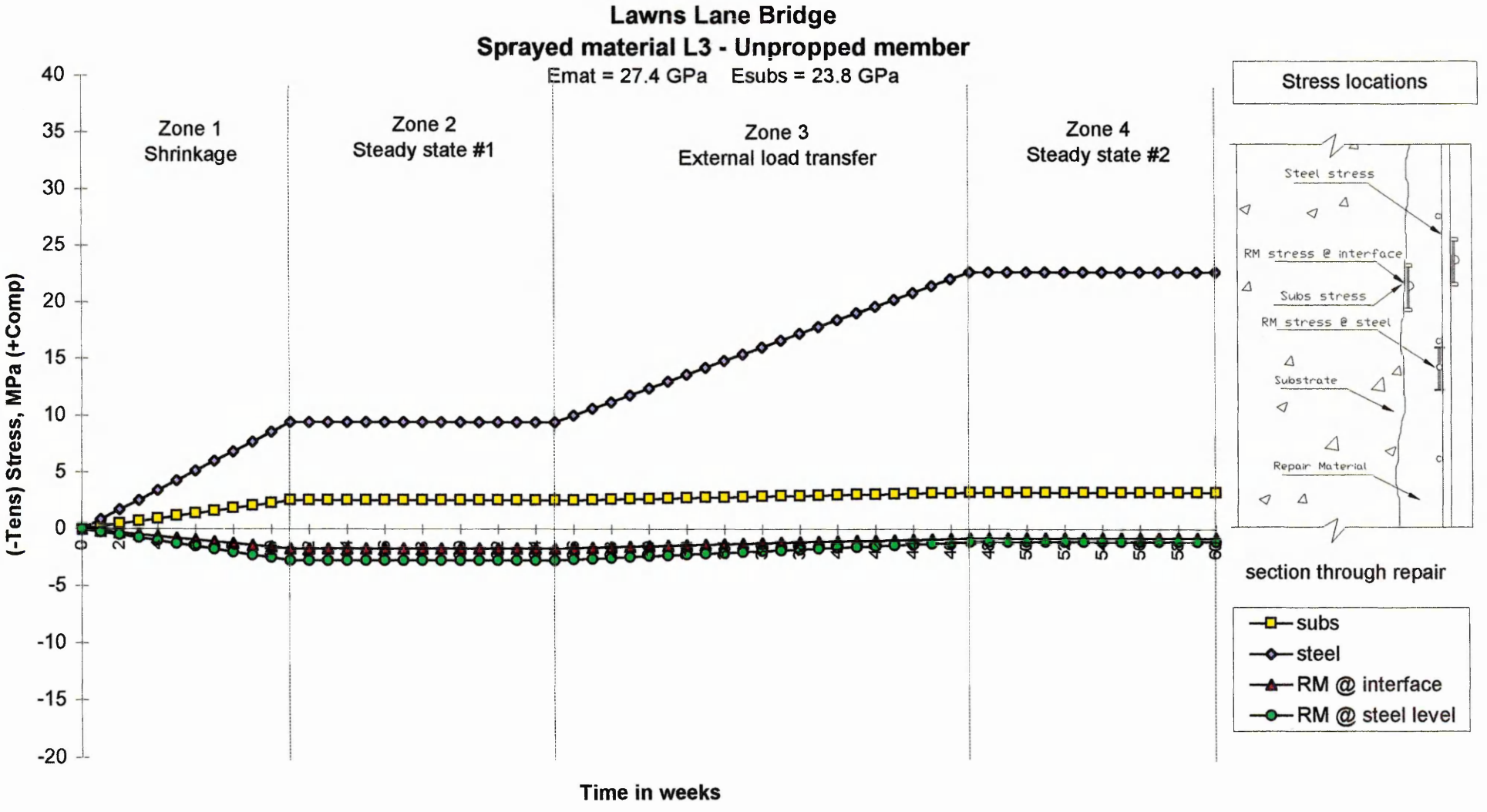

Figure 10.21 Simplified stress distribution in repair patch of material L3 at Lawns Lane Bridge (Unpropped compression member)

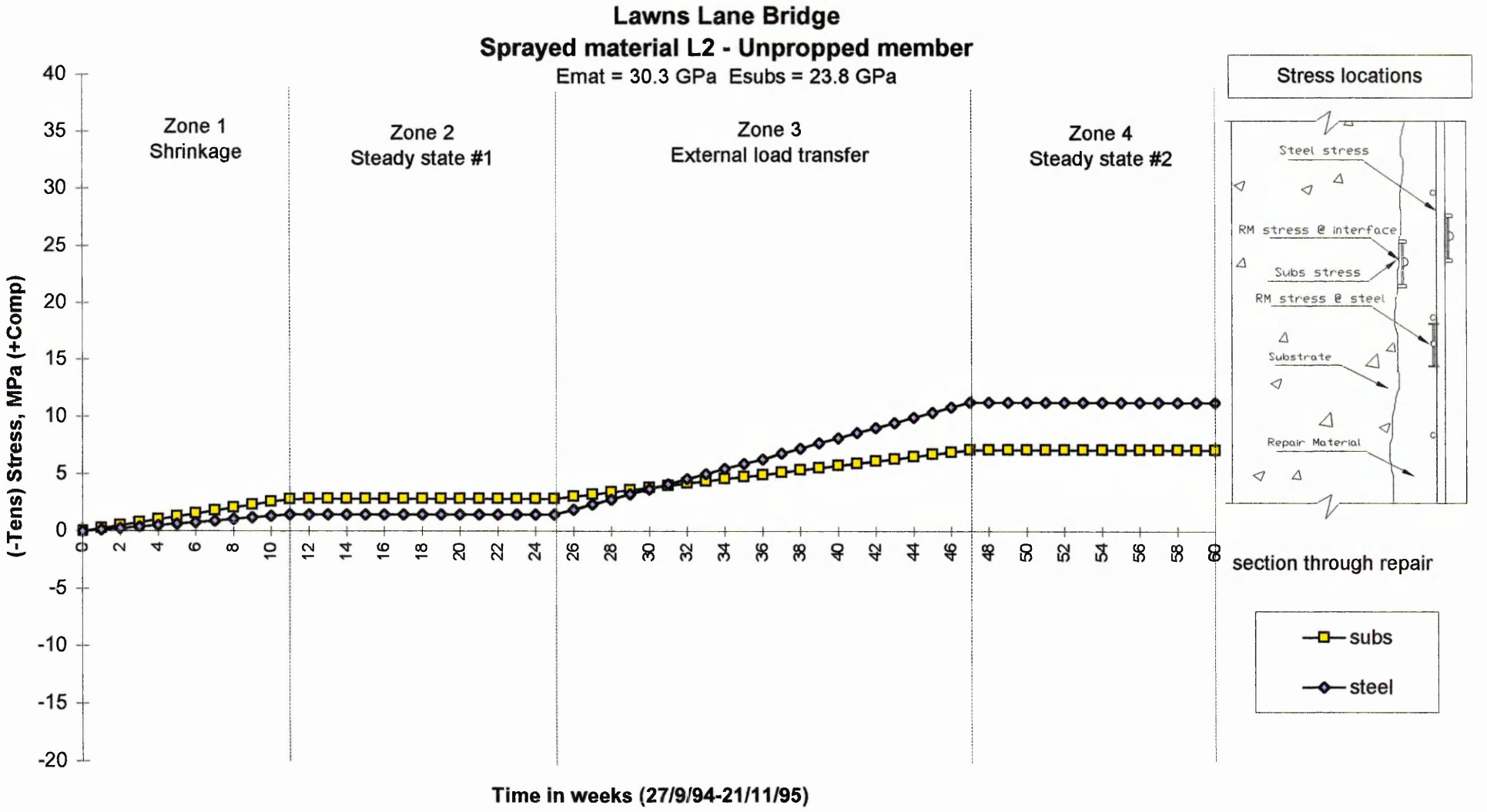

Figure 10.22 Simplified stress distribution in repair patch of material L2 at Lawns Lane Bridge (Unpropped compression member)

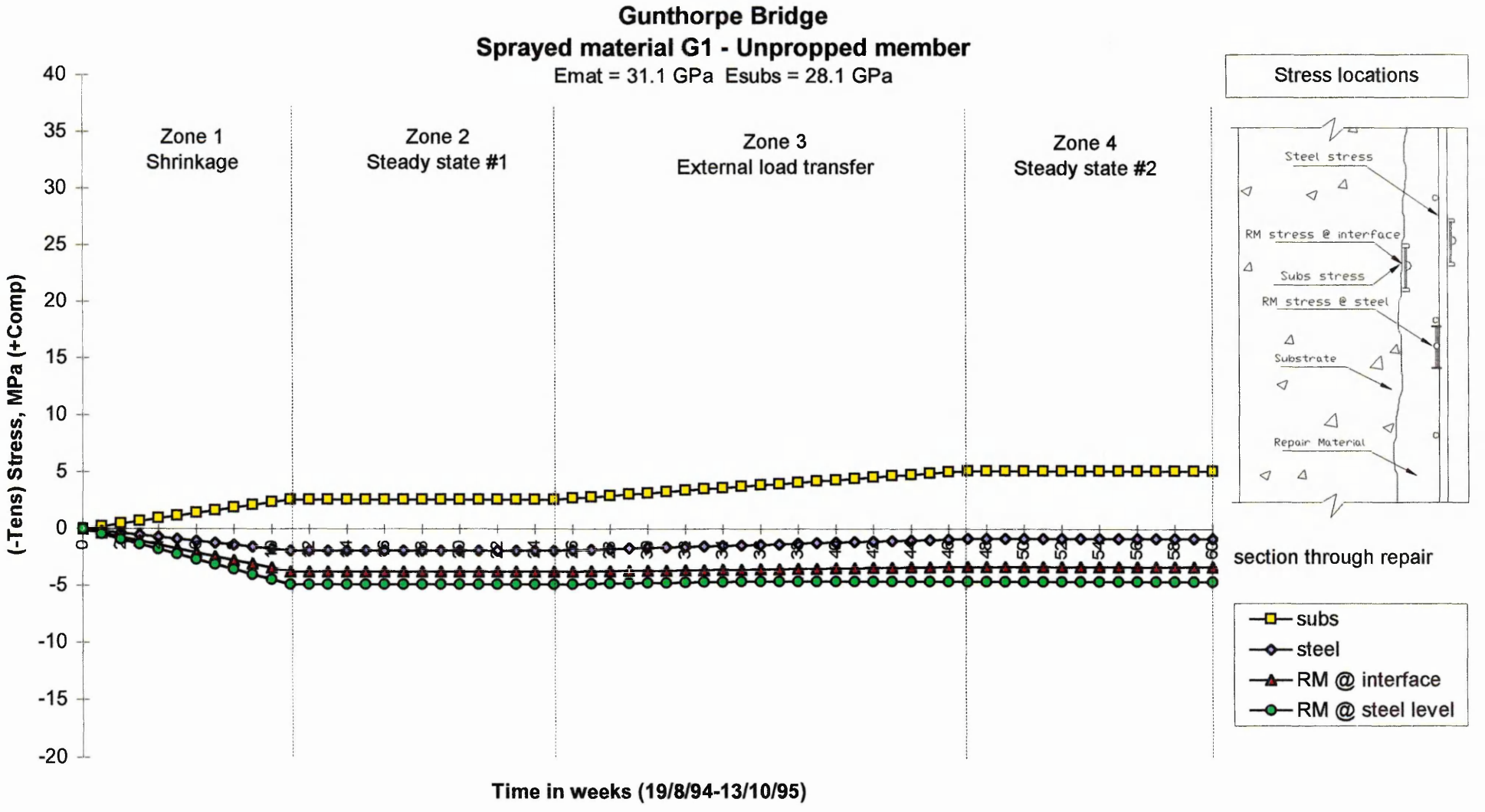

Figure 10.23 Simplified stress distribution in repair patch of material G1 at Gunthorpe Bridge (Unpropped compression member)

Table 10.6 Cumulative shrinkage and external load transfer stress in the repair patch

Material	*Location*	*Cumulative stress at end of: (N/mm²)*			
		Zone 1	*Zone 2*	*Zone 3*	*Zone 4*
		(week 11)	*(week 25)*	*(week 47)*	*(week 60)*
L4	subs	+3.7	+3.7	+ 7.1	+ 7.1
	steel	+8.8	+8.8	+29.8	+29.8
	RM @ interface	- 2.2	-2.2	+ 1.4	+ 1.4
	RM @ steel	- 4.2	-4.2	- 0.6	- 0.6
L3	subs	+2.5	+2.5	+ 3.3	+ 3.3
	steel	+9.5	+9.5	+22.7	+22.7
	RM @ interface	- 1.7	-1.7	- 0.8	- 0.8
	RM @ steel	- 2.7	-2.7	- 1.1	- 1.1
L2	subs	+2.8	+2.8	+ 7.1	+ 7.1
	steel	+1.5	+1.5	+11.3	+11.3
	RM @ interface	NA	NA	NA	NA
	RM @ steel	NA	NA	NA	NA
G1	subs	+2.6	+2.6	+ 5.1	+ 5.1
	steel	-1.9	-1.9	- 0.8	- 0.8
	RM @ interface	-3.8	-3.8	- 3.3	- 3.3
	RM @ steel	-4.9	-4.9	- 4.6	- 4.6

Note: Positive values indicate compressive stress; negative values indicate tensile stress (or loss in compression)

is tensile. The stress in steady state #1 remains constant for the substrate concrete, steel reinforcement and repair material from weeks 11 to 25 (Figures 10.20 to 10.23). In the external load transfer stage (Zone 3, Figures 10.20 to 10.23), the compressive stress increases linearly in the substrate concrete and steel reinforcement whereas the tensile

stress decreases in the repair material. In Zone 4, the steady state #2 period, the stress in the substrate concrete, steel reinforcement and repair material remain constant for the remainder of the monitoring period, weeks 47 to 60.

Referring to Figure 10.20 and Table 10.6, the stress in the substrate concrete at the end of Zone 1 is 3.7 N/mm^2. This stress is assumed to remain constant throughout Zone 2. The stress in the substrate concrete at the end of Zone 3, the external load transfer stage, increases to 7.1 N/mm^2 (compression). From week 47 onwards (Zone 4), the stress in the substrate concrete remains constant. The stress in the steel reinforcement also increases in compression throughout the monitoring period. The stress at the end of the shrinkage period, week 11, is 8.8 N/mm^2. This stress remains steady in Zone 2, before an increase is again observed in Zone 3 to 29.8 N/mm^2. The stress in the steel reinforcement remains constant in Zone 4. The tensile stress in the repair material at the substrate concrete/repair patch interface ("RM @ interface") and at the steel reinforcement level ("RM @ steel") is 2.2 and 4.2 N/mm^2 respectively at week 11. This stress remains constant in Zone 2 (weeks 11 to 25). The stress in "RM @ interface" changes to 1.4 N/mm^2 (compression) in Zone 3, whereas the stress in "RM @ steel" decreases to 0.6 N/mm^2 (tension). The stress in the repair material subsequently remains constant in Zone 4.

The simplified distribution of stress in the repair patch of material L3 is shown in Figure 10.21 and Table 10.6. The stress in the substrate concrete and steel reinforcement increases in compression to reach 2.5 N/mm^2 and 9.5 N/mm^2 respectively at week 11. These stresses remain constant in Zone 2, but an increase in compression is again

observed in Zone 3, the external load transfer stage to 3.3 N/mm^2 and 22.7 N/mm^2 respectively. From week 47 onwards, the stress in the substrate concrete and steel reinforcement remain constant. The stress in the repair material ("RM @ interface" and "RM @ steel") in Zone 1 is 1.7 N/mm^2 and 2.7 N/mm^2 (tension) respectively. These stresses remain constant in Zone 2 before a slight decrease in tension is observed in Zone 3 to 0.8 and 1.1 N/mm^2 respectively. The stresses in the repair material at the end of Zone 3 remain constant in Zone 4.

The stress in the substrate concrete and steel reinforcement for material L2 is given in Figure 10.22 and Table 10.6. The stress in the repair material was not obtained since data on creep was not available for this material. The compressive stress in the substrate concrete and steel reinforcement increase linearly to 2.8 and 1.5 N/mm^2 respectively at the end of the shrinkage period, week 11. These stresses remain constant until the end of Zone 2. The stress in the substrate concrete and steel reinforcement increase to 7.1 and 11.3 N/mm^2 by the end of Zone 3 when external load is transferred into the repair patch. The stresses are constant throughout Zone 4.

Figure 10.23 and Table 10.6 show the stresses in the substrate concrete and steel reinforcement in the shrinkage period for material G1 at Gunthorpe Bridge. The stress in the substrate concrete at the end of the shrinkage period (week 11) is 2.6 N/mm^2. This stress is assumed to remain constant in Zone 2 but increases to 5.1 N/mm^2 by the end of Zone 3. This stress remains constant throughout Zone 4. The stress in the steel reinforcement in the repair patch of material G1 exhibits a different stress pattern to previous cases. It shows a reduction in compression in the shrinkage period (-1.9

N/mm^2) and remains constant throughout Zone 2. The stress decreases in tension to -0.8 N/mm^2 by the end of Zone 3 and remains constant in Zone 4. The tensile stress in the repair material ("RM @ interface" and "RM @ steel") at the end of Zone 1 (week 11) is 3.8 N/mm^2 and 4.9 N/mm^2 respectively. These stresses remain constant in Zone 2. A very slight reduction in tensile stress is observed in Zone 3, as external stress is attracted into the repair patch (3.3 N/mm^2 and 4.6 N/mm^2 in tension respectively). As before, these stresses remain constant in Zone 4.

Table 10.7 shows the stress developed in the substrate concrete, steel reinforcement and repair material in Zone 1 and Zone 3 from Figures 10.20 to 10.23. Tensile stress is apparent in the repair material in Zone 1. In Zone 3, the repair materials go into compression along with the substrate concrete steel reinforcement. Referring to Table 10.7, Zone 1, the compressive stress in the substrate concrete for materials L4, L3, L2 and G1 ranges between 2.5 N/mm^2 and 3.7 N/mm^2. This variation is due to the varying differences in the elastic modulii of repair materials and substrate concretes, and also due to the different shrinkage of the repair materials (see Table 10.3). The stress in the steel reinforcement ranges from a loss in compression of 1.9 N/mm^2 to a gain in compression of 9.5 N/mm^2. Again, repair material properties (elastic modulus and shrinkage) are responsible for these variations. Repair material properties are not responsible for the loss in compression of the steel reinforcement in material G1 - this loss of compressive stress is probably attributed to experimental error (i.e. the strain gauge may have malfunctioned in the repair patch). The stresses in the repair materials during the shrinkage stage are all tensile, since the substrate concrete and steel reinforcement provide a partial restraint to shrinkage. The highest tensile stress is

Table 10.7 Average stress due to restraint to shrinkage and external load transfer

Material	*Location*	*Stress in: (N/mm²)*	
		Zone 1	*Zone 3*
		(weeks 0 to 11)	*(weeks 25 to 47)*
L4	subs	+3.7	+3.4
	steel	+8.8	+21.0
	RM @ interface	-2.2	+3.6
	RM @ steel	-4.2	+3.6
L3	subs	+2.5	+0.8
	steel	+9.5	+13.2
	RM @ interface	-1.7	+0.9
	RM @ steel	-2.7	+1.6
L2	subs	+2.8	+4.3
	steel	+1.5	+9.8
	RM @ interface	NA	NA
	RM @ steel	NA	NA
G1			
	subs	+2.6	+2.5
	steel	-1.9	+1.1
	RM @ interface	-3.8	+0.5
	RM @ steel	-4.9	+0.3

Note: Positive values indicate compressive stress; negative values indicate tensile stress

in material G1 (4.9 N/mm^2) at the steel reinforcement level. This is because repair material G1 has the highest modified free shrinkage and lowest transfer of shrinkage to the steel reinforcement (see Table 10.3). In the External load transfer stage (Zone 3, Table 10.7), the substrate concrete for all materials (L4, L3, L2 and G1) exhibits varying compressive stress (0.8 N/mm^2 to 3.4 N/mm^2). This is because different levels of

external stress is attracted into the repair patches. For instance, material L3 has the lowest elastic modulus (Table 10.3) of the four materials under observation, and as a result, attracts the lowest magnitude of stress. The stress in the steel reinforcement after transfer of external stress also shows a wide variation for the repair materials (1.1 to 21.0 N/mm^2), again due to a variation in repair material properties. The stress attracted into the repair materials varies from 0.3 N/mm^2 (material G1) to 3.6 N/mm^2 (material L4). The difference in elastic modulus between the substrate concrete and repair material L4 is greater than the corresponding difference between the substrate concrete and repair material G1 (Table 10.3). As a result, material L4 attracts more external stress into the repair patch (see Table 10.7).

10.3 CONCLUSIONS

The following conclusions are based on the information presented in this chapter:

- Four stages of stress are evident in spray applied repairs to unpropped compression members:
  - (i) shrinkage stage (Zone 1, weeks 0 to 11)
  - (ii) steady state #1 (Zone 2, weeks 11 to 25)
  - (iii) external load transfer (Zone 3, weeks 25 to 47)
  - (iv) steady state #2 (Zone 4, weeks 47 to 60)
- Tensile stress is evident in the repair material in Zone 1 (weeks 0 to 11) due to the partial restraint to shrinkage provided by the substrate concrete and steel reinforcement.

- Compressive stress is transferred to the substrate concrete and steel reinforcement during shrinkage (contraction) of the repair material within Zone 1.
- Stresses in the repair material, substrate concrete and steel reinforcement remain constant in Zone 2 (weeks 11 to 25) since shrinkage in the repair material had reached negligible levels.
- Tensile stress in the repair material is reduced (or changes to compression) after external (compressive) load is transferred from the substrate concrete in Zone 3 (weeks 25 to 47).
- Stresses in the repair material, substrate concrete and steel reinforcement at the end of Zone 3 remain constant in Zone 4 (weeks 47 to 60) since the transfer of external load transfer from the substrate concrete has ceased.
- Tensile stress may be evident in the repair material in the long term if insufficient external load is attracted into the repair material to neutralise the tensile stress.
- Stress relaxation due to tensile creep in the repair material reduces the tensile stress caused by the restraint to shrinkage provided by the substrate concrete and steel reinforcement.

CHAPTER 11

A THEORY FOR REPAIR MATERIAL INTERACTION IN COMPRESSION MEMBERS

11.1 INTRODUCTION

Reinforced concrete is the most widely used construction material in the world due to its relatively low cost and ease of placing. It gives excellent durability when designed, constructed and maintained correctly, justifying the design lives of 60 or 120 years [102]. However, when the effects of inadequate detailing, poor workmanship or severe exposure to harsh environments are experienced, the steel reinforcement corrodes which leads to spalling of the concrete. The design life of the structure can be extended by replacing the damaged concrete with a new material. This process can prove to be successful if the repair material is selected on the basis of an adequate understanding of the interaction between the substrate concrete and repair material. Too often, this is not the case and materials are applied with little knowledge of their long term performance under service conditions. Therefore, information is required that will allow repair materials to be used that will restore the integrity of the structure.

In this chapter, simple mathematical expressions to predict the distribution of stress across the repair patch due to shrinkage in the repair material and redistribution of external load into the repair patch are derived. A brief review is also given on the

current literature on predictive procedures for the performance of repair patches under service conditions.

11.2 LITERATURE REVIEW

11.2.1 Analytical models for concrete repair

Previous research into the performance of reinforced concrete repair carried out at Sheffield Hallam University [24] involved deriving a mathematical expression to predict the total strain ratio between the repair material and substrate concrete at any time, *t*. Column specimens measuring 150mm x 150mm x 750mm long were used in the investigation and reinforced with four 12mm diameter high yield steel bars.

The specimens were loaded in compression 28 days after casting and the deformation due to shrinkage and creep was monitored for 120 days. To simulate deterioration due to reinforcement corrosion, centrally located voids on two opposite faces of the columns were cut to a depth of 55mm and length 220mm and patch repaired. A simple mathematical expression to determine the total strain ratio, $(\varepsilon_R/\varepsilon_C)_t$, between the repair material and concrete substrate was derived as [24]:

$$\left(\frac{\varepsilon_R}{\varepsilon_C}\right)_t = \left[\frac{\left(\frac{\sigma_R}{E_R}\right)_{to}\left[1+\phi_{R(to,t)}\right]+\frac{\sigma_{R(t)}-\sigma_{R(to)}}{E_{R(to)}}x\left[1+\chi_{R(to,t)}\phi_{R(to,t)}\right]+K_1\varepsilon_{shR(to,t)}}{\left(\frac{\sigma_C}{E_C}\right)_{to}\left[1+\phi_{C(to,t)}\right]+\frac{\sigma_{C(to,t)}-\sigma_{C(to)}}{E_{C(to)}}x\left[1+\chi_{C(to,t)}\phi_{C(to,t)}\right]+K_2\varepsilon_{shC(to,t)}}\right]$$

Equation 11. 1

where

ε_R = total strain on repair patch

ε_C = total strain on substrate concrete, at any time t, in terms of the creep properties and modulus of elasticity of the materials, and the varying sustained stress applied on the concrete and repair cross-section.

t_0 = age at first application of load

E_C = modulus of elasticity of concrete substrate

E_R = modulus of elasticity of repair material

ϕ = creep coefficient

χ = ageing coefficient

K_1 ,K_2 = constants for volume/surface correction

A comparison between the experimental and theoretical total strain (including elastic, creep and shrinkage strain) of the repair patch and substrate concrete at different ages under load showed close agreement. Equation 11.1 relates to the performance of repair to a propped compression member (column) under serviceability conditions.

Yuan and Marosszeky [103] reported on long term tests to investigate the performance of structural concrete repair. Reinforced concrete beams with repair patches in both the tension and compression zones were repaired using three types of polymer-cement concrete. These repair concretes were formed by modifying concrete with acrylic, SBR and styrene-acrylic. A lever-arm load system (lever arm ratio 1:9) was used for the long term tests. Their results show that the major factors which influence the performance of

structural repair include free shrinkage, creep coefficient and tensile strength. The ultimate tensile strain at early ages was also shown to be very important. An analytical method for predicting the strain in a repair patch was developed [103] and compared with the results of the test beams. The effect of free shrinkage, tensile creep, tensile strength and modulus of elasticity of the repair material on restrained shrinkage were included in the analytical method. The strain in the repair concrete obtained from laboratory tests showed good correlation with values obtained from the analytical method (see Figure 11.1 [103]).

Yuan and Marosszeky [103] found that a tensile strain of 109 microstrain occurred in the substrate concrete near the repair interface on the first day after repair. This tensile strain was reportedly due to the expansion of the SBR modified concrete within 24 hours. Based on the results from the current project, a repair material with an elastic modulus greater than that of the substrate concrete is able to transfer some strain to the substrate concrete. It is unlikely, however, that the elastic modulus of the repair concrete in the previous research [103] was sufficient to transfer shrinkage strain to the substrate concrete after 24 hours, hence, the increase in strain on the substrate concrete must be due to other effects. No information was given on the elastic modulus of the repair concrete.

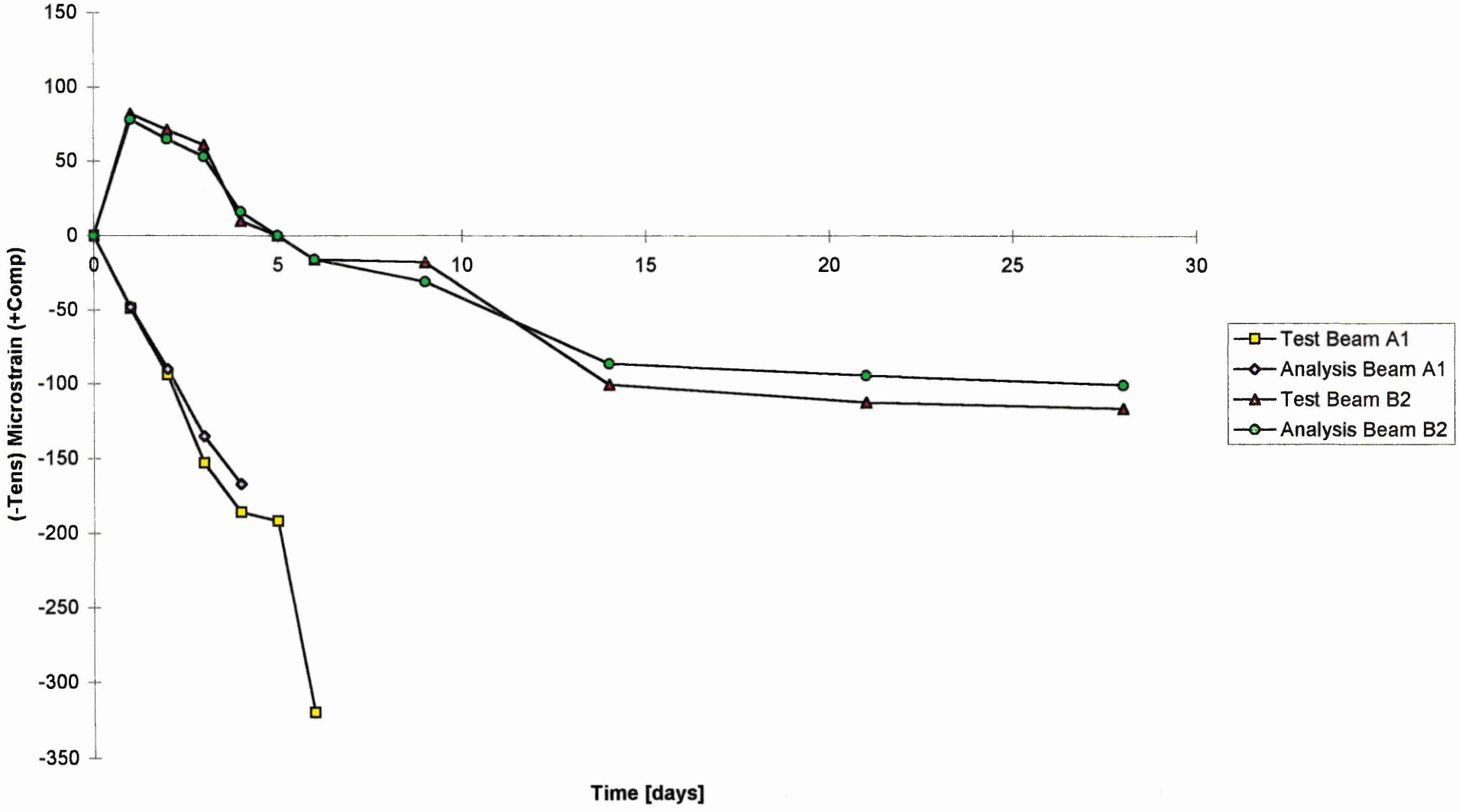

Figure 11.1 Comparison between laboratory tests and analysis [103]

11.3 A THEORY TO PREDICT THE STRUCTURAL INTERACTION IN REPAIRED MEMBERS

In this section, a theory is presented that predicts the structural interaction in repaired reinforced concrete structures. The theory is applicable to all repair techniques, but the field data from the spray applied repair materials to unpropped members in compression is used to verify the validity of the analysis. It also assumes that the elastic modulus of the repair material is greater than the elastic modulus of the substrate concrete.

It has been stated previously that a repair material with an elastic modulus greater than the elastic modulus of the substrate concrete will transfer a portion of the shrinkage strain to the substrate concrete. The amount of shrinkage strain that is transferred to the substrate concrete depends on the difference in elastic modulus between the repair material and substrate concrete (i.e. the modular ratio). The higher the modular ratio, the higher the shrinkage transfer to the substrate concrete. This is shown with reference to Figure 11.2. The relationship between m, the modular ratio (E_{rm} / E_{sub}), and λ, the percentage of free shrinkage strain transferred to the substrate concrete, is given for the four spray applied materials to unpropped members in compression. λ is obtained by dividing the strain in the substrate concrete at the end of the shrinkage period at week 11, $\varepsilon_{sub(shr)}$ (Table 10.2 and Figures 10.5 to 10.8, week 11) by the free shrinkage strain in the repair material at the same age, Table 10.3. The strain in the substrate concrete, $\varepsilon_{sub(shr)}$, was measured by means of a vibrating wire strain gauge attached to the cut-back substrate in the abutments/columns of the bridges investigated (see Figure 5.5). The free shrinkage of the repair materials, $\varepsilon_{shr(free)}$, was obtained by casting prisms in the laboratory and monitoring the shrinkage deformation that occurred over a period of

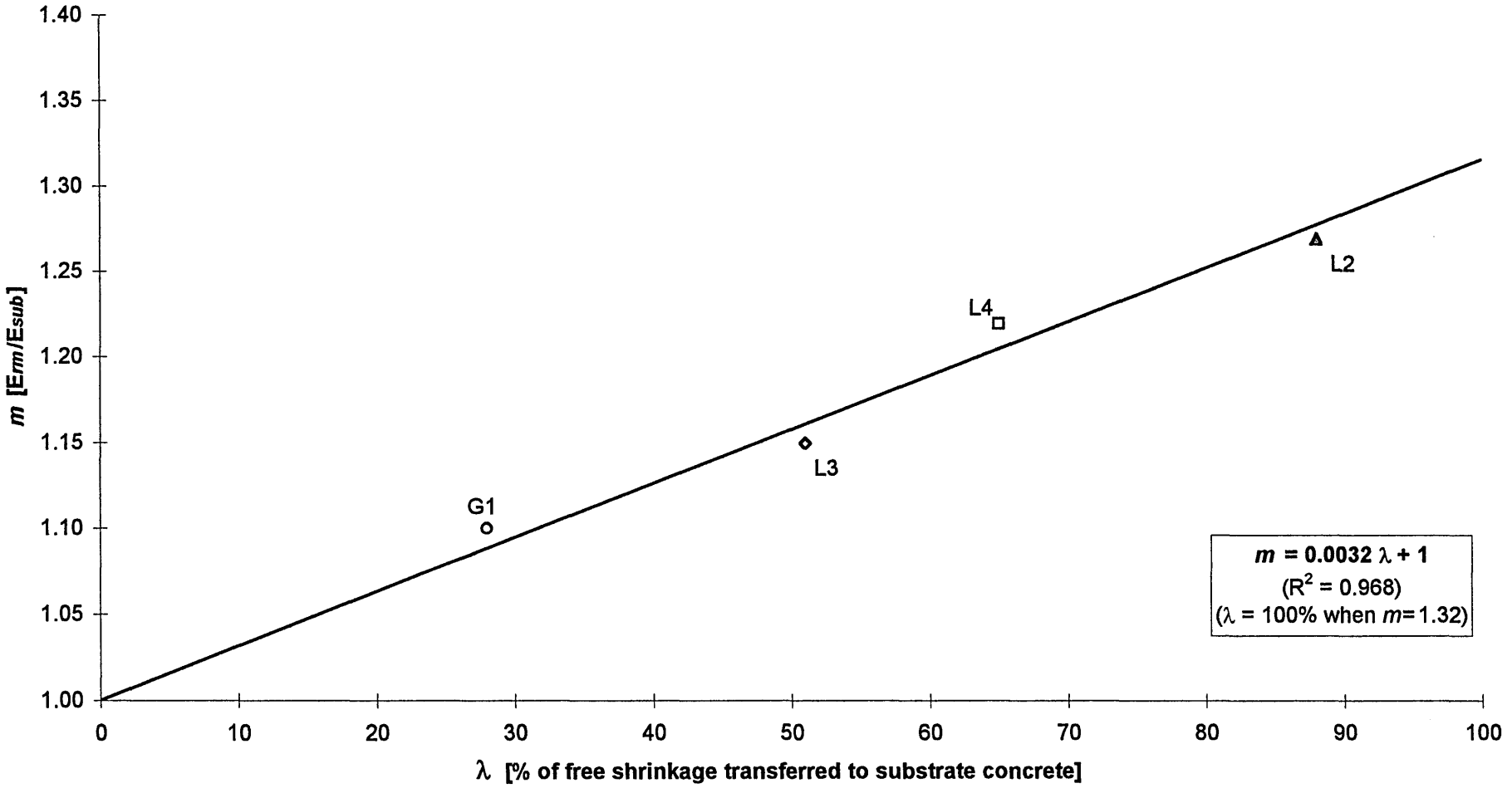

Figure 11.2 Modular ratio versus percentage of free shrinkage transferred to the substrate concrete, $E_{rm} > E_{sub}$ (spray applied materials to unpropped members in compression)

100 days (curing conditions: 20°C and 55% RH - full details are given in Chapter 8, Sections 8.3 and 8.4). These free shrinkage readings were then modified to take into account differences that existed between laboratory and field specimens. For instance, the surface/volume ratio differed for both laboratory and field materials (a higher surface/volume ratio would contribute to higher free shrinkage), therefore an allowance was made for this. Corrections, where applicable, were made to take into account the difference in temperature and relative humidity between laboratory and field materials. Finally, a correction for the efficiency of the curing compounds that were applied to the surface of the repair materials at Lawns Lane Bridge was also made. A summary of Figure 11.2 is also given in Table 11.1. Referring to Table 11.1, the abbreviations of the four repair materials under observation are given in column 1. The modular ratio between the repair material and substrate concrete (E_{rm} / E_{sub}) is given in column 2. The deformation in the substrate concrete, $\varepsilon_{sub(shr)}$, after transfer of shrinkage strain from the repair material at week 11 is shown in column 3. The free shrinkage of the repair materials, $\varepsilon_{shr(free)}$, at the end of the shrinkage period, week 11, is shown in column 4. Finally, λ, the ratio of transferred shrinkage strain to the free shrinkage strain, is given in column 5.

Figure 11.2 shows a strong linear relationship between m and λ, even though data from only four repair materials were available on different bridges (materials L4, L3 and L2 from Lawns Lane Bridge, and material G1 from Gunthorpe Bridge). The coefficient of variation (R^2) is 0.968. Referring to Figure 11.2, when the elastic modulus of the repair material is equal (or less) than the elastic modulus of the substrate concrete (m =1), then the repair material is fully restrained by the substrate concrete and, therefore, it is

Table 11.1 Percentage of free shrinkage strain transferred to substrate concrete, λ

		Column		
1	2	3	4	5
Repair material	m $\left(\frac{E_{rm}}{E_{sub}}\right)$	$\varepsilon_{sub(shr)}$ (microstrain)	$\varepsilon_{shr(free)}$ (microstrain)	λ (%)
L4	1.22	154	238	65
L3	1.15	107	210	51
L2	1.27	120	136	88
G1	1.10	92	329	28

unable to transfer shrinkage strain to the substrate concrete (λ = 0%). On the other hand, full shrinkage strain transfer will occur (λ = 100%) when the modular ratio between the repair material and substrate concrete is approximately 1.32 (see Figure 11.2). For example, the elastic modulus of the substrate concrete at Lawns Lane Bridge is 23.8 kN/mm^2. A repair material with an elastic modulus of 31.4 kN/mm^2 (E_{sub} x 1.32) would then theoretically transfer all free shrinkage to the substrate concrete.

11.3.1 Spring analogy to represent interaction between repair material and substrate concrete

Figure 11.3 (a) shows an oblique view of a compression member repaired in the unpropped state. The repair material has an elastic modulus that is greater than the elastic modulus of the substrate concrete, and as a result, transfers shrinkage strain to the substrate concrete in the shrinkage stage, week 0 to week 11, see Figures 10.5 to 10.8. The influence of the steel reinforcement on the transfer of shrinkage strain is omitted for simplification and clarity. Since the substrate concrete has an infinite thickness

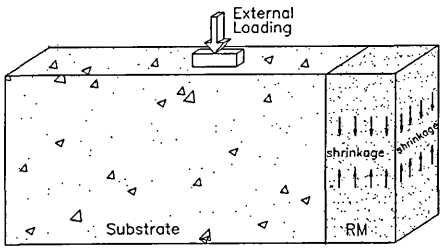

(a) oblique view of repaired compression member

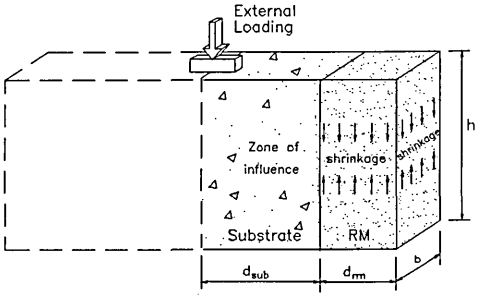

(b) shrinking repair material assumed to influence the substrate concrete to a depth of d_{sub}

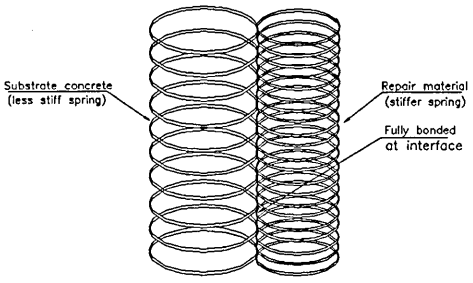

(c) springs of different stiffness represent the repair material and substrate concrete

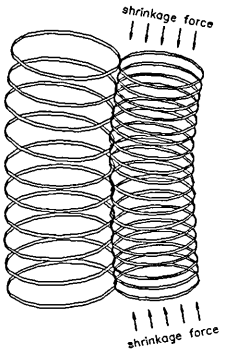

(d) stiffer spring deforms and simultaneously transfers strain to less stiff spring (strain compatibility).

Figure 11.3 Spring analogy to represent the interaction between the the repair material and substrate concrete
Method of repair: spray applied
Properties: repair material stiffer than substrate concrete
Support during repair: unpropped
Steel reinforcement omitted for clarity

compared with the thickness of repair material, it is impossible for the repair material to transfer strain across the full depth of the substrate concrete. Therefore, the shrinking repair material is assumed only to influence an area adjacent to the interface between the repair material and substrate concrete. This zone of influence, as shown in Figure 11.3 (b), is assumed to have a depth of d_{sub}. Knowing that the repair material is dimensionally unstable (i.e. shrinkage will cause contraction of the repair material), compression will be forced into the substrate concrete as the stiffer repair material deforms. Consequently, deformation is evident in both the repair material and substrate concrete, since full bond exists between both materials. The simultaneous deformation of the repair material and substrate concrete in the shrinkage period (Zone 1, Figure 10.5 to 10.8), can be represented by the analogy of two deforming springs connected in parallel, as shown in Figure 11.3 (c). The repair material is represented by a spring with a high stiffness whereas the substrate concrete is represented by a spring with a lower stiffness. Both springs are assumed to be fully bonded at the interface. When the stiffer spring deforms due to shrinkage (in the repair material), the less stiff spring will provide partial restraint to deformation in the stiffer spring. Nevertheless, net deformation will occur in the stiffer spring (repair material), and as a result, compression will be forced into the less stiff spring (substrate concrete). Both springs will exhibit similar strains at the interface due to strain compatibility. The free surface of the stiffer spring will undergo greater compressive strain (equivalent to the net shrinkage of the repair material) than the interface with the substrate concrete due to shrinkage restraint. This will result in a bending effect in the spring system, as shown in Figure 11.3 (d). This bending effect is used as a basis to predict the distribution of shrinkage strain across the repair patch as described in the next section.

11.3.2 Distribution of shrinkage strain using analogy of bi-metallic strip

Referring to Section 11.3, the eccentric effects resulting on the spring system in Figure 11.3 (d) causes bending in the system which represents the repair material and the 'zone of influence' of the substrate concrete. Therefore, the deformation in the spring system, and consequently in the repair patch, can be compared to the analogy of a bi-metallic strip undergoing differential contraction. A bi-metallic strip consists of two dissimilar materials which are perfectly joined at the interface so that they deform together when the temperature is raised or decreased. The coefficients of thermal expansion are different for both metals, therefore, one metal has the tendency to deform more than the other metal when the temperature is decreased (or raised). An elevation of a bi-metallic strip is shown in Figure 11.4 (a). The strip consists of two dissimilar materials, labelled A and B, which exhibit different coefficients of expansion (or in the context of the research, shrinkage strain). Figure 11.4 (b) shows an enlarged elevation of a portion of the bi-metallic strip at the datum temperature. Assuming that the materials are not joined at their common interface, both materials would contract freely as shown in Figure 11.4 (c) when the temperature is decreased, since the coefficient of expansion is different for both materials. The contraction shown from Figure 11.4 (c) onwards is exaggerated for clarity. Material A contracts from the datum position (Level 0) to Level 1. On the other hand, material B contracts from Level 0 to Level 2. In reality, due to perfect bond at the interface, both materials contract equally at the interface (Level 0 to Level 3) under a drop in temperature, as shown in Figure 11.4 (d), although a strain gradient will be evident across the strip. Referring to Figure 11.4 (d), material A will be forced to contract more due to the action of the bi-metallic strip. Therefore,

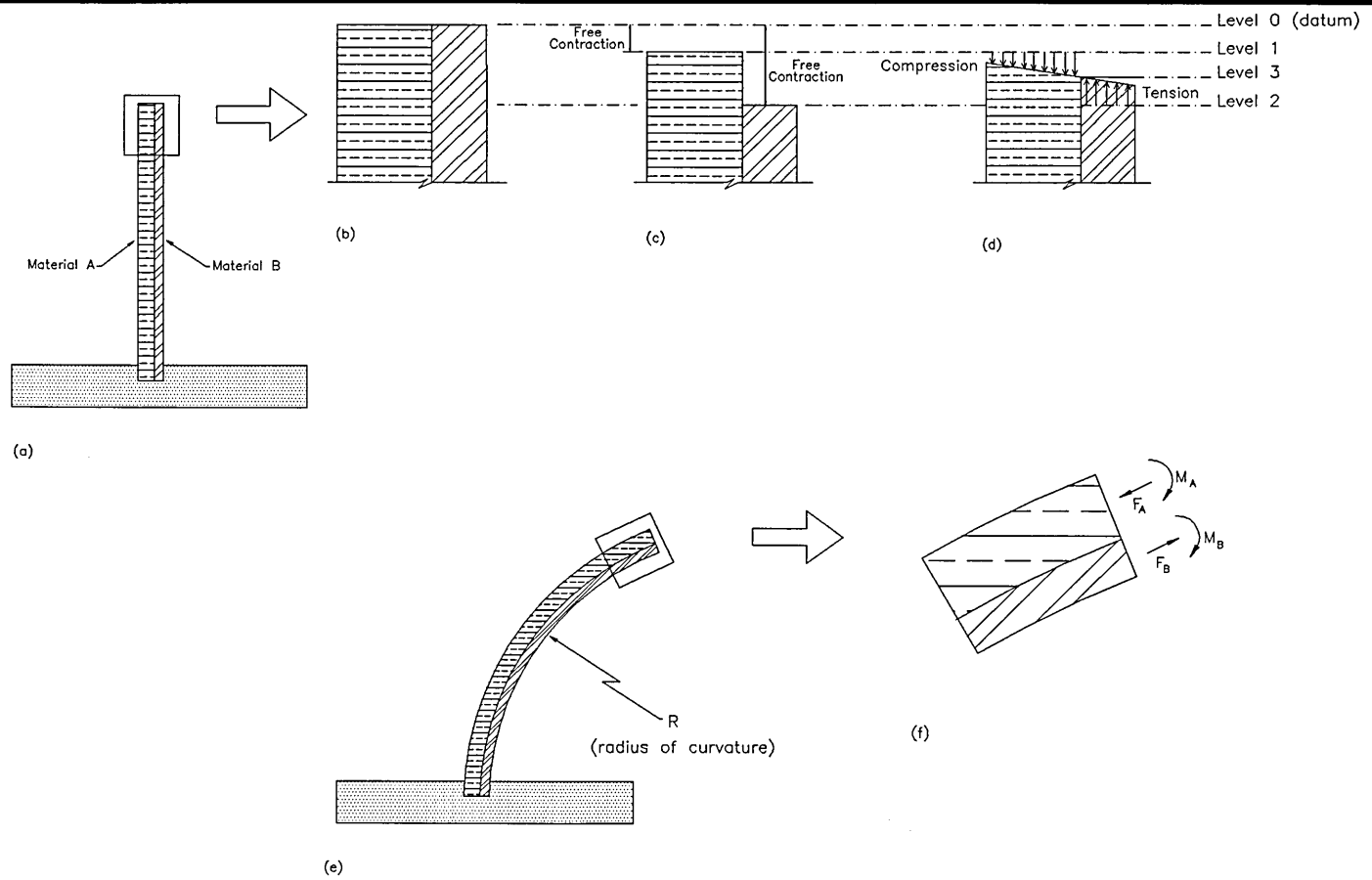

Figure 11.4 Deformation in a bi–metallic strip when subjected to a drop in temperature
(a) Bi–metallic strip consisting of material A and material B (b) Enlarged elevation of an element of bi–metallic strip
(c) Contraction in materials A and B if allowed to deform freely (d) Actual deformation in bi–metallic strip after drop in temperature
(e) Bending in bi–metallic strip due to drop in temperature (f) Internal force system for materials A and B

compression is forced into material A to deform it from Level 1 to Level 3 [Figure 11.4 (d)] at the interface. Material B, however, is restrained by material A and is prevented from undergoing its full free contraction. As a result, tension is induced in material B equivalent to the material being stretched from Level 2 to Level 3 at the interface [Figure 11.4 (d)]. The tension is less at the free surface of material B. The differential strains in the bi-metallic strip lead to circular arc bending as shown in Figure 11.4 (e). The radius of curvature of the deflection curve, R, is so large compared to the cross sectional dimensions of the strip that it may be taken as the same for both materials A and B. The internal force system for materials A and B can be reduced to a longitudinal force, F_A and F_B respectively, and bending moment, M_A and M_B respectively, as shown in Figure 11.4 (f). Therefore, material A compresses under the longitudinal force, F_A and bends under the action of the moment M_A (compression will be induced at the common interface for material A). Material B will exhibit tension under the action of the central force, F_B and also exhibit tension at the interface with material A due to the action of the moment, M_B [see Figure 11.4 (f)].

11.3.2.1 Analysis of shrinkage stress in a repair patch

The analogy of a bi-metallic strip contracting due to a drop in temperature can be used to represent the distribution of shrinkage strain in a repair patch. The two materials of the bi-metallic strip are represented by the "zone of influence" of the substrate concrete and repair material. Both the substrate concrete and repair material undergo deformation when shrinkage strain is transferred from the stiffer repair material to the

less stiff substrate concrete (see Zone 1, Figures 10.5 to 10.8). Figure 11.5 (a) shows a cross-section through an unpropped member in compression, repaired with a spray applied material that is stiffer than the substrate concrete. The external load remained in place throughout the application of the repair material. Immediately after application of the repair material and before shrinkage begins in the repair patch, the repair material extends the full length of the repair patch, labelled Level 0 to Level 1 in Figure 11.5 (b). Assuming the substrate concrete has a negligible elastic modulus ($E_{rm} \approx 0$), the repair material could shrink freely from Level 0 to Level 2 in Figure 11.5 (b), displaying a free shrinkage strain, $\varepsilon_{shr(free)}$ [the strains shown from Figure 11.5 (b) onwards are exaggerated for clarity]. In an actual repair situation, the substrate concrete has a stiffness which in the case being considered is less than the stiffness of the repair material ($E_{sub} < E_{rm}$). The repair material, therefore, is prevented from deforming freely due to the partial restraint provided by the substrate concrete (the influence of the steel reinforcement on the restraint to shrinkage is omitted for simplicity and to aid clarity). This restraint will be maximum at the substrate concrete/repair material interface, but will gradually reduce as the distance from the interface increases. Nevertheless, since the repair material has an elastic modulus which is greater than the elastic modulus of the substrate concrete, it is able to transfer a portion of its shrinkage strain to the substrate concrete during the shrinkage period (Figures 10.5 to 10.8, Zone 1). Due to the restraint at the interface, deformation in the form of a circular arc [see Figure 11.5 (c)] will occur similar to deformation of the bi-metallic strip [Figure 11.4 (e)]. This will cause bending in the zone of the substrate concrete that is influenced by the shrinking repair material. The repair material is, therefore, assumed to contract from Level 0 to Level 3 at the interface [see Figure 11.5 (d)] due to the restraint provided by the

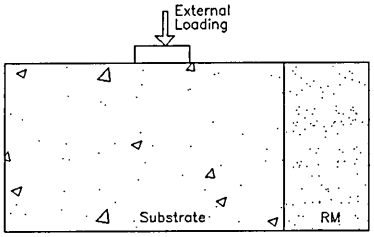

(a) repair material applied and undergoes shrinkage

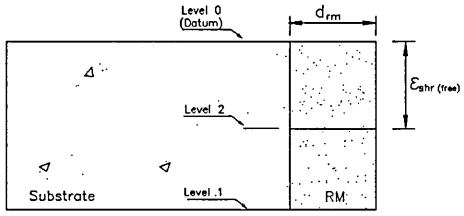

(b) idealised free shrinkage in repair material

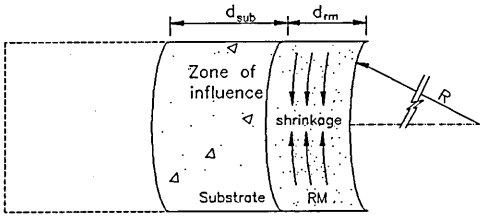

(c) stiffer repair material shrinks which leads to circular arc bending of radius R

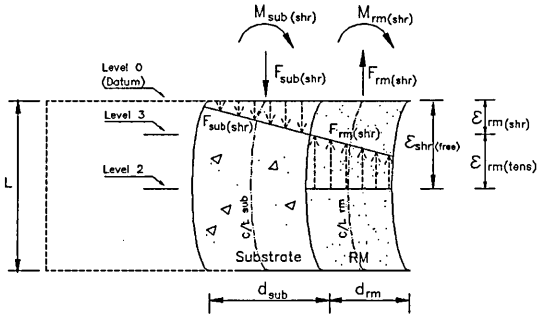

(d) idealised forces due to distribution of shrinkage strain

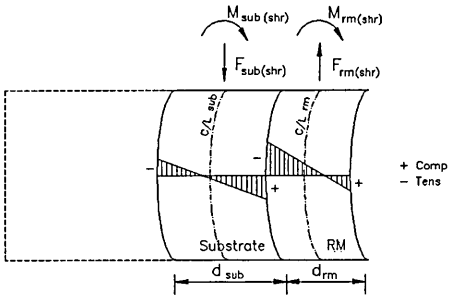

(e) idealised force system and resulting strain distribution for each material

Figure 11.5 Simplified representation of shrinkage forces in the repair patch of a compression member
Method of repair: spray application
Support during repair: unpropped
Properties: repair material stiffer than substrate concrete
Steel reinforcement omitted for clarity

substrate concrete. Due to the interfacial bond between the substrate concrete and repair material (assuming no slip), the substrate concrete also deforms from Level 0 to Level 3 at the interface due to the shrinkage of the stiffer repair material [see Figure 11.5 (d)]. A strain gradient will be evident across the repair material and zone of influence in the substrate concrete, since the restraint decreases as the distance form the interface increases. This is similar to the strain gradient across the bi-metallic strip in Figure 11.4 (d). This deformation will induce compression in the substrate concrete which can be related to a compressive force, $F_{sub(shr)}$ [Figure 11.5 (d)]. On the other hand, the stiffer repair material is prevented from deforming freely from Level 0 to Level 2 [Figure 11.5 (d)]. It can therefore be assumed that at the interface, the repair material is stretched from Level 2, the free shrinkage depth, to Level 3 [see Figure 11.5 (d)]. This induces a tensile strain in the repair material which can be related to a tensile force, $F_{rm(shr)}$, in the repair material. The internal force system for both the repair material and substrate concrete can be reduced to a central force acting along the centre line plus a bending moment [see Figure 11.5 (d)]. The central force in the substrate concrete will be compressive, whereas the central force in the repair material is tensile. The bending moment in the substrate concrete will induce compression in the substrate concrete at the interface, while the bending moment in the repair material will induce tension in the repair material at the interface [Figure 11.5 (d)].

The distribution of stress across the repair patch as a result of the loading in Figure 11.5 (d) is shown in Figure 11.5 (e). The stress in the substrate concrete at the interface is compressive, whereas the stress in the repair material, due to the restraint to shrinkage provided by the substrate concrete, is tensile. These stresses reduce in magnitude as the

distance form the interface increases, since the level of restraint to shrinkage decreases. The stresses at the free face of the repair material, and at the face furthest from the interface in the zone of influence of the substrate, may change from compression to tension, or vice versa, due to the bending effects as shown in Figure 11.5 (e).

11.3.2.2 Depth of substrate concrete affected by shrinkage of the repair material (zone of influence)

The magnitude of d_{sub}, the depth of the substrate concrete (zone of influence) affected through transfer of shrinkage strain from the repair material can be calculated by applying the concepts of conservation of strain energy to the repair patch [106]. When a tensile force is applied to a material, it will cause an increase in strain in the material. This force, therefore, does work on the material. When the force is removed, the strain disappears (assuming deformation occurred within the elastic range) and the material returns to its original position. Therefore, the energy stored in the material when subjected to such a force is called strain energy. For example, a spring is an elastic component which absorbs energy when compressed under a load. This energy is stored as recoverable strain energy in the spring which disappears when the load is removed [104].

Strain energy can be used to estimate the depth of substrate concrete, d_{sub}, influenced through transfer of shrinkage strain from the repair material. Referring to Figure 11.6 (a), the repair material extends the full depth of the repair patch immediately after application (Level 0 to Level 1). Upon completion of shrinkage (and assuming the

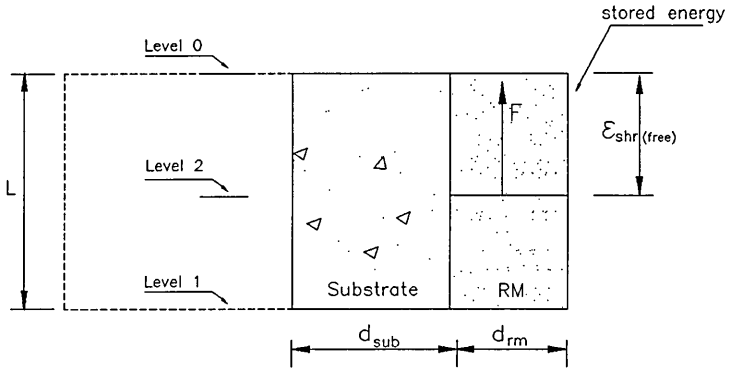

(a) loading on repair material to deform it by $\varepsilon_{sub(free)}$

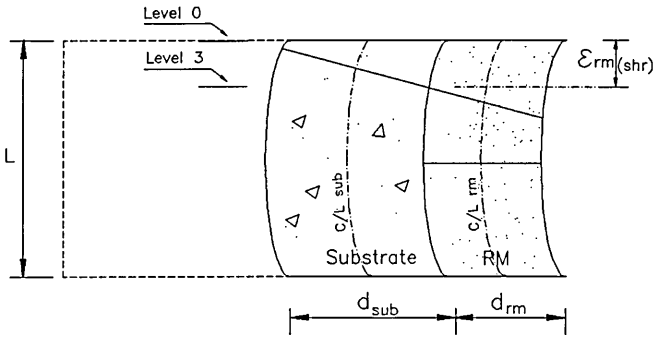

(b) repair material deforms after partial release of load (equivalent to restrained shrinkage)

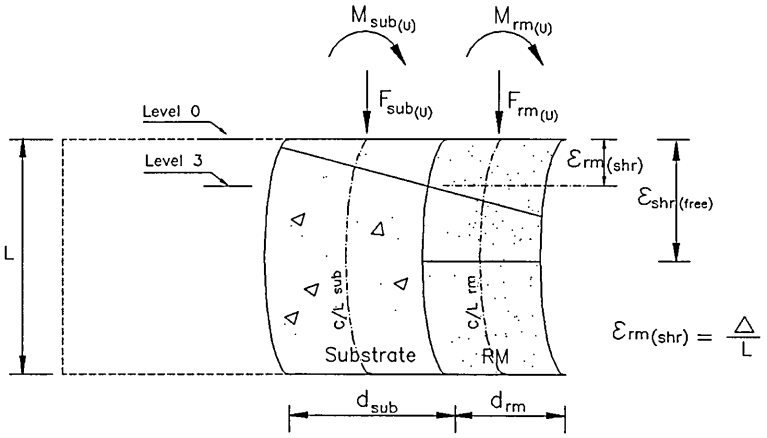

(c) loading on repair patch to represent partial release of strain energy

Figure 11.6 Loading on repaired section to determine depth of substrate concrete influenced through transfer of shrinkage from the repair material

repair material was allowed to shrink freely), it would deform by $\varepsilon_{shr(free)}$, the free shrinkage strain. Hence, the free shrinkage can be considered as stored energy in the repair material which is released through shrinkage. The repair, therefore, can be considered as a material upon which a tensile force, F, acts to extend it by $\varepsilon_{shr(free)}$ [Level 2 to Level 0, Figure 11.6 (a)]. Upon partial removal of this force in the repair material, some of the stored strain in the repair material is lost and the repair material deforms by $\varepsilon_{rm(shr)}$ at the interface [Level 0 to Level 3, Figure 11.6 (b)]. This release in stored energy, U, is equal to the restrained shrinkage strain in the repair material. Since the repair material is stiffer than the substrate concrete, and fully bonded at the interface, the substrate concrete also deforms a similar amount when the virtual tensile load on the repair material is decreased. The repair material deforms more at the free face due to the lower restraint [Figure 11.6 (b)] causing bending to occur in the repair material. Therefore, an axial load, $F_{rm(U)}$, and bending moment, $M_{rm(U)}$, can be considered to act on the repair material to deform it to Level 3 [Figure 11.6 (c)]. Concentrating on the axial force, strain energy equals the average load times the extension. Hence, the energy due to the axial force in the repair material can be estimated from [105]:

$$U_{rm(axial)} = \frac{1}{2} F_{rm(U)} \Delta$$

Equation 11. 2

where $F_{rm(U)}$ is the imaginary force in the repair material to cause a displacement, Δ [Δ is equal to $(\varepsilon_{rm(shr)})(L)$ which is common to both the repair material and substrate concrete at the interface after shrinkage has occurred in the repair material]. The force in the repair material can be written as:

$$F_{rm(u)} = \frac{\Delta A_{rm} E_{rm}}{L}$$

Equation 11. 3

Substituting Equation 11. 3 into Equation 11. 2 gives:

$$U_{rm(axial)} = \frac{1}{2} \frac{A_{rm} E_{rm}}{L} \Delta^2$$

Equation 11. 4

Equation 11. 4 can be expanded to give:

$$U_{rm(axial)} = \frac{1}{2} \frac{A_{rm} E_{rm}}{L} [(\varepsilon_{rm(shr)}(L)]^2$$

Equation 11. 5

But since

$$A_{rm} = d_{rm} b$$

Equation 11. 6

Equation 11. 5 can be written as:

$$U_{rm(axial)} = \frac{(\varepsilon_{rm(shr)})^2 E_{rm} b d_{rm} L}{2}$$

Equation 11. 7

Similarly, the release of stored energy in the repair material due to bending can be estimated from [106]:

$$U_{rm(bend)} = \frac{1}{2}\frac{M_{rm(U)}{}^2 L}{E_{rm} I_{rm}}$$

Equation 11. 8

But since

$$M_{rm(U)} = \frac{\sigma_{rm(U)} I_{rm}}{y_{rm}}$$

Equation 11. 9

and

$$\sigma_{rm(U)} = E_{rm}(\varepsilon_{rm(shr)})$$

Equation 11. 10

Equation 11. 9 and Equation 11. 10 can be substituted into Equation 11. 8 to give:

$$U_{rm(bend)} = \frac{1}{2}\left(\frac{(\varepsilon_{rm(shr)}{}^2) E_{rm} I_{rm} L}{y_{rm}{}^2}\right)$$

Equation 11. 11

Similarly, since

$$y_{rm} = \frac{d_{rm}}{2}$$

Equation 11. 12

and

$$I_{rm} = \frac{bd_{rm}^3}{12}$$

Equation 11. 13

Equation 11. 12 and Equation 11. 13 can be substituted into Equation 11. 11 to give:

$$U_{rm(bend)} = \frac{(\varepsilon_{rm(shr)}^2)E_{rm}bd_{rm}L}{6}$$

Equation 11. 14

The total strain energy lost in the repair material due to shrinkage can be calculated by adding Equation 11. 14 to Equation 11. 7 and simplifying to give:

$$U_{rm(total)} = 0.67E_{rm}(\varepsilon_{rm(shr)}^2)bd_{rm}L$$

Equation 11. 15

The strain lost due to release of strain energy in the repair material (shrinkage) is equal to the strain energy gained by the substrate concrete at the interface. This increase in strain can be estimated in terms of a direct force, $F_{sub(U)}$, and bending moment, $M_{sub(U)}$, in the substrate concrete to deform it by $\varepsilon_{rm(shr)}$ at the interface [Figure 11.6 (c)]. Therefore, the total strain gained by the substrate concrete due to transfer of shrinkage from the repair material can be shown to be:

$$U_{sub(total)} = 0.67 E_{sub}(\varepsilon_{rm(shr)}^{2}) b d_{sub} L$$

Equation 11. 16

Equating Equation 11. 15 and Equation 11. 16 and simplifying gives:

$$E_{rm} d_{rm} = E_{sub} d_{sub}$$

Equation 11. 17

Since the modular ratio, m, equals E_{rm} / E_{sub}, Equation 11. 17 can be simplified to give:

$$d_{sub} = m d_{rm}$$

Equation 11. 18

Therefore, the depth of substrate concrete influenced through transfer of shrinkage strain from the repair material is equal to the depth of repair material times the modular ratio between the repair material and substrate concrete. Hence, the depth of substrate concrete influenced through transfer of shrinkage strain increases as the modular ratio increases. The distribution of stress in the repair patch can now be determined by applying the principles of a bi-metallic strip [106] to the repair material/substrate concrete section [see Figure 11.5 (d)]. Two compatibility equations are derived which allow the force in the repair patch due to shrinkage, F_{shr}, and the radius of curvature due to bending, R, to be determined.

11.3.2.3 Equilibrium of forces in the repaired section

Considering the equilibrium of forces in Figure 11.5 (e), it can be stated that:

$$F_{rm(shr)} = F_{sub(shr)} = F_{shr}$$

Equation 11. 19

The normal distance between forces [Figure 11.4 (e)] is $\frac{1}{2}(d_{rm} + d_{sub})$. The couple produced by these forces must, for equilibrium, balance the sum of the moments of resistance of the repair and substrate materials. Thus:

$$\frac{F_{shr}}{2}(d_{sub} + d_{rm}) = M_{sub(shr)} + M_{rm(shr)}$$

Equation 11. 20

The elastic theory of bending gives the following relationship for the substrate concrete:

$$\frac{M_{sub(shr)}}{I_{sub}} = \frac{f_{sub(shr)}}{y_{sub}} = \frac{E_{sub}}{R}$$

Equation 11. 21

Similarly, the general expression for simple bending in the repair material is defined as:

$$\frac{M_{rm(shr)}}{I_{rm}} = \frac{f_{rm(shr)}}{y_{rm}} = \frac{E_{rm}}{R}$$

Equation 11. 22

Excluding the $\frac{f}{y}$ term from Equation 11. 21 and Equation 11. 22 and rearranging gives:

$$M_{sub(shr)} = \frac{E_{sub}I_{sub}}{R}$$

Equation 11. 23

and

$$M_{rm(shr)} = \frac{E_{rm}I_{rm}}{R}$$

Equation 11. 24

Therefore substituting Equation 11. 23 and Equation 11. 24 into Equation 11. 20 gives:

$$\frac{F_{shr}}{2}(d_{sub} + d_{rm}) = \frac{E_{sub}I_{sub}}{R} + \frac{E_{rm}I_{rm}}{R}$$

Equation 11. 25

Rearranging Equation 11. 25 gives:

$$F_{shr} = 2\left[\frac{E_{sub}I_{sub} + E_{rm}I_{rm}}{d_{sub} + d_{rm}}\right]\frac{1}{R}$$

Equation 11. 26

The only unknowns in Equation 11. 26 are the force due to shrinkage, F_{shr}, and the radius of curvature due to bending, R.

11.3.2.4 Strain compatibility at the interface

A second relationship can be obtained by considering the strain compatibility of the two materials (repair and substrate) at the interface. These strains are made up of three components, (i) the free shrinkage of the repair material $\varepsilon_{shr(free)}$, (ii) the strains due to the bending moments, $M_{sub(shr)}$ and $M_{rm(shr)}$, and (iii) the strain due to the longitudinal forces, F_{shr}.

(i) Strains due to free shrinkage, $\varepsilon_{shr(free)}$

The free shrinkage strains of the repair materials under observation, $\varepsilon_{shr(free)}$, were determined in the laboratory, and are given in Table 11.1, column 2.

(ii) Strains due to bending, $\varepsilon_{sub(bend)}$ and $\varepsilon_{rm(bend)}$

Excluding the $\frac{M}{I}$ term in Equation 11. 21 and Equation 11. 22 and transposing gives:

$$\frac{f_{sub(shr)}}{E_{sub}} = \frac{y_{sub}}{R}$$

Equation 11. 27

and

$$\frac{f_{rm(shr)}}{E_{rm}} = \frac{y_{rm}}{R}$$

Equation 11. 28

Assuming the centroidal axis of the individual materials in Figure 11.5 (e) to be at half the depth (ignoring the effects of the steel reinforcement), the distance to the interface is:

$$y_{sub} = \frac{d_{sub}}{2}$$

Equation 11. 29

and

$$y_{rm} = \frac{d_{rm}}{2}$$

Equation 11. 30

Substituting Equation 11. 29 into Equation 11. 27 and Equation 11. 30 into Equation 11. 28 and rearranging gives the following expressions for stress at the interface between repair and substrate materials:

$$f_{sub(shr)} = \frac{d_{sub}E_{sub}}{2R}$$

Equation 11. 31

and

$$f_{rm(shr)} = \frac{d_{rm}E_{rm}}{2R}$$

Equation 11. 32

Dividing Equation 11. 31 by the elastic modulus of the substrate concrete gives the strain at the interface due to bending in the substrate concrete, hence:

$$\varepsilon_{sub(bend)} = \frac{d_{sub}}{2R}$$

Equation 11. 33

Similarly, the strain at the interface of the repair material, due to bending, can be obtained from Equation 11. 32 to give:

$$\varepsilon_{rm(bend)} = \frac{d_{rm}}{2R}$$

Equation 11. 34

(iii) Strains due to longitudinal force, $\varepsilon_{sub(shr)}$ and $\varepsilon_{rm(tens)}$

The strain due to axial force, F_{shr}, in the substrate concrete is given by:

$$\varepsilon_{sub(shr)} = \frac{F_{shr}}{A_{sub}E_{sub}}$$

where

$$A_{sub} = mA_{rm}$$

Equation 11. 35

Similarly, the strain due to the axial force, F_{shr}, in the repair material is given by:

$$\varepsilon_{rm(tens)} = \frac{F_{shr}}{A_{rm}E_{rm}}$$

Equation 11. 36

where A_{rm} is obtained from Equation 11. 6.

(iv) Net Strain

At the common interface between the repair material and substrate concrete, the net strain for the substrate concrete is equal to net strain for the repair material. Therefore:

$$\left[\frac{F_{shr}}{d_{sub}bE_{sub}}\right] + \frac{d_{sub}}{2R} = \varepsilon_{shr(free)} - \left[\frac{F_{shr}}{d_{rm}bE_{rm}}\right] - \frac{d_{rm}}{2R}$$

Equation 11. 37

(direct strain) + (bending strain) = (free shrinkage strain) - (direct strain) - (bending strain)

Rearranging Equation 11. 37 gives

$$\frac{F_{shr}}{b}\left[\frac{1}{d_{sub}E_{sub}} + \frac{1}{d_{rm}E_{rm}}\right] + \frac{1}{2R}[d_{sub} + d_{rm}] = \varepsilon_{shr(free)}$$

Equation 11. 38

Equation 11. 38 can also be rearranged to give F_{shr} in terms of R:

$$F_{shr} = \frac{\left(\varepsilon_{shr(free)} - \frac{1}{2R}(d_{sub} + d_{rm})\right)b}{\left(\frac{1}{d_{sub}E_{sub}} + \frac{1}{d_{rm}E_{rm}}\right)}$$

Equation 11. 39

The only unknowns in Equation 11. 39 are again the force due to shrinkage, F_{shr}, and the radius of curvature, R. Therefore, simultaneous equations (Equation 11. 26 and Equation 11. 39) can be solved to determine the values F_{shr} and R. Knowing the value of R, the moment due to bending in both the substrate concrete, $M_{sub(shr)}$, and repair material, $M_{rm(shr)}$, can be obtained by substituting the value of R into Equation 11. 23 and Equation 11. 24. Therefore, the compressive stress in the substrate concrete due to a transfer of shrinkage strain from the stiffer repair material at the end of Zone 1 (Figures 10.20 to 10.23, week 11) can be determined from the sum of the direct stress and bending stress as follows:

$$\sigma_{sub(shr)} = \frac{F_{shr}}{A_{sub}} \pm \frac{M_{sub(shr)} y_{sub}}{I_{sub}}$$

Equation 11. 40

Equation 11. 40 can be simplified by substituting Equation 11. 23 for the moment term as follows:

$$\sigma_{sub(shr)} = \frac{F_{shr}}{A_{sub}} \pm \frac{E_{sub} y_{sub}}{R}$$

Equation 11. 41

The tensile stress in the repair material due to the restraint to shrinkage provided by the substrate concrete at the end of Zone 1 (Figures 10.20 to 10.23, week 11) can be determined from the sum of the stress due to the direct stress and bending stress as follows:

$$\sigma_{rm(shr)} = -\frac{F_{shr}}{A_{rm}} \pm \frac{M_{rm(shr)} y_{rm}}{I_{rm}}$$

Equation 11. 42

Equation 11. 42 can be simplified by substituting Equation 11. 24 for the moment term as follows:

$$\sigma_{rm(shr)} = -\frac{F_{shr}}{A_{rm}} \pm \frac{E_{rm} y_{rm}}{R}$$

Equation 11. 43

Therefore, Equation 11. 41 and Equation 11. 43 and can be used to predict the stress in the repair material and substrate concrete after transfer of shrinkage strain from a stiffer, spray applied repair material to an unpropped compression member.

11.3.3 External load transfer

11.3.3.1 Stress in the repaired section

Shrinkage in the repair material is considered to have ceased at the end of Zone 1 followed by a steady state period (Zone 2). External load is then transferred from the substrate concrete to the repair patch in Zone 3 (see Figures 10.5 to 10.8). Table 11.2 gives a summary of the strains (and corresponding stresses) in the repair materials at the end of the external load transfer stage (materials L4, L3, L2 and G1). These strains in

Table 11.2 External load transfer strains and stresses in the repair material

	Column				
	1	*2*	*3*	*4*	*5*
Repair material/ location	*Strain (microstrain)*	*Elastic modulus (kN/mm^2)*	*Stress (N/mm^2)*	*Cube strength (N/mm^2)*	$\frac{stress}{strength}$ *(%)*
L4		29.1		73	
RM @ interface	+143		4.2		5.8
RM @ steel	+100		2.9		4.0
L3		27.4		35	
RM @ interface	+ 30		0.8		2.3
RM @ steel	+ 63		1.7		4.9
L2		30.3		60	
RM @ interface	+ 18		0.5		0.8
RM @ steel	+ 47		1.4		2.3
G1		31.1		50	
RM @ interface	+ 82		2.6		5.2
RM @ steel	+ 5		0.2		0.4

the repair material are at the repair material/substrate concrete interface (denoted "RM @ interface" in Table 11.2) and the strains in the repair material at the steel reinforcement level (denoted "RM @ steel" in Table 11.2). The 28 day elastic modulus of the repair material is given in column 2. The resulting stress given in column 3, due to external load transfer, is obtained by multiplying the strain by the 28 day elastic modulus of the repair material. The cube strengths of the repair materials are given in

column 4. The resulting maximum stress/strength ratios on the repair materials under load are given in column 5. Referring to Table 11.2, the highest stress/strength ratio was observed in material L4 at the interface between the substrate concrete and repair material (5.8%). A stress/strength ratio of this magnitude, which was obtained over a period of 22 weeks (Figure 10.20 to 10.23, weeks 25 to 47), would induce negligible compressive creep in the repair material. As a result, the effects of creep can be ignored and analysis of the external load transfer stage can be based on elastic analysis. The substrate concrete is stressed as a result of external service loading, as shown in Figure 11.7 (a), before repair work is carried out on the abutment. The external load remains on the substrate concrete during removal of the deteriorated concrete, as shown in Figure 11.7 (b). Therefore, the stress in the damaged concrete before removal can be considered to be taken by the existing substrate concrete throughout the repair period and Zones 1 and 2 until this stress is transferred back into the repaired section of the abutment. During the load transfer stage to the repair material (Zone 3), an area of adjacent substrate concrete, similar to the zone of influence as described in Section 11.3.2.2, is assumed to shed load to the repair patch, as shown in Figure 11.7 (c) (this assumption is substantiated later in the chapter). The depth of this zone is taken as md_{rm}, as established earlier (Equation 11. 18). It is virtually impossible to calculate accurately the stress in the substrate concrete due to external load during the service life of a structure since the precise loading and material properties are not known. Therefore, Figure 11.7 (c) shows that the substrate concrete in the zone of influence is stressed to αf_{cu}, where α is the ratio of the 28 day design cube strength of the substrate concrete. This stress can be related to a force due to external loading in the zone of

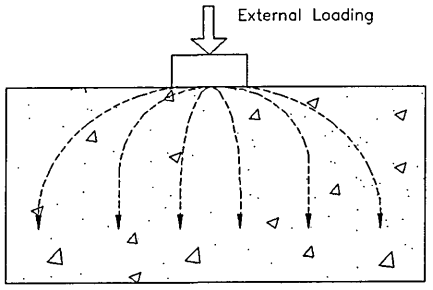

(a) substrate concrete under load before repair

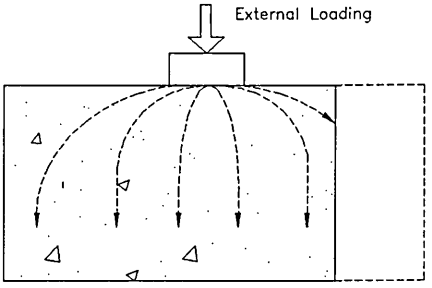

(b) deteriorated concrete removed whilst substrate concrete remains under load

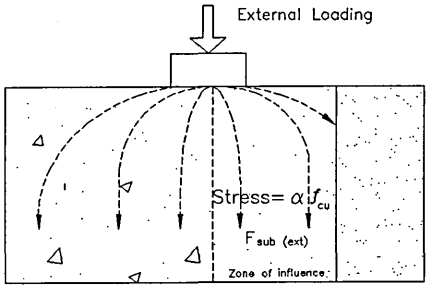

(c) Force in the 'zone of influence' of substrate concrete due to external loading (Stress= αf_{cu})

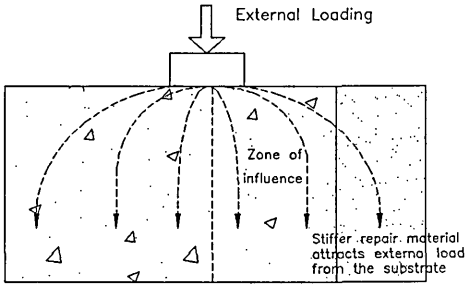

(d) External load transfer from adjacent substrate concrete (zone of influence) into repair material (weeks 25 to 47)

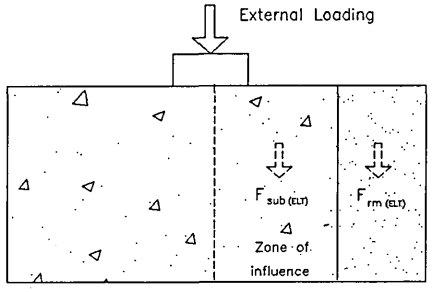

(e) Force, $F_{rm\ (ELT)}$ redistributed into repair patch leaving a force, $F_{sub\ (ELT)}$ in the substrate concrete

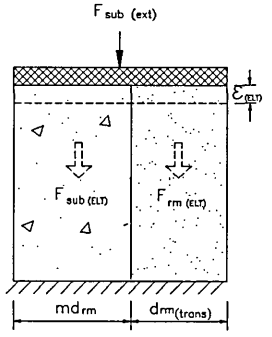

(f) Equivalent loading in repaired section after transfer of external load into repair material

Figure 11.7 Simplified representation of stress due to external load transfer in the repair patch of a compression member
Method of repair: spray application
Support during repair: unpropped
Properties: repair material stiffer than substrate concrete
(Steel reinforcement omitted for clarity)

influence, $F_{sub(ext)}$. An approximate estimation of the maximum substrate concrete stress, and subsequently maximum substrate concrete force, is made by adopting the *Campaign for Practical Codes of Practice* (CPCP) [107] recommendation that the permissible stress in a member in direct compression should not exceed $0.275 f_{cu}$, where f_{cu} is the cube strength. Assuming that the in-service stress in the compression member, $\sigma_{sub(ext)}$, equals the permissible (maximum) stress:

$$\sigma_{sub(ext)} = 0.275 f_{cu}$$

Equation 11. 44

The compressive strength of the substrate concrete, f_{cu}, can be obtained by extracting cores and testing to failure in the laboratory. In this investigation, cores of dimensions 200 x 100mm diameter were extracted from the substrate concretes and their compressive strength determined. Kong and Evans [82] report that the cylinder (or core) strength of concrete is approximately 70-90% of the cube strength. Assuming the core strength of concrete to be 80% of the cube strength, therefore,

$$f_{cu} = \frac{f_{co}}{0.80}$$

Equation 11. 45

where f_{co} is the core strength. Therefore, the maximum in-service stress in the substrate concrete can be obtained by substituting Equation 11. 45 into Equation 11. 44 as follows:

$$\sigma_{sub(ext)} = 0.34 f_{co}$$

Equation 11. 46

Therefore, Equation 11. 46 gives an estimation of the permissible stress in the substrate concrete in terms of the core strength, f_{co}.

Since the abutment is now a composite member with three different materials (i.e. concrete, steel reinforcement and repair material), Figure 11.7 (d) shows the stiffer repair material attracting stress from the zone of influence of the substrate concrete. The repair patch now assists in carrying external load resulting in stress paths similar to those which existed before repair as shown in Figure 11.7 (a) (i.e. the abutment has returned to distributing the load as before repair). Steel reinforcement also provides continuity between the substrate concrete and repair material which assists in the transfer of load from the substrate concrete. It has been observed in many instances in the project that a repair material that has an elastic modulus greater than the elastic modulus of the substrate concrete will attract load from the adjacent substrate concrete in the long term (Figures 10.5 to 10.7, weeks 25 to 47). This will cause a force, $F_{rm(ELT)}$, in the repair material as shown in Figure 11.7 (e). For equilibrium, this force, plus the force remaining in the substrate concrete after transfer of external load, $F_{sub(ELT)}$, should equal the original force in the substrate concrete due to external loading, $F_{sub(ext)}$. Therefore,

$$F_{sub(ext)} = F_{sub(ELT)} + F_{rm(ELT)}$$

Equation 11. 47

The force in the zone of influence in the substrate concrete, $F_{sub(ext)}$, can be calculated by multiplying the stress by the cross-sectional area of the zone of influence:

$$F_{sub(ext)} = (\alpha f_{cu})(md_{rm})(b)$$

Equation 11. 48

where α can be assumed to equal the maximum permissible value (0.275). The transferred stress will cause elastic deformation in the repair material (creep effects can be neglected due to the low stress/strength ratios involved as described earlier). Referring to Figures 10.20 to 10.23, Zone 3, the stress in the substrate concrete interface (with the repair material) also increases as external load is transferred into the repair material. This is opposite to what might be expected. This can be explained with reference to concepts that were described earlier. Referring to Section 11.3, it was stated that when the elastic modulus of the repair material was greater than the elastic modulus of the substrate concrete, the deforming repair material was able to transfer a portion of the shrinkage strain to the substrate concrete. A similar phenomenon occurs when external load is attracted into the repair material. When the repair material deforms elastically due to the increase in external stress, the stiffer repair material, due to full bond at the interface, also causes deformation in the substrate concrete interface. Therefore, the substrate concrete interface shows similar deformation as the repair material (strain compatibility at the interface). Hence an increased compressive strain will also be evident in the substrate concrete after transfer of external load into the repair material. Since the increase in strain in the repair material is similar to the increase in strain in the substrate concrete, the concept of conservation of strain energy, as

described earlier in Section 11.3.2.2, can be used to predict the depth of substrate concrete shedding load to the repair patch. The strain deformation in the repair material can be considered as a loss in strain energy (similar to the loss in stored energy due to shrinkage). Therefore, this strain energy can be related to an axial force (similar to Equation 11. 4). Likewise, the increase in strain in the substrate concrete can also be related to an axial force (the substrate concrete can be assumed to gain the dissipated strain from the repair material). Therefore, by equating these forces, it can be shown that $d_{sub} = md_{rm}$ (similar to Equation 11. 18).

For simplicity, strain compatibility is assumed to occur across the full depth of the repair patch and zone of influence of the substrate concrete (see also the increase in strain in the substrate concrete in Figures 10.5 to 10.8, Zone 3). Therefore, referring to Figure 11.7 (f), the deformation in the substrate concrete and repair material can be estimated from analysis of a compound member. A compound member is made up of two (or more) components of different materials and constructed in such a way that the components deform equally under axial loading [105]. The axial load in this instance is assumed as $F_{sub(ext)}$, since this is the force in the zone of influence of the substrate concrete due to external loading, and is responsible for deforming both materials. Figure 11.7 (f) shows that the thickness of the substrate concrete is md_{rm}, as derived earlier (see Equation 11. 18). Since most of the steel reinforcement in the abutments/columns in the highways structures investigated in this project was near the surface of the repair, the area of the repair material, therefore, is modified to take into account the area of the steel reinforcement. Therefore:

$$A_{rm(trans)} = A_{rm} + m_{st}A_{st}$$

Equation 11. 49

where $A_{rm(trans)}$ is the transformed area of the repair material, A_{rm} is the area of the repair material, m_{st} is the modular ratio of the steel reinforcement and repair material and A_{st} is the area of the steel reinforcement. Since $A_{rm(trans)} = bd_{rm(trans)}$, and $A_{rm} = bd_{rm}$, Equation 11. 49 can be simplified to give the transformed depth of repair material:

$$d_{rm(trans)} = d_{rm} + \frac{m_{st}A_{st}}{b}$$

Equation 11. 50

Referring to Figure 11.7 (f), the deformation in the substrate concrete and repair material, $\varepsilon_{(ELT)}$, due to external load transfer, can be estimated from:

$$\frac{F_{sub(ELT)}}{A_{sub}E_{sub}} = \frac{F_{rm(ELT)}}{A_{rm(trans)}E_{rm}}$$

Equation 11. 51

Transposing Equation 11. 47 and inserting into Equation 11. 51 gives:

$$\frac{F_{sub(ext)} - F_{rm(ELT)}}{A_{sub}E_{sub}} = \frac{F_{rm(ELT)}}{A_{rm(trans)}E_{rm}}$$

Equation 11. 52

The only unknown in Equation 11. 52 is the portion of load that is transferred into the repair material, $F_{rm(ELT)}$. Since:

$$A_{sub} = md_{rm}b$$

Equation 11. 53

and $F_{sub(ext)}$ and $A_{rm(trans)}$ are obtained from Equation 11. 48 and Equation 11. 49 respectively, Equation 11. 52 can be transposed to give the force in the repair material after transfer of external load:

$$F_{rm(ELT)} = \frac{\alpha bmd_{rm}f_{cu}(bd_{rm} + mA_{st})}{(2bd_{rm} + m_{st}A_{st})}$$

Equation 11. 54

Therefore, Equation 11. 54 gives the force in the repair material due to the portion of external load attracted into the repair patch. Dividing this force by the transformed area of the repair patch (Equation 11. 49) gives the maximum stress in the repair patch after external load transfer (Figures 10.20 to 10.23, week 47), thus:

$$\sigma_{rm(ELT)} = \frac{F_{rm(ELT)}}{A_{rm(trans)}}$$

Equation 11. 55

The deformation in the repair material in Zone 3 (Figures 10.20 to 10.23) also causes deformation in the substrate concrete, since the stiffer repair material is fully bonded to

the substrate concrete. Assuming strain compatibility at the interface between the repair material and substrate concrete, the increase in strain in the substrate concrete can be determined by dividing the predicted stress in the repair patch (Equation 11. 55) by the elastic modulus of the repair patch. This strain is then multiplied by the elastic modulus of the substrate concrete to give the increase in stress in the substrate concrete:

$$\sigma_{sub(ELT)} = \frac{F_{rm(ELT)}}{E_{rm}A_{rm(trans)}} E_{sub}$$

Equation 11. 56

Equation 11. 56 can be simplified by replacing the elastic modulus terms by the reciprocal of m, the modular ratio:

$$\sigma_{sub(ELT)} = \frac{1}{m} \frac{F_{rm(ELT)}}{A_{rm(trans)}}$$

Equation 11. 57

Therefore, Equation 11. 55 can be used to predict the increase in stress in the repair material after transfer of external load from the substrate concrete. Similarly, Equation 11. 57 can be used to predict the increase in compressive stress in the substrate concrete after deformation occurs due to full bond with the repair material.

11.3.4 Cumulative stress in the repaired section

The total stress in the substrate concrete at the end of the 60 week monitoring period, $\sigma_{sub(wk60)}$ (Figures 10.20 to 10.23) is the sum of stresses obtained from the analysis in the shrinkage period (Equation 11. 41) and the external load transfer period (Equation 11. 57), i.e.

$$\sigma_{sub(wk60)} = \frac{F_{shr}}{A_{sub}} \pm \frac{E_{sub} y_{sub}}{R} + \frac{1}{m} \frac{F_{rm(ELT)}}{A_{rm(trans)}}$$

Equation 11. 58

The maximum stress in the substrate concrete will be at the interface between the substrate concrete and the repair material. This stress will gradually decrease within the 'zone of influence', as the distance from the interface increases.

The stress in the repair material at the end of the 60 week monitoring period, $\sigma_{rm(wk60)}$, (Figure 10.20 to 10.23), is the sum of the stresses predicted from the shrinkage period (Equation 11. 43) and the stress predicted through analysis of the external load transfer (Equation 11. 55) i.e.

$$\sigma_{rm(wk60)} = -\frac{F_{shr}}{A_{rm}} \pm \frac{E_{rm} y_{rm}}{R} + \frac{F_{rm(ELT)}}{A_{rm(trans)}}$$

Equation 11. 59

Equation 11. 58 and Equation 11. 59 assumes that the elastic modulus of the repair material is greater than the elastic modulus of the substrate concrete and that the repair material remains crack free. The equations are based on the performance of spray applied repair materials to unpropped members in compression.

11.3.5 Comparison between experimental and predicted stresses

Table 11.3 gives the key repair material properties, repair patch dimensions and calculated values which are needed for determining the stress across the repair patches of materials L4, L3, L2 and G1 (Equation 11. 58 and Equation 11. 59). The repair material reference is given in column 1. The elastic modulus of both the repair material and substrate concrete, E_{rm} and E_{sub}, is given in columns 2 and 3 respectively. The modified free shrinkage of the repair materials, $\varepsilon_{shr(free)}$, is given in column 4. The equivalent cube strength of the substrate concrete, f_{cu}, obtained from Equation 11. 45, at both Lawns Lane Bridge and Gunthorpe Bridge is given column 5. The transformed depth of the repair patch, $d_{rm(trans)}$, is given in column 6. The depth of the zone of influence in the substrate concrete, (d_{sub}, Equation 11. 18) is given shown in column 7. The breadth of the repair patch, b, is given in column 8 and the amount of longitudinal steel in the repair patches is given in column 9. The calculated force in the repair patch/substrate concrete due to shrinkage in the repair material, F_{shr}, is given in column 10 (Equation 11. 26 and Equation 11. 39). The resulting radius of curvature of the substrate concrete/repair patch, R, due to shrinkage in the repair material is given in

Table 11.3 Properties of repair materials, patch dimensions and other key values for calculating stresses in the substrate concrete and repair materials

					Column						
1	*2*	*3*	*4*	*5*	*6*	*7*	*8*	*9*	*10*	*11*	*12*
Repair patch	E_{rm} (GPa)	E_{sub} (GPa)	$\varepsilon_{shr(free)}$ (μstrain)	f_{cu} (MPa)	$d_{rm(trans)}$ (mm)	d_{sub} (mm)	*b* (mm)	*Longitud. steel* (Ømm)	F_{shr} (kN)	*R* ($x10^3$) (mm)	$F_{rm(ELT)}$ (α=0.275) (kN)
L4	29.1	23.8	238	42.6	148	171	1500	5x20	184.5	861	1540
L3	27.4	23.8	210	42.6	148	161	1500	5x20	151.5	957	1452
L2	30.3	23.8	136	42.6	148	178	1035	5x20	77.5	1522	1119
G1	31.1	28.1	329	45.1	148	155	2300	5x20	249.8	520	2228

column 11 (Equation 11. 26 and Equation 11. 39). Finally, the calculated force transferred to the repair patch from the substrate, $F_{rm(ELT)}$, concrete is given in column 12 [Equation 11. 54]

Referring to Table 11.3, column 7, it is evident that the depth of substrate concrete affected by transfer of shrinkage strain from the repair patch increase as the difference in elastic modulus between the substrate concrete and repair material increases (compare d_{sub} for material L2 with d_{sub} for material G1, Table 11.3). The high modular ratio between the repair material and substrate concrete is responsible for this (Equation 11. 18). Referring to column 10, the virtual force in the repair patch due to shrinkage in the repair material ranges between 77.5 kN to 249.8 kN. This virtual force is high when the free shrinkage (column 4) of the repair material is high (compare material L2 with material G1, Table 11.3). The radius of curvature of the deflection curve of the repair patch/substrate concrete due to the restraint to shrinkage in the repair material ranges between 520 x 10^3 and 1522 x 10^3 mm. It is noticeable that this radius increases as the

virtual force due to shrinkage decreases (compare material L2 with material G1). This is since a lower shrinkage force will cause less deformation, and as a result, the bending effects in the repair patch will be reduced accordingly. With regards to the virtual force that is attracted into the repair patch (column 12), it is evident that the cross sectional area of the repair patch has an influence on the magnitude of the force. The larger the cross-sectional area of the repair patch, the larger the virtual force (compare the force in the repair patch of material G1 with the force in the repair patch of material L2).

Figures 11.8 to 11.11 show the comparison between the actual interfacial stress in the substrate concrete and repair material, with the predicted stresses in the substrate concrete and repair material at the same location obtained from the analytical models (Equation 11. 58 and Equation 11. 59). A summary of the comparisons are also given in Table 11.4. Initially, when calculating the portion of the load that is transferred to the repair material in the long term, the value of $\alpha = 0.275$ is used which is the maximum allowed by the CPCP design recommendations [107]. Referring to Figure 11.8 and Table 11.4, the comparisons between the stress in the repair material and substrate concrete at the end of the shrinkage stage (week 11) are given for repair material L4. Referring to Zone 1 (Figure 11.8 and Table 11.8), the actual compressive stress in the substrate concrete after transfer of shrinkage from the repair material is 3.7 N/mm^2. The predicted compressive stress from the analysis in the shrinkage period is slightly less at 3.1 N/mm^2 (at week 11). The actual tensile stress in repair material L4 at the end of the Zone 1 is 2.2 N/mm^2 (Figure 11.8 and Table 11.4). The predicted tensile stress in the repair material is higher at 3.2 N/mm^2. Therefore, comparing the actual stresses with

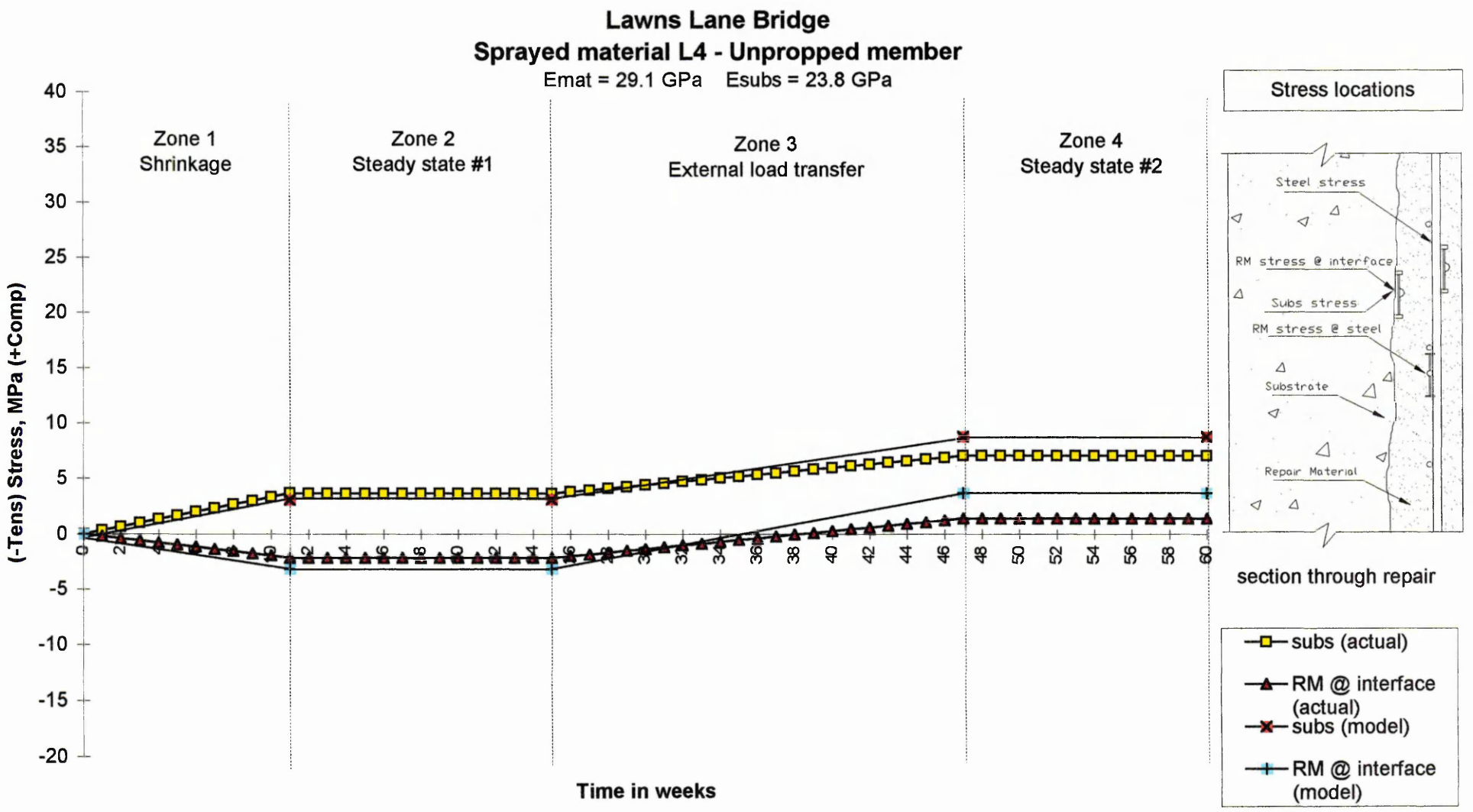

Figure 11.8 Comparison between actual and predicted stress in repair patch of material L4 at Lawns Lane Bridge (Unpropped compression member)

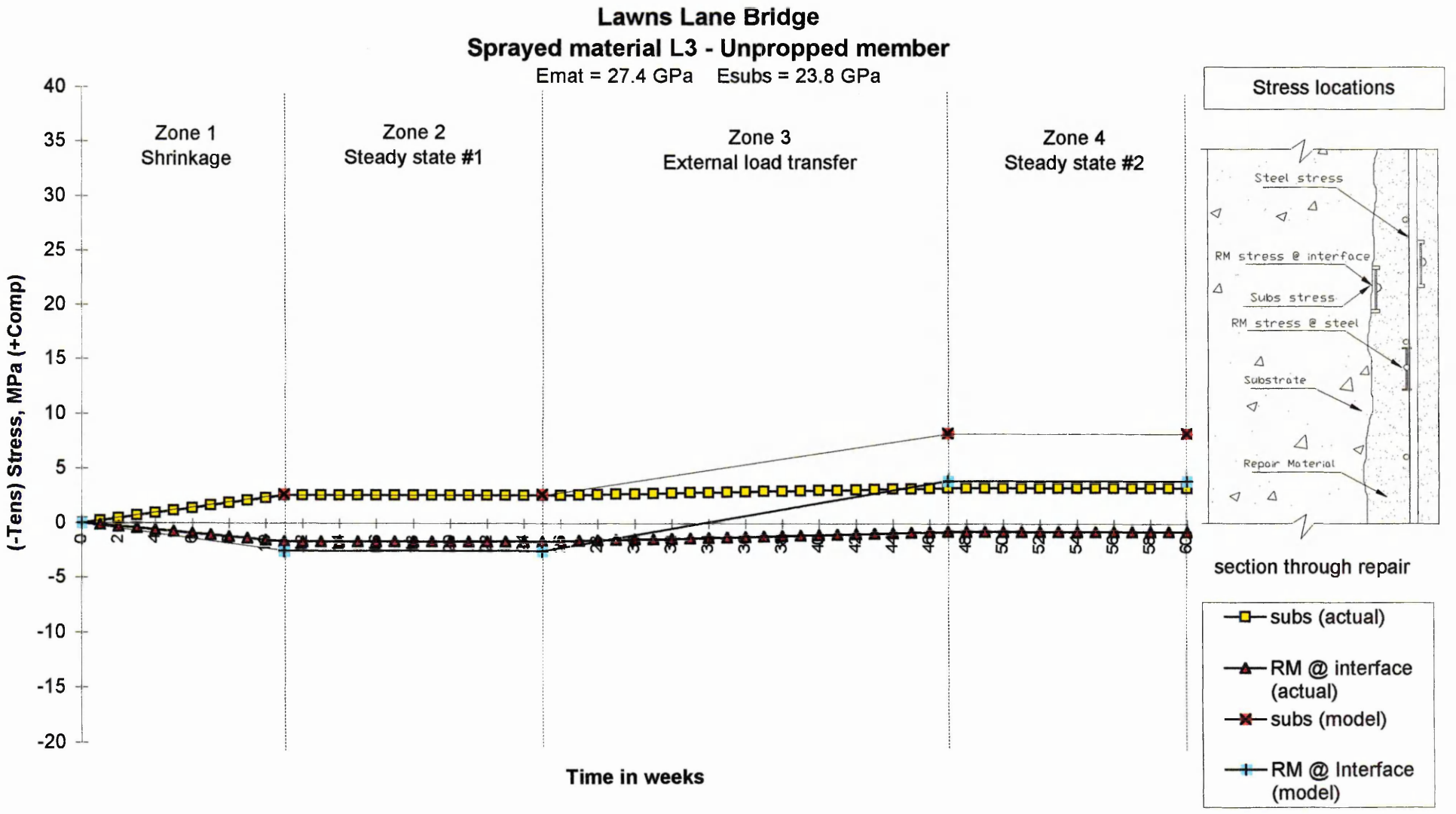

Figure 11.9 Comparison between actual and predicted stress in repair patch of material L3 at Lawns Lane Bridge (Unpropped compression member)

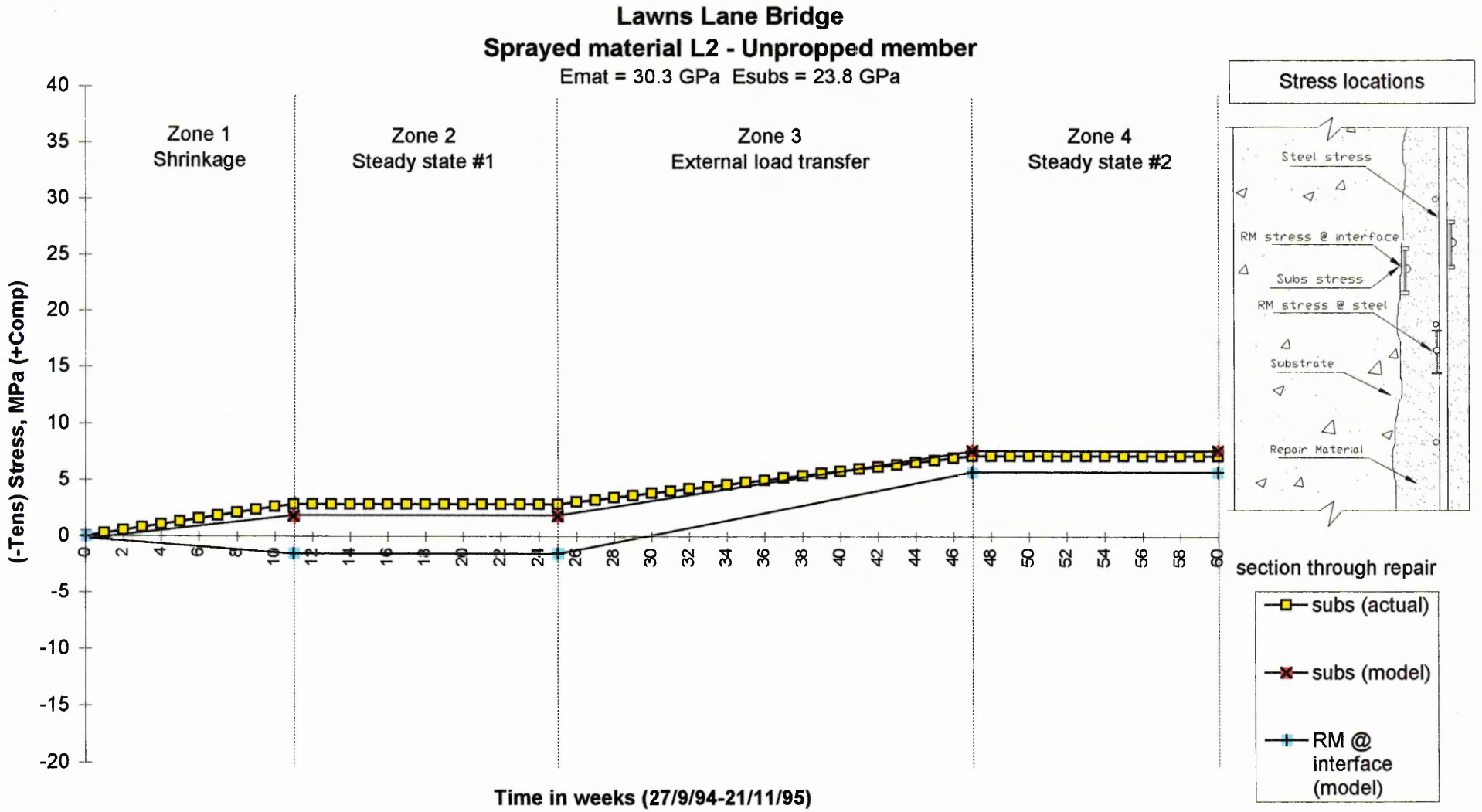

Figure 11.10 Comparison between actual and predicted stress in repair patch of material L2 at Lawns Lane Bridge (Unpropped compression member)

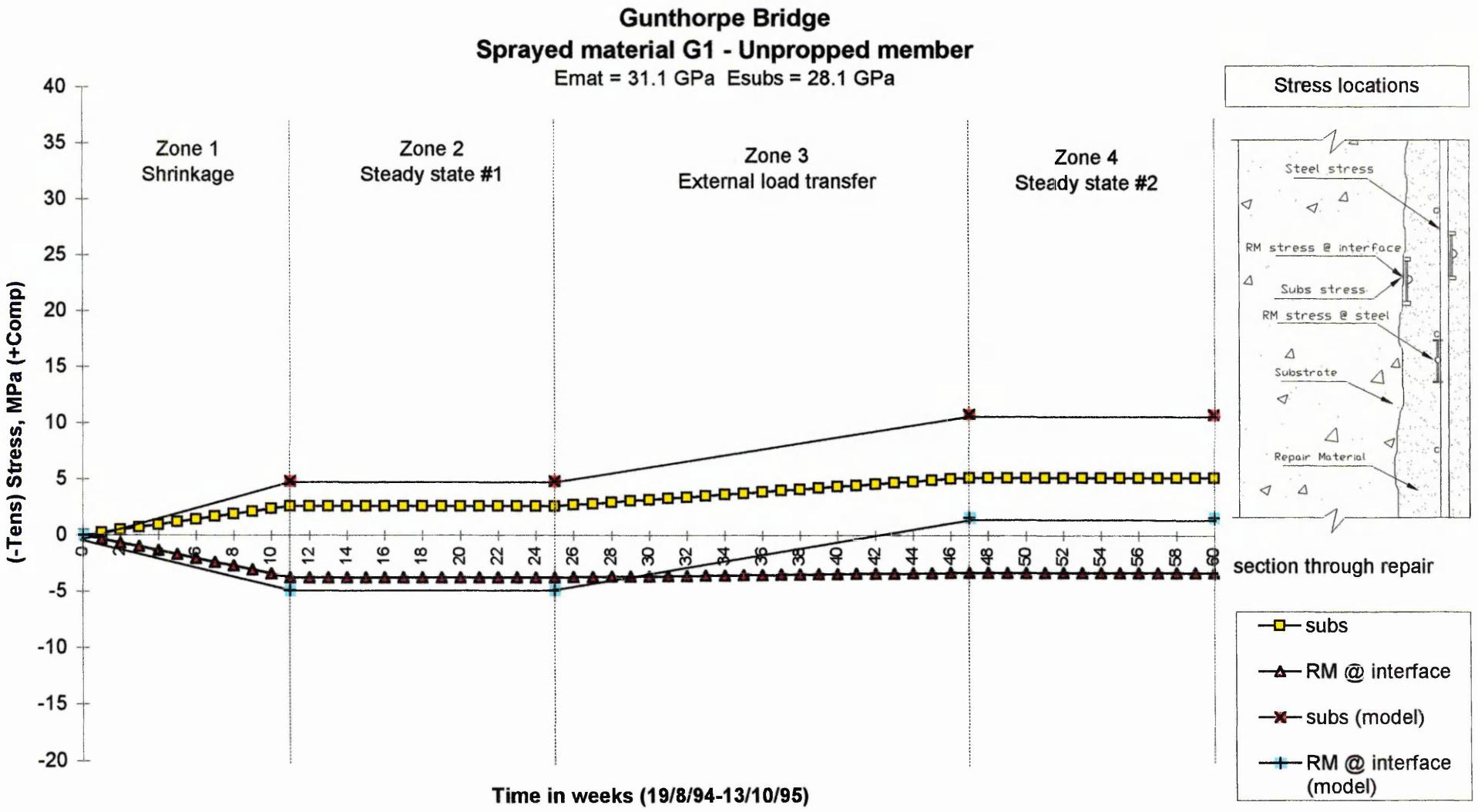

Figure 11.11 Comparison between actual and predicted stress in repair patch of material G1 at Gunthorpe Bridge (Unpropped compression member)

Table 11.4 Comparison between actual and predicted cumulative stress in the repair patch

Material/ location	*Cumulative stress at end of: (MPa)*			
	Zone 1 (week 11)	*Zone 2 (week 25)*	*Zone 3 (week 47)*	*Zone 4 (week 60)*
	Actual/Predicted	Actual/Predicted	Actual/Predicted	Actual/Predicted
L4				
subs	+3.7 / +3.1	+3.7 / +3.1	+ 7.1 / + 8.8	+7.1 / +8.8
RM @ interface	-2.2 / -3.2	-2.2 / -3.2	+ 1.4 / + 3.7	+ 1.4 / +3.7
L3				
subs	+2.5 / +2.6	+ 2.5 / +2.6	+3.3 /+8.3	+3.3 / +8.3
RM @ interface	-1.7 / -2.6	-1.7 / -2.6	-0.8 / +3.9	-0.8 / +3.9
L2				
subs	+2.8 / +1.8	+2.8 / +1.8	+7.1 / + 7.6	+7.1 / + 7.6
RM @ interface	NA / -1.6	NA / -1.6	NA / + 5.7	NA / + 5.7
G1				
subs	+2.6 / +4.8	+2.6 / +4.8	+5.1 / + 10.8	+5.1 / + 10.8
RM @ interface	-3.8 / -4.9	-3.8 / -4.9	-3.3 / + 1.6	-3.3 / + 1.6

Note: Positive values indicate compressive stress; negative values indicate tensile stress

the predicted stresses, the shrinkage model reasonably predicts the stresses in the repair patch of material L4. The actual and predicted stresses at the end of Zone 1 (Figure 11.8 and Table 11.4) are assumed to remain constant in Zone 2 (Figure 11.8 and Table 11.4), therefore, the same differences exist between the actual and predicted stresses at the end of Zone 2 for repair material L4. At the end of Zone 3, Figure 11.8, the actual stress in the substrate concrete is 7.1 N/mm^2. The cumulative predicted stress in the

substrate concrete at the end of Zone 3 is slightly higher at 8.8 N/mm^2 (the predicted cumulative stress in the substrate concrete is the sum of the predicted stress from Equation 11. 58). The actual stress in the repair material at the end of Zone 3 is 1.4 N/mm^2 (compression), whereas the predicted cumulative stress is 3.7 N/mm^2 (compression). Therefore, the analytical model slightly overestimates the cumulative stress in the repair material and substrate concrete at the end of Zone 3. The stress in the substrate concrete and repair material in Zone 4 is again assumed equal to the stress at the end of Zone 3 (Figure 11.8), therefore the differences are again similar.

Referring to Figure 11.9 and Table 11.4, the actual and predicted stresses are given for material L3. In the shrinkage stage (weeks 0 to 11), the actual compressive stress in the substrate concrete at the end of Zone 1 is 2.5 N/mm^2. The predicted compressive stress in the substrate concrete is very close to the actual at 2.6 N/mm^2. At the end of the same period (Zone 1), the actual tensile stress in the repair material is 1.7 N/mm^2. The predicted tensile stress is slightly higher at 2.6 N/mm^2. Hence, for repair material L3, the shrinkage model accurately predicts the stress in the substrate concrete, but slightly overestimates the tensile stress in the repair material. The stress values in the substrate concrete and repair material at the end of Zone 1 are considered to be the same at the end of Zone 2 (Figure 11.9, weeks 11 to 25). The compressive stress in the substrate concrete at the end of Zone 3, after external load transfer has taken place, is 3.3 N/mm^2. The cumulative predicted stress in the substrate concrete at the end of the same period (Zone 3) is well overestimated at 8.3 N/mm^2. The actual stress in the repair material at the end of Zone 3 is 0.8 N/mm^2 (tensile), but the cumulative predicted stress in the repair material at the end of the same period is 3.9 N/mm^2 (compressive). Therefore,

the shrinkage and external load transfer models overestimate the stress in the repair patch at the end of Zone 3. As before, the stress at the end of Zone 4 is assumed to be similar to the stress in the repair material and substrate concrete at the end of Zone 3 (see Figure 11.9).

In Figure 11.10 and Table 11.4, a comparison is made between the actual and predicted stress in the substrate concrete in the repair patch of material L2. The predicted stress in the repair material is also given (the actual stress in repair material L2 is unavailable since data was unavailable on the creep of this repair material). Referring to Zone 1 (Figure 11.10 and Table 11.4), the actual compressive stress in the substrate concrete at week 11 is 2.8 N/mm^2. The predicted stress from the shrinkage model is slightly lower at 1.8 N/mm^2. At the end of the same period, the predicted stress in the repair material is 1.6 N/mm^2 (tensile). The same stresses are evident in the substrate concrete and repair material at the end of Zone 2 (Figure 11.10, week 25). At the end of Zone 3, the actual stress in the substrate concrete is 7.1 N/mm^2. The cumulative compressive stress from the analytical model is 7.6 N/mm^2, marginally higher than actual stress. The predicted stress in the repair material is 5.7 N/mm^2 in compression at the end of Zone 3 (Figure 11.10, week 47). Therefore, the shrinkage and external load transfer models reasonably predicts the stress in the substrate concrete for material L2. Finally, the stresses at the end of Zone 4 are the same as the stresses at the end of Zone 3 in the substrate concrete and repair material (Figure 11.10).

Figure 11.11 and Table 11.4 show the comparison between the actual and predicted stresses in the repair patch of material G1. Referring to Zone 1 (Figure 11.11 and Table

11.4), the actual stress in the substrate concrete at week 11 is 2.6 N/mm^2 (compressive). The predicted stress in the substrate concrete at the end of the same period is higher at 4.8 N/mm^2 (compressive). With regards to the stress in the repair material at the end of Zone 1, the actual stress is 3.8 N/mm^2 (tension), whereas the predicted tensile stress is marginally higher at 4.9 N/mm^2. Hence, the shrinkage model overestimates the stress in the substrate concrete for material G1. The substrate concrete and repair material are assumed to be stressed to the same level at the end of Zone 2 (Figure 11.11 and Table 11.4). At the end of Zone 3 in repair material G1, there is poor correlation between the actual and predicted stress in the substrate concrete and repair material (Figure 11.11 and Table 11.4). The actual stress in the substrate concrete at week 47, Figure 11.11 and Table 11.4, is 5.1 N/mm^2 (compression). The cumulative predicted stress in the substrate concrete at the end of the same period 10.8 N/mm^2. The actual stress in the repair material at the end of Zone 3 is 3.3 N/mm^2 in tension. The analytical models predicts an cumulative value of 1.6 N/mm^2 in compression. The stresses in the substrate concrete and repair material at the end of Zone 4 is again similar to the stresses in the repair patch at the end of Zone 3 (Figure 11.11).

11.3.5.1 Discussion

Referring to Figures 11.8 to 11.11, and Table 11.4, the shrinkage model used to predict the stress in the substrate concrete and repair material shows a reasonable comparison with the actual values in the substrate concrete and repair material. In three of the four materials (L4, L3 and L2, Figures 11.8 to 11.11), the predicted stress in the substrate concrete at the end of Zone 1 is very similar to the actual stress in the substrate concrete.

On the other hand, the predicted compressive stress in the substrate concrete for material G1 is higher than the actual stress (4.8 N/mm^2 versus 2.6 N/mm^2). Overall, this analytical model can be used to reasonably predict the stress in the substrate concrete due to transfer of shrinkage from a spray applied repair material to an unpropped compression member.

Referring to Figures 11.8 to 11.11, and Table 11.4, the comparison between the actual and predicted stresses in the substrate concrete and repair material at the end of Zone 3 (external load transfer) show varying accuracy. The analytical models show reasonable accuracy for predicting the stress in the substrate concrete and repair material at the end of Zone 3 for materials L4 and L2, Figures 11.8 and 11.10 respectively, although the predicted stresses in the repair patch of material L4 are marginally higher than the actual stresses. In materials L3 and G1 (Figures 11.9 to 11.11 respectively), the predicted stresses in the substrate concrete and repair material do not have the same accuracy as the predicted stresses in materials L4 and L2 (compare Figures 11.9 and 11.11 with Figures 11.8 and 11.10). This could be due to the fact that these repair materials did not attract as much externally applied stress into the repair patch as materials L4 and L2. Furthermore, the predicted stress in the substrate concrete and repair material at the end of Zone 3 is higher for all materials, see Table 11.4 (with the exception of the substrate concrete stress for material L2, Figure 11.10). This could be due to the assumption that the stress in the substrate concrete in the zone of influence was 27.5% ($\alpha = 0.275$) of the cube strength (Equation 11. 44), the maximum permissible stress. In reality, the substrate concrete may not be stressed to this extent which would not only reduce the force in the substrate concrete due to external loading, but also reduce the proportion of

this force that is transferred to the repair material (Equation 11. 54). Furthermore, α from the design recommendations is based on the 28 day cube strength. Since the abutments in the field have been in service for many years, the cube strength obtained from core testing will be higher than the 28 day value. Therefore, the cores extracted from the substrate concretes in the field will have a higher strength, which will mean that the long term equivalent cube strength will be higher. A higher stress will, therefore, be calculated in the zone of influence, and subsequently, the load transferred to the repair material will be greater than indicated by field monitoring. Therefore, if a lower α is used in the analysis, the predicted compressive stress in the repair material and substrate concrete would be lower than those presented Table 11.4. This would yield better comparisons between some of the actual and predicted stresses in the substrate concrete and repair material at the end of Zone 3. Each highway structure is unique so it is impossible to obtain one α that satisifies all conditions. For example, Gunthorpe Bridge was built in 1927 and Lawns Lane Bridge in 1965, therefore, the design codes would vary for these bridges. Gunthorpe Bridge, which is highly over-designed, would rely less on the repair patch to carry some of the external load since the area of the repair patch is insignificant compared to the area of the substrate concrete. Nevertheless, the results presented when using the maximum permissible stress in the substrate concrete are sufficiently accurate since the relatively low (compressive) stresses in the repair material and substrate concrete at week 60 are unlikely to cause overstressing. Problems may occur if insufficient external stress is attracted into the repair patch to neutralise the tensile stress due to the restraint to shrinkage (materials L3 and G1, Figures 11.9 and 11.11). The analytical models show compressive stress in the repair materials at week 60. In reality, this may not always be the case as tensile stress

may still be evident in the repair patch. It was observed that the modulus of rupture, and consequently, the tensile strength, decrease with time in repair materials. Therefore, if the tensile strength of the repair material drops below the residual tensile stress in the repair material, then cracking will occur (see material L4, Section 9.3.1.1.1.2). The theoretical model is not able to predict the effects of cracking on stress distribution.

Overall, the difficulties associated with correlating field data with properties of repair materials obtained under laboratory conditions are such that it is perhaps too much to expect close agreement between theoretical and actual results. Various modifications had to be made to apply laboratory data to field studies. For example, the influence of surface/volume ratio on shrinkage of the repair materials, measured on prisms in the laboratory, was determined before applying to field monitoring. Compressive creep only was studied in the laboratory - an estimate of tensile creep was obtained from this and applied to the results from the field. Likewise, the compressive elastic modulus was determined in the laboratory. From this, the tensile elastic modulus was estimated and applied to the field data. Differences in temperature and humidity also existed between laboratory and field data and was accounted for in the analysis. Curing compounds were applied to the repair materials at Lawns Lane Bridge. Their effect on shrinkage could only be provided with considerable approximation. An estimation of the external load that was attracted into the repair patch was obtained from assumed service stresses since precise loading and design data for the substrate concretes was not available. Since the laboratory data was substantially modified to represent field conditions, the likelihood of cumulative error is high. Therefore, the predicted results are satisfactory under the circumstances.

11.3.5.2 Limitations of the analytical models

This model only takes into account the stress in the substrate concrete and the stress in the repair material at the interface between the substrate concrete and repair material. Referring to Figure 11.5 (e), the tensile stress in the repair material at the steel reinforcement level (centre of repair patch), due to the restraint to shrinkage, is less than the tensile stress in the repair material at the interface under simplified modelling conditions. In practice, this was not the case, since the steel reinforcement provided a higher restraint to shrinkage, and therefore, the tensile stress in the repair material should be greater at this point (see Figures 10.20 to 10.22). The model, therefore, is not sensitive enough to predict the tensile stress in the repair material at the steel reinforcement level at the end of the shrinkage period. Besides, the stress in the repair material at the interface and at the steel reinforcement level is relatively similar after modifications were made to the properties of the repair materials to compensate for the effects of tensile creep and different surface/volume ratios etc. (see Figures 10.20, 10.21 and 10.23). Therefore, for simplicity, the stress calculated in the repair material at the interface due to the restraint to shrinkage can be considered similar to the stress in the repair material at the steel reinforcement level.

The stress in the steel reinforcement due to transfer of shrinkage strain is also omitted from Figures 11.8 to 11.11. This is since the stress predicted by the model at the steel reinforcement level is a tensile stress [i.e. the stress in the repair material - see Figure 11.5 (e)]. The stress in the steel reinforcement is compressive due to the transfer of shrinkage from the repair material (see Figures 10.20 to 10.22). However, the restrained shrinkage that was transferred to the steel reinforcement could be estimated from the

tensile stress predicted in the repair material at steel reinforcement level. The virtual tensile strain in the repair material at the steel reinforcement level could be obtained from the tensile stress in the repair material [i.e. by dividing the tensile stress as calculated by the analytical model (Equation 11. 59) by the elastic modulus of the repair material]. This virtual tensile strain could then be subtracted from the modified free shrinkage strain in the repair material to give the contraction in the repair material at the steel reinforcement level. This strain, due to strain compatibility between the repair material and steel reinforcement, could then be converted to a compressive stress in the steel reinforcement by multiplying by the elastic modulus of the steel reinforcement. The stress transferred to the steel reinforcement was found to be negligible compared with the ultimate strength of the steel reinforcement. Therefore, overstressing will not be a problem in the steel reinforcement, and consequently, prediction of this stress is not crucial.

11.4 DISCUSSION

The aim of this chapter is to present simple theoretical models which describe the mechanics of concrete repair. Consequently, the material properties used in the models were limited to basic properties such modulus of elasticity, shrinkage and creep, all of which can easily be determined in the laboratory. An interaction between the repair material and the substrate concrete can only occur if there is a full bond between the two mediums. This is assumed to be true in all cases considered in this project.

Specification of repair materials at present is based on short term properties such as compressive strength, bond and early age plastic-shrinkage/expansion etc. [24]. Basic repair material properties such as elastic modulus, shrinkage and creep which control the long term performance of the repair material are glaring omissions from the current repair specification, BD 27/86 [1]. More often than not, repair materials exhibit significant shrinkage characteristics, regardless of the manufacturers literature stating otherwise. When this occurs, the shrinkage strain that is not transferred to the substrate concrete will cause tensile stress in the repair material. Furthermore, a material with high tensile creep characteristics will relieve some of the tensile stress induced (compare Figures 10.13, 10.14 and 10.16 with 10.20, 10.21 and 10.23).

If the difference in elastic modulus between the repair material and substrate concrete is significant (i.e. the repair material is much stiffer than the substrate concrete), then the repair material is able to transfer more of the shrinkage strain to the substrate, thus reducing the tensile strain induced in the repair material (see Figure 10.2 and Figures 10.9 to 10.12). Obviously, the tensile strain in the repair material due to the restraint to shrinkage provided by the substrate concrete and steel reinforcement will be low if the free shrinkage in the repair material is low. Therefore, a crack free repair material can be virtually guaranteed if the elastic modulus of the repair material is high ($m \geq 1.32$) and the free shrinkage of the repair material is low. An uncracked material, one which is able to withstand the tensile stresses induced, will attract externally applied stress from the substrate concrete to become a load sharing repair (it has been observed that a cracked material will not attract stress into the material). This externally applied load will also serve to reduce the tensile stress remaining in the repair material from the

shrinkage stage, zone 1 (see Figure 10.21) or even completely neutralise the tensile stress in the repair material (see Figure 10.20, "RM @ interface", week 39).

11.5 CONCLUSIONS

The following conclusions are based on the results obtained from the various repair materials under test:

- A spray applied repair material that has an elastic modulus which greeter than the elastic modulus of the substrate concrete will:
  - (i) transfer a portion of the shrinkage strain to the substrate concrete
  - (ii) attract external applied stress into the repair patch
- Four stages of stress are evident in spray applied repairs to unpropped compression members:
  - (i) shrinkage stage (weeks 0 to 11)
  - (ii) steady state #2 (weeks 11 to 25)
  - (iii) external load transfer (weeks 25 to 47)
  - (iv) steady state #2 (weeks 47 to 60)
- Stress relaxation due to creep reduces the tensile stress in the repair material caused by the restraint to shrinkage provided by the substrate concrete and steel reinforcement
- The depth of substrate concrete affected by transfer of shrinkage strain from the repair material can be calculated from:

$$d_{sub} = m(d_{rm})$$

- The virtual force in the substrate concrete and repair patch due to shrinkage in the repair material, F_{shr}, and the radius of curvature caused by bending of the substrate concrete and repair patch, R, can be obtained from the following simultaneous equations:

$$F_{shr} = 2\left[\frac{E_{sub}I_{sub} + E_{rm}I_{rm}}{d_{sub} + d_{rm}}\right]\frac{1}{R}$$

$$F_{shr} = \frac{\left(\varepsilon_{shr(free)} - \frac{1}{2}(d_{sub} + d_{rm})\right)b}{\left(\frac{1}{d_{rm}E_{rm}} + \frac{1}{d_{sub}E_{sub}}\right)}$$

- The bending moment in the substrate concrete caused by the restraint to shrinkage in the repair material can be determined from:

$$M_{sub(shr)} = \frac{E_{sub}I_{sub}}{R}$$

- The bending moment in the repair patch caused by the restraint to shrinkage provided by the substrate concrete can be determined from:

$$M_{rm(shr)} = \frac{E_{rm}I_{rm}}{R}$$

- The compressive stress across the zone of influence of the substrate concrete due to transfer of shrinkage from the repair material can be determined from:

$$\sigma_{sub(shr)} = \frac{F_{shr}}{A_{sub}} \pm \frac{E_{sub}y_{sub}}{R}$$

- The tensile stress across the repair patch due to the restraint to shrinkage provided be the substrate concrete can be determined from:

$$\sigma_{rm(shr)} = -\frac{F_{shr}}{A_{rm}} \pm \frac{E_{rm}y_{rm}}{R}$$

- The force in the repair material due to transfer of external load from the substrate concrete can be estimated from

$$F_{rm(ELT)} = \frac{\alpha b m d_{rm} f_{cu}(b d_{rm} + m_{st} A_{st})}{(2b d_{rm} + m_{st} A_{st})}$$

- The stress in the repair patch due to transfer of external load from the substrate concrete can be estimated from

$$\sigma_{rm(ELT)} = \frac{F_{rm(ELT)}}{A_{rm(trans)}}$$

- The stress in the substrate concrete due to deformation in the repair patch after transfer of external load can be calculated from

$$\sigma_{sub(ELT)} = \frac{1}{m} \frac{F_{rm(ELT)}}{A_{rm(trans)}}$$

- The total stress in the substrate concrete at week 60, the end of the monitoring period, after transfer of shrinkage from the repair material and transfer of external load into the repair patch can be estimated from

$$\sigma_{sub(wk60)} = \frac{F_{shr}}{A_{sub}} \pm \frac{E_{sub} y_{sub}}{R} + m \frac{F_{rm(ELT)}}{A_{rm(trans)}}$$

- The total stress in the repair material at week 60, the end of the monitoring period, can be estimated from

$$\sigma_{rm(wk60)} = -\frac{F_{shr}}{A_{rm}} \pm \frac{E_{rm} y_{rm}}{R} + \frac{F_{rm(ELT)}}{A_{rm(trans)}}$$

CHAPTER 12

CONCLUSIONS AND RECOMMENDATIONS FOR FURTHER WORK

12.1 CONCLUSIONS

The following conclusions are based on the theoretical and experimental work reported in this thesis:

Properties of repair materials

1. Repair materials which contain coarse aggregate exhibit lower free shrinkage and creep compared with repair materials which contain fine aggregate only.
2. Spray applied and flowable repair materials shrink and creep less than repair materials which are hand applied due to the inclusion of coarse aggregates in the spray applied and flowing repair materials.
3. All the cementitious repair materials tested in this project exhibited significant free shrinkage regardless of some manufacturers' claims that their materials were shrinkage compensated or non-shrinking repair materials.
4. The free shrinkage of repair materials is reduced when the specimens are initially cured in water for 28 days after casting as opposed to curing in air from the age of 24 hours onwards.

5. Repair materials which contain coarse aggregates exhibit lower creep recovery than repair materials with fine aggregates.
6. The addition of polymers and coarse aggregates generally increases the elastic modulus of a repair material.
7. Repair materials with fine aggregates, with or without polymer additives, generally have lower elastic modulus.
8. Repair materials which contain coarse aggregates generally exhibit higher modulus of rupture than repair materials with fine aggregate.
9. The modulus of rupture of some repair materials decreases with time.

Performance of repair materials

1. Recommendations given in the current repair specification, BD 27/86 [1], are not suitable for all concrete repairs. The specification does not adequately take into account the potential mismatch in key properties which may occur between the repair material and substrate concrete. It also gives emphasis to some properties of repair materials which are of secondary importance.
2. The long term performance of a repair is superior when the repair is applied to an unpropped member as opposed to a propped member.
3. The risk of cracking in the repair patch is greatly increased when the repair material is applied to a propped flexural member.
4. Spray applied repair materials to unpropped members perform better than flowing repair materials applied to unpropped members.
5. Increasing the depth of repair behind the steel reinforcement in repairs to flexural members does not significantly influence the performance of the repair.

6. The elastic modulus is a vitally important property to be considered when selecting a repair material for concrete repairs. The elastic modulus of the repair material should be 32% (or more) greater than the elastic modulus of the substrate concrete ($m = 1.32$) to provide optimum performance
7. The possibility of cracking in the repair patch is greatly increased when the repair material exhibits high shrinkage.
8. If the elastic modulus of the repair material is greater than the elastic modulus of the substrate in a compression member repaired in the unpropped state, the stiffer repair is able to transfer shrinkage strain to the concrete substrate.
9. A spray applied repair material of $E_{rm} > E_{sub}$, when applied to an unpropped member in compression, will attract externally applied load into the repair patch in the long term.
10. A spray applied repair material of $E_{rm} < E_{sub}$, when applied to an unpropped member in compression, will not attract externally applied load into the repair patch in the long term.
11. A flowing repair material of $E_{rm} > E_{sub}$, when applied to a propped member in compression, will not attract externally applied load into the repair patch.
12. Repair materials for both flexural and compression members should have low shrinkage and creep characteristics.
13. Cracking will occur in a repair material when the tensile strain due to restraint to shrinkage is greater than the tensile strain capacity of the repair material (including creep effects).
14. Repairs to flexural members carried out with high modulus materials ($E_{rm} > E_{sub}$) attract tensile load from the steel reinforcement.

15. Four stages (or zones) of distribution of strain (and consequently stress) are evident in spray applied repairs to unpropped compression members:

    (i) shrinkage stage (zone 1, weeks 0 to 11)

    (ii) steady state #1 (zone 2, weeks 11 to 25)

    (iii) external load transfer (zone 3, weeks 25 to 47)

    (iv) steady state #2 (zone 4, weeks 47 to 60)

16. Tensile stress is evident in the repair material in stage 1 (zone 1, weeks 0 to 11) due to the partial restraint to shrinkage provided by the substrate concrete and steel reinforcement.

17. Compressive stress is transferred to the substrate concrete and steel reinforcement during the shrinkage (contraction) of the repair material within stage 1.

18. Stresses in the repair material, substrate concrete and steel reinforcement remain constant in stage 2 (zone 2, weeks 11 to 25) since the shrinkage in the repair material reaches negligible levels.

19. Tensile stress in the repair material is reduced (or changes to compression), after external (compressive) load is transferred from the substrate concrete in stage 3 (zone 3, weeks 25 to 47).

20. Stresses in the repair material, substrate concrete and steel reinforcement at the end of stage 3 remain constant in stage 4 (zone 4, weeks 47 to 60) since the transfer of external load transfer from the substrate concrete has ceased.

21. Residual tensile stress may be evident in the repair material in the long term if insufficient compressive stress is attracted into the repair material to neutralise the tensile stress.

22. Stress relaxation due to tensile creep in the repair material reduces the tensile stress caused by the restraint to shrinkage provided by the substrate concrete and steel reinforcement.

Properties of repaired section

1. The depth of substrate concrete (zone of influence) affected by transfer of shrinkage strain from the repair material can be calculated from:

$$d_{sub} = m(d_{rm})$$

2. The virtual force in the substrate concrete and repair patch due to shrinkage in the repair material, F_{shr}, and the radius of curvature caused by bending of the substrate concrete and repair patch, R, can be obtained from the following simultaneous equations:

$$F_{shr} = 2\left[\frac{E_{sub}I_{sub} + E_{rm}I_{rm}}{d_{sub} + d_{rm}}\right]\frac{1}{R}$$

$$F_{shr} = \frac{\left(\varepsilon_{shr(free)} - \frac{1}{2}(d_{sub} + d_{rm})\right)b}{\left(\frac{1}{d_{rm}E_{rm}} + \frac{1}{d_{sub}E_{sub}}\right)}$$

3. The bending moment in the substrate concrete caused by the restraint to shrinkage in the repair material can be determined from:

$$M_{sub(shr)} = \frac{E_{sub}I_{sub}}{R}$$

4. The bending moment in the repair patch caused by the restraint to shrinkage provided by the substrate concrete can be determined from:

$$M_{rm(shr)} = \frac{E_{rm}I_{rm}}{R}$$

5. The compressive stress across the zone of influence of the substrate concrete due to transfer of shrinkage from the repair material can be determined from:

$$\sigma_{sub(shr)} = \frac{F_{shr}}{A_{sub}} \pm \frac{E_{sub} y_{sub}}{R}$$

6. The tensile stress across the repair patch due to the restraint to shrinkage provided be the substrate concrete can be determined from:

$$\sigma_{rm(shr)} = -\frac{F_{shr}}{A_{rm}} \pm \frac{E_{rm} y_{rm}}{R}$$

7. The force in the repair material due to transfer of external load from the substrate concrete can be estimated from:

$$F_{rm(ELT)} = \frac{\alpha b m d_{rm} f_{cu} (b d_{rm} + m_{st} A_{st})}{(2 b d_{rm} + m_{st} A_{st})}$$

8. The stress in the repair patch due to transfer of external load from the substrate concrete can be estimated from:

$$\sigma_{rm(ELT)} = \frac{F_{rm(ELT)}}{A_{rm(trans)}}$$

9. The stress in the substrate concrete due to deformation in the repair patch after transfer of external load can be calculated from:

$$\sigma_{sub(ELT)} = \frac{1}{m} \frac{F_{rm(ELT)}}{A_{rm(trans)}}$$

10. The total stress in the substrate concrete at week 60, the end of the monitoring period, after transfer of shrinkage from the repair material and transfer of external load into the repair patch can be estimated from:

$$\sigma_{sub(wk60)} = \frac{F_{shr}}{A_{sub}} \pm \frac{E_{sub} y_{sub}}{R} + m \frac{F_{rm(ELT)}}{A_{rm(trans)}}$$

11. The total stress in the repair material at week 60, the end of the monitoring period, can be estimated from:

$$\sigma_{rm(wk60)} = -\frac{F_{shr}}{A_{rm}} \pm \frac{E_{rm} y_{rm}}{R} + \frac{F_{rm(ELT)}}{A_{rm(trans)}}$$

12.2 RECOMMENDATIONS FOR FURTHER WORK

The following points may be considered for future research in the investigation of long term performance of concrete repair in highway structures:

1 Determine the relationship between the modulus of rupture and direct tensile strength of repair materials

2 Determine the relationship between tensile and compressive creep of repair materials

3 Determine the influence of curing membranes on the free shrinkage of repair materials under field conditions

CHAPTER 13

REFERENCES

1 Department of Transport (1986). Materials for the repair of concrete highway structures, BD 27/86.

2 Swiss Bank Corporation (Stockbrokers). *Quarterly building bulletin,* 26 Jan. 1989, London

3 British Standards Institution. (1983) *Method for determination of static modulus of elasticity in compression.* BSI, London. BS 1881, Part 121.

4 British Standards Institution. (1978). *Specification for ordinary and rapid hardening Portland cement,* BSI, London, 1978. BS 12.

5 British Standards Institution. (1983). *Specification for aggregates from natural sources for concrete,* BSI, London, 1983. BS 882.

6 Hornby, I.W., "The vibrating wire strain gauge", Strain Gauge Technology (ed. A.L. Window), Elsevier Applied Sciences, Great Britain, 1989, pp. 325-345.

7 Davidenkoff, N., "The vibrating wire method of measuring deformations, *Zh prikl. Fiziki (Journal of Applied Physics),* Leningrad, 1928, **5.**

8 Jerrett, R.S., "The acoustic strain gauge, *J. Sci. Inst.,* 1945, **22**

9 Mainstone, R.J., Vibrating wire strain gauge for long term tests on structures, *Engineering,* July 1953.

10 Whiffin, A.C., "Some special techniques developed at the Road Research Laboratory for testing roads and other structures, *RILEM Sypm. On the observation of structures,* Lisbon, 1955.

11 Chalmers, G.F., "Materials, construction, performance and characteristics", Strain Gauge Technology (ed. A.L. Window), Elsevier Applied Sciences, Great Britain, 1989, pp. 1-38.

12 Micro-Measurements Division, Measurements Group, Inc. "Strain gauge application with M-Bond AE-10, AE-15 and GA-2 adhesive systems". Instruction Bulletin B-137-16, 1979.

13 TML Strain Gauges. Catalogue TML pam E-101 Z, 1990.

14 SBD Ltd., *Construction and Repair Products (1994),* Technical data sheets.

15 Flexcrete Ltd,. *Repair and Protection Systems (1995),* Technical data sheets.

16 Proton Group Limited. *Portland Cement Systems (1994).* Technical data sheet.

17 Nufins Limited. Technical data sheet (1994).

18 Fosroc Expandite Limited. Technical data sheet (1993).

19 Pozament Limited. Technical data sheet (1994).

20 British Standards Institution. (1983). *Method for determination of compressive strength of concrete cubes*. BSI. London. BS 1881 Pt 116.

21 British Standards Institution. (1982). *Specification for pulverised fuel ash for use as a cementitious component in structural concrete*. BSI. London. BS 3892 Pt 1.

22 British Standards Institution. (1982). *Specification for accelerating admixtures, retarding admixtures and water-reducing admixtures*. BSI. London. BS 5075 Pt 3.

23 British Standards Institution. (1985) *The Structural Use of Concrete.* BSI, London. BS 8110.

24 Limbachiya, M.K. A thesis submitted in fulfilment of the requirement of Sheffield Hallam University for the degree of Doctor of Philosophy, November 1995.

25 Emberson, N.K.; Mays, G.C., "Significance of property mismatch in the patch repair of structural concrete. Part 1: Properties of the repair system", *Mag. Con. Res.,* 1990, 42, No. 152, Sept., 147-160.

26 Emmons, P.H.; Vaysburd, A.M.; McDonald, J.E., "Concrete repair in the future turn of the century - Any problems?, *Concrete International,* March 1994, pp 42-49.

27 Alberta concrete patch evaluation program, Report No. ABTR/RD/RR-87/05, Alberta Transportation and Utilities, Edmonton, 1987.

28 Morgan, D.R., "Compatibility of concrete repair materials and systems", *Construction and Building Materials,* Vol 10, No.1, pp 57-67, 1996.

29 Mangat, P.S., Limbachiya, M.K., "Repair materials properties which influence long-term performance of concrete structures", *Construction and Building Materials,* Vol. 9, No. 2, pp. 81-90, 1995.

30 Mangat, P.S., Limbachiya, M.K., "Repair material properties for effective structural application", *Cement and Concrete Research,* Vol. 27, No. 4, pp. 601-617, 1997.

31 Dector, M.H.; Lambe, R.W., "New materials for concrete repair - Development and testing", *The Indian Concrete Journal,* October 1993, pp 475-480.

32 Australian Standards (1983). *Methods of testing concrete - methods for the determination of properties related to the consistence of concrete.* AS 1012, Part 3.

33 *New Civil Engineer.* "Midland Links analysis offers full repair range" 9 April 1987, pp 6-8.

34 Coutinho, A., "The influence of the type of cement on its cracking tendency", *RILEM Bulletin,* 5, December 1959, 26-40.

35 Department of Transport (1994). Specification for the repair of concrete highway structures, Draft standard BD /94.

36 Maultzch, M., *"Properties of PCC for repair of concrete structures", Proceedings of 5th International Congress on Polymers in Concrete,* Brighton, UK, 22-24 September 1987, 301-304.

37 Yuan, Y.S., Marosszeky, M., "Major factors affecting the performance of structural repair", in Proceedings of the ACI International Conference on Evaluation and Rehabilitation of Concrete Structures and Innovations in Design, Hong Kong, 1991, ACI-SP128, Vol. 2, pp. 819-837.

38 Brull, L., Komlos, K., Majzlan, B., "Early shrinkage of cement pastes, mortars and concretes", *Mater. Struct.* 13(73), (1980), pp. 41-45.

39 Staynes, B.W., "Delamination of polymer composite sandwich structures - the interaction of the controlling parameters. *Proc. 2nd Int. Symp. on Brittle Matrix Composites,* Cedyna, Poland, Sept. 1988. Elsevier, London, pp 462-473.

40 Schrader, E.K., "Mistakes, misconceptions and controversial issues concerning concrete and concrete repairs", *Concrete International,* September 1992, pp 53-56.

41 Lea, F.M., "The chemistry of cement and concrete", 3rd Edition, Edward Arnold (Publishers) Ltd., 1970.

42 Hamad, B.S., "Evaluation and repair of war-damaged concrete structures in Beirut", *Concrete International,* March 1993, pp 47-51.

43 Pinelle, D.J., "Curing stresses in polymer modified repair mortars", *Cement, Concrete and Aggregates,* CCAGDP, Vol. 17, No. 2, Dec. 1995, pp 195-200.

44 Cusson, D., Mailvaganam, N., "Durability of Repair Materials", *Concrete International,* March 1996, pp. 34 - 38.

45 Saucier, F., Detriche, C.H., Pigeon, M., "Tensile relaxation capacity of a repair concrete", *Materials and Structures,* 25, 1992, pp. 335-346 (in French)

46 Illston, J.M., "The creep of concrete under uniaxial tension", *Magazine of Concrete Research,* Vol. 17, No. 51, June 1965. pp. 77-84.

47 Brooks, J.J., Neville, A.M., "A comparison of creep, elasticity and strength of concrete in tension and in compression", *Magazine of Concrete Research,* Vol. 29, No. 100, September 1978. pp. 131-141.

48 Johnston, C.D., "Strength and deformation of concrete in uniaxial tension and compression", *Magazine of Concrete Research,* Vol. 22, No. 70, March 1970. pp. 5-16.

49 Emmons, P.H., Vaysburd, A.M., "A total system concept - Necessary for improving the performance of repaired structures", *Concrete International,* March 1995, pp 31-36.

50 Rots, J.G., De Borst, R., "Analysis of concrete in "direct" tension", *Int. J. Solids and Structures,* Vol. 25, No. 12, 1989. pp. 1381-1394.

51 Cedolin, L., Dei Poli, S., Iori, I, "Tensile behaviour of concrete", *Journal of Engineering Mechanics,* Vol. 113, No. 3, March 1988. pp. 431-449.

52 Mangat, P.S., O'Flaherty, F.J., "Long Term Performance of Sprayed Concrete Repair in Highway Structures", *Proceedings of the ACI/SCA International Conference on Sprayed Concrete/Shotcrete - Sprayed Concrete Technology for the 21st Century,* (Ed. S. Austin), Edinburgh University, 10-11 September 1996, E & FN Spon, London, pp. 196-205.

53 Bissonnette, B., Pigeon, M., "Tensile creep at early ages of ordinary, silica fume and fibre reinforced concretes", *Cement and Concrete Research,* Universite Laval, 1995.

54 Emmons, P.H., Vaysburd, A.M., Pinelle, D.J., Poston, R.W., and Walkowicz, S., "The origin and durability of concrete repairs", Int. Association for Bridge and Structural Engineering Symposium, San Francisco, 23-25 Aug, 1995.

55 Kovler, K., "Testing system for determining the mechanical behaviour of early age concrete under restrained and free uniaxial shrinkage", *Materials and Structures,* Vol. 27, 1994, pp. 324-330.

56 Emmons, P., "*Concrete Repair and Maintenance Illustrated*, R.S. Means Company, Inc., Kingston, MA, 1993, pp. 128-129.

57 Ramachandran, V.S., "*Concrete Admixtures Handbook - Properties, Science and Technology,* Noyes Publications, Park Ridge, New Jersey, 1984 p. 388.

58 Glanville, W.H., Thomas, F.G., *Further investigations on the creep or flow of concrete under load,* London, H.M.S.O., 1939, pp. 5-8. Building Research Technical Paper No. 21.

59 Hanson, J.A., *A 10-year study of creep properties of concrete.* United States Department of the Interior, Bureau of Reclamation, July 1953, Laboratory Report, No. SP-38.

60 Davis, R.E., Davis, H.E., Brown, E.H., "Plastic flow and volume changes in concrete. *Proceedings of the American Society for Testing and Materials,* Vol. 37, Part II, 1937, pp. 317-330.

61 Ross, A.D., "Experiments on the creep of concrete under two-dimensional stressing. *Magazine of Concrete Research,* Vol. 6, No. 16, June 1954, pp. 3-10.

62 Neville, A.M. (with Chapters 17-20 written in collaboration with W. Dilger), *Creep of concrete:, plain, reinforced and prestressed,* Amsterdam, North-Holland Publishing Co., 1970, pp. 622.

63 Kuhlman, L, "Styrene -Butadiene Latex-Modified Concrete: The Ideal Concrete Repair Material?", *Concrete International,* October 1990, pp 59-65.

64 Mosley, W.H., Bungey, J.H., "Reinforced Concrete Design", Fourth Edition, McMillan Press, London 1990, p 362, ISBN 0-333-53718-1.

65 Neville, A.M., "Properties of concrete, London, Pitman Publishing Ltd., 1972, p. 686.

66 Chan, S.T., Ainsworth, P.R., Read, A.S., "A classification and quality system for concrete repair mortars", *Proc. of ACI International Conference on Evaluation and Rehabilitation of Concrete Structures and Innovations in Design,* Hong Kong, 1991, 609-623.

67 Watkins, R.A.M., McNicholl, D.P., "Statistics applied to the analysis of test data from low strength concrete cores", *The Structural Engineer,* 68, No. 16, 21 August 1990.

68 RILEM. Direst tensile tests of concrete. *RILEM Bulletin,* No. 20, September 1963, pp. 84-90.

69 Johnston, C.D., Sidwell, E.H., "Testing concrete in tension and compression", *Magazine of Concrete Research,* Vol. 20, No. 65, December 1968, pp. 221-228.

70 Gonnerman, H.F., Shuman, E.C., "Compression, flexure and tension tests of plain concrete", *Proceedings of the American Society for Testing Materials,* Vol. 28, Part 2. pp. 527-552.

71 O'Cleary, D.P., Byrne, J.G., "Testing of concrete and mortar in tension. *Engineering.* Vol 189, No. 4900, 18 March 1960, pp. 384-385.

72 Ward, M.A., "*The testing of concrete materials by precisely controlled uniaxial tension.* Thesis presented to the University of London for the degree of PhD. 1964. p 12.

73 Schuman, L., Tucker, J., "Tensile and other properties of concretes made with various cements. *Journal of Research of the National Bureau of Standards.* Vol. 31, August 1943, pp. 107-124.

74 Todd, J.D., "The determination of tensile stress-strain curves for concrete". *Proceedings of the Institution of Civil Engineers.* Part 1, Vol. 4. March 1955, pp. 201-211.

75 Humphreys, R., "Direct tensile strength of concrete. *Civil Engineering and Public Works Review.* Vol. 52, No. 614. August 1958. pp. 882-883.

76 Hughes, B.P., Chapman, G.P., "Direct tensile test for concrete using modern adhesives. *RILEM Bulletin,* No. 26, March 1965. pp. 77-80.

77 Domone, P.L., "Uniaxial tensile creep and failure of concrete", Vol. 26, No. 88, September 1974, pp. 144-152.

78 British Standards Institution (1970). *Methods for testing concrete for strength.* London. BSI, 1970, BS 1881:Part 4, pp. 28.

79 Elvery, R.H., Haroun, W., "A direct tensile test for concrete under long- and short-term loading." *Magazine of Concrete Research,* Vol. 20, No. 63, June 1968, pp. 111-116.

80 British Standards Institution. (1983) *Testing Concrete.* BSI. London. BS 1881.

81 British Standards Institution. (1983) *Testing of Resin Compositions for use in Construction.* BSI. London. BS 6319.

82 British Standards Institution. (1983) *Method for making test cylinders from fresh concrete.* BSI. London. BS 1881 Part 110.

83 Illston, J.M., Pomeroy, C.D., "Recommendations for a standard creep test", *Concrete,* December 1975, pp. 24-25.

84 Kong and Evans, Reinforced and Prestressed Concrete, 3rd Edition. Van Nostrand Reinhold (UK), Hong Kong, 1987, ISBN 0-278-00016-9.

85 Neville, A.M., Dilger, W.H., Brooks, J.J., "Creep of plain and structural concrete", Construction Press, New York, 1983.

86 Roll, F., "Long-term creep-recovery of highly stressed concrete cylinders ", Symposium on Creep of Concrete, *American Concrete Institute Special Publication No. 9,* 1964, pp. 95-114.

87 British Standards Institution. (1983) *Method for determination of flexural strength.* BSI. London. BS 1881 Part 118.

88 British Standards Institution. (1980) *Methods of testing mortars, screeds and plasters.* BSI. London. BS 4551.

89 British Standards Institution. (1990) *Methods for measurement of modulus of elasticity in flexure and flexural strength.* BSI. London. BS 6319 Part 3.

90 British Standards Institution. (1983) *Method for preparation of test specimens.* BSI. London. BS 6319 Part 1.

91 Rizzo, E.M., Sobelman, M.B., "Selection criteria for concrete repair materials", *Concrete International,* September 1989, pp. 46-49.

92 Browne, R.D., *Durability of Building Materials,* Elsevier Science Publishers, Amsterdam, 1982.

93 Plum, D.R., "Repair materials and repaired structures in a varying environment", *Proc. 3rd. Int. Seminar on the Life of Structures - the Role of Physical testing,* Brighton, 1989, pp. 77-84.

94 Emmons, P.H., Vaysburd, A.M., "*Performance Criteria for Concrete Repair Materials, Phase 1,* Technical Report for the U.S. Army Corps of Engineers (in publication).

95 Emberson, N.K., Mays, G.C., "Significance of property mismatch in the patch repair of concrete. Part 3: Reinforced concrete members in flexure", *Magazine of Concrete Research,* 1996, 48, No. 174, Mar., pp. 45-57.

96 Wood, J.G.M., King, E.S., Leek, D.S., "Defining the properties of concrete repair materials for effective structural application", *International Conference on Structural Faults and Repair-89,* **2,** London, 1989.

97 British Standards Institution (1992). *Method of test for curing compounds for concrete.* BSI, London, BS 7542.

98 Wang, J., Dhir, R.K., Levitt, M., "Membrane curing of concrete: Moisture loss", *Cement and Concrete Loss,* Vol. 24, No. 8, pp. 1463-74, 1994.

99 Senbetta, E., Scholer, C., "A new approach for testing concrete curing efficiency", *ACI Journal,* January/February 1984, pp. 82-86.

100 Cabrera, J.G., Gowripalan, N., Wainwright, P.J., "An assessment of concrete curing efficiency using gas permeability", *Mag. Con. Repair materials.,* 1989, 41, No. 149, Dec., pp. 193-198.

101 Russell, Peter, "The curing of concrete", C&CA, 2nd Edition, 1976, ISBN 0 7210 0902 6

102 Bennison, P., "Materials for concrete repair and protection - innovation and performance", *Construction Repair,* July/August 1992, pp. 31-35

103 Yuan, Y.S., Marosszeky, M., "Major factors affecting the performance of structural repair", in Proceedings of the ACI International Conference on Evaluation and Rehabilitation of Concrete Structures and Innovations in Design, Hong Kong, 1991, ACI-SP128, Vol. 2, pp. 819-837.

104 Cain, J.A., Hulse, R, "Structural Mechanics", Macmillan, London 1990. ISBN 0 333 48078 3

105 Whitlow, R., "Materials and Structures", Longman Group Ltd., Tenth impression, New York 1986. ISBN 0 582 42006 7

106 Urry, S.A., Turner, P.J., "Solution of problems in strength of materials and mechanics of solids", Pitman Publishing Ltd., London, Fourth edition, 1981. ISBN 0 273 01590 7

107 Reynolds, C.E., Steedman, J.C., "Reinforced Concrete Designer's Handbook", Tenth Edition, E & FN Spon, London, 1988, pp. 43

LIST OF PUBLICATIONS

1. Mangat, P.S., O'Flaherty, F.J., "Long Term Performance of Sprayed Concrete Repair in Highway Structures", *Proceedings of the ACI/SCA International Conference on Sprayed Concrete/Shotcrete - Sprayed Concrete Technology for the 21st Century,*(Ed. S. Austin), Edinburgh University, 10-11 September 1996, E & FN Spon, London, pp. 196-205.